Faculty of Science and Technology

BACHELOR`S THESIS

Study program/Specialization: B.Sc. Geo/and energy resources	Spring semester, 2021 Open
Writer: Kolbrun Mari Kristjansdottir	……………………………………… (Writer's signature)
Faculty supervisor: Udo Zimmermann External supervisor(s):	
Thesis title: **Provenance of Lower Cambrian rocks in Northern Spain – U-Pb isotope ages on detrital zircons in different lithofacies**	
Credits (ECTS): 20	
Key words: Provenance U-Pb detrital zircon dating Whole-rock geochemistry Petrography Cantabrian Mountains	Pages: 38 + enclosure: 72 Stavanger, 26.06.2021

Provenance of Lower Cambrian rocks in Northern Spain – U-Pb isotope ages on detrital zircons in different lithofacies

By

Mari Kristjansdottir

BSc. Thesis

Presented to the Department of Energy Resources

The University of Stavanger

The University of Stavanger

June 2021

Acknowledgement

I need to express my sincere gratitude towards my very patience supervisor, Dr. Udo Zimmermann. Without your continuous motivation, support and guidance, it would have been difficult to finish this thesis. I would also like to extend my gratitude towards Tom Andersen and Magnus Kristoffersen at UiO for their guidance and support through the U-Pb analysis. My gratitude also goes to Caroline Ruud for assisting me through the rock analysis and preparation of rock samples at the laboratory at UiS. Finally, I would like to thank my better half Thomas Meldahl Olsen for his patience, motivation, support and for pushing me to the limit.

Abstract

The Herrería Formation with a Lower Cambrian depositional age exposed in the Cantabrian Mountains of northern Spain is the focus of this study. The motivation of this study is related to recognized significant provenance changes between the base of the formation and the top, which would have allowed fundamentally different provenance interpretations (Zimmermann, et al., 2015). Therefore, this study concentrates on a similar lithotype (quartz-arenites), which show a variety of differing sedimentary structures pointing to different sedimentary processes including sorting. The quartz-arenites are intercalated with shales devoid of carbonate material. The recognition of acritarchs pinpoints a marine depositional environment. The youngest detrital zircon age of the Herreria Formation is 524 ± 3Ma (Zimmermann, et al., 2015). Total of four samples were collected and to identify the differences and similarities of the provenance signals of these clastic sedimentary rocks, we apply optical petrography and whole-rock geochemistry, detrital zircon age. The results indicate that: All four lithotypes point to different possible maximum depositional age ranging from 549 Ma to 581 Ma with 32 Ma in difference and even more when comparing to the previous study (Zimmermann, et al., 2015). Although the rocks are supposed to be deposited in the same tectonic event, all samples fail to provide any younger depositional age than around 560 Ma. The detrital zircon population seem to differ between arenites and quartz-arenites where the latter see to reflect a more complete population. Therefore, studies with detrital zircon populations should be treated with great caution before being interpreted in stratigraphic context. Even with the large variety of different lithofacies sampled in this study it could not reflect the real Paleozoic depositional age, with an error of about 10 %. For the maximum depositional age determination, the base of the Herrería Formation would be the most ideal one studied, but not when trying to gain the entire provenance. I would argue for only using detrital zircon data with a detailed sedimentological background in addition to a known geological substructure.

Content

1. Introduction

This study focuses on the top of the Herreria Formation which is located in the Cantabrian Zone in northern Spain (Figure 1) within the province of Castilla y León in the northern part of Spain, close to the town Los Barrios de Luna (Figure 5). The top of the Herrería Formation is an ideal study object as the outcrop is well exposed, where the Formation has an accurate constrained age dated by paleontological material (Moczydowska, 1991 Vidal, et al., 1999), and which makes it an ideal candidate for the determination of the maximum depositional age. Another reason for selecting the Herrería Formation is due to lack of metamorphism and the domination of sandstones which are well dated and well understood in terms of the major source areas (Vidal, et al., 1999; Zimmermann, et al., 2015). The Herrería Formation represents individual lithofacies, which are well defined by different types of clastic sediments and sedimentary structures produced by hydrodynamic parameters within varying depositional environments. Previous attempts to U-Pb zircon date these rocks have yielded interesting results, which does not coincide with the provenance in this region (Zimmermann, et al., 2015). In many cases when determining the maximum depositional age, samples for detrital zircon dating are taken as a single rock sample. By mixing different lithofacies sorting effects could be decreased, as within specific facies, (e.g. fluvial or alluvial) those are affecting heavy mineral composition and therefore the possibility of interpretation of detrital zircon dating using U-Pb isotopes (DeGraaff-Surpless, et al., 2002; Garzanti, et al., 2010; Zimmermann, et al., 2015). Significant differences of the maximum depositional age in the different lithofacies would question the validity of interpretation in articles where the sorting effects based on different facies has not been recognized (Zimmermann, et al., 2019). This would lead to a massive re-evaluation process in many already published articles. The main objective of this thesis is to unravel significant differences in the maximum depositional ages by sampling four identified, individual lithofacies of the Herrería Formation and comparing the data to one mixed sample from the same outcrop. By performing U-Pb zircon dating, combined with petrography and whole-rock geochemical analysis, we will unravel subtle to large variations between the individual lithofacies.

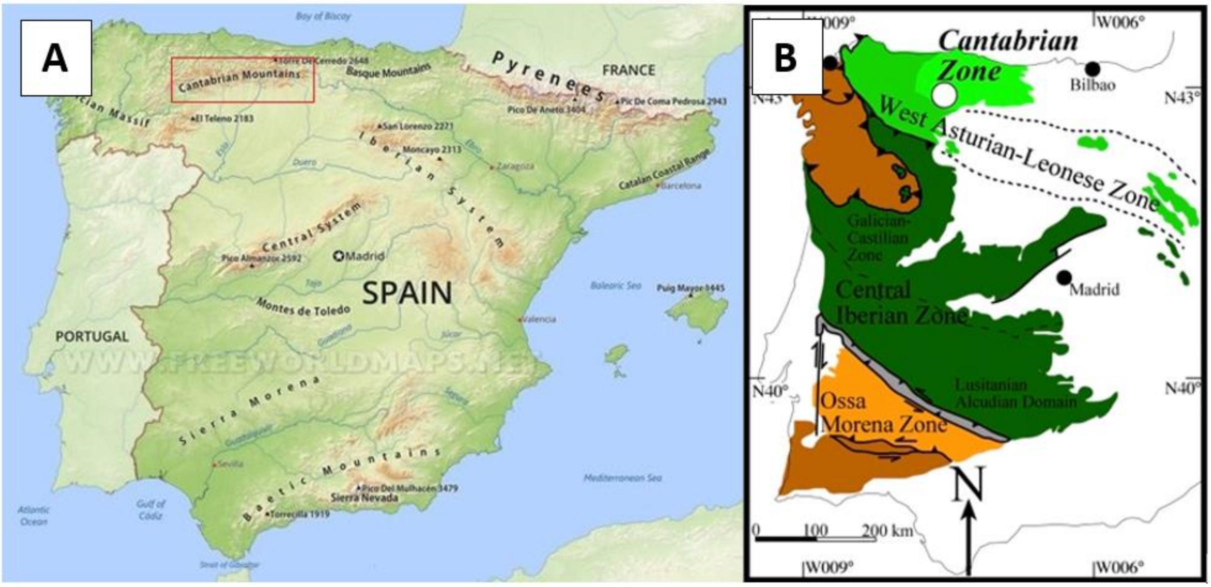

Figure 1 Map over the studied area in the northern part of Spain(A, Feher,), in the Cantabrian mountains within the Cantabrian zone (B, López-Guijarro, et al., 2008).

2. Geology

The area of interest is located in northern Spain within the Variscan nappe system of the Cantabrian Mountains within the Cantabrian zone (Figure 2 ;Linan, et al., 2002).

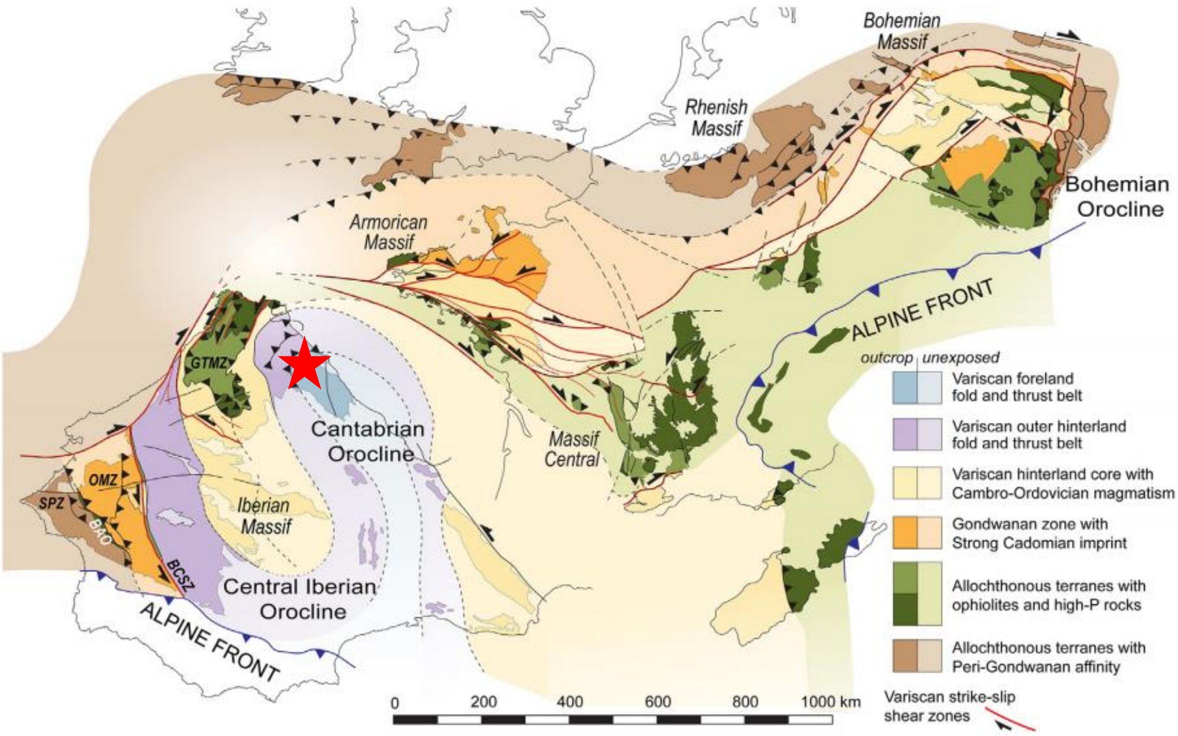

Figure 2 Tectonostratigraphic map of the Western European Variscan belt. Study area is marked by a red star. (Martínez Catalán, et al., 2007; Shaw, et al., 2012)

The oldest rock formation of the area is called the Mora Formation (Zimmermann, et al., 2015). These meta-turbidites are of Ediacaran age (Naidoo, et al., 2017) and lie underneath the Herrería Formation, separated by a regional unconformity defined by a conglomerate layer (Ábalos, et al., 2012;Ugidos, et al., 2010) which last for not more than 30 My (Zimmermann, et al., 2015; Naidoo, et al., 2017).

The Mora Formation is a part of the Narcea Group with an age from the Ediacaran to the Lowermost Cambrian (Valladares, et al., 2002). The Mora Formation was a part of the Iberian plate during deposition and was located in an active continental margin (Naidoo, et al., 2017). During the Cadomian Orogeny there was a series of tectonic events in the late Neoproterozoic (650 – 550 Ma) along the active margin of Gondwana involving numerous terranes (Figure 3). Based on the sedimentary structures and large-scale turbiditic shale sequences (Marcos, 1973) the Mora Formation has been interpreted as a deep-sea fan deposit. The Upper part of the Mora Formation consists of meta-greywackes with a maximum depositional age of 565 ± 11 Ma and reflects magmatism at this active margin (Naidoo, et al., 2017). The boundary separating the Mora Formation and the Herrería Formation contain the fossils *Rusophycus avalonensis* and *Treptichnus (Phycodes) pedum* indicating a depositional age of 530 Ma (Vidal, et al., 1999) which is confirmed by detrital zircon ages from the same exposure (524 Ma; Zimmermann, et al., 2015). The Herrería Formation can be divided into three members (Aramburu, et al., 1992), where the here studied part represents the top of Member 2 and shows the transition to Member 3, the youngest (Figure 4). With its conformable and transitional contact to the overlying Láncara Formation, the top of the Herrería Formation is younger than Atdabanian in age (517 – 521 Ma) according to microfossil stratigraphy (Moczydowska, 1991).

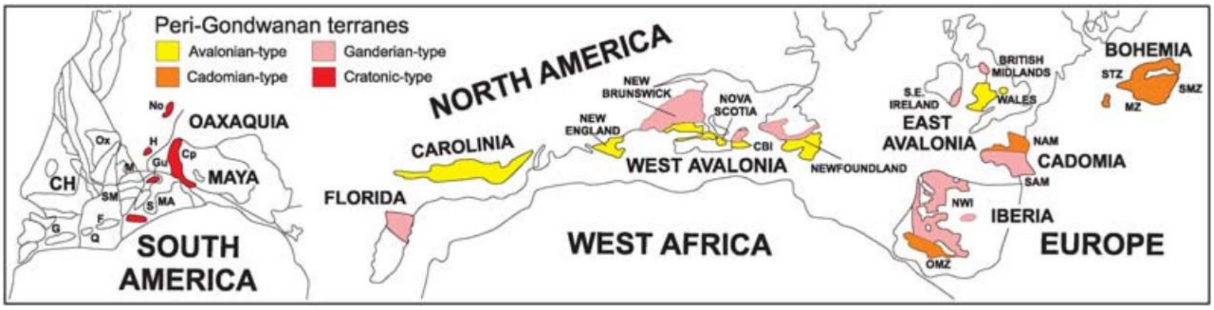

Figure 3 The location of the peri-Gondwanan terranes during the Early Mesozoic (Nance, et al., 2008)

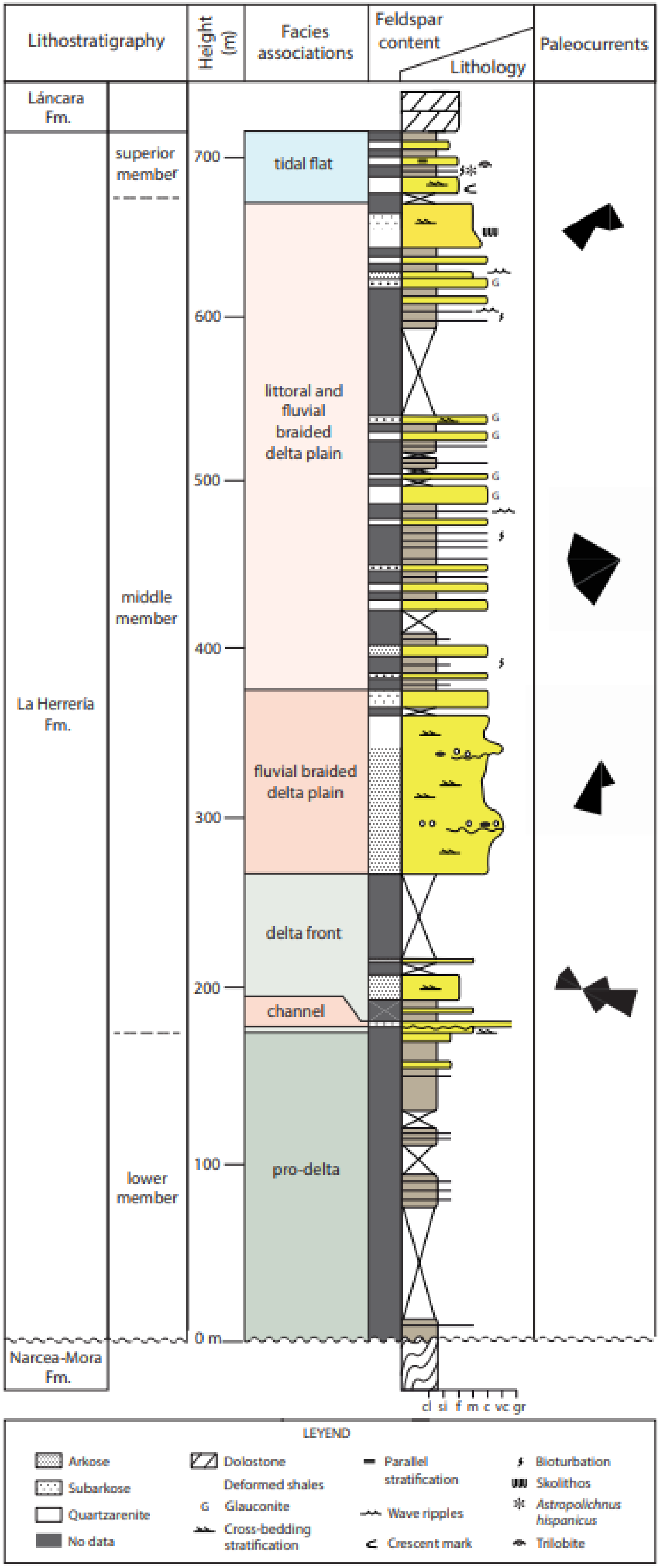

Figure 4 Stratigraphy of the 3 divided Members from the Herrería Formation(after Flórez, et al., 2017).

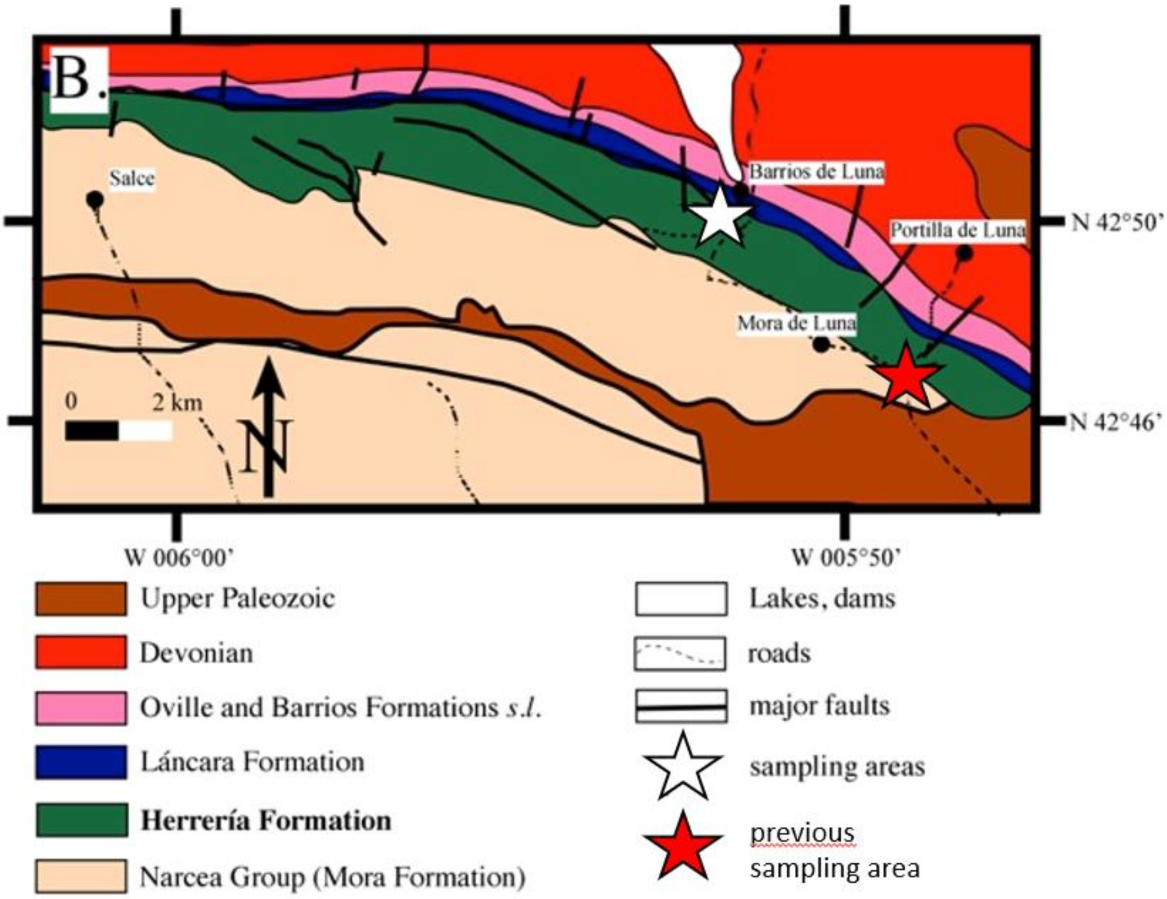

Figure 5 Overview of the sampled area for this study, showing previous sampling in addition (Rodríguez Fernández, 1984; Martín Parra, 1989)

During the deposition of the Herrería Formation extension was dominating the tectonic setting and subduction processes ceased (Zimmermann, et al., 2015). The Cantabrian zone was a part of the Peri-Gondwanan terranes which were located along the northern margin of Gondwana. Located on the Ganderian-type terrane, the Herrería Formation had been deposited during the slow rift northwards away from the northern Gondwanan margin resulting in the opening of the Rheic ocean during Late Cambrian-Early Ordovician time (Figure 6) (Brendan Murphy, et al., 2010; Nance, et al., 2008) including the overlying Láncara, Oville and Barrios Formations as representing a passive or rifted margin affected by sea level changes. The overall thickness of the Herrería Formation is around 800 m deposited during 13 My with a sedimentary rate of 61,5 m/1 My if unconformities are absent, which is improbable considering the interpretation of a rift-related succession (Zimmermann, et al., 2015; Vidal, et al., 1999; Fischer, 1969). In the study area, the formation is mostly covered by overgrowth and regolith but well exposed along road cuts for example between Mallo de Luna and Los Barrios de Luna close to Río Luna.

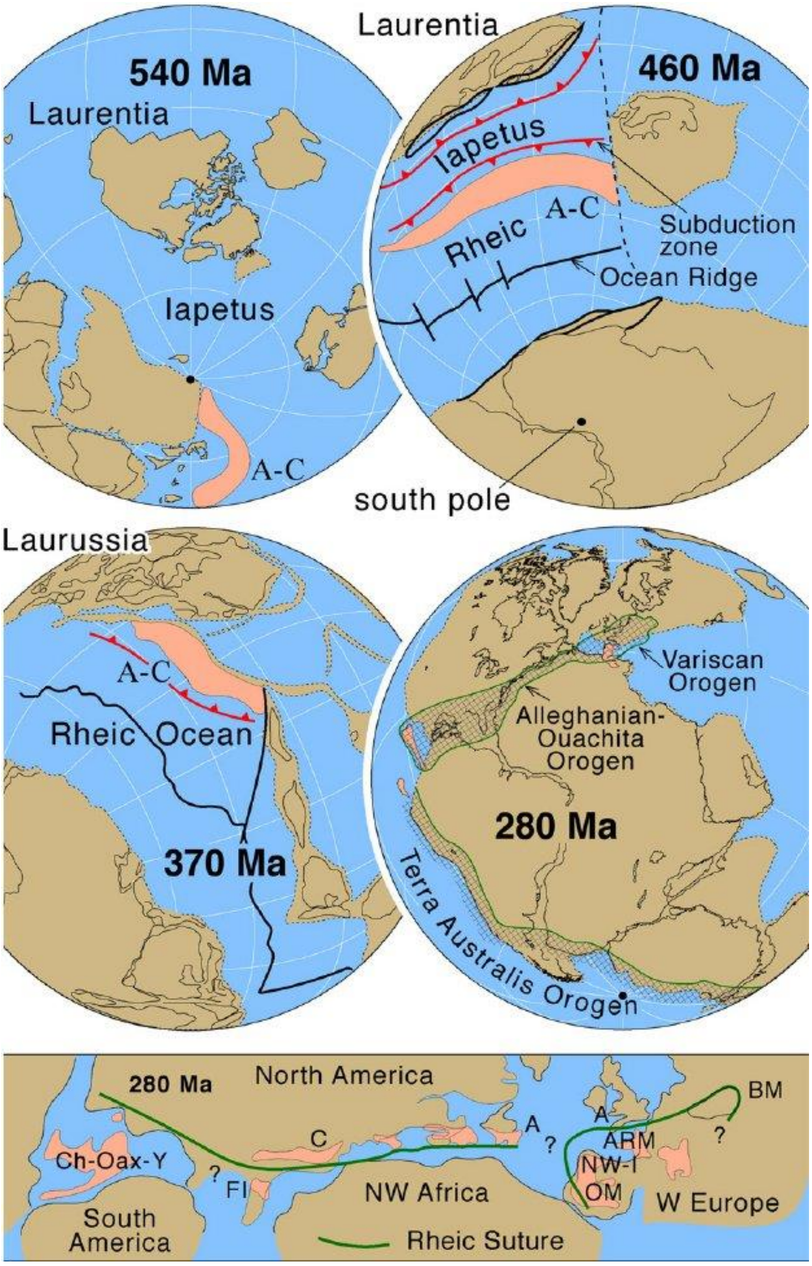

Figure 6 The reconstruction of the position of the peri-Gondwanan terranes along the northern margin of Gondwana, the opening of the Rheic ocean and closing of the Iapetus.(after Stampfli and Borel, 2002)

Sedimentology of the sampled section

The subject of sampling is the well exposed Herrería Formation as well as the transition to the Láncara Formation. Sampling and methodology as well as new data for these layers are described below. A total of four samples were taken as shown in Figure 7. The profile starts with sample CB (Figure 8A), a thick layer of cross-bedded quartz-arenite interpreted to be deposited in shallow-marine environment reflecting large sandbars on a platform. These are followed by the cast-rich layer FM (‘flute-marks’, although the marks are groove marks) which point to a beach environment where tidal effects and strong water flow affected the sand deposition (Figure 8B). Those are followed stratigraphically up by several thick sandstone packages with no clear thinning and thickening upwards. These facies represent steady deposition of sand fed by larger supply systems possibly at the mouth of a delta. These beds lead to the very hard cross-bedded coarser-grained bed: CG2 (Figure 9A). The facies for this bed is interpreted as a minute sea-level rise with a higher degree of sorting, resulting in more effective compaction during lithification. This very hard arenite is covered by the bed CG1 (Figure 9B), which is exceptional as it is highly friable compared to all occurring arenites in the section. The rock seemed to be affected by being exposed to oxygen and allowed the oxygenation of iron-rich minerals (see chapter 4.1 Petrography) together with a remarkable large-scale cross bedding (see Figure 7 above the yellow cross within the same bed). Then the transition to the Láncara Formation is marked by thin shales and a sudden income of carbonates followed by a thick block of dolomitic ooids.

Figure 7 The sampled section in the Herrería Formation.

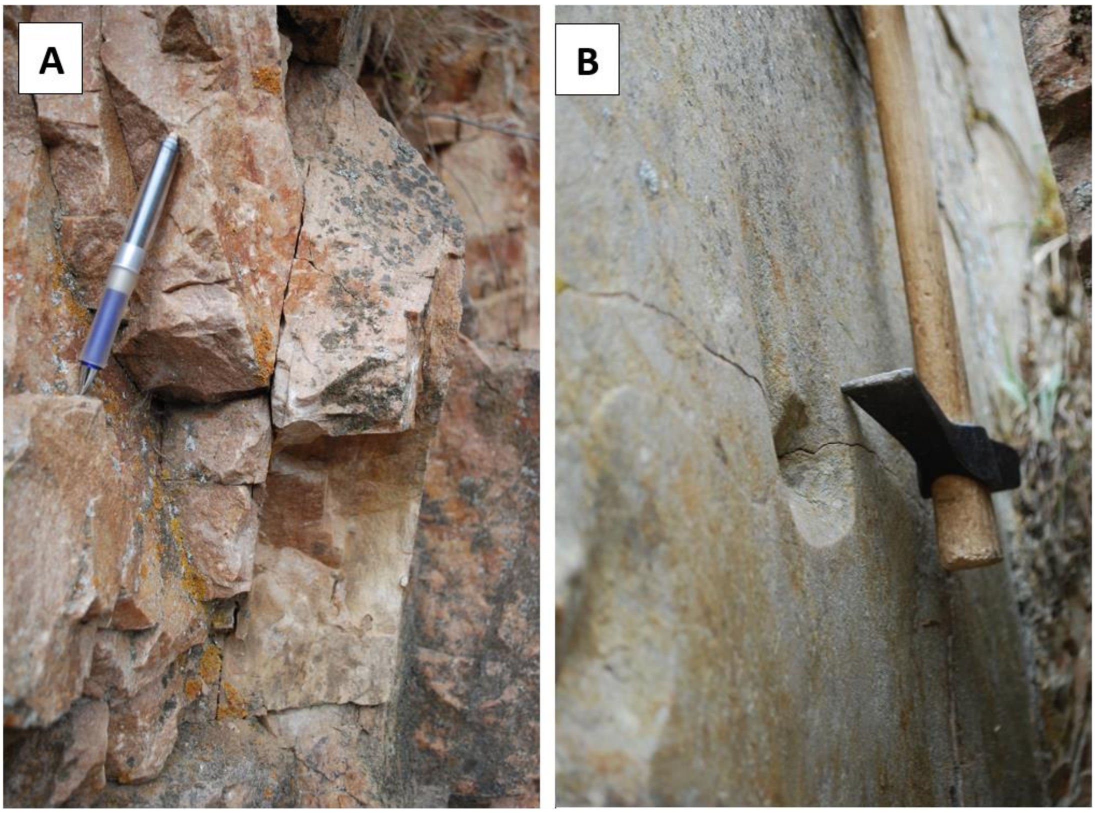

Figure 8 A – Sample CB, B – Sample FM

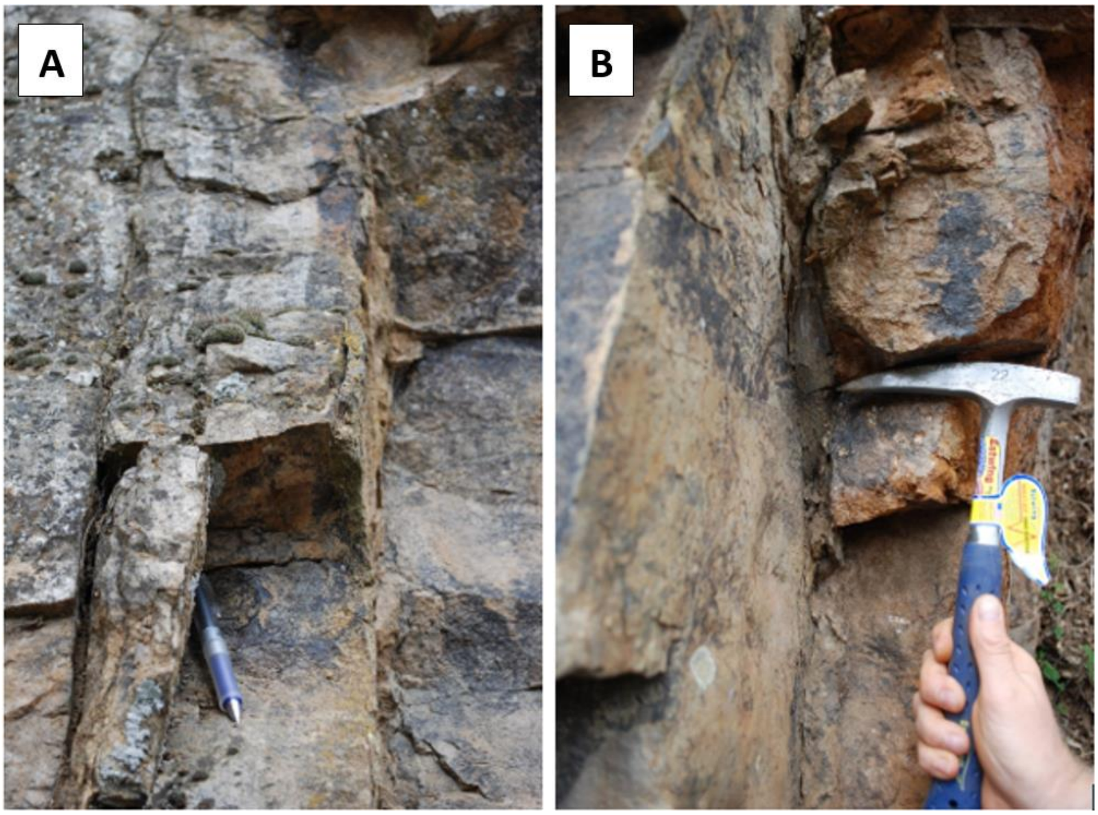

Figure 9 A – Sample CG2, B – Sample CG1

3. Methodology

3.1 Fieldwork

The sampling was done at the top of Herrería Formation along a 10 m stratigraphy, where four different facies of quartz dominated arenites were collected. The selection criteria for sampling for study of the abundance of specific aged detrital zircons was the obvious variation in sedimentary structures in the field. The quartz dominated arenites are intercalated with very thin layers of shales which lack any carbonate material. The recognition of acritarchs argues for a marine environment, the abundance of flute marks in the lowermost layer of the section indicates sub-aqueous deposition, most probably sub-marine. Samples will be analyzed using optical petrography, whole-rock chemistry, U-Pb detrital zircon analysis.

3.2 Petrography

Preparation

First step to prepare for petrography is to craft thin sections of the four lithotypes, using a frosted glass which is polished for a flat and even surface. The samples must be cut into sizes around 2 cm by 4 cm and then sliced further parallel. The sample is then polished using 340 to 1000 grid silicon carbide powder on glass plates for a smoother surface. With both the glass and rock samples prepared the sample is glued on the glass plate. The samples are then further sliced and polished until the minerals show the correct birefringence under a common optical microscope.

3.3 Optical Petrography

A Zeiss polarized light microscope is then used to analyze the thin section, with both plane and double-polarized light. The identification of minerals is mainly based on extinction, birefringence, cleavages and shape.

3.3 Geochemical analysis

Preparation and analysis

All 23 samples were milled with a weight between 70 and 80 grams each in the Retch Vibratory Disc Mill machine with an agate of 100 ml. Approximately 12 grams of each prepared sample were sent to ACME Laboratory in Canada where geochemical analysis were completed.

The milled samples were analyzed by ICP-MS at Acme laboratory in Vancouver, Canada. Details for the analytical method and processing can be found at http://acmelab.com and in

Minde, et al., 2018. Although 23 samples were analyzed through whole-rock geochemistry analysis, only four samples are mentioned under the results chapter. All samples are included in the discussion chapter.

3.4 U-Pb isotopes of detrital zircon grains

Preparation

Heavy minerals of all four samples were separated as routinely crushed carefully with a jawbreaker, sieved and separated with heavy liquids (bromoform and diiodomethane) according to common procedures. The zircons were then separated using the Frantz magnetic separation techniques with 10° full scale, non-magnetic and density > 2.95 g/cm³.

Approximately 200 zircon grains were randomly and nonrandomly mounted, ensuring that all grain sizes and geometric shapes were covered for each sample. The zircons were then mounted on 1- inch epoxy mounts with a fine polish to reveal the center of the zircon grains. The zircon mounts were then analyzed with cathodoluminescence in a Zeiss Supra 35VP field emission gun scanning electron microscope (SEM)

U-Pb Analysis

A selection of approximately 150 detrital zircons were U-Pb analyzed at the Department of Geosciences in the University of Oslo using a Nu Plasma HR multi-collector ICP-MS equipped with a Cetac LSX-G2 and laser microprobe (with HelEx cell). The masses 204, 206 and 207 were all measured in ion counters and the mass 238 was measured in a Faraday cup by using the U-Pb collector block of the Nu Plasma instrument. By using 238/235U=137,88 the 235U was estimated from measured 238U. Reference zircons used for calibrating isotope fractionations were GJ-1 (609 ±1 Ma, Jackson, et al., 2004, 91500 (1065 ±1 Ma, Wiedenbeck, et al., 1995) and A382 (1876 ± 2 Ma, Huhma, et al., 2012). The Plešovice (337 Ma, Sláma, et al., 2008) ran as an unknown at regular intervals. The data reduction was done following Rosa, et al., 2008 reduction protocols by using an interactive spreadsheet based on Excel 2003/Visual Basic. The U-Pb was plotted and the ages were calculated using Isoplot 4.15 (Ludwig, 2003). The reproducibility of this method is within c. 1 – 2 %. During the U-Pb isotope analysis a 40 µm beam diameter with a 10 Hz pulse was used with a focused laser beam in aperture mode to produce circular ablation pits. Reference zircons used for calibrating isotope fractionations were GJ-03, GJ-04, A382-04 and A382-05. As concordant are U-Pb isotope values classified if they fall in the window of 90 to 105 % discordance from the Concordia (Stacey and Kramers, 1975) and the data have been corrected for common lead with 206Pb/204Pb N 1000.

4. Results

4.1 Petrography

Optical petrography

The oldest sample CB is very poorly sorted with the largest grains ranging from 0,25 mm – 2 mm, the grains are rounded to well-rounded within the secondary cementation (Figure 10) and has high sphericity. As it is quartz-arenite it contains mostly of quartz with only accessory muscovite, biotite and few feldspar (e.g., plagioclase and microcline). The rock has only around 5 % of matrix and is dominated by a well-developed quartz cementation rimming the quartz grains.

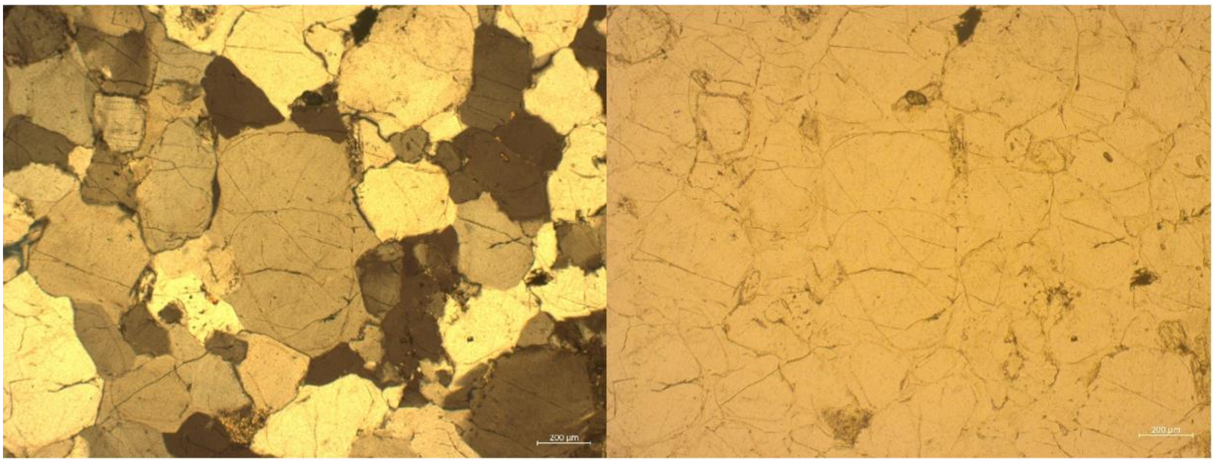

Figure 10 Secondary cementation in sample CB.

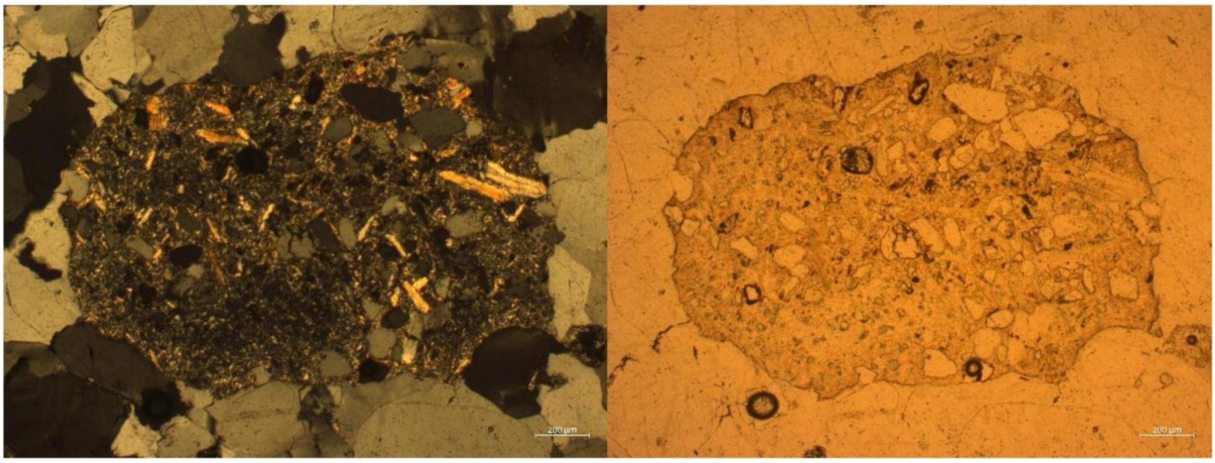

Figure 11 Lithoclast from Mora Formtaion found in sample CB.

Sample FM is poorly to moderately sorted with smaller grains than CB ranging from 0,125 mm – 0,5 mm, mostly around 0,25 mm. The grains are subangular to subrounded and the sphericity is low. The texture of the sample is remarkable as most of the grains are parallel aligned and may be a reflection of the high energy regime of these facies (Figure 12). The bed consists mainly of quartz, with only few grains of plagioclase and muscovite. The rock has a higher amount of matrix around 20% compared to the other samples (Figure 13).

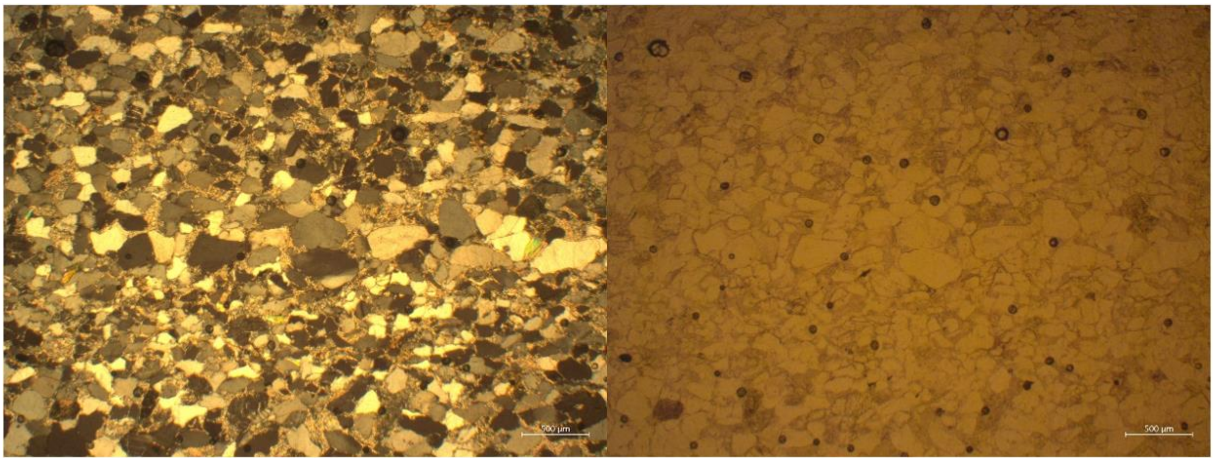

Figure 12 Alignment in sample FM.

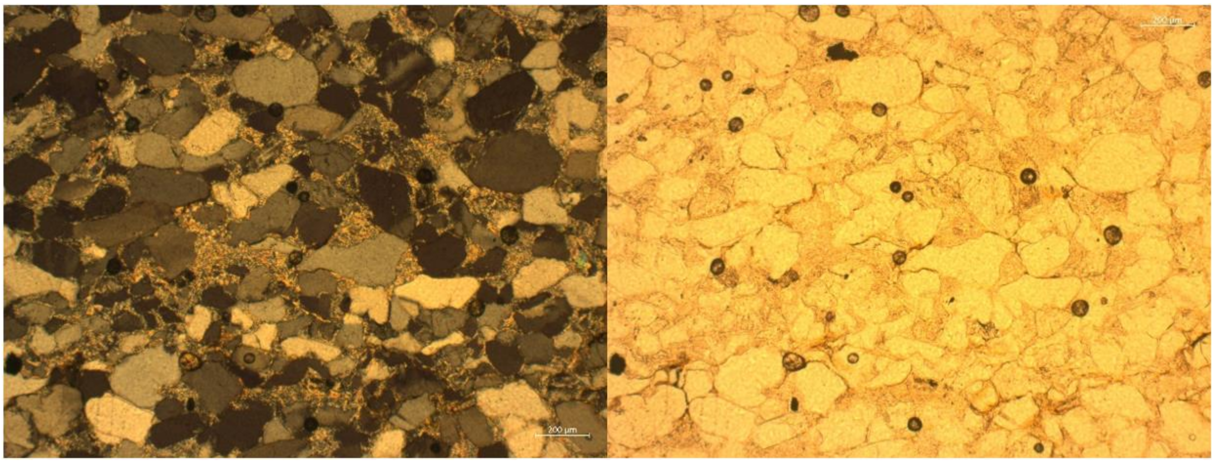

Figure 13 Around 20% matrix in sample FM.

Sample CG2 is poorly sorted with grains ranging from 0,05 mm to 1 mm. The sorting of grains is totally different from the other samples with either big (0.25 mm – 1 mm) or small grains (0.05 mm – 0,150 mm). The biggest grains are well rounded with low sphericity and the smallest ones are angular with low sphericity (Figure 16). This sample has around 5 – 10 % mica-rich matrix and a few small zircons (Figure 15 and 17). This is a very hard rock which might be due to compaction, figure 14 shows mica which is deformed which might be due to high compaction and therefore heavier sediments?

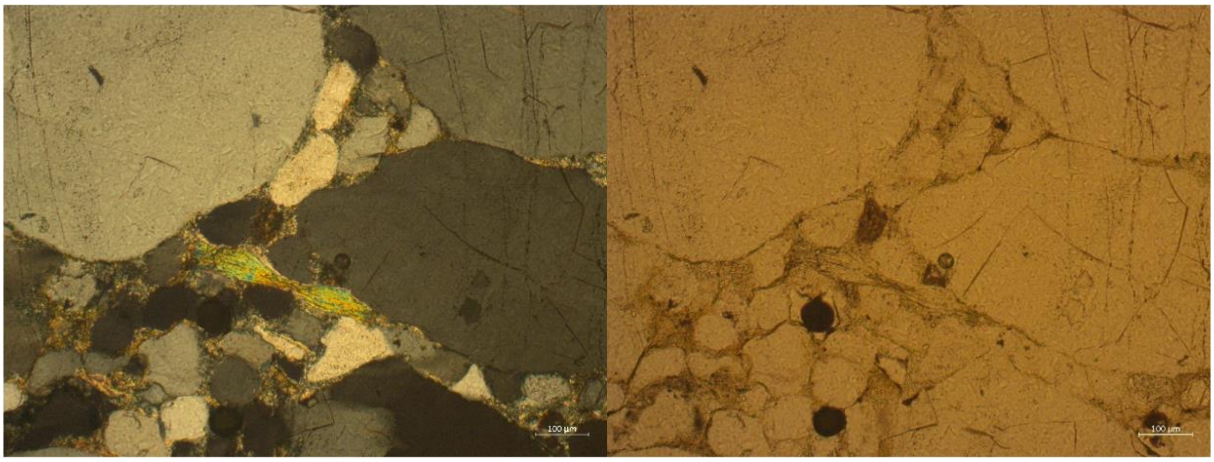

Figure 14 Mica deformed by compaction in sample CG2.

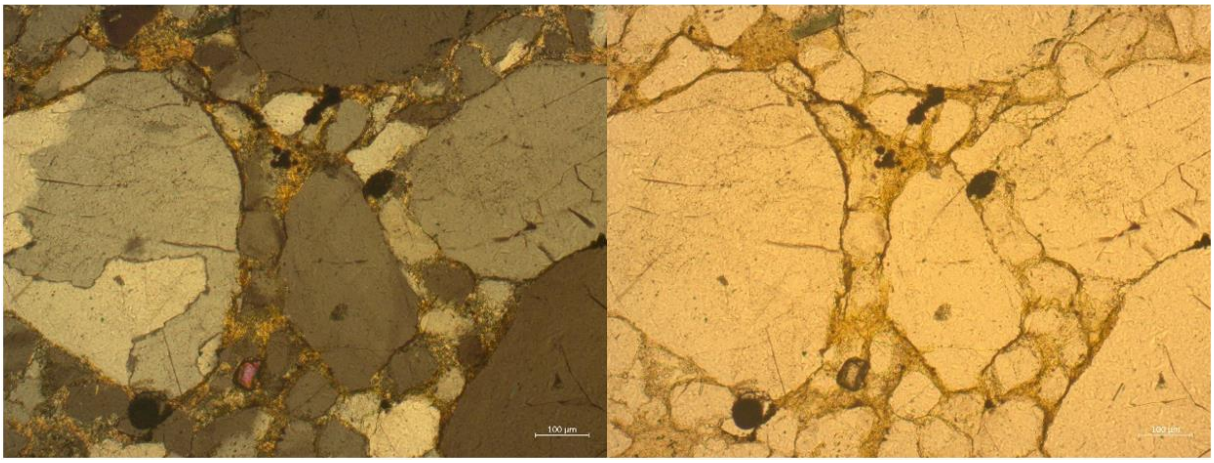

Figure 15 Zircon found in sample CG2.

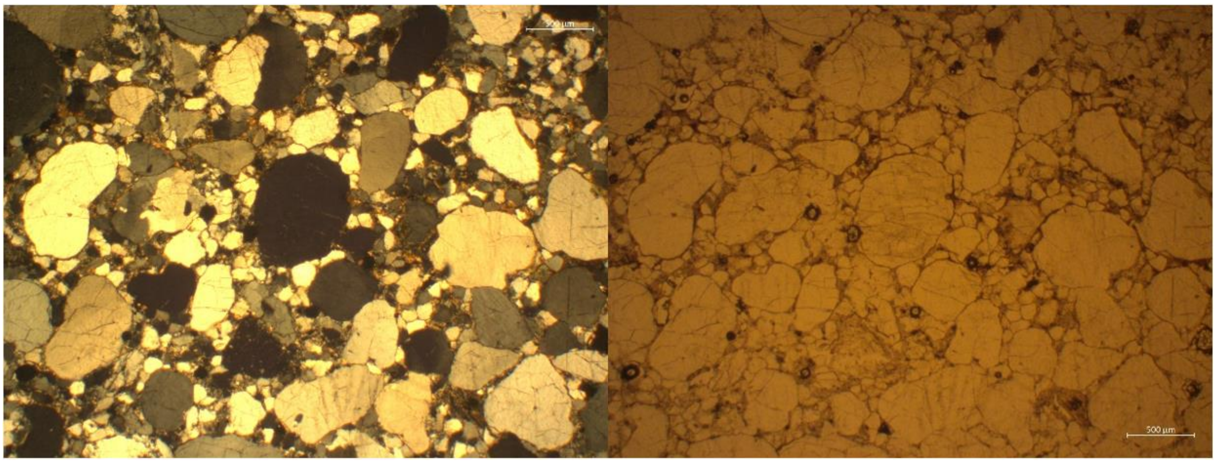

Figure 16 Overview of sample CG2

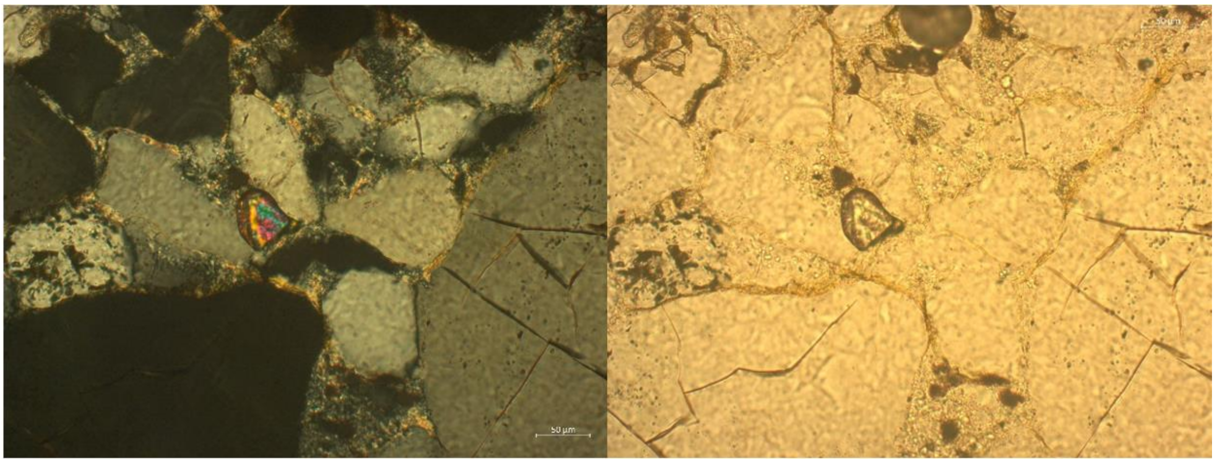

Figure 17 Zircon found in sample CG2.

The highly friable sample CG1 is very moderately to well sorted with big size variation 0,25 mm – 0,5 mm, mostly 0,5 mm (Figure X). The grains are subangular to subrounded with a lot of iron overgrowth seen with a strong reddish color in the thin section (Figure 18, 19, 20 and 21). Matrix is almost non existing in this sample with maybe 1 – 2 %.

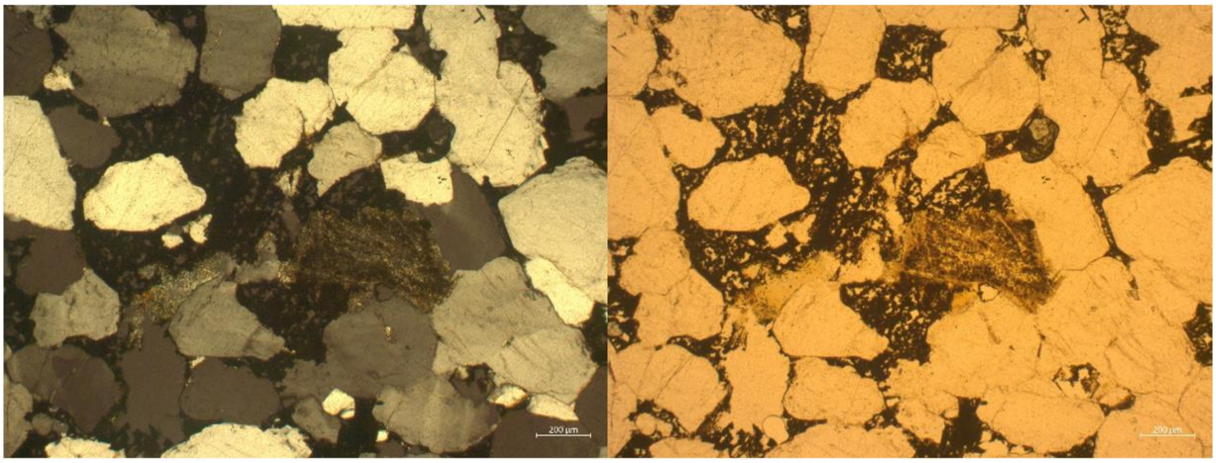

Figure 18 Overgrowth of iron in sample CG1.

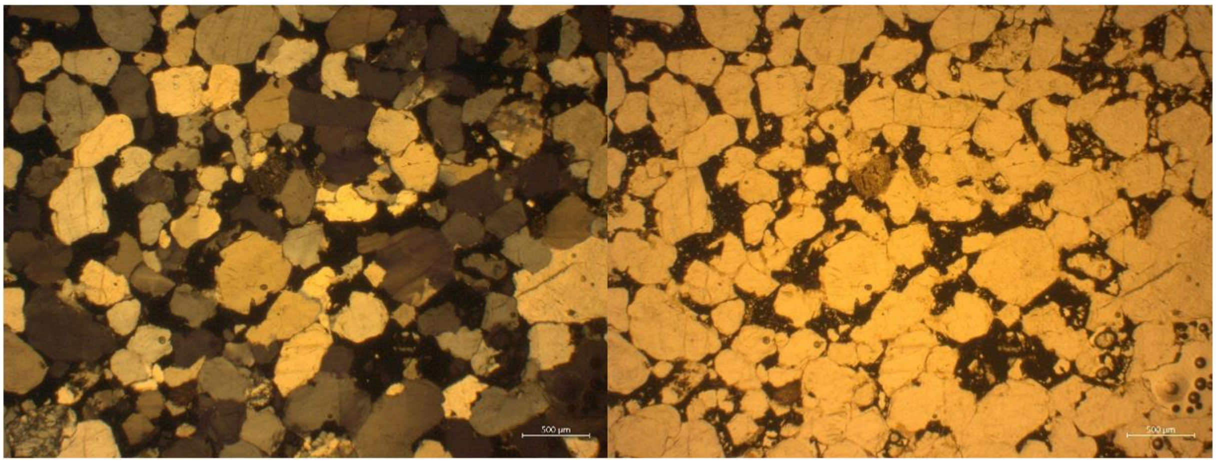

Figure 19 Overgrowth of iron in sample CG1.

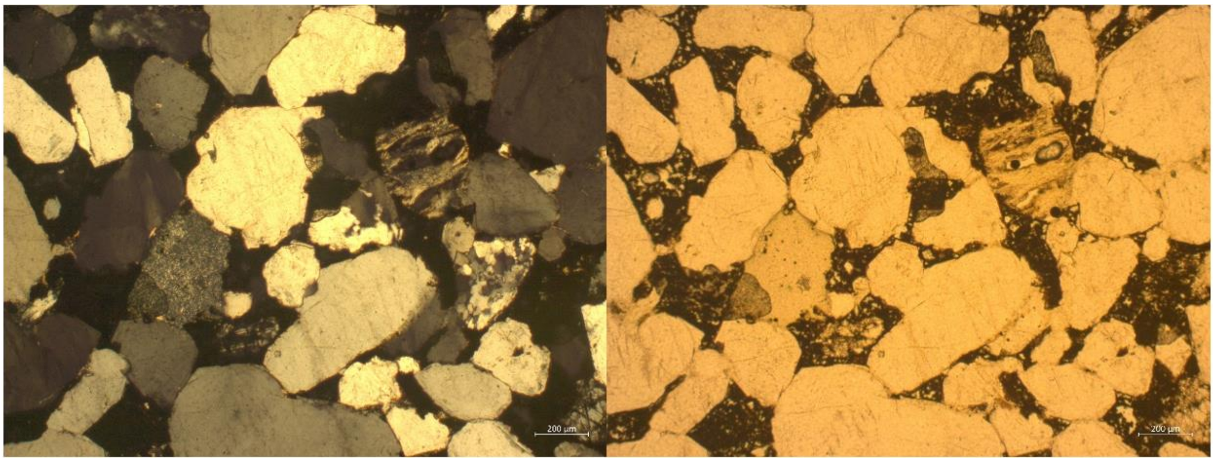

Figure 20 Overgrowth of iron in sample CG1.

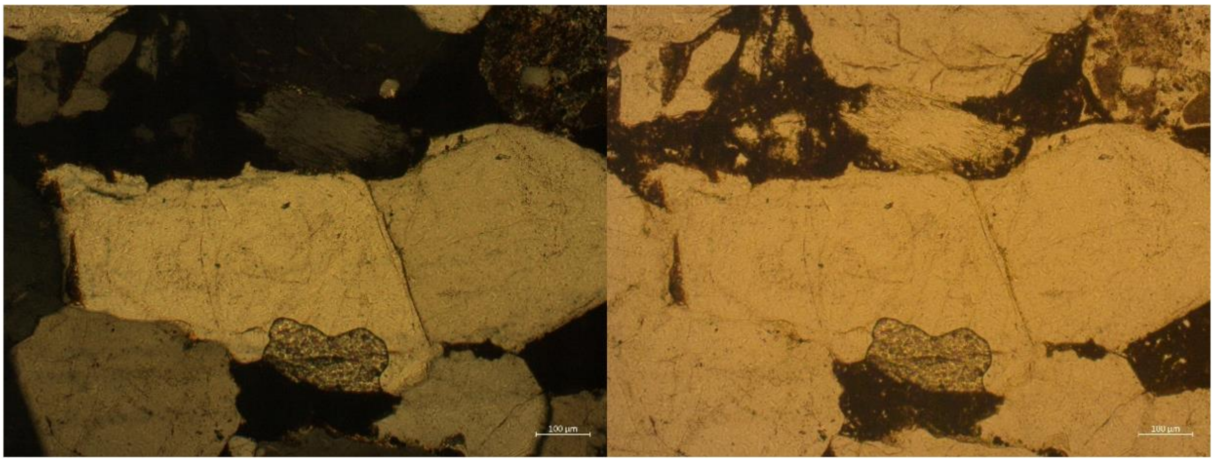

Figure 21 Overgrowth of iron in sample CG1.

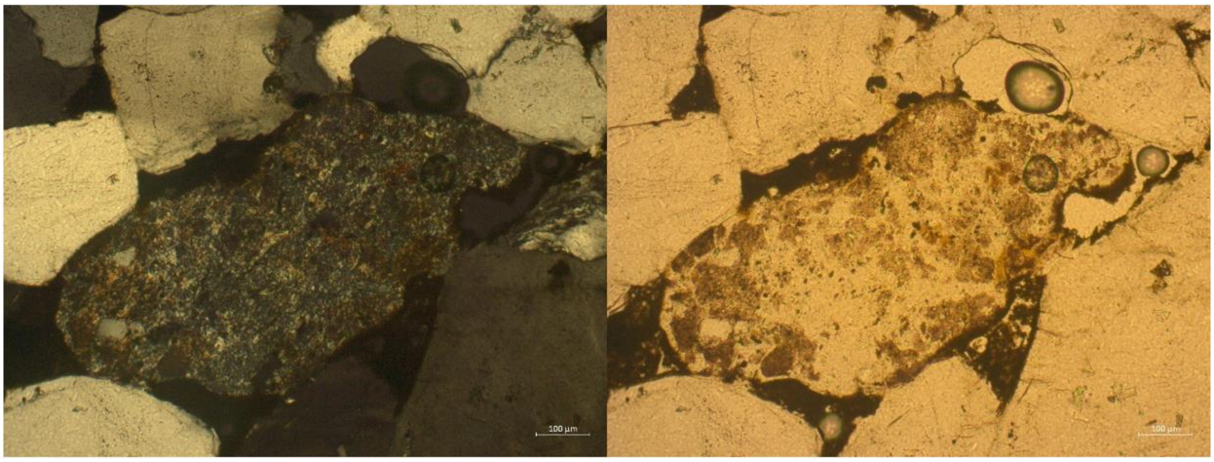

Figure 22 Lithoclast in sample CG1

4.2 Whole rock geochemical composition
Major-element composition

The oldest sample CB has the highest content of SiO_2 with a value of 95,42 wt% (weight percent), whereas the lowest value of 79,94 wt% is seen in the overlaying sample FM. The other samples are ranging from 91,88 wt% to 95,25 wt%. Sample FM has the highest content of Al_2O_3 with a value of 11,45 wt% while the other samples have values 2,26 wt% or lower. FM has also the highest value of K_2O at 4,56 wt% where the other samples range between 0,29 wt% to 0,93 wt%. The youngest samples CG1.1 and CG1.2 have the highest value of Fe_2O_3 compared to the other samples with values below 1,08 wt%. All the samples have extremely low values of CaO, Na_2O and TiO_2 (Appendix 8.1, Table 2)

The rare earth elements

The ΣREE (sum of rare earth elements) of the four samples are from bottom to top:

CB: 46,9 ppm

FM: 155,52 ppm

CG2: 30,8 ppm

CG1: 61,9 ppm and 63,8 ppm

This confirms the petrography reflecting the amount of non-quartz minerals in the samples. The relatively high amount of ΣREE within the sample FM reflects the amount of clay minerals as the main carrier of REE. This is close to typical upper continental crust composition (after Taylor and McLennan, 1985) with 183 ppm and allows to speculate about a different source component. The most friable sample CG1 is rather affected by oxidized iron-minerals and is a typical quartz-arenite. This amount of iron is, besides one sample which is, an arenite (see Appendix 8.1, Table 2) unique.

Trace-element composition

All of the samples within table X reveal that not only the major and minor elements are strongly depleted with a few exceptions but also most of the trace elements La, Sc, Zr, Th and Ti, which are the provenance indicators (according Floyd and Leveridge, 1987; Bhatia and Crook, 1986; Taylor and McLennan, 1985). Therefore, the ratios and absolute amounts are difficult to interpret as mostly the element concentrations are very close to the detection limits (e.g. Zimmermann and Spalletti, 2009). As seen in appendix 8.1 in table 1 by using Zr/Sc ratio as a tool for recycling effects most of the samples are obviously recycled but as often seen in quartz-arenites the values may have been expected to be higher (Zimmermann and Spalletti, 2009). Nevertheless, the high friable sample CG1 (CG1.1 and CG1.2) show less higher values compared to the other samples.

4.3 U-Pb isotope determination in detrital zircons

Overview cathodoluminescence (CL) images of the detrital zircons are given in appendix 8.3 were also a complete data tables of the isotopic determinations can be found with an organized table with the grains from young to old and discordant grains at the bottom.

Grains from sample CB vary between 100 and 200 µm containing mostly sizes around 100 µm and are subrounded to rounded. Most of the grains are transparent and mostly without a zoned core. A total of 175 grains were analyzed (Appendix 8.2, Table 7-10 for compilation), of which 119 are concordant according to the given criteria (chapter 3.4, methodology). The youngest concordant age 581 Ma ± 7 Ma (sub-rounded shape, 100 µm; Figure 10A) while the first cluster of 3 or more detrital zircons reflects a rough average age of 587 Ma. The major clusters of ages are listed from young to old: Cadomian – Early Neoproterozoic – Rodinia Formation – Late Paleoproterozoic – Early Archean and few older grains than 2,8 Ga with the oldest 3312 Ma ± 21 Ma.

Grains from sample FM vary between 50 and 200 µm with mostly sizes 100 µm and are subrounded to rounded. Most of the grains are transparent and mostly well zoned. A total of 150 grains were analyzed (Appendix 8.2, Table 17-18 for compilation) of which 125 are concordant according to the given criteria. The youngest concordant age is 549 Ma ± 6 Ma (rounded shape, 100 µm; Figure 10C) while the first cluster of 3 or more detrital zircons reflects an rough average age of 585 Ma. Major cluster of ages are from younger to old: Cadomian – Early Neoproterozoic – Rodinia Formation – Late Paleoproterozoic – Early Archean but none older than 2,8 Ga with the oldest one 2685 Ma ± 39 Ma.

Grains from sample CG2 vary between 100 and 200 µm but the most abundant size is at 100 µm and are subangular to subrounded. Most of the grains are transparent and broken without a zoned core. A total of 150 grains were analyzed (Appendix 8.2, Table 14-16 for compilation), of which 92 are concordant according to the given criteria. The youngest concordant age is 550 Ma ± 12 Ma (elongated and angular in shape, broken, 100 µm; Figure 10E) while the first cluster of 3 or more detrital zircons reflects on a rough average of 568 Ma. The major clusters of ages are from young to old: Cadomian – few Early Neoproterozoic – Rodinia Formation – Late Paleoproterozoic – Early Archean and none older than 2,8 Ga with the oldest one 2766 Ma ± 10 Ma.

Zircon grain sizes from sample CG1 vary between 100 and 200 µm but the most abundant size is at 200 µm and are subrounded to rounded. Most of the grains are transparent and broken without a zoned core. A total of 150 grains were analyzed (Appendix 8.2, Table 11-13 compilation), of which 129 are concordant according to the given criteria. The youngest concordant age is 566 Ma ± 6 Ma (rounded shape, 200 µm; Figure 10G) while the first cluster of 3 or more detrital zircons reflects on a rough average of 569 Ma. The major clusters of ages are from young to old: Cadomian – few Early Neoproterozoic – Late Paleoproterozoic – Early Archean and none older than 2,8 Ga with the oldest one 2662 Ma ± 14 Ma.

Conclusively, all the samples in this study cover the major provenance or source regions as expected as determined by various authors (e.g. Zimmermann, et al., 2015; Naidoo, et al., 2017). But only one of the samples, the one in Zimmermann, et al., 2015 (HE3) could catch the syn-sedimentary rift magmatism during the lower Cambrian and in all other sources the Cadomian orogeny represents the youngest source cluster.

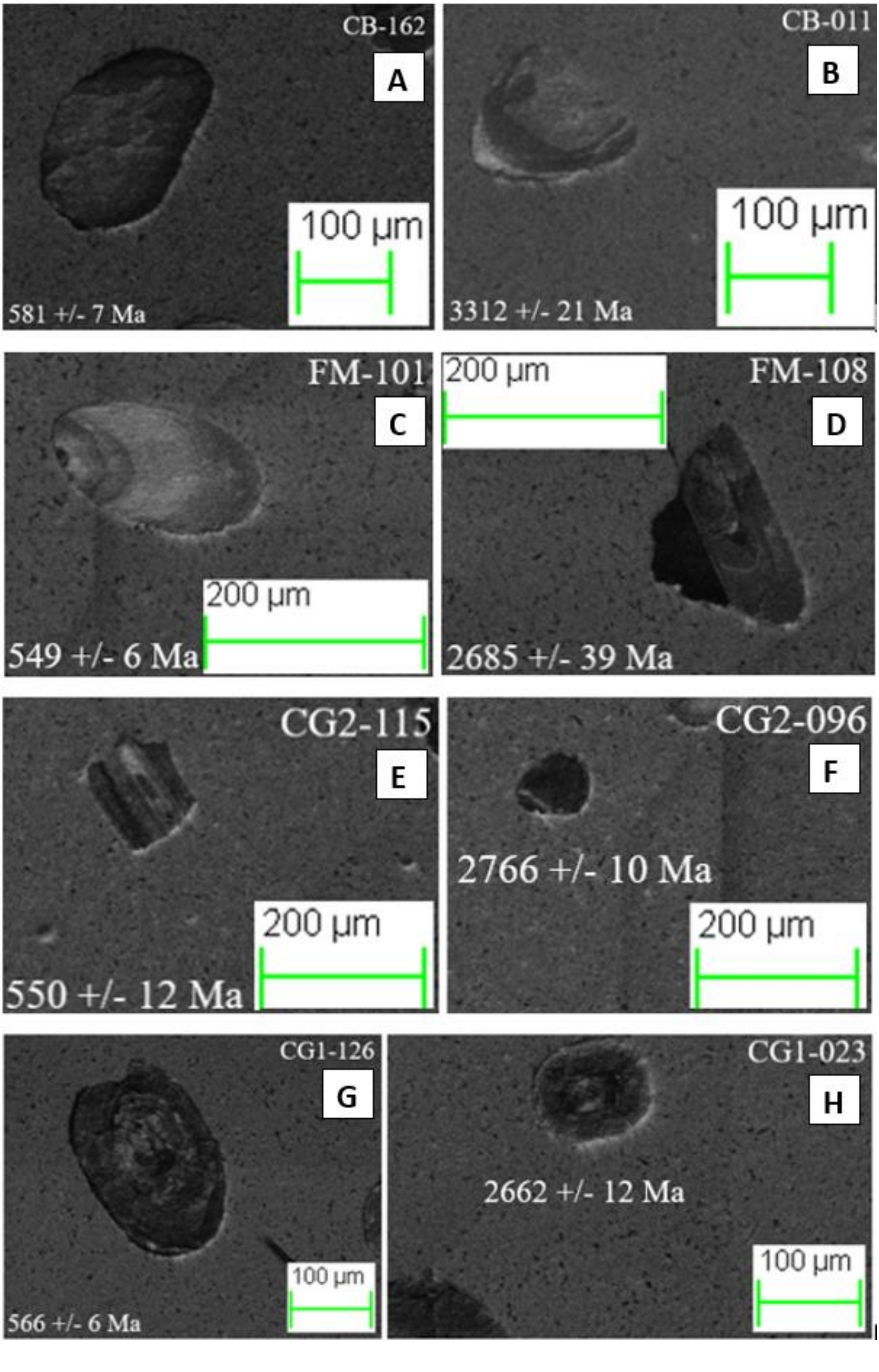

Figure 23 A – Youngest zircon in sample CB, B – Oldest zircon in sample CB, C – Youngest zircon in sample FM, D – Oldest zircon in sample FM, E – Youngest zircon in sample CG2, F – Oldest zircon in sample CG2, G – Youngest zircon in sample CG1, H – Oldest zircon in sample CG1.

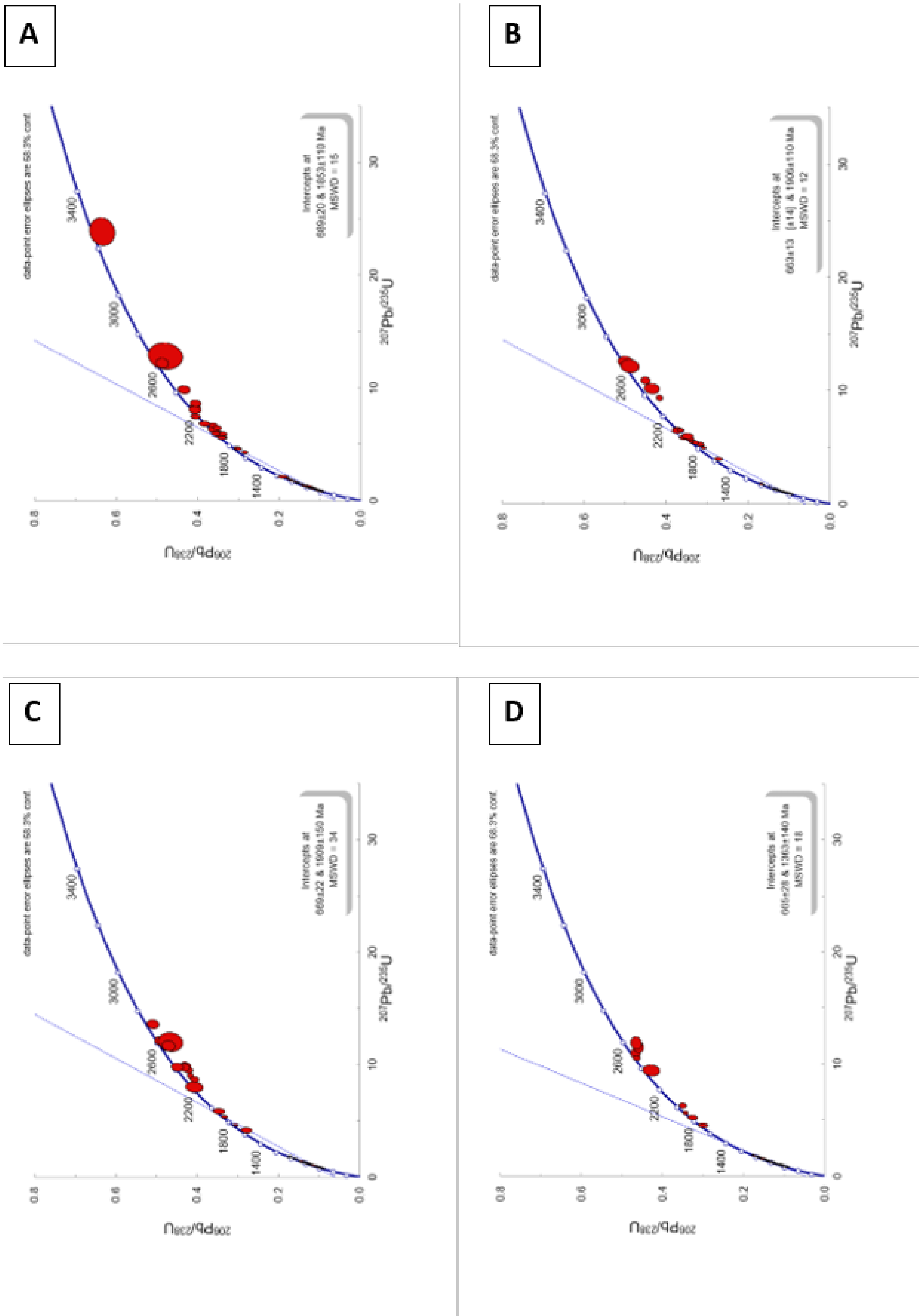

Figure 24 Concordia plot for all the samples. A – CB, B – CG1, C – CG2, D – FM

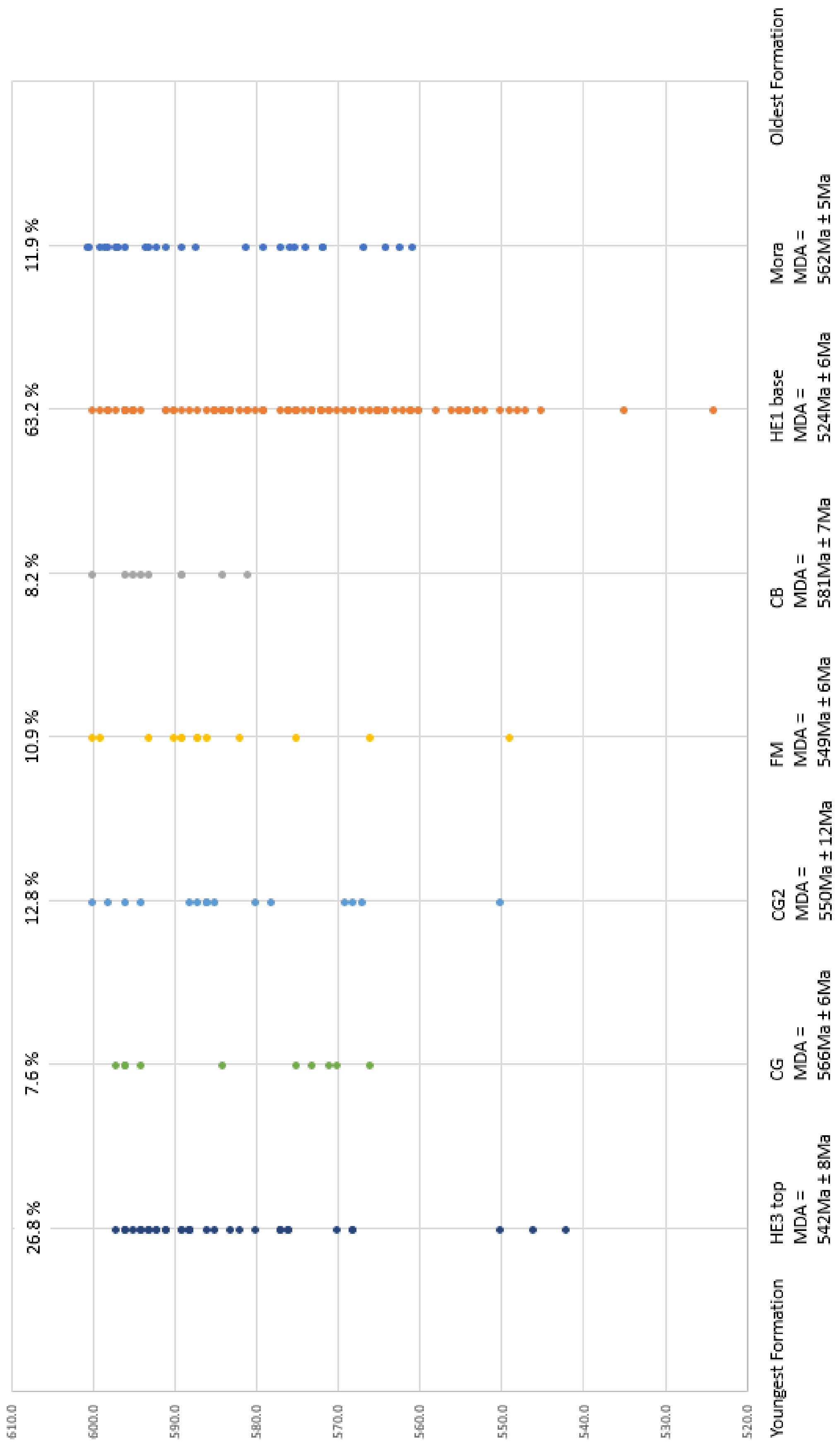

Figure 25 The youngest cluster of detrital zircons from the ages 520 - 600 Ma

5. Discussion

The Herrería Formation consists of four different types of clastic rocks: shales, carbonate-rich arenites, arenites and quartz-arenites. All the lithotypes are well distributed at the top of the formation except for the carbonate-rich arenites which are only abundant at the base of the formation. This exposure at Barrios de Luna has been sampled from the top part. Here, four different lithofacies have been targeted for detrital zircon dating in combination with geochemical and petrography analysis to study differences: CB, FM, CG2, CG1.

The petrography shows differences in grain sizes, especially the sample FM with much smaller grains compared to the other samples (0,125 mm – 0,5 mm, mostly around 0,25 mm). The grains in FM are parallel aligned which indicates a higher energy rate, not observed within the other samples. This can explain the sediment transport marks in this section. Matrix content is only evident within FM, and the only common connection the samples have is that they are quartz-rich, which may point to a quartz-rich precursor. The grains in the samples are all poor to moderately sorted.

The geochemical data shows that the samples are relatively similar except for FM, which has much less SiO_2 than the others classifying it an arenite (70% versus > 90% respectively). The other samples are definitely quartz-arenites due to the high content of SiO_2 with values over 90%. Another difference is found in the friable sample CG1 which contains higher amount of Fe_2O_3, besides that it is geochemically very similar to the other quartz-arenites. CG1 and CG2 have lower Zr/Sc ratios and may point to a less effective sorting. As observed in the petrography analysis, FM contains a higher amount of clays and may possibly reflect a second source of sediment which has not been sorted.

The major elements of the typical quartz-rich rocks within Herreria Formation are mostly depleted. Previous studies show that the base is starting with a conglomerate with a larger variation existing in iron and titanium abundances (Appendix 8.1, Table 2; Zimmermann, et al., 2015). Carbonate is also found in some of the layers which some are affected by higher CaO abundance. The trace elements in this part are relatively similar in its abundance except for Zr and Hf.

The middle part of the formation (HE2; Zimmermann, et al., 2015) with its thick quartz-arenite dominated layers does not differ from the main trend at the base or the top (HE1, HE3) (Appendix 8.2, Table 1-6).

The top of the Herreria Formation is by far more heterogeneous, which represents the transition to the dolomites of the Láncara Formation. At the exposure at Barrios de Luna the base of the top starts with the extreme hard quartz-arenites which are depleted for almost every element (Appendix 8.2, Table 1-6). The sample CB is one of these lithofacies, devoid of Na_2O but containing some few mica and alkali feldspar.

The next overlying layers are less quartz-rich and containing some K_2O and few iron-rich grains. TiO_2 is slightly enriched compared to other major and minor elements. It is a thick sequence of layers abundant with sediment transport marks (HE12, 16, 18 and FM, Appendix 8.2, Table 1-6). The totals of REE (rare earth elements) are relatively high compared to the quartz-arenites and reflects specific heavy minerals enriched in REE like apatite or even monazite.

The thick cross-bedded typical quartz-arenite (CG2) is comparable with the middle part (HE2) of the Herreria Formation but in comparison slightly enriched in REE, Th, Al_2O_3 and K_2. This might be due to some alkali feldspar or few clay mineral. The sample CG1 with the high amount of iron-oxides has a high value of REE compared to CG2, this may point to a depletion of feldspar and using Al_2O_3 for clay-minerals or sericite as K_2O are as low as in CG2. None of the key elements for specific heavy minerals are enriched, like P_2O_5 for phosphates (monazite and apatite), Zr and Hf (for zircon), Cr (for chromite) or TiO2 (for rutile) or higher amounts of heavy minerals.

All four samples show differences from the U-Pb data collected, Cadomian ages are dominating in sample FM, CG2 and CG1 with much lower value in the oldest layer CB. There is high number of zircons from the Lower Neoproterozoic from all samples except for the youngest highly friable iron rich CG1. All samples have a few zircons with Late Mesoproterozoic ages (1000 – 1200 Ma; from here on called Rodinia-related) except the youngest sample CG1 which is completely lacking zircons from this age frame. The Late Paleoproterozoic is dominated in the oldest and the youngest samples CB and CG1 with very few in the other ones. The sample CG2 has higher amount of the Early Paleoproterozoic and the Late Archean compared to the other samples. From this layer to the next overlying layer CG1 there is a shift from older to younger source. There is a trend observable reflecting a correlation between more quartz-rich the samples and more abundant older zircons: the least quartz-rich sample FM have very few older grains than of Neoproterozoic.

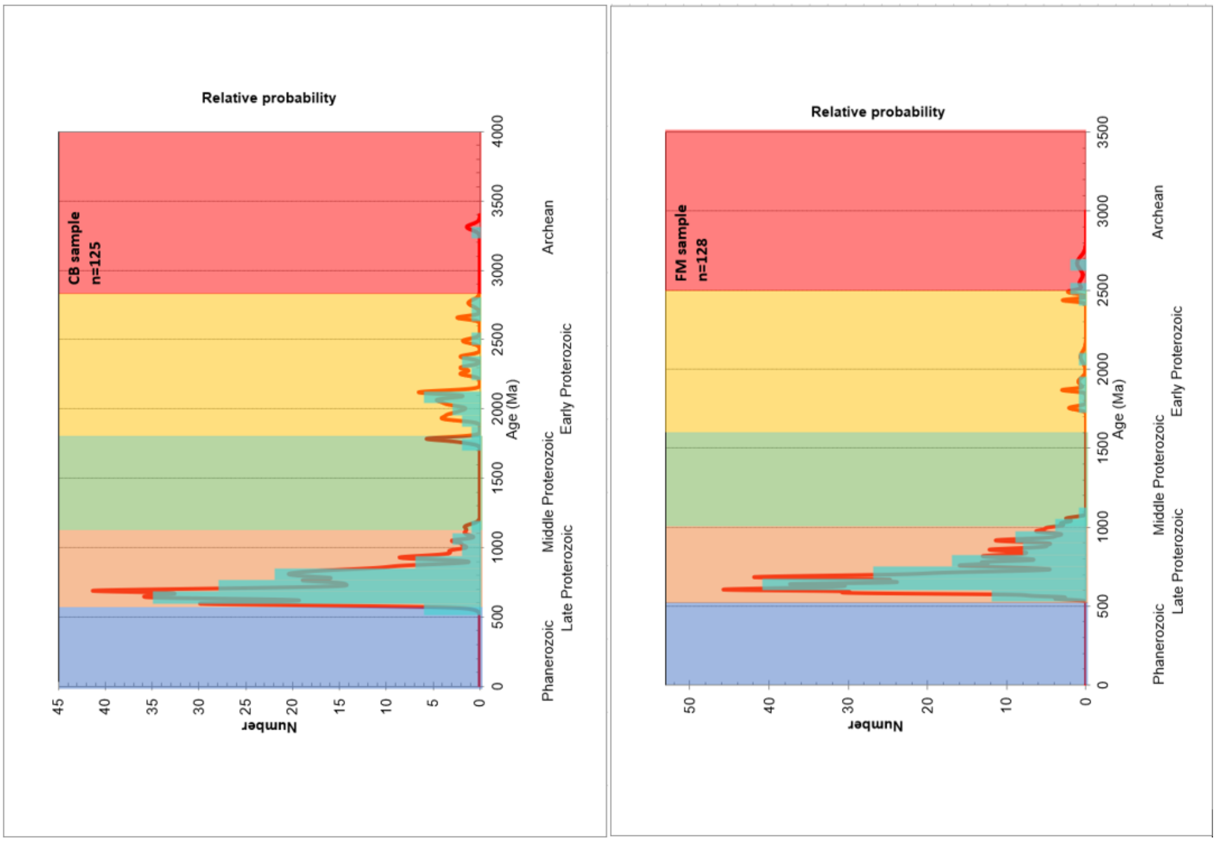

Figure 26 Relative probability plot of CB (left) and FM (right).

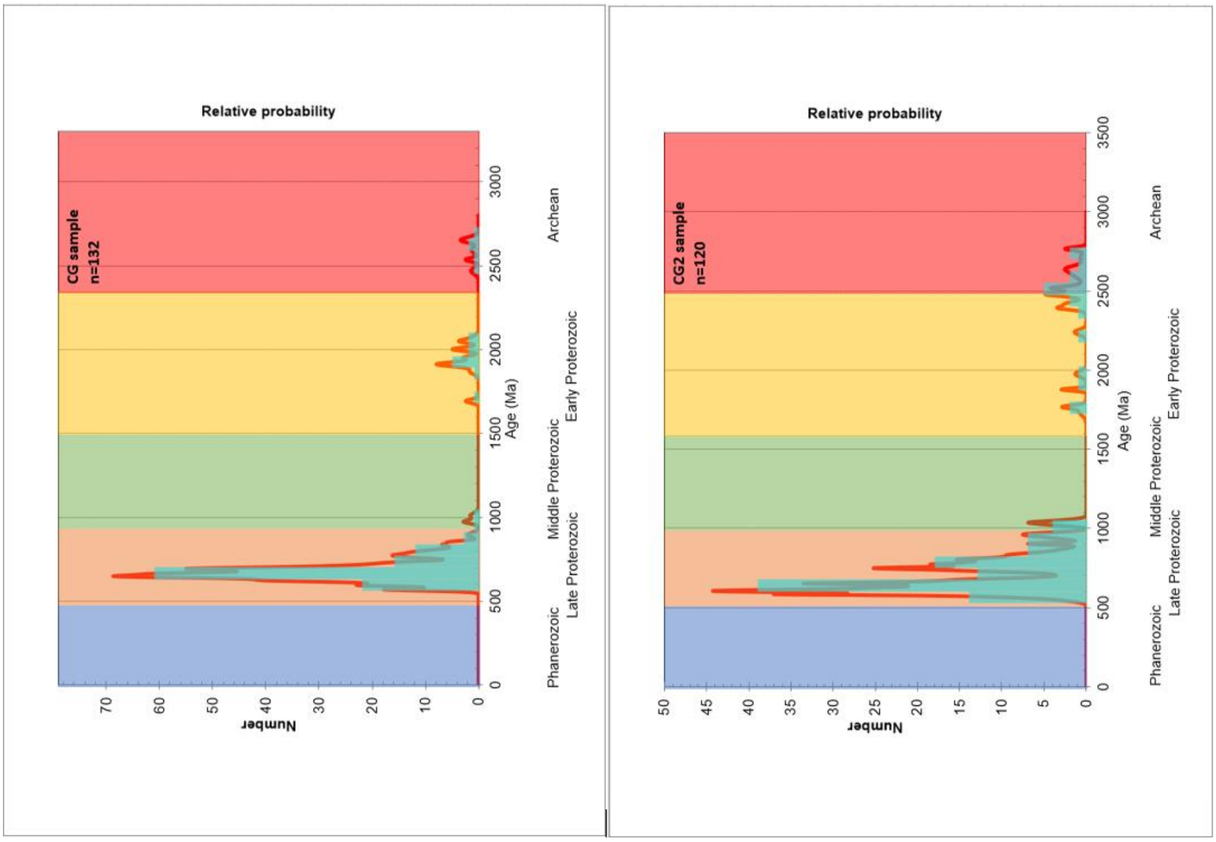

Figure 27 Relative probability plot of CG (left) and CG2 (right).

When comparing previous U-Pb zircon dating from the Herrería Formation (Zimmermann, et al., 2015) and Mora Formation (Naidoo, et al., 2017) to samples here discussed it reveals a difference. The published samples have been taken from the base (HE1) and the top (HE3) of the formation, mixing all the different lithofacies. These two samples are very different when comparing U-Pb data. The sample HE3 has a peak in the Middle to Early Paleoproterozoic (nearly 45%; Figure 28) where the sample HE1 only have few. The sample HE1 is dominated by detrital zircons from the Ediacaran age (nearly 80% of all dated grains; Figure 28). All of the samples collected in this study are collected in the same section as HE3. Sample CB is the most similar to HE3 for the Paleoproterozoic, although it is still missing that high peak from the Paleoproterozoic. None of the new samples have the high peak in the Paleoproterozoic like the HE3. Another distinct difference is seen in the Neoproterozoic ages which is dominating in all the samples CB, FM, CG1 and CG2 but very few in both HE1 and HE3. This detrital zircon age peak is actually more similar to the Mora Formation. Even with a more detailed sampling from the top of the Herrería Formation the peak of the Paleoproterozoic was not detected, as well as the youngest 524 ± 6 Ma detrital zircon and the youngest population around 525 Ma (Zimmermann et al, 2015) reflecting nearly the depositional age, found in the base HE1 is absent in the top layers. If only one sample would have been taken from the whole formation this would not represent the formation at all, like with the sample FM which is very different from the others. The high cluster of Early Paleoproterozoic age found in HE3 is still enigmatic and more research is needed to define which lithofacies layer it belongs to, and why it is only found in one specific layer.

On the other hand, since the maximum sedimentation age is often derived from the detrital zircon dating, caution should be taken when interpreting the results. In this situation the combined sample HE3 from Zimmermann, et al., 2015 points to a maximum depositional age of c. 550 Ma but the definite clustering of ages takes place in at c. 575 Ma (Figure 25). The youngest grains dated within the formation belongs to the base and reflects the biostratigraphic ages at 525 Ma. Samples CG1 and CG2 may point to an age at 570 Ma with only single zircons slightly younger but not pre-Ediacaran. There is not observed any clear clustering in sample FM but more detrital zircons occur with ages older than 580 Ma. The quartz-arenite CB shows a wide range of ages, but the oldest younger cluster is at 590 Ma. The last mentioned contains therefore an error of over 10 % for the maximum depositional age, while the base HE1 reflects the real age. These differences can be damaging within Paleozoic geology and shows that detrital zircons should only be used carefully when determining maximum depositional ages.

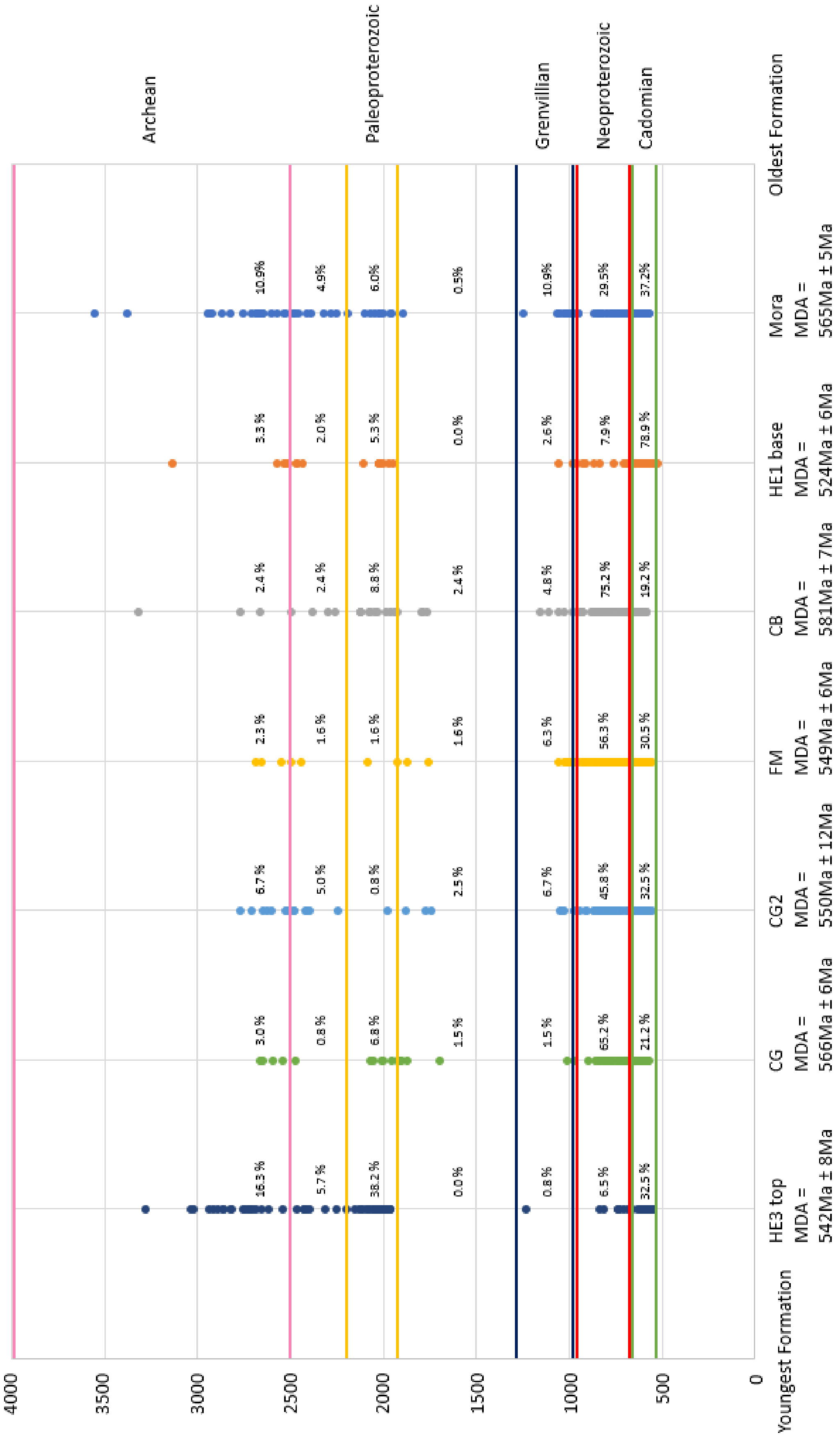

Figure 28 Overview of detrital zircon ages in Herrería and Mora Formations.

6. Conclusion

Four samples were collected from the Lower Cambrian Herrería Formation in the Cantabrian mountains in northern Spain. The samples were compared to each other as well to other studies from this formation. The previous studies show extremely different provenance interpretations when comparing the base (HE1) and top (HE3) of the actual formation. By sampling only from the top of the formation choosing very different lithofacies and then analyzing them with geochemistry, U-Pb zircons and petrography the purpose is to see if there are big differences. The main differences in the petrography part was the grainsizes, sorting and the amount of matrix seen in sample FM which might have been interpreted very differently compared to the other samples. Within the geochemical data it is also observed differences in the chemical composition, also in FM with only 79,94 % SiO_2 compared to the other samples with >90% classifying FM as an arenite and the other samples CB, CG2 and CG1 as quartz-arenites. The high value of Fe_2O_3 observed in sample CG1 is unusual for quartz-arenites but besides this it is similar to the other quartz-arenites.

When comparing these studied samples to the previous study from the of the Herrería Formation (Zimmermann, et al., 2015), there are differences in the U-Pb data collected. The youngest detrital zircon dated previously is from the base of the Herrería Formation at 524 Ma (HE1) while the youngest detrital zircons from this study range from 549 Ma to 581 Ma with the youngest found in sample FM. So none of the samples can provide a depositional age as young as HE1. Even from a larger variety of lithotypes within the formation could not reflect the real depositional age. The sample HE3 has a peak in the Middle to Early Paleoproterozoic (nearly 45%; Figure 28) where the sample HE1 only have few. The sample HE1 is dominated by detrital zircons from the Ediacaran age (nearly 80% of all dated grains; Figure 28). This is not observed in this study and there are also differences seen in the clusters of younger grains, where the biggest cluster of younger grains are actually found in the base of the formation (HE1, Figure 25).

These results show the importance of how you sample and analyze sedimentary rocks. These big differences could mean very different interpretations, as well the big differences found in the detrital zircon ages which is used to determine the maximum depositional age. The ideal sample area for the maximum depositional in this case would be the base of the Herrería Formation, however, would not represent the entire provenance. If only choosing one of these samples, it would mean very different interpretations in every level of the provenance study.

The importance of combining the detrital zircon data with a detailed sedimentological background and a known geological substructure should not be underestimated.

7. References

Ábalos, B., J.I. Gil Ibarguchi, M.E. Sánchez-Lorda, and J.L. Paquette. "African/Amazonian Proterozoic Correlations of Iberia: A Detrital Zircon U-Pb Study of Early Cambrian Conglomerates from the Sierra De La Demanda (Northern Spain)." *Tectonics* 31 (2012). http://dx.doi.org/10.1029/2011TC0030413.

Aramburu, C., J. Tryols, M. Arbizu, I. Méndez Bedia, I. Zamarreño, J.C. García Ramos, C. Suárez de Centi, and M. Valenzuela. "El Palaeozoico Inferior En La Zona Cantábrica. In: Gutiérrez Marco, J.C., Saavedra, J., Rábano, I. (Eds.)." *Palaeozoico Inferior de Ibero-America* (1992): 397-421.

Bhatia, M. R., and K. A. Crook. "Trace Element Characteristics of Graywackes and Tectonic

Setting Discrimination of Sedimentary Basins.". *Contributions to mineralogy and petrology* 92, no. 2 (1986): 181-93.

Brendan Murphy, J., J. Duncan Keppie, R. Damian Nance, and Jaroslav Dostal. "Comparative Evolution of the Iapetus and Rheic Oceans: A North America Perspective." *Gondwana Reasearch* 17 (2010): 482-99.

DeGraaff-Surpless, K., S.A. Graham, J.L. Wooden, and M.O. McWilliams. "Detrital Zircon Provenance Analysis of the Great Valley Group, California: Evolution of an Arc-Forearc System." *GSA Bulletin* 114(12) (2002): 1564-80. https://doi.org/10.1130/0016-7606(2002)114<1564:DZPAOT>2.0.CO;2.

Feher, D. "Spain Physical Map." https://www.freeworldmaps.net/europe/spain/map.html.

Fischer, A.G. "Geological Time-Distance Rates -- the Bubnoff Unit." *Geological Society of America Bulletin* 80 (1969): 549-51.

Flórez, A.G., C. Aramburu, and J.M. Toyos. "Stratigraphy and Sedimentology of the Cambrian Base (La Herrería Formation) in the Area of Los Barrios De Luna (N of Spain)." *European Geoscience Union General Assembly* (2017).

Floyd, P.A. , and B.E. Leveridge. "Tectonic Environment of the Devonian Gramscatho

Basin, South Cornwall: Framework Mode and Geochemical Evidence from Turbiditic

Sandstones.". *Journal of the Geological Society* 144, no. 4 (1987): 531-42.

Garzanti, E., S. Andò, C. France-Lanord, G. Vezzoli, P. Censi, V. Galy, and Y. Najman. "Mineralogical and Chemical Variability of Fluvial Sediments 1. Bedload Sand (Ganga-Brahmaputra, Bangladesh).". *Earth and Planetary Science Letters* 299 (2010): 368-81.

Huhma, H., I. Mänttäri, P. Peltonen, A. Kontinen, T. Halkoaho, E. Hanski, T. Hokkanen*, et al.* "The Age of the Archaen Greenstone Belts in Finland." *Geological Survey of Finland, Special Paper* 54 (2012): 74-175.

Jackson, S.E., N.J. Pearson, W.L. Griffin, and E.A. Belousova. "The Application of Laser Ablation-Inductively Coupled Plasma-Mass Spectrometry to in Situ U-Pb Zircon Geochronology." *Chemical Geology* 211 (2004): 47-69.

Linan, E., R. Gozalo, T. Palacios, Vintaned Gámez, J.A., J.M. Ugidos, and E. Mayoral. "Cambrian. In: Gibbons, W., Moreno, T. (Eds), the Geology of Spain.". *Geological Society of London* (2002): 17-29.

López-Guijarro, R., M. Armendáriz, C. Quesada, J. Fernándes-Suárez, J. Brendan Murphy, C. Pin, and F. Bellido. "Ediacaran-Paleozoic Evolution of the Ossa Morena and Central Iberian Zones (Sw Iberia) as Revealed by Sm-Nd Isotope Systematics.". *Tectonophysics* 461 (2008): 202-14.

Ludwig, K. "User's Manual for Isoplot 3.00 - a Geochronological Toolkit for Microsoft Excel. Geochronology Center, Berkeley, California." *Geochronology Center, Berkeley, California* (Special Publication 4) (2003).

Marcos, A. "Las Series Del Paleozoico Inferior Y La Estructura Herciniana Del Occidente De Asturias (Nw De Espana)." *Trab Geol* 6 (1973): 1-113.

Martín Parra, L.M. "Riello. Mapa Geologica De Espana. 1:50000." *ITGE* 128 (1989): 1-119.

Martínez Catalán, J.R., R. Arenas, F. Díaz García, P. González Cuadra, J. Gómez-Barreiro, J. Abati, P. Castiñeiras*, et al.* "Space and Time in the Tectonic Evolution of the Northwestern Iberian Massif: Implications for the Variscan Belt.". *Geological Society of America Memoirs* 200 (2007): 403-23.
Minde, M.W., W. Wenxia, M. V. Madland, U. Zimmermann, R.I. Korsnes, S.R.A. Bertolino, and P.Ø. Andersen. "Temperature Effects on Rock Engineering Properties and Rock-Fluid Chemistry in Opal-Ct-Bearing Chalk.". *Journal of Petroleum Science and Engineering* 169 (2018): 454-70.
Moczydowska, M. "Acritarch Biostratigraphy of the Lower Cambrian and the Precambrian–Cambrian Boundary in Southeastern Poland." *Fossils and Strata* 29 (1991): 1-127.
Naidoo, T., U. Zimmermann, J. Vervoort, and J. Tait. "Evidence of Early Archean Crust in Northwest Gondwana, from U– Pb and Hf Isotope Analysis of Detrital Zircon, in Ediacaran Surpacrustal Rocks of Northern Spain." *International Journal of Earth Science* 107 (2017): 409-29.
Nance, R. D., J. B. Murphy, R. A. Strachan, J. D. Keppie, G. Gutiérrez-Alonso, J. Fernándes-Suárez, C. Quesada*, et al.* "Neoproterozoic–Early Palaeozoic Tectonostratigraphy and Palaeogeography of the Peri-Gondwanan Terranes: Amazonian V. West African Connections." *Geological Society* 297 (2008): 345-83.
Rodríguez Fernández, L.A. "La Robla. Mapa Geologica De Espana, 1:50000." *IGME* 129 (1984): 1-98.
Rosa, D.R.N., A.A. Finch, and C.M.C. Inverno. "U-Pb Geochronology of Felsic Volcanic Rocks Hosted in the Gafo Formation, South Portuguese Zone: The Relationship with Iberian Pyrite Belt Magmatism.". *Mineralogical Magazine* 72 (2008): 1103-18.
Shaw, J., S.T. Johnston, G. Gutiérrez-Alonso, and A.B. Weil. "Oroclines of the Variscan Orogen of Iberia: Paleocurrent Analysis and Paleogeographic Implications." *Earth Planet. Sci. Lett.* (2012): 329-30, 60-70. http://dx.doi.org/10.1016/j.epsl.2012.02.014.
Sláma, J., J. Kosler, D.J. Condon, A. Gerdes, J.M. Hanchar, M.S.A. Horstwood, G. Morris*, et al.* "Plesovice Zircon - a New Natural Reference Material for U-Pb and Hf Isotopic Microanalysis." *Chemical Geology* 249(1-2) (2008): 1-35.
Stacey, J.S., and J.D. Kramers. "Approximation of Terrestrial Lead Isotope Evolution by a Two-Stage Model." *Earth and Planetary Science Letters* 26, no. 2 (1975): 207-21. https://doi.org/10.1016/0012-821X(75)90088-6.
Stampfli, G.M., and G.D. Borel. "A Plate Tectonic Model for the Paleozoic and Mesozoic Constrained by Dynamic Plate Boundaries and Restored Synthetic Oceanic Isochrones.". *Earth and Planetary Science Letters* 196 (2002): 17-33.
Taylor, S. R., and S. M. McLennan. "The Continental Crust: Its Composition and Evolution.". *Blackwell, Oxford* (1985).
Ugidos, J.M., J.M. Sánchez-Santos, P. Barba, and M.I. Valladares. "Upper Neoproterozoic Series in the Central Iberian, Cantabrian and West Asturian Leonese Zones (Spain): Geochemical Data and Statistical Results as Evidence for a Shared Homogenised Source Area." *Precambrian Research* 178, no. 1-4 (2010): 51-58.
Valladares, M.I., P. Barba, and J.M. Ugidos. "Precambrian. In: Gibbons, W., Moreno, T. (Eds.), the Geology of Spain.". *Geological Society of London* (2002): 9-16.
Vidal, G., T. Palacios, M. Moczydowska, and A. P. Gubanov. "Age Constraints from Small Shelly Fossils on the Early Cambrian Terminal Cadomian Phase in Iberia ". *Geologiska Föreningens i Stockholm Förhandlingar* 121, no. 2 (1999): 137-43.
Wiedenbeck, M., P. Allé, F. Corfu, W.L. Griffin, M. Meier, F. Oberli, A. Von Quadt, J.C. Roddick, and W. Spiegel. "Three Natural Zircon Standards for U-Th-Pb, Lu-Hf, Trace Element and Ree Analyses." *Geostandards newsletter* 19, no. 1 (1995): 1-23.
Zimmermann, U., T. Andersen, M. V. Madland, and I. S. Larsen. "The Role of U-Pb Ages of Detrital Zircons in Sedimentology-an Alarming Case Study for the Impact of Sampling for Provenance Interpretation.". *Sedimentary Geology* 320 (2015): 38-50.
Zimmermann, U., J. Dieset, L.J. Watson, and T. Lapen. "Sedimentological Constraints and Provenance of Eocene and Miocene Successions from Barbados, in C. Bartolini, Ed., Eastern Caribbean-Northeastern South American Boundary: Tectonic Evolution, Basin Architecture, and

Petroleum Systems." *AAPG Memoir* 123 (2019). https://doi.org/10.1306/13692244M1233846.
Zimmermann, Udo, and Luis A Spalletti. "Provenance of the Lower Paleozoic Balcarce Formation (Tandilia System, Buenos Aires Province, Argentina): Implications for Paleogeographic Reconstructions of Sw Gondwana." *Sedimentary Geology* 219, no. 1-4 (2009): 7-23.

8. Appendix

8.1 Whole-rock geochemical analysis

Table 1 Overview of concentrations of major elements and trace elements from the whole-rock geochemical analysis.

	outcrop	rocktype	La/Th	La/Sc	Th/Sc	Co/Th	Zr/Sc	sum ree ppm
HE 2	Pontedo	shale	3,0	2,4	0,8	0,8	11,7	210,09
HE 4	Pontedo	shale	3,0	2,0	0,7	1,0	7,6	210,47
HE 7	Pontedo	shale	3,2	2,3	0,7	0,6	8,9	204,78
HE 1	Pontedo	qa-conglomerate	2,8	5,4	1,9	1,4	52,4	61,43
HE 3	Pontedo	arenite	2,6	2,6	1,0	1,7	25,4	59,32
HE 5	Pontedo	quartz arenite	2,3	3,8	1,6	1,7	39,8	58,52
HE 6	Pontedo	quartz arenite	4,0	6,4	1,6	1,8	17,0	71,65
HE 8	BdL road	quartz arenite	2,1	16,1	7,7	0,1	n.a.	70,33
HE 9	BdL road	quartz arenite	2,0	14,1	6,9	0,4	163,0	59,08
HE 14	BdL section	shale	4,1	5,5	1,3	0,2	19,9	317,31
HE 15	BdL section	shale	2,7	3,4	1,3	0,3	28,5	201,23
HE 17	BdL section	shale	4,0	2,5	0,6	0,5	9,5	254,85
HE 19	BdL section	shale	2,6	3,0	1,1	0,3	9,7	187,22
HE 10	BdL section	quartz arenite	2,2	4,6	2,1	0,1	n.a.	24,26
HE 13	BdL section	quartz arenite	2,1	2,7	1,3	1,0	n.a.	21,15
CB	**BdL section**	**qa-cross bedded**	3,1	10,4	3,4	0,1	65,1	**46,91**
HE 12	BdL section	arenite	2,4	7,3	3,0	0,2	125,4	100,9
HE 16	BdL section	arenite	2,2	5,1	2,3	0,1	31,8	103,65
HE 18	BdL section	arenite	8,0	5,9	0,7	1,6	28,8	191,84
FM	**BdL section**	**flute marks arenite**	4,5	8,2	1,8	0,1	47,7	**155,52**
HE 11	BdL section	quartz arenite	3,1	8,2	2,6	0,2	n.a.	37,53
CG2	**BdL section**	**hard quartz-arenite**	1,9	3,6	1,9	3,3	n.a.	**30,8**
CG1.2	**BdL section**	**friable quartz-arenite**	4,4	4,0	0,9	9,8	20,9	**61,92**
CG1.1	**BdL section**	**friable quartz-arenite**	3,6	0,9	0,2	8,7	6,4	**63,86**

in caption:
%=, ppm=, ppb=, n.a.= not applicable as one value below detection limit; b.d.l.= below detection limi
replace <xxx with b.d.l.

Table 2 Overview of concentrations of major elements and trace elements from the whole-rock geochemical analysis.

	SiO2	Al2O3	Fe2O3	MgO	CaO	Na2O	K2O	TiO2	P2O5	MnO	LOI	Sum
	%	%	%	%	%	%	%	%	%	%	%	%
HE 2	64,26	18,46	4,14	1,65	0,17	0,07	6,47	0,87	0,11	0,01	3,4	99,65
HE 4	58,6	20,61	5,14	1,97	0,22	0,07	7,12	0,81	0,11	0,03	4,9	99,58
HE 7	59,92	19,95	5,29	1,59	0,21	0,07	6,94	0,8	0,13	0,13	4,6	99,61
HE 1	95,22	1,58	1,2	0,28	0,13	0,02	0,36	0,5	0,09	0,01	0,6	99,94
HE 3	55,01	3,32	4,47	5,81	11,91	0,34	0,97	0,15	0,02	0,45	17,4	99,85
HE 5	90,03	3,45	2,8	0,3	0,06	0,02	1,08	0,21	0,1	0,13	1,7	99,9
HE 6	91,22	3,37	2,29	0,38	0,08	0,02	0,99	0,11	0,05	0,05	1,4	99,92
HE 8	93,61	2,87	0,59	0,06	0,04	0,03	1,83	0,31	0,04	<0.01	0,6	99,94
HE 9	93,4	3,37	0,3	0,06	0,02	0,02	1,85	0,18	0,02	<0.01	0,7	99,95
HE 14	58,21	20,59	5,14	1,43	0,03	0,06	7,23	0,98	0,23	0,03	5,5	99,45
HE 15	65,35	17,85	1,71	1,06	0,21	0,1	8,42	0,84	0,3	<0.01	3,8	99,61
HE 17	55,16	21,18	7,17	1,62	0,35	0,08	8,02	1,06	0,26	0,01	4,6	99,57
HE 19	60,22	20,98	2,48	1,97	0,48	0,05	7,22	0,72	0,18	<0.01	5,3	99,59
HE 10	98,42	0,71	0,07	0,02	<0.01	<0.01	0,25	0,04	0,01	<0.01	0,5	100,01
HE 13	98,38	0,57	0,41	0,03	0,01	<0.01	0,17	0,04	0,05	0,02	0,3	99,99
CB	**95,42**	**2,26**	**0,46**	**0,06**	**<0.01**	**0,01**	**0,93**	**0,09**	**0,02**	**<0.01**	**0,7**	**99,99**
HE 12	85,16	8,02	0,83	0,25	0,05	0,05	3,56	0,53	0,08	<0.01	1,3	99,84
HE 16	78,36	12,25	0,84	0,42	0,1	0,05	5,73	0,4	0,09	<0.01	1,6	99,84
HE 18	76,16	10,81	4,39	0,42	0,04	0,06	4,91	0,33	0,11	0,13	2,4	99,74
FM	**79,94**	**11,45**	**1,08**	**0,36**	**0,05**	**0,05**	**4,56**	**0,3**	**0,05**	**<0.01**	**2,1**	**99,91**
HE 11	96,35	1,81	0,34	0,05	0,01	0,01	0,81	0,06	0,02	<0.01	0,5	99,99
CG2	**95,25**	**1,78**	**0,76**	**0,06**	**0,28**	**<0.01**	**0,53**	**0,07**	**0,25**	**0,03**	**1**	**99,98**
CG1.2	**93,68**	**1,15**	**3,12**	**0,08**	**0,02**	**<0.01**	**0,29**	**0,04**	**0,14**	**0,13**	**1,3**	**99,97**
CG1.1	**91,88**	**1,87**	**3,62**	**0,12**	**0,04**	**0,02**	**0,51**	**0,06**	**0,21**	**0,23**	**1,4**	**99,95**

Table 3 Overview of concentrations of major elements and trace elements from the whole-rock geochemical analysis.

	TOT/C	TOT/S	Ba	Rb	Sr	Cs	Cr	V	Co	Ga	Nb	Sn	Ta
	%	%	ppm	ppm	ppm	ppm	ppm	ppm	ppm	ppm	ppm	ppm	ppm
HE 2	0,07	0,04	738	234,9	34,4	29,1	68,5	108	12,1	23,1	15,6	7	1,1
HE 4	0,05	<0.02	536	261,8	30,7	31	109,6	124	15	26,9	13,2	6	1
HE 7	0,06	<0.02	574	240,3	30,3	22,3	89,05	126	7,7	25,1	13,8	6	1,2
HE 1	<0.02	<0.02	355	13,4	13,1	1,4	BDL	12	5,2	2,2	7,6	2	0,5
HE 3	4,94	0,05	145	30,7	229,3	2,1	BDL	11	5,2	3,2	2,8	2	0,3
HE 5	0,03	<0.02	164	34,9	7,5	2,4	BDL	9	5,5	3,3	2,8	2	0,3
HE 6	<0.02	<0.02	209	34,1	7	2,8	BDL	12	5,9	3,2	2	2	0,2
HE 8	0,07	<0.02	366	41,5	24,4	0,6	BDL	8	0,6	3,2	11	<1	0,9
HE 9	0,02	<0.02	148	37,7	20,1	0,5	BDL	11	2,9	4,2	5,1	<1	0,5
HE 14	0,05	<0.02	1191	188,4	153,5	40,5	95,9	130	3,7	26,1	18,3	4	1,3
HE 15	0,14	<0.02	714	149,5	129,9	19,1	82,2	105	5,2	20,7	14	4	1,3
HE 17	0,13	<0.02	558	229,8	113,6	37,3	109,6	177	6,8	29,3	16,5	4	1,3
HE 19	0,07	<0.02	382	201,7	75,5	35,4	102,75	141	5,9	28,3	14	5	1
HE 10	<0.02	<0.02	17	5,2	9,3	0,2	BDL	<8	0,3	0,9	0,9	<1	0,2
HE 13	0,02	<0.02	21	3	13,2	0,2	BDL	<8	1,3	1,1	0,8	<1	0,1
CB	**<0.02**	**<0.02**	**109**	**16,7**	**15**	**0,6**	**BDL**	**11**	**0,3**	**1,6**	**1,6**	**<1**	**0,2**
HE 12	0,03	<0.02	384	69,5	51,8	2,2	27,4	27	1,4	7,9	8	2	0,7
HE 16	0,03	<0.02	424	99,6	61,3	6	34,25	41	1,5	12	6,3	2	0,5
HE 18	0,04	<0.02	739	94,9	86,7	7,8	20,55	50	7	11,6	5,5	<1	0,4
FM	**0,03**	**<0.02**	**314**	**87,8**	**72,7**	**2,7**	**13,7**	**29**	**1**	**9,7**	**5,2**	**<1**	**0,4**
HE 11	<0.02	<0.02	80	15,4	13,3	0,5	BDL	<8	0,4	2,3	1,1	<1	<0.1
CG2	**<0.02**	**<0.02**	**111**	**10,3**	**18,4**	**0,6**	**BDL**	**9**	**6,2**	**1,8**	**1,2**	**<1**	**0,1**
CG1.2	**<0.02**	**<0.02**	**130**	**6**	**44,1**	**0,6**	**BDL**	**16**	**17,7**	**0,9**	**0,7**	**<1**	**0,1**
CG1.1	**<0.02**	**<0.02**	**267**	**10,2**	**38,9**	**0,9**	**BDL**	**20**	**19,2**	**2,1**	**1,2**	**<1**	**<0.1**

Table 4 Overview of concentrations of major elements and trace elements from the whole-rock geochemical analysis.

	Th	**U**	**Sc**	**Hf**	**Zr**	**Y**	**La**	**Ce**	**Pr**	**Nd**	**Sm**	**Eu**	**Tb**	**Dy**
	ppm	ppm	ppm	ppm	ppm	ppm	ppm	ppm	ppm	ppm	ppm	ppm	ppm	ppm
HE 2	14,4	3,7	18	6,5	210,6	38,2	43,3	82,7	10,29	40,6	7,91	1,48	1,01	6,67
HE 4	14,3	3,5	21	4,4	158,6	36	42,7	81,2	10,52	43,8	7,65	1,34	0,95	6,36
HE 7	13,4	3,7	19	4,9	169,6	31,1	43,4	82,2	10,3	39,7	7,12	1,42	0,84	5,53
HE 1	3,8	0,9	2	3	104,8	11,5	10,8	23	2,95	12,3	3,28	0,69	0,43	2,11
HE 3	3	0,7	3	2,4	76,3	21,8	7,7	17,9	2,39	12,4	3,83	0,99	0,66	4,1
HE 5	3,2	1,2	2	2,3	79,5	18,1	7,5	16,7	2,45	11,8	4,59	1,2	0,79	4,12
HE 6	3,2	0,7	2	1	34	11,7	12,8	29,5	3,42	13,7	3,19	0,66	0,4	2,21
HE 8	7,6	1,1	<1	4,1	145,8	6,8	15,9	31,8	3,32	12,1	1,85	0,27	0,22	1,18
HE 9	6,9	9,3	1	4,8	163	9,2	14,1	25,7	2,87	8,5	1,73	0,39	0,26	1,36
HE 14	20,1	3,4	15	8,2	298,4	53,2	83,1	135,8	14,39	49,6	8,55	1,45	0,76	5,58
HE 15	17,8	3,1	14	11	399,2	32,4	47,4	83,8	9,63	31,6	6,33	1,38	0,92	5,89
HE 17	13,9	4,2	22	6,3	209,4	46,1	55,9	99,6	12,08	45,7	9,36	2,22	1,23	8,36
HE 19	16,9	3,7	15	4,6	145,5	26,6	44,5	77,7	9,24	31,7	6,19	1,21	0,68	4,31
HE 10	2,1	0,4	<1	1,3	51,5	3,2	4,6	9,6	1,24	5,7	0,79	0,15	0,08	0,61
HE 13	1,3	0,4	<1	1	31,7	7,6	2,7	6,9	0,9	3,3	1,36	0,43	0,28	1,55
CB	**3,4**	**0,5**	**1**	**1,7**	**65,1**	**3,5**	**10,4**	**21,1**	**2,22**	**8,8**	**1,31**	**0,27**	**0,12**	**0,59**
HE 12	9,1	1,4	3	10,3	376,2	9,5	21,9	42,3	5,13	20,1	3,08	0,66	0,3	1,97
HE 16	11,7	1	5	4,6	158,9	10,7	25,4	47,1	5,1	17,4	2,08	0,38	0,21	1,45
HE 18	4,4	1,8	6	4,4	172,7	54,3	35,4	71	8,61	34,1	7,06	1,91	1,59	10,41
FM	**7,2**	**1,1**	**4**	**4,8**	**190,8**	**10,1**	**32,7**	**69,7**	**8,15**	**31,4**	**5,21**	**0,91**	**0,28**	**1,72**
HE 11	2,6	0,5	<1	1,5	42	3,1	8,1	16,6	1,93	7,5	1,06	0,22	0,08	0,46
CG2	**1,9**	**2,6**	**<1**	**2,2**	**81,1**	**12,8**	**3,6**	**9,9**	**1,14**	**5,3**	**2,21**	**0,63**	**0,44**	**2,15**
CG1.2	**1,8**	**4,5**	**2**	**1,3**	**41,7**	**17,9**	**7,9**	**25,5**	**2,92**	**11**	**2,53**	**0,64**	**0,59**	**3,44**
CG1.1	**2,2**	**5,7**	**9**	**1,6**	**57,4**	**20,1**	**7,9**	**23,9**	**2,89**	**11,8**	**2,91**	**0,73**	**0,68**	**3,91**

Table 5 Overview of concentrations of major elements and trace elements from the whole-rock geochemical analysis.

	Ho	Er	Tm	Yb	Lu	sum ree	Mo	Cu	Pb	Zn	Ni		Be	Cd
	ppm	ppm	ppm	ppm	ppm	ppm	ppm	ppm	ppm	ppm	ppm		ppm	ppm
HE 2	1,3	3,48	0,53	3,66	0,58	203,51	<0.1	19	1,6	34	29,2	HE 2	3	<0.1
HE 4	1,21	3,4	0,5	3,83	0,53	203,99	<0.1	16	1,4	39	49,1	HE 4	6	<0.1
HE 7	0,94	3,24	0,5	3,01	0,52	198,72	<0.1	0,8	0,9	18	16,1	HE 7	4	<0.1
HE 1	0,42	0,94	0,14	0,88	0,12	58,06	0,1	23,8	1,1	12	9,7	HE 1	<1	<0.1
HE 3	0,72	1,89	0,31	1,92	0,29	55,1	0,1	24,4	1,7	18	5,7	HE 3	<1	<0.1
HE 5	0,58	1,52	0,2	1,21	0,17	52,83	0,1	8,1	1,3	18	8,3	HE 5	<1	<0.1
HE 6	0,4	0,97	0,15	1,03	0,1	68,53	<0.1	0,9	0,3	19	10	HE 6	1	<0.1
HE 8	0,23	0,74	0,11	0,93	0,1	68,75	<0.1	0,4	0,6	<1	0,5	HE 8	1	<0.1
HE 9	0,28	0,91	0,15	1	0,13	57,38	<0.1	15	11,4	2	1,9	HE 9	2	<0.1
HE 14	1,21	4,21	0,73	5,12	0,73	311,23	0,8	0,6	1,7	9	9,6	HE 14	9	<0.1
HE 15	1,02	2,75	0,46	3,4	0,46	195,04	0,1	37,6	4,2	7	6,9	HE 15	4	<0.1
HE 17	1,45	4,37	0,66	4,46	0,62	246,01	0,7	0,1	2,2	18	10,5	HE 17	3	<0.1
HE 19	0,83	2,63	0,39	2,48	0,38	182,24	<0.1	39,9	2,6	3	2,5	HE 19	6	<0.1
HE 10	0,09	0,36	0,05	0,34	0,06	23,67	<0.1	0,4	0,4	<1	0,4	HE 10	<1	<0.1
HE 13	0,26	0,61	0,09	0,59	0,08	19,05	<0.1	0,4	0,3	2	1,4	HE 13	1	<0.1
CB	**0,13**	**0,42**	**0,06**	**0,45**	**0,07**	**45,94**	**0,1**	**0,7**	**0,8**	**1**	**0,6**	**CB**	**<1**	**<0.1**
HE 12	0,36	1,14	0,18	1,39	0,2	98,71	0,1	0,3	1,2	<1	0,8	HE 12	1	<0.1
HE 16	0,28	1,03	0,16	1,35	0,16	102,1	0,3	0,5	0,3	<1	1	HE 16	2	<0.1
HE 18	1,91	4,86	0,74	4,74	0,63	182,96	<0.1	0,2	0,9	25	11	HE 18	<1	<0.1
FM	**0,4**	**1,08**	**0,19**	**1,28**	**0,21**	**153,23**	**<0.1**	**0,7**	**1**	**1**	**0,5**	**FM**	**<1**	**<0.1**
HE 11	0,07	0,26	0,05	0,37	0,06	36,76	<0.1	0,7	0,6	<1	0,5	HE 11	1	<0.1
CG2	**0,43**	**1,02**	**0,13**	**0,81**	**0,12**	**27,88**	**0,6**	**17,1**	**4**	**3**	**6,8**	**CG2**	**2**	**<0.1**
CG1.2	**0,61**	**1,64**	**0,23**	**1,39**	**0,18**	**58,57**	**7**	**35,1**	**8,7**	**16**	**24,4**	**CG1.2**	**<1**	**<0.1**
CG1.1	**0,81**	**2,02**	**0,29**	**1,62**	**0,24**	**59,7**	**8,4**	**39,2**	**5,4**	**23**	**17,4**	**CG1.1**	**2**	**0,1**

Table 6 Overview of concentrations of major elements and trace elements from the whole-rock geochemical analysis.

	Bi	**Ag**	**Au**	**Hg**	**Tl**	**W**	**Se**
	ppm	ppm	ppb	ppm	ppm	ppm	ppm
HE 2	0,4	<0.1	0,9	0,03	0,1	2,6	<0.5
HE 4	0,3	<0.1	0,5	<0.01	0,1	2,5	<0.5
HE 7	<0.1	<0.1	<0.5	<0.01	<0.1	2,5	0,6
HE 1	0,4	<0.1	1,1	0,03	<0.1	3,6	0,5
HE 3	0,3	<0.1	0,7	0,03	<0.1	0,9	<0.5
HE 5	0,4	<0.1	<0.5	0,04	<0.1	<0.5	<0.5
HE 6	<0.1	<0.1	1,7	0,04	<0.1	<0.5	<0.5
HE 8	<0.1	<0.1	<0.5	0,03	<0.1	<0.5	<0.5
HE 9	0,2	<0.1	0,8	0,46	<0.1	<0.5	<0.5
HE 14	0,1	<0.1	0,9	0,11	0,1	1,4	<0.5
HE 15	0,3	0,1	4,4	0,16	<0.1	1,8	<0.5
HE 17	0,1	<0.1	2,9	1,26	0,3	3,2	<0.5
HE 19	0,3	0,1	1,5	0,28	<0.1	3	<0.5
HE 10	<0.1	<0.1	0,7	0,07	<0.1	<0.5	<0.5
HE 13	<0.1	<0.1	1	0,04	<0.1	<0.5	<0.5
CB	**<0.1**	**<0.1**	**<0.5**	**0,08**	**<0.1**	**<0.5**	**<0.5**
HE 12	<0.1	<0.1	<0.5	0,15	<0.1	0,6	<0.5
HE 16	0,2	<0.1	2,5	0,24	<0.1	<0.5	<0.5
HE 18	<0.1	<0.1	<0.5	0,54	<0.1	<0.5	<0.5
FM	**<0.1**	**<0.1**	**<0.5**	**0,14**	**<0.1**	**<0.5**	**<0.5**
HE 11	<0.1	<0.1	1,3	0,1	<0.1	<0.5	<0.5
CG2	**<0.1**	**0,1**	**0,9**	**0,4**	**0,2**	**<0.5**	**<0.5**
CG1.2	**<0.1**	**<0.1**	**<0.5**	**0,15**	**0,3**	**<0.5**	**<0.5**
CG1.1	**<0.1**	**0,1**	**<0.5**	**0,12**	**0,3**	**<0.5**	**<0.5**

8.2 Raw data of concordant and disconcordant U-Pb analysis of all samples

Table 7 Raw data of concordant and disconcordant U-Pb analysis of all samples.

Name	ppm U	^{206}Pb	$^{206}Pb_c$(%)	206/204	Ratios $^{207}Pb/^{206}Pb^*$	1SE	$^{207}Pb/^{235}U^*$	1SE	$^{206}Pb/^{238}U^*$	1SE	Rho	Discordance Central (%)	Minimum rim (%)	Ages 207/206	1σ	207/235	1σ	206/238	1σ	Preferred Age	1σ
CB-162	148	11.3	0.00E+00	16009	0.0598	0.00032	0.7775	0.01004	0.094298	0.001107	0.909	-2.7		596	11	584	6	581	7	581	7
CB-025	81	6.7	0.00E+00	2303	0.0606	0.00049	0.79206	0.01523	0.094793	0.001657	0.909	-6.9	-0.4	625	17	592	9	584	10	584	10
CB-141	189	16.4	0.00E+00	6609	0.05911	0.00053	0.77978	0.02982	0.09568	0.003558	0.973	3.3		571	18	585	17	589	21	589	21
CB-078	83	5.8	0.00E+00	3640	0.05947	0.00055	0.78433	0.01392	0.095652	0.001451	0.855	0.8		584	20	588	8	589	9	589	9
CB-160	161	12.6	0.00E+00	11596	0.05976	0.00034	0.79335	0.01018	0.096278	0.001112	0.9	-0.4		595	12	593	6	593	7	593	7
CB-155	57	4.4	0.00E+00	1852	0.06066	0.00049	0.80668	0.01104	0.096451	0.00107	0.810	-5.6		627	17	601	6	594	6	594	6
CB-069	51	3.6	0.00E+00	1657	0.05946	0.00058	0.79313	0.01437	0.096747	0.001481	0.845	2		584	21	593	8	595	9	595	9
CB-125	86	8.4	0.00E+00	7704	0.05969	0.00046	0.79672	0.01348	0.096806	0.001461	0.892	0.6		592	16	595	8	596	9	596	9
~~CB-148~~	~~111~~	~~9.7~~	~~0.00E+00~~	~~4382~~	~~0.06011~~	~~0.00062~~	~~0.80239~~	~~0.0355~~	~~0.096821~~	~~0.004167~~	~~0.973~~	~~-2~~		~~607~~	~~21~~	~~598~~	~~20~~	~~596~~	~~24~~	~~596~~	~~24~~
CB-136	41	3.6	0.00E+00	2874	0.05959	0.00066	0.80152	0.02958	0.097547	0.003435	0.954	2		589	23	598	17	600	20	600	20
CB-144	236	21	0.00E+00	9015	0.06103	0.00056	0.82279	0.03311	0.097785	0.003833	0.974	-6.3		640	19	610	18	601	23	601	23
CB-115	37	3.6	0.00E+00	2011	0.06001	0.00058	0.81198	0.0139	0.098142	0.001385	0.825			604	20	604	8	604	8	604	8
CB-099	674	66.5	0.00E+00	33003	0.05938	0.00036	0.80612	0.01144	0.098453	0.001261	0.903	4.3		581	13	600	6	605	7	605	7
CB-111	22	2.2	0.00E+00	999	0.0599	0.00061	0.81917	0.01426	0.099193	0.001406	0.814	1.7		600	21	608	8	610	8	610	8
CB-001	56	5	0.00E+00	2826	0.06004	0.00052	0.83429	0.01508	0.100785	0.001603	0.880	2.4		605	18	616	8	619	9	619	9
CB-037	86	7.6	0.00E+00	5666	0.06126	0.00041	0.86212	0.016	0.102061	0.001768	0.933	-3.6		649	14	631	9	626	10	626	10
CB-075	186	14	0.00E+00	8851	0.06128	0.0005	0.86206	0.0147	0.102031	0.001528	0.878	-3.7		649	16	631	8	626	9	626	9
CB-133	562	52.9	0.00E+00	30037	0.05982	0.0005	0.8474	0.02992	0.102749	0.003525	0.972	5.9		597	18	623	16	630	21	630	21
CB-129	365	34.4	0.00E+00	18115	0.06018	0.0005	0.85463	0.02949	0.103001	0.003447	0.970	3.8		610	17	627	16	632	20	632	20
CB-163	412	34.3	0.00E+00	22662	0.06043	0.00029	0.9	0.01083	0.103146	0.001199	0.922	2.3		619	10	630	6	633	7	633	7
~~CB-147~~	~~141~~	~~13.2~~	~~0.00E+00~~	~~6598~~	~~0.06102~~	~~0.0006~~	~~0.87368~~	~~0.03809~~	~~0.103851~~	~~0.004411~~	~~0.974~~	~~-0.5~~		~~640~~	~~21~~	~~638~~	~~21~~	~~637~~	~~26~~	~~637~~	~~26~~
CB-021	136	12.3	0.00E+00	4819	0.06164	0.00043	0.88404	0.01459	0.104021	0.001559	0.908	-3.8		662	14	643	8	638	9	638	9
CB-159	629	53	0.00E+00	24190	0.0618	0.00028	0.88584	0.01124	0.10396	0.00123	0.932	-4.7	-1.1	667	9	644	6	638	7	638	7
CB-120	51	5.3	0.00E+00	6057	0.06192	0.00053	0.88786	0.01556	0.104002	0.001591	0.873	-5.2		671	18	645	8	638	9	638	9
CB-109	287	30.2	0.00E+00	12690	0.06054	0.0004	0.87441	0.01271	0.104754	0.00136	0.893	3.2		623	14	638	7	642	8	642	8
CB-077	234	18.1	0.00E+00	9219	0.06256	0.00052	0.90468	0.01564	0.104877	0.001591	0.878	-7.7	-1.7	693	17	654	8	643	9	643	9
CB-048	130	10.2	0.00E+00	4002	0.06085	0.00049	0.8888	0.0137	0.105934	0.001392	0.853	2.5		634	16	646	7	649	8	649	8
CB-012	90	8.4	0.00E+00	4182	0.0612	0.00043	0.89553	0.016	0.10613	0.001742	0.919	0.6		646	15	649	9	650	10	650	10
CB-114	246	26.4	0.00E+00	15481	0.06065	0.00042	0.8924	0.01382	0.106713	0.001479	0.895	4.5		627	14	648	7	654	9	654	9
CB-166	211	18.1	0.00E+00	11051	0.06166	0.00033	0.90755	0.01199	0.106751	0.001293	0.916	-1.3		662	11	656	6	654	8	654	8
CB-043	34	3.1	0.00E+00	868	0.06277	0.00067	0.92345	0.01883	0.1067	0.001854	0.852	-7		700	21	664	10	654	11	654	11
CB-008	7	0.6	0.00E+00	290	0.06103	0.0013	0.90328	0.02848	0.10734	0.002499	0.739	2.8		640	45	653	15	657	15	657	15
CB-139	29	2.9	0.00E+00	1107	0.06221	0.00069	0.92274	0.03548	0.107576	0.003959	0.957	-3.5		681	23	664	19	659	23	659	23
CB-067	58	4.6	0.00E+00	2118	0.06179	0.00052	0.91844	0.0153	0.107807	0.001552	0.864	-1.1		667	18	662	8	660	9	660	9
CB-003	407	38.7	0.00E+00	19815	0.06216	0.00038	0.92404	0.01536	0.107814	0.001665	0.929	-3		680	13	664	8	660	10	660	10
CB-116	30	3.3	0.00E+00	2173	0.06062	0.00061	0.9041	0.01573	0.108176	0.001534	0.815	6.1		626	21	654	8	662	9	662	9
CB-073	125	10.1	0.00E+00	5024	0.06206	0.00053	0.9312	0.01612	0.108819	0.001636	0.869	-1.6		676	18	668	8	666	10	666	10
CB-175	93	8.1	0.00E+00	11501	0.06183	0.00035	0.93464	0.01283	0.109633	0.001373	0.912	0.4		668	12	670	7	671	8	671	8
CB-093	599	66.3	0.00E+00	25529	0.06169	0.00038	0.93405	0.01307	0.109814	0.001382	0.899	1.3		663	12	670	7	672	8	672	8
CB-010	226	21.9	0.00E+00	7624	0.06089	0.00036	0.92416	0.01523	0.110072	0.001691	0.932	6.2	0.8	635	12	665	8	673	10	673	10
CB-072	78	6.4	0.00E+00	3363	0.06257	0.00056	0.95497	0.01681	0.110694	0.00168	0.862	-2.6		694	19	681	9	677	10	677	10
CB-124	138	15.5	0.00E+00	8232	0.06275	0.00047	0.96784	0.01578	0.111869	0.001622	0.889	-2.4		700	15	687	8	684	9	684	9
CB-119	16	1.8	0.00E+00	704	0.06302	0.00066	0.97203	0.01868	0.111858	0.001802	0.839	-3.8		709	22	690	10	684	10	684	10
CB-168	300	27.1	0.00E+00	16003	0.06224	0.00031	0.96206	0.01268	0.112112	0.001365	0.924	0.4		682	10	684	7	685	8	685	8
CB-156	122	11.1	0.00E+00	6694	0.06283	0.00035	0.97049	0.01414	0.112029	0.001509	0.925	-2.7		702	12	689	7	685	9	685	9
CB-103	125	14.2	0.00E+00	5379	0.06205	0.00044	0.96077	0.01389	0.112294	0.001418	0.873	1.6		676	15	684	7	686	8	686	8
CB-083	281	23.3	0.00E+00	15150	0.06254	0.00052	0.96763	0.01676	0.112208	0.00171	0.880	-1.1		693	16	687	9	686	10	686	10
CB-052	115	9.6	0.00E+00	6244	0.06125	0.0005	0.9515	0.01484	0.112666	0.001503	0.855	6.5	0.2	648	16	679	8	688	9	688	9
CB-096	313	35.6	0.00E+00	4265	0.06217	0.00039	0.96798	0.01374	0.11292	0.001435	0.895	1.5		680	14	687	7	690	8	690	8
CB-004	10	1	0.00E+00	510	0.06254	0.0011	0.9755	0.02721	0.11312	0.002455	0.778	-0.3		693	35	691	14	691	14	691	14

Table 8 Raw data of concordant and disconcordant U-Pb analysis of all samples.

					Ratios											Ages								
Name	ppm U	^{206}Pb	$^{206}Pb_c$(%)	206/204	$^{207}Pb/^{206}Pb^*$	1SE	$^{207}Pb/^{235}U^*$	1SE	$^{206}Pb/^{238}U^*$	1SE	Rho	Discordance Central (%)	Minimum rim (%)			207/206	1σ	207/235	1σ	206/238	1σ		Preferred Age	1σ
CB-110	137	15.7	0.00E+00	6211	0.06335	0.00063	0.99204	0.0166	0.113577	0.001524	0.802	-3.9	.			720	20	700	8	693	9		693	9
CB-045	84	7.1	0.00E+00	2530	0.06245	0.00052	0.98308	0.01589	0.114162	0.001577	0.854	1.1	.			690	17	695	8	697	9		697	9
CB-102	373	42.9	0.00E+00	12019	0.06175	0.00039	0.97441	0.01394	0.114441	0.001467	0.896	5.2	0.1			666	13	691	7	698	8		698	8
CB-106	355	41	0.00E+00	18458	0.06205	0.00039	0.98047	0.0139	0.114607	0.001457	0.897	3.7	.			676	13	694	7	699	8		699	8
CB-053	223	19.1	0.00E+00	11924	0.06197	0.00048	1.0	0.01516	0.115211	0.001537	0.866	4.7	.			673	15	696	8	703	9		703	9
CB-092	276	32.4	0.00E+00	14274	0.06344	0.00041	1.0	0.01403	0.116094	0.001415	0.882	-2.2	.			723	13	712	7	708	8		708	8
CB-152	106	10	0.00E+00	6895	0.06331	0.00035	1.01656	0.01297	0.116447	0.001335	0.899	-1.3	.			719	11	712	7	710	8		710	8
~~CB-145~~	~~193~~	~~20.6~~	~~0.00E+00~~	~~9808~~	~~0.06313~~	~~0.00061~~	~~1.02085~~	~~0.04393~~	~~0.117272~~	~~0.004916~~	~~0.974~~	~~0.3~~	~~.~~			~~713~~	~~20~~	~~714~~	~~22~~	~~715~~	~~28~~		~~715~~	~~28~~
CB-070	61	5.4	0.00E+00	3071	0.06363	0.00057	1.03115	0.0189	0.117529	0.00188	0.873	-1.9	.			729	19	720	9	716	11		716	11
CB-020	38	3.9	0.00E+00	1683	0.06321	0.0006	1.02708	0.01869	0.117854	0.00183	0.853	0.4	.			715	19	717	9	718	11		718	11
CB-031	63	6.6	0.00E+00	4648	0.06402	0.0005	1.05728	0.01877	0.119782	0.001907	0.897	-1.8	.			742	16	732	9	729	11		729	11
CB-128	175	21.1	0.00E+00	8659	0.06327	0.00043	1.04634	0.01716	0.119939	0.001791	0.911	1.9	.			717	14	727	9	730	10		730	10
CB-057	41	3.7	0.00E+00	2760	0.0637	0.00057	1.07086	0.01836	0.121917	0.001784	0.853	1.4	.			732	19	739	9	742	10		742	10
CB-064	17	1.5	0.00E+00	4507	0.06372	0.00083	1.07615	0.02302	0.122493	0.002071	0.79	1.8	.			732	27	742	11	745	12		745	12
CB-130	57	6.4	0.00E+00	3723	0.06401	0.00064	1.08345	0.03875	0.122766	0.004218	0.960	0.7	.			742	20	745	19	746	24		746	24
CB-132	149	17	0.00E+00	9453	0.06414	0.00056	1.09793	0.03896	0.124159	0.004273	0.970	1.2	.			746	18	752	19	754	25		754	25
CB-121	271	33.9	0.00E+00	8664	0.06451	0.00043	1.10613	0.01757	0.124365	0.001791	0.907	-0.4	.			758	14	756	8	756	10		756	10
CB-076	181	16.8	0.00E+00	9586	0.06659	0.00055	1.14705	0.01993	0.124936	0.001911	0.881	-8.5	-3.4			825	16	776	9	759	11		759	11
CB-016	27	3	0.00E+00	1175	0.06704	0.00053	1.16039	0.02133	0.125527	0.002083	0.903	-9.7	-4.9			839	16	782	10	762	12		762	12
CB-170	99	10	0.00E+00	4378	0.06452	0.0004	1.12139	0.01564	0.126048	0.001571	0.893	0.9	.			759	13	764	7	765	9		765	9
CB-173	53	5.3	0.00E+00	4209	0.06499	0.00045	1.13562	0.01631	0.126736	0.001593	0.875	-0.6	.			774	14	770	8	769	9		769	9
CB-138	27	3.2	0.00E+00	1720	0.06584	0.0007	1.2	0.04426	0.127621	0.004682	0.96	-3.6	.			801	22	781	21	774	27		774	27
CB-137	212	25	0.00E+00	10249	0.06433	0.00057	1.14195	0.04384	0.128755	0.004809	0.973	4	.			752	18	773	21	781	27		781	27
CB-054	110	10.6	0.00E+00	9504	0.06438	0.00056	1.15176	0.01934	0.129746	0.001865	0.856	4.5	.			754	18	778	9	786	11		786	11
CB-056	18	1.7	0.00E+00	2019	0.06592	0.0007	1.1816	0.02171	0.130004	0.001954	0.818	-2.1	.			804	22	792	10	788	11		788	11
CB-030	50	5.7	0.00E+00	2081	0.06656	0.00051	1.19799	0.02165	0.130538	0.002138	0.906	-4.3	.			824	15	800	10	791	12		791	12
CB-041	194	21.9	0.00E+00	11456	0.06583	0.00043	1.18966	0.02186	0.131064	0.002253	0.935	-0.9	.			801	13	796	10	794	13		794	13
CB-063	147	14.4	0.00E+00	32802	0.06617	0.00053	1.2	0.02143	0.131082	0.002098	0.893	-2.3	.			812	16	799	10	794	12		794	12
CB-087	256	34.5	0.00E+00	10048	0.06607	0.00045	1.21019	0.01843	0.132844	0.001808	0.894	-0.6	.			809	14	805	8	804	10		804	10
CB-174	882	94.3	0.00E+00	37688	0.06463	0.00032	1.18736	0.01605	0.133237	0.001678	0.932	6.1	2.1			762	10	795	7	806	10		806	10
CB-097	147	20	0.00E+00	7095	0.066	0.00045	1.22313	0.01791	0.134414	0.001744	0.886	0.9	.			806	15	811	8	813	10		813	10
CB-074	243	24.2	0.00E+00	40090	0.06643	0.00054	1.23217	0.02105	0.134528	0.00202	0.879	-0.8	.			820	15	815	10	814	11		814	11
CB-172	664	72.3	0.00E+00	40554	0.06451	0.00031	1.20814	0.01629	0.135829	0.001708	0.932	8.8	4.7			758	10	804	7	821	10		821	10
CB-007	43	5.2	0.00E+00	1915	0.0662	0.00057	1.24172	0.02366	0.136048	0.002316	0.894	1.3	.			813	16	820	11	822	13		822	13
CB-135	196	24.6	0.00E+00	10310	0.06676	0.00061	1.2655	0.04766	0.137485	0.005025	0.970	.	.			830	18	830	21	830	28		830	28
CB-117	259	35.8	0.00E+00	30142	0.06655	0.00046	1.26022	0.02048	0.137345	0.00202	0.905	0.8	.			824	14	828	9	830	11		830	11
CB-049	70	7.2	0.00E+00	5722	0.06654	0.00057	1.26271	0.02091	0.13763	0.00195	0.856	1	.			823	17	829	9	831	11		831	11
CB-085	106	14.9	0.00E+00	4508	0.06728	0.00048	1.28263	0.01976	0.138263	0.001892	0.888	-1.5	.			846	14	838	9	835	11		835	11
CB-134	78	9.8	0.00E+00	3763	0.0673	0.00063	1.28386	0.04735	0.138349	0.004937	0.968	-1.5	.			847	19	839	21	835	28		835	28
CB-055	39	4.1	0.00E+00	2414	0.0681	0.00065	1.31407	0.02287	0.139942	0.002037	0.836	-3.4	.			872	19	852	10	844	12		844	12
CB-098	246	35.1	0.00E+00	9952	0.06701	0.00044	1.29778	0.01903	0.14046	0.001843	0.895	1.2	.			838	14	845	8	847	10		847	10
CB-107	175	25.2	0.00E+00	12584	0.06776	0.00044	1.33156	0.02039	0.14253	0.001974	0.904	-0.3	.			861	13	860	9	859	11		859	11
CB-088	133	19.5	0.00E+00	6801	0.06841	0.00045	1.35702	0.01954	0.143879	0.001844	0.890	-1.7	.			881	13	871	8	867	10		867	10
CB-100	246	36.2	0.00E+00	26372	0.07128	0.00046	1.4	0.02077	0.145356	0.001894	0.896	-10	-6.6			965	12	901	9	875	11		875	11
CB-105	334	52.1	0.00E+00	20269	0.06962	0.00045	1.47803	0.02222	0.153963	0.002089	0.902	0.7	.			917	13	921	9	923	12		923	12
CB-094	32	5	0.00E+00	7494	0.07233	0.00058	1.54056	0.02573	0.154475	0.002267	0.879	-7.5	-3.2			995	16	947	10	926	13		926	13
CB-028	69	9.3	0.00E+00	10245	0.07184	0.0005	1.53625	0.02717	0.155094	0.002523	0.920	-5.7	-1.8			981	14	945	11	929	14		929	14
CB-079	53	6.1	0.00E+00	4870	0.07203	0.00065	1.54592	0.02821	0.155669	0.002475	0.871	-5.9	-1			987	18	949	11	933	14		933	14
CB-013	43	6	0.00E+00	3638	0.07124	0.00052	1.57435	0.02801	0.160283	0.002604	0.913	-0.7	.			964	14	960	11	958	14		958	14
CB-086	85	14.2	0.00E+00	5331	0.07308	0.00052	1.65535	0.02464	0.164273	0.002149	0.879	-3.8	.			1016	14	992	9	980	12		980	12

Table 9 Raw data of concordant and disconcordant U-Pb analysis of all samples.

					Ratios											Ages								
Name	ppm U	^{206}Pb	$^{206}Pb_c$(%)	206/204	$^{207}Pb/^{206}Pb^*$	1SE	$^{207}Pb/^{235}U^*$	1SE	$^{206}Pb/^{238}U^*$	1SE	Rho	Discordance Central (%)	Minimum rim (%)			207/206	1σ	207/235	1σ	206/238	1σ		Preferred Age	1σ
CB-167	88	12.2	0.00E+00	5702	0.07432	0.00044	1.75413	0.02477	0.171173	0.002194	0.907	-3.3	-0.1			1050	11	1029	9	1019	12		1050	11
CB-062	238	30.7	0.00E+00	14874	0.0732	0.00059	1.74065	0.03007	0.172456	0.002634	0.884	0.6	.			1020	16	1024	11	1026	14		1020	16
CB-050	30	4	0.00E+00	2679	0.07634	0.00075	1.8748	0.03309	0.178127	0.002608	0.829	-4.6	.			1104	19	1072	12	1057	14		1104	19
CB-143	36	6.4	0.00E+00	4104	0.07817	0.0008	2.0652	0.08804	0.191614	0.007931	0.971	-2	.			1151	19	1137	29	1130	43		1151	19
CB-089	33	9.9	0.00E+00	4808	0.10797	0.00087	4.25213	0.07873	0.28563	0.004766	0.901	-9.3	-6.5			1765	14	1684	15	1620	24		1765	14
CB-153	140	35.2	0.00E+00	22673	0.10909	0.00062	4.53827	0.07989	0.301717	0.005022	0.946	-5.4	-3.3			1784	10	1738	15	1700	25		1784	10
CB-026	42	11.3	0.00E+00	3678	0.10945	0.00082	4.58858	0.09769	0.304058	0.006059	0.936	-5	-2.2			1790	13	1747	18	1711	30		1790	13
CB-108	566	202.6	0.00E+00	53088	0.12585	0.00105	5.87854	0.12238	0.338782	0.006465	0.917	-9	-6.3			2041	15	1958	18	1881	31		2041	15
CB-032	56	16.7	0.00E+00	4722	0.11874	0.00092	5.57176	0.12418	0.340314	0.007109	0.937	-2.9	-0.1			1937	14	1912	19	1888	34		1937	14
CB-036	236	70.6	0.00E+00	27371	0.11783	0.0009	5.567	0.1236	0.342665	0.007145	0.939	-1.4	.			1924	13	1911	19	1899	34		1924	13
CB-015	17	5.1	0.00E+00	2530	0.12182	0.00114	5.85514	0.15099	0.348582	0.008373	0.931	-3.2	.			1983	16	1955	22	1928	40		1983	16
CB-123	423	156.5	0.00E+00	110	0.1314	0.00115	6.39069	0.14038	0.352748	0.007101	0.916	-9.2	-6.5			2117	15	2031	19	1948	34		2117	15
CB-039	184	57.1	0.00E+00	31131	0.12015	0.00092	5.88133	0.13321	0.355017	0.007568	0.941	.	.			1958	13	1958	20	1959	36		1958	13
CB-035	30	9.3	0.00E+00	4786	0.12823	0.00105	6.3247	0.15308	0.357717	0.008144	0.941	-5.7	-3			2074	13	2022	21	1971	39		2074	13
CB-095	434	166.6	0.00E+00	167481	0.13181	0.00112	6.59923	0.13532	0.363108	0.006774	0.91	-6.9	-4.1			2122	14	2059	18	1997	32		2122	14
CB-066	207	58.2	0.00E+00	31187	0.12487	0.00126	6.28774	0.14697	0.365192	0.007699	0.902	-1.2	.			2027	17	2017	20	2007	36		2027	17
CB-034	361	121.3	0.00E+00	51764	0.12734	0.001	6.75018	0.15903	0.384469	0.008543	0.943	2	.			2062	13	2079	21	2097	40		2062	13
CB-169	988	333.9	0.00E+00	1178947	0.13157	0.00083	7.4	0.1467	0.405464	0.00767	0.948	4.2	.			2119	11	2156	18	2194	35		2119	11
CB-027	403	144	0.00E+00	29743	0.15272	0.00132	8.55402	0.20873	0.406221	0.009266	0.935	-8.9	-6.3			2377	14	2292	22	2198	42		2377	14
CB-040	54	19.1	0.00E+00	38282	0.14208	0.00121	7.98861	0.19786	0.407791	0.009488	0.939	-2.5	.			2253	14	2230	22	2205	43		2253	14
CB-002	256	93.1	0.00E+00	27	0.14578	0.00122	8.20163	0.19564	0.408031	0.009112	0.936	-4.7	-2			2297	14	2254	22	2206	42		2297	14
CB-112	53	24.6	0.00E+00	7678	0.16326	0.00164	9.78312	0.23746	0.434606	0.009607	0.911	-7.8	-4.9			2490	16	2415	22	2326	43		2490	16
CB-131	912	426.9	0.00E+00	56672	0.19252	0.00287	12.74055	0.77499	0.479958	0.028304	0.969	-10.3	-6.3			2764	24	2661	57	2527	123		2764	24
CB-171	147	60.2	0.00E+00	30118	0.18056	0.00142	12.13089	0.2675	0.487266	0.010042	0.935	-4.5	-2.2			2658	12	2615	21	2559	44		2658	12
CB-011	23	13	0.00E+00	5340	0.27108	0.00361	23.76812	0.81914	0.635922	0.020218	0.923	-5.3	-1.8			3312	21	3259	34	3173	80		3312	21
CB-014	67	4.8	0.00E+00	1468	0.06035	0.0005	0.67052	0.01285	0.080578	0.00139	0.9	-19.7	-13.8			616	17	521	8	500	8		500	8
CB-068	126	8	0.00E+00	698	0.0638	0.00055	0.75579	0.01462	0.085923	0.001487	0.895	-28.8	-24.2			735	18	572	8	531	9		531	9
CB-044	532	36.3	0.00E+00	2141	0.06571	0.00056	0.83198	0.01395	0.091822	0.00133	0.864	-30.3	-26.2			797	18	615	8	566	8		566	8
CB-154	616	46.7	0.00E+00	2120	0.07057	0.00035	0.90057	0.0133	0.092559	0.00129	0.944	-41.4	-39.6			945	10	652	7	571	8		571	8
CB-142	761	68.4	0.00E+00	12225	0.06246	0.00056	0.84399	0.03307	0.098	0.003738	0.974	-13.2	-6.7			690	18	621	18	603	22		603	22
CB-140	1094	101.2	0.00E+00	3557	0.06476	0.00057	0.90575	0.03457	0.101442	0.003766	0.973	-19.7	-14.2			766	18	655	18	623	22		623	22
CB-090	206	21.7	0.00E+00	878	0.07751	0.00163	1.11362	0.02716	0.104201	0.001293	0.509	-45.8	-40.6			1134	40	760	13	639	8		639	8
CB-071	84	6.6	0.00E+00	4338	0.06902	0.0006	0.99939	0.02003	0.105021	0.001897	0.901	-29.8	-26			899	17	704	10	644	11		644	11
CB-018	23	2.1	0.00E+00	615	0.06587	0.00099	1.0	0.02348	0.106522	0.002026	0.784	-19.6	-11.6			802	30	687	12	653	12		653	12
CB-080	167	13.5	0.00E+00	6031	0.06518	0.00071	0.98316	0.01834	0.109405	0.001661	0.814	-14.9	-8.7			780	22	695	9	669	10		669	10
CB-165	510	45.2	0.00E+00	3936	0.06589	0.00034	1.00011	0.01378	0.110085	0.001404	0.925	-17	-14			803	11	704	7	673	8		673	8
CB-158	79	7.9	0.00E+00	3209	0.06886	0.00048	1.16251	0.01643	0.122447	0.001504	0.869	-17.7	-14.2			894	14	783	8	745	9		745	9
CB-005	61	6.7	0.00E+00	11295	0.06151	0.00046	1.05368	0.01864	0.124231	0.001988	0.905	15.7	8.9			657	15	731	9	755	11		755	11
CB-113	141	19.3	0.00E+00	3152	0.07237	0.00137	1.34613	0.0315	0.134908	0.001846	0.585	-19.3	-11.5			996	36	866	14	816	10		816	10
CB-006	3	0.5	0.00E+00	225	0.06434	0.00207	1.48499	0.09972	0.167401	0.009862	0.877	35.1	8.2			753	62	924	41	998	54		998	54
CB-091	170	31.4	0.00E+00	7183	0.1063	0.00082	2.63768	0.04302	0.179958	0.002587	0.882	-41.8	-40.1			1737	14	1311	12	1067	14		1737	14
CB-058	20	2.7	0.00E+00	1404	0.097	0.00104	2.44395	0.04867	0.182736	0.003071	0.844	-33.6	-30.8			1567	20	1256	14	1082	17		1567	20
CB-127	708	152.5	0.00E+00	2399	0.14377	0.00134	4.16702	0.07964	0.210216	0.003507	0.873	-50.3	-48.8			2273	16	1668	16	1230	19		2273	16
~~CB-146~~	~~16~~	~~3.5~~	~~0.00E+00~~	~~1861~~	~~0.11771~~	~~0.00173~~	~~3.8~~	~~0.19735~~	~~0.236492~~	~~0.011653~~	~~0.958~~	~~-31.9~~	~~-28.1~~			~~1922~~	~~26~~	~~1601~~	~~41~~	~~1368~~	~~61~~		~~1922~~	~~26~~
CB-157	98	19.6	0.00E+00	14865	0.13505	0.0009	4.51837	0.06991	0.242656	0.003392	0.904	-39.2	-37.8			2165	11	1734	13	1400	18		2165	11
CB-065	309	56.3	0.00E+00	7069	0.16516	0.00197	5.54502	0.1283	0.243495	0.004826	0.857	-48.8	-47			2509	19	1908	20	1405	25		2509	19
CB-082	82	15	0.00E+00	20680	0.10312	0.001	3.46735	0.07084	0.243877	0.004388	0.881	-18.1	-15			1681	17	1520	16	1407	23		1681	17
CB-164	137	27.4	0.00E+00	11738	0.09836	0.00055	3.31042	0.05149	0.244095	0.003544	0.934	-12.9	-10.9			1593	10	1484	12	1408	18		1593	10

Table 10 Raw data of concordant and disconcordant U-Pb analysis of all samples.

Name	ppm U	^{206}Pb	$^{206}Pb_c$(%)	206/204	Ratios $^{207}Pb/^{206}Pb^*$	1SE	$^{207}Pb/^{235}U^*$	1SE	$^{206}Pb/^{238}U^*$	1SE	Rho	Discordance Central (%)	Minimum rim (%)			Ages 207/206	1σ	207/235	1σ	206/238	1σ		Preferred Age	1σ
CB-051	40	7.5	0.00E+00	4381	0.09965	0.00093	3.38774	0.06363	0.246554	0.004012	0.866	-13.6	-10.3			1618	17	1502	15	1421	21		1618	17
CB-024	132	29.6	0.00E+00	7783	0.11655	0.00089	4.14101	0.08724	0.257692	0.005057	0.931	-25	-22.9			1904	14	1662	17	1478	26		1904	14
CB-084	893	256.5	0.00E+00	19592	0.12037	0.001	4.54853	0.09383	0.27407	0.005178	0.916	-22.9	-20.6			1962	14	1740	17	1561	26		1962	14
CB-118	139	53.5	0.00E+00	15300	0.16092	0.0016	8.06056	0.17952	0.3633	0.007245	0.895	-22	-19.6			2465	16	2238	20	1998	34		2465	16
CB-101	231	91.5	0.00E+00	7902	0.1595	0.00155	8.2049	0.17971	0.373085	0.007328	0.897	-19.3	-16.8			2450	16	2254	20	2044	34		2450	16
CB-009	22	7.9	0.00E+00	3456	0.16199	0.00154	9.2	0.23614	0.411789	0.009822	0.929	-12.1	-9.4			2477	15	2358	24	2223	45		2477	15
CB-126	180	83.9	0.00E+00	38080	0.1788	0.00192	10.68019	0.26807	0.433218	0.009827	0.904	-14.5	-11.7			2642	18	2496	23	2320	44		2642	18
CB-029	152	58.3	0.00E+00	23235	0.17281	0.00164	10.38337	0.27649	0.43579	0.010843	0.934	-11.7	-9			2585	15	2470	25	2332	49		2585	15
CB-122	140	67.1	0.00E+00	29873	0.17653	0.00192	10.79063	0.2799	0.443339	0.010444	0.908	-11.6	-8.6			2621	17	2505	24	2366	47		2621	17
CB-046	198	70.2	0.00E+00	39357	0.2064	0.0029	12.94018	0.35292	0.454701	0.010623	0.857	-19.2	-16			2877	21	2675	26	2416	47		2877	21

Table 11 Raw data of concordant and disconcordant U-Pb analysis of all samples.

Name	ppm U	^{206}Pb	$^{206}Pb_c$(%)	206/204	Ratios $^{207}Pb/^{206}Pb^*$	1SE	$^{207}Pb/^{235}U^*$	1SE	$^{206}Pb/^{238}U^*$	1SE	Rho	Discordance Central (%)	Minimum rim (%)	Ages 207/206	1σ	207/235	1σ	206/238	1σ	Preferred Age	1σ
CG-126	322	24.6	0.00E+00	10416	0.05968	0.00047	0.8	0.01027	0.091726	0.00102	0.817	-4.6	.	592	17	571	6	566	6	566	6
CG-044	325	30.6	0.00E+00	8472	0.05964	0.0003	0.76058	0.01139	0.092498	0.001306	0.943	-3.6	.	590	10	574	7	570	8	570	8
CG-109	474	36.9	0.00E+00	3354	0.0589	0.00044	0.75185	0.00894	0.092577	0.000858	0.779	1.3	.	563	15	569	5	571	5	571	5
CG-096	151	12	0.00E+00	4790	0.06094	0.00034	0.78139	0.01453	0.092992	0.001651	0.954	-10.5	-6.1	637	11	586	8	573	10	573	10
CG-079	71	5.8	0.00E+00	1919	0.05943	0.00042	0.76395	0.01526	0.093235	0.001743	0.936	-1.5	.	583	15	576	9	575	10	575	10
CG-063	188	18	0.00E+00	9035	0.0589	0.00035	0.77007	0.01381	0.094822	0.001603	0.943	3.8	.	563	13	580	8	584	9	584	9
CG-130	106	8.5	0.00E+00	2995	0.05975	0.00048	0.79589	0.00964	0.096603	0.000881	0.752	.	.	595	16	595	5	594	5	594	5
CG-138	89	7.2	0.00E+00	2614	0.05922	0.00051	0.79056	0.01049	0.096822	0.000978	0.761	3.7	.	575	18	591	6	596	6	596	6
CG-147	18	1.4	0.00E+00	228	0.06072	0.00086	0.81128	0.01557	0.096904	0.001254	0.674	-5.5	.	629	30	603	9	596	7	596	7
CG-112	47	3.8	0.00E+00	422	0.05992	0.0006	0.80133	0.01253	0.096987	0.001169	0.771	-0.7	.	601	22	598	7	597	7	597	7
CG-093	69	5.9	0.00E+00	5000	0.05986	0.00039	0.809	0.01568	0.098012	0.001791	0.943	0.7	.	599	14	602	9	603	11	603	11
CG-123	115	9.5	0.00E+00	584	0.05973	0.0005	0.81008	0.01045	0.098361	0.000962	0.758	1.9	.	594	17	602	6	605	6	605	6
CG-150	201	16.4	0.00E+00	8119	0.06031	0.0005	0.82401	0.01074	0.099094	0.000994	0.770	-1	.	615	17	610	6	609	6	609	6
CG-006	64	4.8	0.00E+00	2608	0.06109	0.00048	0.84297	0.01377	0.100073	0.00143	0.875	-4.5	.	643	17	621	8	615	8	615	8
CG-037	761	78.2	0.00E+00	23756	0.06021	0.00027	0.83483	0.01231	0.100564	0.001414	0.954	1.1	.	611	10	616	7	618	8	618	8
CG-015	90	6.8	0.00E+00	5073	0.06073	0.00042	0.84274	0.01385	0.100637	0.001497	0.905	-2	.	630	14	621	8	618	9	618	9
CG-040	193	19.9	0.00E+00	9715	0.061	0.00033	0.84846	0.01292	0.100877	0.001435	0.934	-3.2	.	639	11	624	7	620	8	620	8
CG-118	217	18.4	0.00E+00	8700	0.06013	0.00047	0.8	0.01022	0.101156	0.000941	0.764	2.2	.	608	16	618	6	621	6	621	6
CG-113	125	10.7	0.00E+00	3126	0.06048	0.0005	0.84798	0.01101	0.101695	0.001014	0.768	0.6	.	621	17	624	6	624	6	624	6
CG-029	348	36.5	0.00E+00	11151	0.06038	0.00029	0.84714	0.01251	0.101756	0.001421	0.945	1.3	.	617	10	623	7	625	8	625	8
CG-022	385	40.7	0.00E+00	14869	0.06127	0.00031	0.86089	0.01267	0.101903	0.001406	0.937	-3.8	.	649	11	631	7	626	8	626	8
CG-053	247	25.4	0.00E+00	13747	0.06047	0.0003	0.8515	0.01322	0.102132	0.001501	0.947	1.1	.	620	11	625	7	627	9	627	9
CG-039	401	42.2	0.00E+00	13645	0.06132	0.00028	0.9	0.01278	0.102779	0.001435	0.949	-3.2	.	650	10	635	7	631	8	631	8
CG-014	28	2.1	0.00E+00	1258	0.06067	0.00062	0.86379	0.01556	0.103256	0.001535	0.825	1	.	628	21	632	8	633	9	633	9
CG-091	163	14.6	0.00E+00	6732	0.06148	0.00033	0.87509	0.01569	0.103235	0.001769	0.956	-3.6	.	656	11	638	8	633	10	633	10
CG-030	101	10.8	0.00E+00	4379	0.06156	0.00033	0.87654	0.01319	0.103271	0.001453	0.935	-4	.	659	11	639	7	634	8	634	8
CG-027	338	36.1	0.00E+00	21808	0.06113	0.00029	0.87224	0.01274	0.10349	0.001429	0.945	-1.5	.	644	10	637	7	635	8	635	8
CG-013	334	26.5	0.00E+00	11097	0.06045	0.00041	0.86889	0.01614	0.104256	0.001803	0.931	3.3	.	620	14	635	9	639	11	639	11
CG-061	325	34.2	0.00E+00	25303	0.06	0.00033	0.86455	0.01378	0.104501	0.001564	0.939	6.4	1.2	604	12	633	8	641	9	641	9
CG-048	605	64.2	0.00E+00	28004	0.0609	0.00029	0.87861	0.01316	0.104629	0.001486	0.948	0.9	.	636	10	640	7	641	9	641	9
CG-090	680	62.3	0.00E+00	24913	0.06	0.00026	0.86704	0.01619	0.104808	0.001903	0.973	6.8	1.6	604	9	634	9	643	11	643	11
CG-140	279	24.2	0.00E+00	11317	0.06054	0.00046	0.87758	0.01115	0.10513	0.001066	0.798	3.6	.	623	16	640	6	644	6	644	6
CG-110	52	4.6	0.00E+00	1407	0.06113	0.00056	0.88598	0.01311	0.105114	0.001216	0.782	0.1	.	644	18	644	7	644	7	644	7
CG-121	424	37.4	0.00E+00	9821	0.06058	0.00046	0.87879	0.01202	0.105216	0.001194	0.83	3.5	.	624	16	640	6	645	7	645	7
CG-089	61	5.6	0.00E+00	2538	0.06161	0.00037	0.89389	0.01647	0.105228	0.001831	0.944	-2.5	.	661	13	648	9	645	11	645	11
CG-066	85	8	0.00E+00	3058	0.06059	0.00037	0.88123	0.0164	0.105479	0.001853	0.944	3.6	.	625	13	642	9	646	11	646	11
CG-002	191	15.2	0.00E+00	10182	0.05958	0.00038	0.86772	0.01307	0.105619	0.001444	0.907	10.5	4.5	589	14	634	7	647	8	647	8
CG-142	249	21.7	0.00E+00	11075	0.06055	0.00048	0.88086	0.01074	0.105515	0.000984	0.765	4	.	623	16	641	6	647	6	647	6
CG-032	30	3.2	0.00E+00	1537	0.0624	0.0005	0.9088	0.01565	0.105625	0.001607	0.883	-6.2	-0.3	688	16	656	8	647	9	647	9
CG-116	327	29.1	0.00E+00	11361	0.0606	0.00046	0.88499	0.0104	0.105912	0.000949	0.762	4	.	625	15	644	6	649	6	649	6
CG-005	198	15.8	0.00E+00	2555	0.06047	0.00037	0.88489	0.01325	0.106141	0.001447	0.911	5.1	.	620	13	644	7	650	8	650	8
CG-135	116	10.3	0.00E+00	3952	0.06049	0.0005	0.88899	0.01147	0.106595	0.001061	0.771	5.4	.	621	17	646	6	653	6	653	6
CG-081	214	20	0.00E+00	8679	0.06119	0.0003	0.89924	0.01612	0.106585	0.001839	0.962	1.1	.	646	10	651	9	653	11	653	11
CG-004	233	18.8	0.00E+00	1742	0.06043	0.00037	0.89221	0.01299	0.107074	0.001411	0.905	6.2	0.8	619	13	648	7	656	8	656	8
CG-076	137	12.9	0.00E+00	4834	0.06067	0.00033	0.89621	0.01613	0.107138	0.001841	0.955	4.8	.	628	11	650	9	656	11	656	11
CG-120	38	3.4	0.00E+00	1424	0.06162	0.00067	0.90991	0.01416	0.107103	0.001186	0.711	-0.8	.	661	22	657	8	656	7	656	7
CG-104	288	26.7	0.00E+00	11361	0.06065	0.00032	0.89879	0.01697	0.107484	0.00195	0.961	5.3	.	627	11	651	9	658	11	658	11
CG-009	115	9.4	0.00E+00	4897	0.06179	0.00042	0.9188	0.0149	0.107846	0.001586	0.907	-1	.	667	14	662	8	660	9	660	9
CG-051	498	54.5	0.00E+00	51537	0.0611	0.00028	0.9116	0.01463	0.108215	0.001663	0.957	3.2	.	643	10	658	8	662	10	662	10

Table 12 Raw data of concordant and disconcordant U-Pb analysis of all samples.

Name	ppm U	^{206}Pb	$^{206}Pb_c$(%)	206/204	Ratios $^{207}Pb/^{206}Pb^*$	1SE	$^{207}Pb/^{235}U^*$	1SE	$^{206}Pb/^{238}U^*$	1SE	Rho	Discordance Central (%)	Minimum rim (%)	Ages 207/206	1σ	207/235	1σ	206/238	1σ	Preferred Age	1σ
CG-108	155	14.4	0.00E+00	18841	0.06126	0.00033	0.91454	0.01777	0.108281	0.002022	0.961	2.4	.	648	11	659	9	663	12	663	12
CG-137	33	3	0.00E+00	134	0.06131	0.00065	0.91594	0.01383	0.108358	0.001169	0.714	2.1	.	650	22	660	7	663	7	663	7
CG-017	381	32.3	0.00E+00	18079	0.06134	0.00042	0.91575	0.01874	0.108278	0.002087	0.942	1.9	.	651	14	660	10	663	12	663	12
CG-143	224	20	0.00E+00	6294	0.06134	0.0005	0.91574	0.01224	0.108267	0.00115	0.795	1.8	.	651	17	660	6	663	7	663	7
CG-080	493	47.1	0.00E+00	14421	0.06067	0.00026	0.90745	0.01714	0.108484	0.001995	0.974	6.1	1.1	627	9	656	9	664	12	664	12
CG-099	221	20.5	0.00E+00	6422	0.06127	0.00033	0.91641	0.01757	0.108484	0.001995	0.959	2.5	.	649	11	660	9	664	12	664	12
CG-106	171	15.9	0.00E+00	9280	0.06127	0.00038	0.91715	0.01792	0.108563	0.002013	0.949	2.5	.	649	13	661	9	664	12	664	12
CG-074	58	5.6	0.00E+00	2295	0.06132	0.00046	0.91697	0.01863	0.108461	0.002046	0.929	2.2	.	650	16	661	10	664	12	664	12
CG-031	451	50.3	0.00E+00	20733	0.06141	0.00028	0.9	0.01358	0.108592	0.001525	0.951	1.8	.	654	9	662	7	665	9	665	9
CG-133	205	18.6	0.00E+00	14630	0.06123	0.00047	0.92053	0.01089	0.109029	0.000985	0.764	3.2	.	648	16	663	6	667	6	667	6
CG-128	192	17.5	0.00E+00	5710	0.06167	0.00053	0.92711	0.01195	0.109034	0.00105	0.747	0.7	.	663	17	666	6	667	6	667	6
CG-095	262	24.5	0.00E+00	10432	0.06156	0.0003	0.92691	0.01716	0.109209	0.001949	0.964	1.5	.	659	10	666	9	668	11	668	11
CG-021	208	23.5	0.00E+00	8777	0.06305	0.00034	0.94968	0.01431	0.109244	0.001536	0.933	-6.2	-2.2	710	11	678	7	668	9	668	9
CG-008	247	20.6	0.00E+00	11452	0.06256	0.00038	0.94702	0.01772	0.109789	0.001941	0.945	-3.3	.	693	13	677	9	672	11	672	11
CG-016	199	16.9	0.00E+00	8368	0.06163	0.00044	0.94347	0.01868	0.111031	0.002054	0.934	2.8	.	661	14	675	10	679	12	679	12
CG-145	522	48	0.00E+00	25723	0.06196	0.00048	0.94945	0.01197	0.111142	0.001103	0.787	1.1	.	673	16	678	6	679	6	679	6
CG-047	112	12.6	0.00E+00	4255	0.06276	0.00036	0.9627	0.01469	0.111252	0.001571	0.926	-3	.	700	12	685	8	680	9	680	9
CG-038	721	82.2	0.00E+00	21542	0.06245	0.00028	0.96006	0.0152	0.111493	0.001694	0.959	-1.3	.	690	10	683	8	681	10	681	10
CG-067	193	19.2	0.00E+00	7564	0.06153	0.0003	0.94875	0.01648	0.111831	0.001862	0.959	4.1	.	658	11	677	9	683	11	683	11
CG-065	326	36.8	0.00E+00	9893	0.06141	0.00035	0.9488	0.0157	0.112065	0.001744	0.940	5	.	653	12	677	8	685	10	685	10
CG-146	384	35.7	0.00E+00	12165	0.06187	0.00048	0.95684	0.01163	0.112172	0.001045	0.766	2.5	.	670	17	682	6	685	6	685	6
CG-083	406	40	0.00E+00	18271	0.06197	0.00028	1.0	0.01834	0.112363	0.002084	0.971	2.1	.	673	9	683	10	686	12	686	12
CG-054	203	23.1	0.00E+00	7229	0.06218	0.00032	0.96927	0.01513	0.113064	0.00167	0.946	1.6	.	680	11	688	8	691	10	691	10
CG-011	63	5.4	0.00E+00	2764	0.06232	0.00051	0.97405	0.01648	0.113356	0.001675	0.874	1.1	.	685	17	691	8	692	10	692	10
CG-026	130	15.2	0.00E+00	4864	0.06298	0.00031	0.98509	0.01452	0.113432	0.001577	0.943	-2.2	.	708	10	696	7	693	9	693	9
CG-058	328	37.4	0.00E+00	17623	0.06103	0.0003	0.95624	0.0155	0.113633	0.001756	0.953	8.8	3.8	640	11	681	8	694	10	694	10
CG-070	447	44.9	0.00E+00	14093	0.06103	0.00026	0.95635	0.01652	0.113652	0.001903	0.969	8.8	4	640	9	681	9	694	11	694	11
CG-060	431	49.4	0.00E+00	13529	0.06126	0.00034	0.95981	0.01637	0.113626	0.001832	0.945	7.4	2	649	12	683	8	694	11	694	11
CG-139	343	32.3	0.00E+00	8158	0.06181	0.00047	0.9683	0.01176	0.113618	0.001069	0.775	4.1	.	668	16	688	6	694	6	694	6
CG-122	96	9.2	0.00E+00	924	0.06241	0.00055	0.97836	0.01276	0.113688	0.001092	0.736	0.9	.	688	18	693	7	694	6	694	6
CG-149	337	31.6	0.00E+00	13014	0.06232	0.00051	0.9795	0.01281	0.113985	0.001159	0.777	1.6	.	685	17	693	7	696	7	696	7
CG-124	425	40.6	0.00E+00	12588	0.06222	0.00047	0.97967	0.01271	0.114204	0.001202	0.811	2.4	.	682	15	693	7	697	7	697	7
CG-078	269	26.9	0.00E+00	9054	0.0616	0.00031	0.97064	0.01688	0.114281	0.001905	0.958	6	1	660	10	689	9	698	11	698	11
CG-019	144	12.5	0.00E+00	5123	0.06234	0.00043	0.98403	0.01701	0.114492	0.001814	0.917	2	.	686	14	696	9	699	10	699	10
CG-103	371	36.6	0.00E+00	16246	0.06166	0.0003	0.97504	0.01829	0.114692	0.002078	0.965	6	0.8	662	10	691	9	700	12	700	12
CG-018	356	31.6	0.00E+00	13823	0.06281	0.00039	0.99291	0.02076	0.114648	0.002289	0.955	-0.3	.	702	13	700	11	700	13	700	13
CG-042	284	33.3	0.00E+00	13300	0.06443	0.00031	1.02306	0.01528	0.115169	0.001628	0.947	-7.4	-4.1	756	10	715	8	703	9	703	9
CG-117	825	80.9	0.00E+00	38366	0.0616	0.00046	0.98802	0.01244	0.116319	0.001185	0.809	7.8	2.4	660	15	698	6	709	7	709	7
CG-094	361	36.4	0.00E+00	13088	0.06232	0.0003	1.00094	0.01884	0.116486	0.002121	0.968	3.9	.	685	10	704	10	710	12	710	12
CG-088	626	63.9	0.00E+00	30424	0.06208	0.00028	1.00715	0.01851	0.117672	0.002095	0.969	6.3	1.4	677	9	707	9	717	12	717	12
CG-071	138	14.4	0.00E+00	5330	0.06264	0.00034	1.01648	0.01842	0.117698	0.002032	0.953	3.2	.	696	11	712	9	717	12	717	12
CG-049	179	21.4	0.00E+00	8560	0.06338	0.00035	1.0297	0.0159	0.117823	0.0017	0.934	-0.5	.	721	11	719	8	718	10	718	10
CG-086	520	54	0.00E+00	25247	0.06268	0.00028	1.02348	0.01897	0.118424	0.002132	0.971	3.6	.	697	9	716	10	721	12	721	12
CG-007	81	7.3	0.00E+00	3944	0.06532	0.00045	1.07081	0.01773	0.118895	0.001794	0.911	-8.1	-3.7	785	14	739	9	724	10	724	10
CG-055	259	31	0.00E+00	10588	0.06295	0.00032	1.03363	0.01618	0.119088	0.001766	0.947	2.8	.	707	10	721	8	725	10	725	10
CG-141	105	10.5	0.00E+00	5179	0.06436	0.00056	1.07092	0.0139	0.120689	0.001169	0.746	-2.6	.	753	17	739	7	735	7	735	7
CG-107	438	45.6	0.00E+00	19322	0.06389	0.00032	1.06658	0.02061	0.121069	0.002261	0.967	-0.2	.	738	10	737	10	737	13	737	13
CG-085	103	10.9	0.00E+00	3965	0.06421	0.00035	1.07435	0.01948	0.12136	0.002101	0.955	-1.4	.	748	11	741	10	738	12	738	12
CG-119	242	25.5	0.00E+00	16446	0.06468	0.0005	1.11459	0.01366	0.124984	0.001191	0.777	-0.7	.	764	16	760	7	759	7	759	7

Table 13 Raw data of concordant and disconcordant U-Pb analysis of all samples.

Name	ppm U	^{206}Pb	$^{206}Pb_c$(%)	206/204	Ratios $^{207}Pb/^{206}Pb^*$	1SE	$^{207}Pb/^{235}U^*$	1SE	$^{206}Pb/^{238}U^*$	1SE	Rho	Discordance Central (%)	Minimum rim (%)		Ages 207/206	1σ	207/235	1σ	206/238	1σ		Preferred Age	1σ
CG-036	44	5.7	0.00E+00	2393	0.06584	0.0004	1.14952	0.01879	0.12662	0.001919	0.927	-4.3	-0.2		801	12	777	9	769	11		769	11
CG-082	55	6.1	0.00E+00	1754	0.06628	0.0004	1.15993	0.02082	0.126923	0.002144	0.941	-5.9	-1.8		815	12	782	10	770	12		770	12
CG-043	305	39.5	0.00E+00	12760	0.06509	0.00031	1.14039	0.01718	0.127074	0.001819	0.95	-0.8	.		777	10	773	8	771	10		771	10
CG-144	31	3.3	0.00E+00	1032	0.06646	0.00067	1.16409	0.0178	0.12704	0.001466	0.755	-6.4	-0.6		821	20	784	8	771	8		771	8
CG-052	373	48.3	0.00E+00	15172	0.06407	0.0003	1.13439	0.01753	0.128412	0.001888	0.952	5	0.7		744	10	770	8	779	11		779	11
CG-020	397	39.4	0.00E+00	17175	0.06469	0.00039	1.14993	0.02373	0.128922	0.002545	0.956	2.4	.		764	12	777	11	782	15		782	15
CG-001	101	10	0.00E+00	6491	0.06433	0.00042	1.15512	0.01786	0.130221	0.001826	0.907	5.1	0.2		753	14	780	8	789	10		789	10
CG-050	34	4.5	0.00E+00	2788	0.06758	0.00047	1.21433	0.02147	0.130329	0.002116	0.918	-8.2	-3.9		856	14	807	10	790	12		790	12
CG-010	79	7.7	0.00E+00	4287	0.06732	0.00046	1.22415	0.01982	0.131875	0.001936	0.906	-6.2	-1.9		848	14	812	9	799	11		799	11
CG-059	234	31.1	0.00E+00	9666	0.06481	0.00032	1.18546	0.01987	0.132655	0.002126	0.956	4.8	0.4		768	10	794	9	803	12		803	12
CG-072	333	39.6	0.00E+00	24983	0.06581	0.0003	1.21378	0.02207	0.133756	0.002357	0.969	1.2	.		800	9	807	10	809	13		809	13
CG-102	143	17	0.00E+00	5202	0.06654	0.00034	1.25619	0.02491	0.136913	0.002624	0.966	0.5	.		824	10	826	11	827	15		827	15
CG-127	103	12	0.00E+00	8821	0.067	0.0006	1.2798	0.0176	0.138542	0.001449	0.761	-0.2	.		838	18	837	8	836	8		836	8
CG-092	322	39	0.00E+00	6982	0.06683	0.00031	1.28381	0.02571	0.139329	0.002717	0.974	1.1	.		832	9	839	11	841	15		841	15
CG-134	448	53	0.00E+00	12196	0.06781	0.00052	1.32461	0.01584	0.141679	0.001303	0.769	-1.1	.		863	15	857	7	854	7		854	7
CG-035	42	6.4	0.00E+00	2237	0.07167	0.00048	1.47301	0.02417	0.149059	0.002236	0.914	-8.9	-5.3		977	13	919	10	896	13		896	13
CG-132	269	36.7	0.00E+00	14295	0.07198	0.00056	1.61777	0.02151	0.162999	0.001754	0.810	-1.3	.		985	16	977	8	973	10		973	10
CG-077	178	26.8	0.00E+00	14779	0.0722	0.00034	1.68623	0.03165	0.169392	0.00308	0.969	1.9	.		992	9	1003	12	1009	17		992	9
CG-098	52	12.7	0.00E+00	3460	0.10373	0.00066	3.91389	0.09149	0.273646	0.006158	0.963	-8.8	-6.5		1692	11	1617	19	1559	31		1692	11
CG-131	439	116	0.00E+00	37722	0.11429	0.00106	4.88557	0.07098	0.310044	0.003478	0.772	-7.8	-5		1869	16	1800	12	1741	17		1869	16
CG-012	120	29.7	0.00E+00	10144	0.11781	0.00095	5.18402	0.1071	0.319144	0.006075	0.921	-8.2	-5.5		1923	14	1850	18	1786	30		1923	14
CG-041	390	131.5	0.00E+00	50528	0.11687	0.00067	5.32926	0.10525	0.330711	0.006253	0.957	-4	-2		1909	10	1874	17	1842	30		1909	10
CG-025	761	264.2	0.00E+00	88752	0.11643	0.00073	5.39505	0.10825	0.336058	0.006409	0.951	-2.1	.		1902	11	1884	17	1868	31		1902	11
CG-028	124	44.2	0.00E+00	15879	0.11974	0.00069	5.68676	0.11592	0.344443	0.006733	0.959	-2.6	-0.6		1952	10	1929	18	1908	32		1952	10
CG-075	283	91.5	0.00E+00	36101	0.12294	0.00067	5.9	0.15292	0.349941	0.008818	0.977	-3.8	-1.9		1999	10	1966	22	1934	42		1999	10
CG-056	244	88.2	0.00E+00	42768	0.11739	0.00068	5.80947	0.1195	0.358914	0.007087	0.96	3.6	.		1917	10	1948	18	1977	34		1917	10
CG-114	203	64.4	0.00E+00	30468	0.12747	0.00129	6.43368	0.10937	0.366064	0.004995	0.803	-3	.		2063	17	2037	15	2011	24		2063	17
CG-034	377	144.8	0.00E+00	40547	0.12627	0.00075	6.51228	0.13798	0.37405	0.007609	0.96	0.1	.		2047	10	2048	19	2048	36		2047	10
CG-064	355	134.8	0.00E+00	61225	0.12324	0.00082	6.38622	0.14505	0.375841	0.008164	0.956	3.1	.		2004	11	2030	20	2057	38		2004	11
CG-129	313	113.2	0.00E+00	41077	0.16112	0.00184	9.29538	0.16387	0.418411	0.005611	0.761	-10.3	-7.4		2468	19	2368	16	2253	25		2468	19
CG-084	99	40.6	0.00E+00	18419	0.16764	0.00114	10.08817	0.29484	0.436443	0.012404	0.972	-9.4	-7.4		2534	11	2443	27	2335	56		2534	11
CG-125	16	6.3	0.00E+00	2071	0.17367	0.00215	10.83438	0.22138	0.452465	0.00735	0.795	-8.6	-5.5		2593	20	2509	19	2406	33		2593	20
CG-097	274	126	0.00E+00	59038	0.17912	0.00136	12.10518	0.37895	0.490158	0.014884	0.97	-3.4	-1.1		2645	12	2613	29	2571	64		2645	12
CG-023	413	212.8	0.00E+00	45990	0.18099	0.00155	12.48859	0.32211	0.500453	0.012172	0.943	-2.1	.		2662	14	2642	24	2616	52		2662	14
CG-062	183	10.7	0.00E+00	160258	0.06057	0.00038	0.48528	0.00938	0.058111	0.001064	0.947	-42.8	-39.6		624	14	402	6	364	6		364	6
CG-100	236	13.5	0.00E+00	3545	0.06454	0.00037	0.59843	0.01157	0.067247	0.001242	0.955	-46.2	-43.9		759	11	476	7	420	8		420	8
CG-105	730	44.7	0.00E+00	4731	0.06389	0.00039	0.63207	0.01363	0.071747	0.001484	0.959	-40.9	-38.1		738	13	497	8	447	9		447	9
CG-045	185	13.5	0.00E+00	4008	0.06151	0.00035	0.61015	0.01031	0.071941	0.001146	0.943	-33	-29.8		657	12	484	6	448	7		448	7
CG-024	93	7.4	0.00E+00	2566	0.07714	0.00112	0.8131	0.01658	0.076446	0.001091	0.700	-59.9	-57.2		1125	28	604	9	475	7		475	7
CG-057	761	60.9	0.00E+00	1997	0.06708	0.00036	0.73244	0.01213	0.079196	0.00124	0.946	-43.1	-41		840	12	558	7	491	7		491	7
CG-033	112	9.3	0.00E+00	2721	0.06114	0.00034	0.68035	0.01042	0.080708	0.001153	0.933	-23.2	-19.6		644	11	527	6	500	7		500	7
CG-073	122	9.2	0.00E+00	3302	0.06088	0.00031	0.72132	0.01287	0.085935	0.001469	0.958	-17	-13.3		635	10	551	8	531	9		531	9
CG-046	558	50.1	0.00E+00	13815	0.06654	0.00058	0.81077	0.01348	0.088377	0.001253	0.853	-35.1	-31.4		823	17	603	8	546	7		546	7
CG-068	271	23.8	0.00E+00	6905	0.06342	0.00054	0.8688	0.01665	0.099359	0.001708	0.897	-16.2	-10.8		722	18	635	9	611	10		611	10
CG-069	815	74.4	0.00E+00	22984	0.0587	0.00025	0.82714	0.01552	0.102192	0.001866	0.973	13.4	7.7		556	9	612	9	627	11		627	11
CG-148	26	2.2	0.00E+00	849	0.06307	0.00074	0.89968	0.01432	0.103463	0.001104	0.671	-11.2	-3.7		711	24	652	8	635	6		635	6
CG-115	56	5.3	0.00E+00	501	0.19434	0.01941	2.95122	0.31281	0.110141	0.003903	0.334	-79.6	-74.9		2779	156	1395	80	674	23		674	23
CG-003	500	42.5	0.00E+00	7543	0.06036	0.00039	0.93151	0.01417	0.11192	0.001541	0.906	11.5	5.6		617	14	668	7	684	9		684	9

Name	ppm U	^{206}Pb	$^{206}Pb_c$(%)	206/204	Ratios $^{207}Pb/^{206}Pb^*$	1SE	$^{207}Pb/^{235}U^*$	1SE	$^{206}Pb/^{238}U^*$	1SE	Rho	Discordance Central (%)	Minimum rim (%)		Ages 207/206	1σ	207/235	1σ	206/238	1σ		Preferred Age	1σ
CG-136	24	4.5	0.00E+00	1539	0.09349	0.00097	2.83667	0.0442	0.220052	0.002554	0.745	-15.9	-12.7		1498	19	1365	12	1282	13		1498	19
CG-087	26	5.5	0.00E+00	28	0.59582	0.01131	19.18306	0.544	0.23351	0.004919	0.743	-76.9	-75.9		4498	26	3051	27	1353	26		4498	26
CG-111	720	195.2	0.00E+00	60645	0.12486	0.00124	5.4196	0.08696	0.3148	0.003963	0.784	-14.8	-12.1		2027	18	1888	14	1764	19		2027	18
CG-101	203	80.7	0.00E+00	34628	0.17556	0.00126	10.47966	0.31729	0.43293	0.012737	0.972	-13.3	-11.4		2611	11	2478	28	2319	57		2611	11

Table 14 Raw data of concordant and disconcordant U-Pb analysis of all samples.

Name	ppm U	^{206}Pb	$^{206}Pb_c$(%)	206/204	Ratios $^{207}Pb/^{206}Pb^*$	1SE	$^{207}Pb/^{235}U^*$	1SE	$^{206}Pb/^{238}U^*$	1SE	Rho	Discordance Central (%)	Minimum rim (%)	Ages 207/206	1σ	207/235	1σ	206/238	1σ	Preferred Age	1σ
CG2-115	80	5.7	0.00E+00	3327	0.05896	0.00084	0.72343	0.01992	0.088986	0.0021	0.857	-3	.	566	31	553	12	550	12	550	12
CG2-010	285	22.3	0.00E+00	15030	0.05943	0.00049	0.75289	0.01564	0.091881	0.001753	0.919	-2.9	.	583	17	570	9	567	10	567	10
CG2-013	90	7.1	0.00E+00	3940	0.06017	0.00056	0.76359	0.02098	0.092046	0.002381	0.942	-7.2	.	610	19	576	12	568	14	568	14
CG2-143	228	15.8	0.00E+00	6538	0.05967	0.00036	0.75892	0.01111	0.092242	0.00123	0.911	-4	.	592	13	573	6	569	7	569	7
CG2-081	224	15.5	0.00E+00	6981	0.0597	0.00029	0.77241	0.00932	0.093842	0.001034	0.913	-2.5	.	593	10	581	5	578	6	578	6
CG2-076	33	2.3	0.00E+00	1152	0.05981	0.00045	0.77608	0.01073	0.094102	0.001088	0.836	-3	.	597	16	583	6	580	6	580	6
CG2-040	175	14.2	0.00E+00	8456	0.0603	0.00063	0.78993	0.01045	0.095003	0.000781	0.621	-5	.	615	22	591	6	585	5	585	5
CG2-036	432	34.7	0.00E+00	12750	0.05893	0.00057	0.8	0.00937	0.095208	0.000697	0.604	4.1	.	564	20	582	5	586	4	586	4
CG2-058	318	22.8	0.00E+00	8348	0.05981	0.00024	0.78509	0.009	0.095207	0.001019	0.934	-1.8	.	597	9	588	5	586	6	586	6
CG2-037	75	6	0.00E+00	2980	0.05973	0.00066	0.78449	0.01068	0.095263	0.000761	0.587	-1.3	.	594	22	588	6	587	4	587	4
CG2-044	270	19.7	0.00E+00	12100	0.05929	0.00025	0.78104	0.00896	0.095546	0.001021	0.931	1.9	.	578	9	586	5	588	6	588	6
CG2-101	318	24.8	0.00E+00	7867	0.06008	0.00075	0.79888	0.02189	0.096444	0.002351	0.890	-2.2	.	606	27	596	12	594	14	594	14
CG2-048	129	9.5	0.00E+00	2085	0.05977	0.00028	0.79783	0.00928	0.096813	0.001031	0.915	0.1	.	595	9	596	5	596	6	596	6
CG2-118	180	13.8	0.00E+00	9862	0.05923	0.00078	0.79447	0.0218	0.09728	0.002344	0.878	4.2	.	576	28	594	12	598	14	598	14
CG2-089	48	3.5	0.00E+00	1549	0.06055	0.00049	0.81477	0.01164	0.097594	0.001145	0.821	-3.9	.	623	17	605	7	600	7	600	7
CG2-100	198	15.8	0.00E+00	6740	0.06034	0.00077	0.81506	0.02251	0.097972	0.002397	0.886	-2.2	.	616	28	605	13	603	14	603	14
CG2-066	155	11.4	0.00E+00	11773	0.05986	0.00028	0.81122	0.00968	0.09828	0.001075	0.917	1	.	599	10	603	5	604	6	604	6
CG2-059	152	11.2	0.00E+00	7034	0.06011	0.00031	0.81481	0.00954	0.098307	0.00103	0.895	-0.5	.	608	11	605	5	604	6	604	6
CG2-122	226	17.5	0.00E+00	7305	0.05938	0.00079	0.80726	0.02252	0.098592	0.002422	0.881	4.5	.	581	27	601	13	606	14	606	14
CG2-079	18	1.3	0.00E+00	852	0.06041	0.00069	0.82107	0.01419	0.098569	0.001273	0.747	-2.1	.	618	26	609	8	606	7	606	7
CG2-103	1272	101.7	0.00E+00	39254	0.05901	0.00073	0.80322	0.02229	0.098722	0.002455	0.896	7.3	.	567	25	599	13	607	14	607	14
CG2-093	447	32.6	0.00E+00	16091	0.06007	0.00027	0.81742	0.0101	0.098696	0.001137	0.933	0.1	.	606	9	607	6	607	7	607	7
CG2-046	428	32.4	0.00E+00	22514	0.06019	0.00026	0.81941	0.00931	0.098738	0.001039	0.927	-0.6	.	610	9	608	5	607	6	607	6
CG2-128	172	12.8	0.00E+00	6735	0.06123	0.0004	0.83292	0.01195	0.098656	0.00126	0.891	-6.6	-1.6	647	14	615	7	607	7	607	7
CG2-007	462	39.1	0.00E+00	17490	0.05879	0.00049	0.80219	0.01708	0.098957	0.00194	0.920	9.1	1	559	18	598	10	608	11	608	11
CG2-071	109	8	0.00E+00	2515	0.06076	0.00034	0.83152	0.01046	0.099264	0.001115	0.893	-3.4	.	631	11	614	6	610	7	610	7
CG2-045	44	3.4	0.00E+00	2268	0.06052	0.00042	0.83419	0.01082	0.099972	0.001099	0.847	-1.3	.	622	15	616	6	614	6	614	6
CG2-043-c	260	19.9	0.00E+00	10244	0.06039	0.00026	0.83523	0.00916	0.100312	0.001013	0.921	-0.2	.	618	9	617	5	616	6	616	6
CG2-026	283	24	0.00E+00	12685	0.05958	0.00055	0.82459	0.01007	0.100382	0.000807	0.658	5.1	.	588	20	611	6	617	5	617	5
CG2-109	255	20.8	0.00E+00	16159	0.05984	0.00075	0.8314	0.02205	0.100768	0.002352	0.880	3.7	.	598	25	614	12	619	14	619	14
CG2-060	129	9.7	0.00E+00	3735	0.05967	0.00028	0.8	0.00928	0.101243	0.001026	0.91	5.3	1.1	592	10	615	5	622	6	622	6
CG2-021	61	5.3	0.00E+00	2987	0.06026	0.00062	0.84851	0.01063	0.102116	0.000722	0.564	2.3	.	613	21	624	6	627	4	627	4
CG2-052	265	20.5	0.00E+00	14653	0.06058	0.00024	0.85475	0.00941	0.102336	0.001048	0.930	0.6	.	624	8	627	5	628	6	628	6
CG2-098	105	9	0.00E+00	5870	0.06209	0.00087	0.87757	0.02339	0.102503	0.002324	0.851	-7.5	.	677	29	640	13	629	14	629	14
CG2-005	265	23.3	0.00E+00	11726	0.06025	0.00048	0.85707	0.01807	0.103171	0.002014	0.926	3.5	.	613	16	629	10	633	12	633	12
CG2-073	38	2.9	0.00E+00	1597	0.06114	0.0005	0.87535	0.01199	0.10383	0.00114	0.801	-1.2	.	644	17	638	6	637	7	637	7
CG2-062	25	2	0.00E+00	1203	0.06128	0.00062	0.87909	0.01319	0.104048	0.00115	0.737	-1.8	.	649	21	640	7	638	7	638	7
CG2-057	193	15.1	0.00E+00	488	0.06107	0.00029	0.8774	0.01002	0.104201	0.001084	0.911	-0.4	.	642	10	640	5	639	6	639	6
CG2-108	330	28.2	0.00E+00	9341	0.06056	0.00076	0.9	0.02341	0.105313	0.002469	0.881	3.7	.	623	26	641	13	645	14	645	14
CG2-054	587	46.7	0.00E+00	2446	0.06219	0.00024	0.9056	0.01068	0.105608	0.001178	0.946	-5.2	-2.2	681	8	655	6	647	7	647	7
CG2-016	811	73.1	0.00E+00	33717	0.06107	0.00054	0.89626	0.01008	0.106435	0.000744	0.621	1.7	.	642	19	650	5	652	4	652	4
CG2-049	309	25	0.00E+00	8343	0.06143	0.00025	0.9026	0.01023	0.106568	0.001129	0.935	-0.2	.	654	8	653	5	653	7	653	7
CG2-031	270	24.3	0.00E+00	17854	0.06158	0.00061	0.90637	0.01126	0.106747	0.000808	0.61	-0.9	.	660	19	655	6	654	5	654	5
CG2-084	230	18.1	0.00E+00	11538	0.06155	0.00029	0.90978	0.01137	0.107202	0.001243	0.928	-0.3	.	659	10	657	6	656	7	656	7
CG2-051	166	13.5	0.00E+00	4053	0.06179	0.00028	0.9	0.0103	0.10749	0.001104	0.913	-1.4	.	667	10	660	5	658	6	658	6
CG2-083	194	15.5	0.00E+00	18895	0.06189	0.00031	0.91939	0.01133	0.107745	0.001211	0.912	-1.7	.	670	10	662	6	660	7	660	7
CG2-099	272	24.2	0.00E+00	10157	0.06248	0.00079	0.93044	0.02471	0.108008	0.002524	0.880	-4.5	.	691	26	668	13	661	15	661	15
CG2-001	273	24.9	0.00E+00	39583	0.06117	0.0004	0.91265	0.01985	0.108216	0.002244	0.953	2.8	.	645	14	658	11	662	13	662	13
CG2-002	286	26.3	0.00E+00	17058	0.0614	0.00039	0.91847	0.02051	0.108495	0.002321	0.958	1.7	.	653	13	662	11	664	13	664	13

Table 15 Raw data of concordant and disconcordant U-Pb analysis of all samples.

Name	ppm U	^{206}Pb	$^{206}Pb_c$ (%)	206/204	Ratios $^{207}Pb/^{206}Pb^*$	1SE	$^{207}Pb/^{235}U^*$	1SE	$^{206}Pb/^{238}U^*$	1SE	Rho	Discordance Central (%)	Minimum rim (%)			Ages 207/206	1σ	207/235	1σ	206/238	1σ		Preferred Age	1σ
CG2-113	330	28.7	0.00E+00	16159	0.06072	0.00078	0.91286	0.02511	0.109031	0.00265	0.883	6.3	.			629	27	659	13	667	15		667	15
CG2-136	567	46.9	0.00E+00	19412	0.06123	0.00037	0.92512	0.01306	0.109579	0.001399	0.904	3.7	.			647	13	665	7	670	8		670	8
CG2-135	121	10	0.00E+00	5585	0.06209	0.00044	0.93911	0.01368	0.109694	0.001397	0.875	-1	.			677	15	672	7	671	8		671	8
CG2-094	783	64.4	0.00E+00	26585	0.06144	0.00023	0.94238	0.0129	0.111247	0.001463	0.961	4.1	0.3			655	8	674	7	680	8		680	8
CG2-111	45	4	0.00E+00	2341	0.06206	0.00089	0.9555	0.02802	0.111668	0.002853	0.871	1	.			676	30	681	15	682	17		682	17
CG2-047	289	24.5	0.00E+00	17545	0.06216	0.00027	0.95981	0.01139	0.111993	0.001235	0.929	0.7	.			680	9	683	6	684	7		684	7
CG2-124	274	24.8	0.00E+00	22215	0.0617	0.00082	0.97555	0.02738	0.114664	0.002834	0.881	5.7	.			664	27	691	14	700	16		700	16
CG2-114	87	8.1	0.00E+00	3082	0.06271	0.00086	1.02396	0.02969	0.118426	0.003029	0.882	3.5	.			698	28	716	15	721	17		721	17
CG2-074	149	13.3	0.00E+00	8182	0.06398	0.00029	1.05938	0.01331	0.120098	0.001405	0.931	-1.4	.			741	9	734	7	731	8		731	8
CG2-102	325	31.9	0.00E+00	9442	0.0639	0.00081	1.06067	0.03058	0.120393	0.003121	0.899	-0.8	.			738	25	734	15	733	18		733	18
CG2-145	241	22.2	0.00E+00	11182	0.06275	0.00039	1.04578	0.01696	0.120873	0.00181	0.924	5.4	0.3			700	12	727	8	736	10		736	10
CG2-050	428	39.2	0.00E+00	20713	0.06393	0.00026	1.06935	0.01199	0.12131	0.00127	0.933	-0.2	.			739	8	738	6	738	7		738	7
CG2-107	92	9.1	0.00E+00	3305	0.06384	0.00084	1.07345	0.03011	0.121946	0.003022	0.884	0.8	.			736	27	740	15	742	17		742	17
CG2-065	64	5.9	0.00E+00	3055	0.06401	0.00035	1.08008	0.01332	0.122379	0.001351	0.896	0.3	.			742	11	744	7	744	8		744	8
CG2-042	143	14.9	0.00E+00	5974	0.06391	0.00067	1.08587	0.01416	0.123235	0.000959	0.597	1.5	.			739	22	746	7	749	6		749	6
CG2-029	76	7.9	0.00E+00	4357	0.06441	0.00064	1.09411	0.01344	0.123199	0.000887	0.586	-0.9	.			755	20	750	7	749	5		749	5
CG2-030	186	19.6	0.00E+00	8049	0.0644	0.00064	1.10337	0.01383	0.124257	0.00095	0.61	.	.			755	19	755	7	755	5		755	5
CG2-148	288	27.2	0.00E+00	27124	0.06239	0.00038	1.06907	0.01731	0.124272	0.001867	0.928	10.4	5			688	12	738	8	755	11		755	11
CG2-091	109	10	0.00E+00	3604	0.06494	0.00033	1.11328	0.01418	0.124331	0.001452	0.917	-2.3	.			772	10	760	7	755	8		755	8
CG2-104	89	9.1	0.00E+00	5961	0.06573	0.00086	1.13968	0.03275	0.125751	0.003217	0.890	-4.6	.			798	26	772	16	764	18		764	18
CG2-082	135	12.6	0.00E+00	2404	0.06455	0.00031	1.12384	0.01451	0.126277	0.001517	0.930	1	.			760	10	765	7	767	9		767	9
CG2-006	101	10.9	0.00E+00	4219	0.06468	0.00057	1.12717	0.02456	0.126382	0.00252	0.915	0.4	.			764	18	766	12	767	14		767	14
CG2-086	54	5	0.00E+00	3498	0.06498	0.00038	1.13265	0.01538	0.126414	0.001554	0.905	-0.9	.			774	12	769	7	767	9		767	9
CG2-038	239	26	0.00E+00	8475	0.06481	0.00065	1.14306	0.01457	0.127913	0.001015	0.623	1.1	.			768	21	774	7	776	6		776	6
CG2-039	253	27.8	0.00E+00	142412	0.06613	0.0007	1.16653	0.01598	0.127943	0.001117	0.637	-4.5	.			810	22	785	7	776	6		776	6
CG2-149	285	27.8	0.00E+00	9987	0.06355	0.00038	1.12475	0.01662	0.128372	0.001736	0.915	7.6	2.8			727	12	765	8	779	10		779	10
CG2-116	155	16.1	0.00E+00	6034	0.06473	0.00086	1.2	0.03249	0.129876	0.003209	0.882	3	.			766	28	782	15	787	18		787	18
CG2-017	260	28.7	0.00E+00	306933	0.06628	0.00063	1.188	0.01439	0.129992	0.000975	0.619	-3.6	.			815	20	795	7	788	6		788	6
CG2-035	50	5.6	0.00E+00	3154	0.06601	0.00078	1.18824	0.0167	0.130561	0.001003	0.547	-2	.			807	24	795	8	791	6		791	6
CG2-019	140	15.8	0.00E+00	9687	0.06605	0.00061	1.21042	0.01473	0.132917	0.00105	0.649	-0.4	.			808	18	805	7	804	6		804	6
CG2-146	146	14.8	0.00E+00	1852	0.06509	0.00042	1.19504	0.01791	0.133152	0.001802	0.903	3.9	.			777	12	798	8	806	10		806	10
CG2-127	81	8.2	0.00E+00	4778	0.06654	0.00048	1.22465	0.01849	0.133478	0.001772	0.879	-2	.			823	14	812	8	808	10		808	10
CG2-072	83	8.2	0.00E+00	5599	0.06663	0.00037	1.22894	0.01557	0.133778	0.00152	0.896	-2.2	.			826	11	814	7	809	9		809	9
CG2-126	179	18.2	0.00E+00	5003	0.06713	0.0004	1.23842	0.01837	0.133789	0.001813	0.914	-4.1	-0.2			842	12	818	8	809	10		809	10
CG2-088	71	7.1	0.00E+00	4526	0.06709	0.00036	1.26312	0.01655	0.136541	0.001637	0.915	-2	.			841	10	829	7	825	9		825	9
CG2-131	24	2.5	0.00E+00	935	0.06759	0.00063	1.28857	0.02189	0.138259	0.001969	0.838	-2.7	.			856	18	841	10	835	11		835	11
CG2-112	86	9.5	0.00E+00	3036	0.06626	0.00091	1.26491	0.03743	0.138462	0.003625	0.885	2.8	.			814	28	830	17	836	21		836	21
CG2-129	106	11.1	0.00E+00	5840	0.06667	0.00046	1.27498	0.01878	0.138695	0.00181	0.886	1.3	.			828	14	835	8	837	10		837	10
CG2-117	284	31.8	0.00E+00	9604	0.06625	0.00088	1.28085	0.03629	0.140224	0.003512	0.884	4.2	.			814	27	837	16	846	20		846	20
CG2-123	46	5.3	0.00E+00	1549	0.06713	0.00095	1.32113	0.03908	0.142728	0.003713	0.879	2.3	.			842	28	855	17	860	21		860	21
CG2-120	217	24.7	0.00E+00	14820	0.06748	0.00091	1.33381	0.03838	0.143367	0.003649	0.884	1.4	.			852	27	861	17	864	21		864	21
CG2-022	139	17.8	0.00E+00	9426	0.06892	0.00068	1.42866	0.01778	0.150341	0.00115	0.614	0.8	.			896	20	901	7	903	6		903	6
CG2-032	663	85.1	0.00E+00	30575	0.06858	0.00067	1.43156	0.01817	0.151406	0.001218	0.634	2.8	.			886	20	902	8	909	7		909	7
CG2-055	107	12.6	0.00E+00	5050	0.0715	0.00035	1.54434	0.01905	0.156655	0.001775	0.918	-3.7	-0.9			972	10	948	8	938	10		938	10
CG2-067	33	4	0.00E+00	2163	0.07157	0.00053	1.57077	0.02178	0.159173	0.001863	0.844	-2.4	.			974	14	959	9	952	10		952	10
CG2-063	80	9.6	0.00E+00	1267	0.0715	0.00038	1.58511	0.02044	0.160795	0.00189	0.911	-1.2	.			972	11	964	8	961	10		961	10
CG2-068	85	10.3	0.00E+00	5025	0.07247	0.00035	1.61843	0.02123	0.161978	0.001978	0.931	-3.4	-0.7			999	9	977	8	968	11		968	11
CG2-069	373	45.1	0.00E+00	32478	0.0723	0.00031	1.61967	0.0196	0.162468	0.001842	0.937	-2.6	-0.2			994	8	978	8	970	10		970	10
CG2-056	129	16.5	0.00E+00	621	0.07337	0.00033	1.71797	0.02072	0.169831	0.001901	0.928	-1.4	.			1024	9	1015	8	1011	10		1024	9

Table 16 Raw data of concordant and disconcordant U-Pb analysis of all samples.

Name	ppm U	^{206}Pb	$^{206}Pb_c$(%)	206/204	Ratios $^{207}Pb/^{206}Pb^*$	1SE	$^{207}Pb/^{235}U^*$	1SE	$^{206}Pb/^{238}U^*$	1SE	Rho	Discordance Central (%)	Minimum rim (%)	Ages 207/206	1σ	207/235	1σ	206/238	1σ	Preferred Age	1σ
CG2-090	39	5	0.00E+00	3128	0.07416	0.00045	1.77308	0.02549	0.173396	0.002256	0.905	-1.6	.	1046	12	1036	9	1031	12	1046	12
CG2-053	208	27.3	0.00E+00	12435	0.0739	0.00031	1.77188	0.02124	0.173901	0.001953	0.937	-0.5	.	1039	8	1035	8	1034	11	1039	8
CG2-147	228	30.7	0.00E+00	27514	0.07171	0.00045	1.72925	0.02963	0.174894	0.00279	0.931	6.8	2.3	978	12	1019	11	1039	15	978	12
CG2-106	62	14.8	0.00E+00	5388	0.1066	0.00165	4.11425	0.14237	0.279932	0.008664	0.894	-9.8	-4.3	1742	27	1657	28	1591	44	1742	27
CG2-092	51	11.6	0.00E+00	6112	0.1082	0.0006	4.56833	0.07193	0.306223	0.004511	0.936	-3	-0.9	1769	10	1744	13	1722	22	1769	10
CG2-070	111	27.8	0.00E+00	11345	0.1149	0.00056	5.29458	0.08044	0.334217	0.00481	0.947	-1.2	.	1878	8	1868	13	1859	23	1878	8
CG2-004	463	137.4	0.00E+00	113051	0.12137	0.00125	5.79766	0.17027	0.346436	0.009523	0.936	-3.4	.	1977	18	1946	25	1918	46	1977	18
CG2-097	160	48.3	0.00E+00	22483	0.15405	0.00088	8.65446	0.157	0.407449	0.007018	0.949	-9.3	-7.6	2391	10	2302	17	2203	32	2391	10
CG2-012	136	47.7	0.00E+00	7432	0.14103	0.00146	7.93211	0.28803	0.407918	0.014199	0.959	-1.8	.	2240	17	2223	33	2205	65	2240	17
CG2-034	203	75.9	0.00E+00	34702	0.15556	0.00242	8.94092	0.17026	0.416867	0.00456	0.575	-7.9	-4.7	2408	25	2332	17	2246	21	2408	25
CG2-087	35	11.1	0.00E+00	6307	0.16222	0.00102	9.44775	0.17445	0.422394	0.007329	0.940	-9.9	-8.1	2479	10	2382	17	2271	33	2479	10
CG2-028	211	81.2	0.00E+00	30363	0.16434	0.00259	9.7	0.19061	0.429982	0.004973	0.591	-9.3	-6.1	2501	25	2411	18	2306	22	2501	25
CG2-041	396	152.7	0.00E+00	53333	0.166	0.00276	9.86844	0.20158	0.431151	0.005115	0.581	-9.8	-6.5	2518	28	2423	19	2311	23	2518	28
CG2-141	324	112	0.00E+00	35368	0.16183	0.00147	9.67341	0.22524	0.433529	0.0093	0.921	-7.4	-4.7	2475	15	2404	21	2322	42	2475	15
CG2-142	193	69.2	0.00E+00	30417	0.15645	0.00139	9.7063	0.23227	0.449977	0.009997	0.928	-1.1	.	2418	14	2407	22	2395	44	2418	14
CG2-133	112	42.3	0.00E+00	18650	0.1789	0.00186	11.61379	0.29123	0.47084	0.010748	0.91	-7.1	-4.1	2643	16	2574	23	2487	47	2643	16
CG2-018	136	59	0.00E+00	34285	0.17434	0.00275	11.52142	0.23364	0.47929	0.0061	0.628	-3.5	-0.1	2600	26	2566	19	2524	27	2600	26
CG2-025	450	200.9	0.00E+00	153047	0.17662	0.00284	12.05417	0.2468	0.494981	0.006258	0.617	-1.4	.	2621	26	2609	19	2592	27	2621	26
CG2-096	580	221	0.00E+00	94801	0.1928	0.00124	13.54314	0.27425	0.509469	0.009786	0.948	-4.9	-3.1	2766	10	2718	19	2654	42	2766	10
CG2-137	2104	67.8	0.00E+00	1512	0.0658	0.0005	0.39028	0.00665	0.043019	0.000655	0.894	-67.4	-65.7	800	16	335	5	272	4	272	4
STA-01	232	8.7	0.00E+00	2504	0.06347	0.00103	0.38518	0.00974	0.044015	0.000852	0.766	-63	-58.5	724	33	331	7	278	5	278	5
CG2-061	110	4.7	0.00E+00	3925	0.06114	0.00035	0.48571	0.01607	0.057614	0.001877	0.985	-45.2	-42.5	644	12	402	11	361	11	361	11
CG2-077	574	30.2	0.00E+00	1219	0.07215	0.00035	0.70814	0.0086	0.071187	0.000794	0.919	-57.1	-55.9	990	10	544	5	443	5	443	5
CG2-008-c	97	6.3	8.30E-01	2038	0.0669	0.00186	0.71691	0.03087	0.077724	0.002555	0.764	-43.8	-33.1	835	56	549	18	483	15	483	15
CG2-075	261	14.9	0.00E+00	10407	0.05997	0.00028	0.64659	0.01154	0.078199	0.001347	0.965	-20.2	-16.7	602	10	506	7	485	8	485	8
CG2-008	97	6.3	0.00E+00	2038	0.07383	0.00188	0.79879	0.0331	0.078472	0.002565	0.789	-55	-48.8	1037	50	596	19	487	15	487	15
CG2-003	204	14.2	0.00E+00	11639	0.06	0.00066	0.6593	0.01451	0.079693	0.00152	0.867	-18.8	-10.9	604	23	514	9	494	9	494	9
CG2-078	124	7.3	0.00E+00	296	0.11573	0.00419	1.2837	0.0504	0.08045	0.001223	0.387	-76.4	-74	1891	63	838	22	499	7	499	7
CG2-144	461	28.5	0.00E+00	5156	0.06486	0.00042	0.7	0.01117	0.082111	0.001133	0.907	-35.3	-32.3	770	13	559	7	509	7	509	7
CG2-121	54	3.6	0.00E+00	3498	0.06619	0.00098	0.779	0.02491	0.085358	0.00242	0.886	-36.4	-29.8	812	30	585	14	528	14	528	14
CG2-043-rir	896	60.8	0.00E+00	18808	0.07112	0.00067	0.86216	0.01392	0.08792	0.001155	0.814	-45.3	-42.5	961	19	631	8	543	7	543	7
CG2-024	73	5.6	0.00E+00	2829	0.06101	0.00068	0.75811	0.01111	0.090124	0.000865	0.655	-13.6	-6	640	23	573	6	556	5	556	5
CG2-064	324	22.8	0.00E+00	556	0.07339	0.0004	0.9507	0.01136	0.093947	0.000997	0.888	-45.5	-43.8	1025	11	678	6	579	6	579	6
CG2-014	143	11.4	0.00E+00	4944	0.06346	0.00063	0.82697	0.02097	0.094515	0.002205	0.92	-20.4	-14.2	724	21	612	12	582	13	582	13
CG2-134	420	30.9	0.00E+00	8397	0.06374	0.00081	0.9	0.01551	0.097524	0.001264	0.716	-19	-11.9	733	26	629	8	600	7	600	7
CG2-011	198	16.6	0.00E+00	87	0.06188	0.00053	0.83457	0.02137	0.097818	0.002363	0.943	-10.7	-4.2	670	17	616	12	602	14	602	14
CG2-150	72	5.6	0.00E+00	2357	0.06611	0.00052	0.93474	0.01522	0.102549	0.001466	0.878	-23.4	-19.3	810	16	670	8	629	9	629	9
CG2-023	263	25.2	0.00E+00	4410	0.07022	0.00077	1.08768	0.01535	0.112347	0.000989	0.624	-28	-23.8	935	22	747	7	686	6	686	6
CG2-080	283	25.7	0.00E+00	19593	0.06756	0.00033	1.1386	0.01401	0.122228	0.001381	0.919	-13.8	-11.1	855	10	772	7	743	8	743	8
CG2-033	788	83.3	0.00E+00	3569	0.07127	0.00071	1.21433	0.01768	0.123568	0.001306	0.726	-23.5	-19.5	965	20	807	8	751	7	751	7
CG2-085	155	14.3	0.00E+00	9490	0.0699	0.00041	1.22024	0.01912	0.126607	0.001843	0.929	-18	-15	925	12	810	9	768	11	768	11
CG2-130	134	17.5	0.00E+00	11632	0.17185	0.00167	4.07864	0.09558	0.172137	0.003669	0.909	-65	-63.9	2576	16	1650	19	1024	20	2576	16
CG2-140	37	7.6	0.00E+00	3291	0.14986	0.00153	5.50014	0.11246	0.266191	0.004713	0.866	-39.3	-37.3	2344	17	1901	18	1521	24	2344	17
CG2-110	597	137.8	0.00E+00	48710	0.17001	0.00343	6.3813	0.23872	0.272227	0.008572	0.842	-44.1	-40.7	2558	32	2030	33	1552	43	2558	32
CG2-009	360	109.5	0.00E+00	70861	0.15274	0.0019	7.46648	0.22471	0.354539	0.009715	0.911	-20.5	-17.3	2377	20	2169	27	1956	46	2377	20
CG2-009-c	360	109.5	0.00E+00	70861	0.15274	0.0019	7.5	0.22471	0.354539	0.009715	0.911	-20.5	-17.3	2377	20	2169	27	1956	46	2377	20
CG2-139	197	61.1	0.00E+00	53715	0.16987	0.00159	9.16143	0.20659	0.391152	0.008021	0.909	-19.6	-17.3	2556	15	2354	21	2128	37	2556	15
CG2-125	38	13.8	0.00E+00	1738	0.17474	0.00382	10.16527	0.4513	0.421922	0.016299	0.87	-15.2	-9.6	2604	35	2450	41	2269	74	2604	35

Name	ppm U	^{206}Pb	$^{206}Pb_c$(%)	206/204	Ratios $^{207}Pb/^{206}Pb^*$	1SE	$^{207}Pb/^{235}U^*$	1SE	$^{206}Pb/^{238}U^*$	1SE	Rho	Discordance Central (%)	Minimum rim (%)	Ages 207/206	1σ	207/235	1σ	206/238	1σ	Preferred Age	1σ
CG2-095	334	106.5	0.00E+00	53847	0.1661	0.00092	9.78064	0.17973	0.427066	0.007484	0.954	-10.7	-9.1	2519	9	2414	17	2292	34	2519	9
CG2-105	175	67.7	0.00E+00	28206	0.17931	0.00378	10.68729	0.51442	0.432273	0.018707	0.899	-14.8	-9.3	2647	33	2496	45	2316	84	2647	33
CG2-132	292	103.6	0.00E+00	53377	0.17645	0.00181	10.80043	0.25862	0.443934	0.009604	0.903	-11.5	-8.7	2620	16	2506	22	2368	43	2620	16
CG2-119	89	36.2	0.00E+00	13329	0.18586	0.00402	11.94069	0.56531	0.465959	0.019629	0.89	-10.7	-4.8	2706	34	2600	44	2466	86	2706	34
CG2-138	267	113.4	0.00E+00	30276	0.26405	0.00364	19.02469	0.54657	0.522556	0.013176	0.878	-20.9	-18	3271	20	3043	28	2710	56	3271	20

Table 17 Raw data of concordant and disconcordant U-Pb analysis of all samples.

Name	ppm U	^{206}Pb	$^{206}Pb_c$(%)	206/204	Ratios $^{207}Pb/^{206}Pb^*$	1SE	$^{207}Pb/^{235}U^*$	1SE	$^{206}Pb/^{238}U^*$	1SE	Rho	Discordance Central (%)	Minimum rim (%)			Ages 207/206	1σ	207/235	1σ	206/238	1σ		Preferred Age	1σ
FM-101	75	5.6	0.00E+00	1364	0.05979	0.00093	0.73353	0.01453	0.088974	0.001096	0.622	-8.2	.			596	33	559	9	549	6		549	6
FM-013	457	39.7	0.00E+00	15226	0.05834	0.00064	0.73833	0.01098	0.09178	0.000924	0.677	4.5	.			543	23	561	6	566	5		566	5
FM-096	113	9	0.00E+00	4964	0.05958	0.00089	0.76636	0.01437	0.093293	0.001063	0.608	-2.4	.			588	32	578	8	575	6		575	6
FM-131	300	28.8	0.00E+00	10145	0.06029	0.00028	0.7852	0.00715	0.094456	0.000743	0.863	-5.5	-1.8			614	10	588	4	582	4		582	4
FM-149	41	3.9	0.00E+00	1909	0.06025	0.00055	0.79107	0.01033	0.095228	0.000897	0.721	-4.5	.			613	18	592	6	586	5		586	5
FM-056	248	22.5	0.00E+00	4958	0.05939	0.00025	0.78084	0.0149	0.095363	0.001777	0.976	1.1	.			581	9	586	8	587	10		587	10
FM-042	48	4.4	0.00E+00	1980	0.05999	0.00081	0.78833	0.01339	0.095306	0.000988	0.610	-2.8	.			603	28	590	8	587	6		587	6
FM-028	178	16.1	0.00E+00	4700	0.05877	0.00068	0.77492	0.01186	0.095628	0.000955	0.653	5.6	.			559	25	583	7	589	6		589	6
FM-026	49	4.5	0.00E+00	1693	0.05917	0.00074	0.78031	0.01296	0.095651	0.00105	0.661	2.9	.			573	27	586	7	589	6		589	6
FM-119	216	17.1	0.00E+00	12574	0.0602	0.00095	0.7957	0.01706	0.095862	0.001386	0.674	-3.5	.			611	32	594	10	590	8		590	8
FM-067	225	20.5	0.00E+00	5210	0.05986	0.00026	0.79572	0.01598	0.096409	0.00189	0.976	-0.9	.			599	9	594	9	593	11		593	11
FM-081	218	20	0.00E+00	6065	0.0599	0.00026	0.8042	0.01732	0.09738	0.002054	0.979	-0.1	.			600	9	599	10	599	12		599	12
FM-068	153	14.1	0.00E+00	3131	0.06061	0.0003	0.81568	0.01648	0.0976	0.001911	0.969	-4.2	.			626	10	606	9	600	11		600	11
FM-117	119	9.7	0.00E+00	1409	0.06099	0.00098	0.82185	0.01746	0.097732	0.001353	0.652	-6.2	.			639	34	609	10	601	8		601	8
FM-124	255	25.4	0.00E+00	7975	0.05966	0.00029	0.80634	0.0074	0.098023	0.000768	0.853	2	.			591	10	600	4	603	5		603	5
FM-115	232	18.8	0.00E+00	6468	0.06087	0.00095	0.82475	0.01641	0.098263	0.001213	0.62	-5	.			635	33	611	9	604	7		604	7
FM-109	98	8.1	0.00E+00	3307	0.06096	0.00093	0.82661	0.01595	0.098347	0.001154	0.608	-5.4	.			638	32	612	9	605	7		605	7
FM-059	228	21.3	0.00E+00	9194	0.05981	0.00026	0.81343	0.01565	0.098638	0.00185	0.975	1.7	.			597	9	604	9	606	11		606	11
FM-100	699	58.1	0.00E+00	19919	0.06042	0.00089	0.82092	0.01517	0.098536	0.001099	0.604	-2.2	.			619	31	609	8	606	6		606	6
FM-103	123	10.2	0.00E+00	2995	0.06141	0.00094	0.83523	0.01656	0.098642	0.001239	0.634	-7.6	.			654	33	617	9	606	7		606	7
FM-112	85	7	0.00E+00	2177	0.06128	0.00097	0.83486	0.01705	0.098814	0.001269	0.629	-6.7	.			649	33	616	9	607	7		607	7
FM-097	131	10.9	0.00E+00	3776	0.06087	0.00093	0.83061	0.01585	0.098971	0.001129	0.598	-4.3	.			635	32	614	9	608	7		608	7
FM-049	158	14.9	0.00E+00	100	0.05999	0.00037	0.82003	0.01607	0.099142	0.001844	0.949	1.1	.			603	13	608	9	609	11		609	11
FM-048	197	18.7	0.00E+00	6213	0.06117	0.00074	0.83549	0.01396	0.099053	0.00115	0.695	-5.9	.			645	25	617	8	609	7		609	7
FM-076	199	18.7	0.00E+00	7770	0.06021	0.00026	0.82512	0.01698	0.099393	0.002	0.978	.	.			611	9	611	9	611	12		611	12
FM-007	282	26.7	0.00E+00	11581	0.06	0.00068	0.82845	0.01218	0.100148	0.000947	0.643	2.1	.			603	24	613	7	615	6		615	6
FM-004	111	10.5	0.00E+00	2727	0.0604	0.00068	0.83381	0.01206	0.100114	0.000916	0.632	-0.5	.			618	23	616	7	615	5		615	5
FM-018	309	29.5	0.00E+00	8831	0.05933	0.00067	0.8	0.01218	0.101161	0.00095	0.638	7.6	0.6			579	24	612	7	621	6		621	6
FM-021	67	6.4	0.00E+00	2219	0.06008	0.00072	0.8378	0.01415	0.10113	0.0012	0.703	2.5	.			607	25	618	8	621	7		621	7
FM-039	84	8.2	0.00E+00	4859	0.06037	0.00072	0.84367	0.01324	0.101361	0.001037	0.652	1	.			617	24	621	7	622	6		622	6
FM-085	177	16.9	0.00E+00	4196	0.06077	0.00028	0.84878	0.01835	0.101293	0.002138	0.976	-1.5	.			631	10	624	10	622	13		622	13
FM-148	112	11.6	0.00E+00	6141	0.0594	0.00039	0.83619	0.00908	0.102097	0.000879	0.792	8.1	2.8			582	14	617	5	627	5		627	5
FM-089	201	19.3	0.00E+00	5814	0.06061	0.00025	0.85352	0.01879	0.102135	0.002207	0.982	0.2	.			625	9	627	10	627	13		627	13
FM-098	515	44.6	0.00E+00	14538	0.06098	0.0009	0.86106	0.01653	0.102414	0.001251	0.636	-1.6	.			638	31	631	9	629	7		629	7
FM-055	688	67.5	0.00E+00	22792	0.06078	0.00022	0.86432	0.01647	0.103141	0.001929	0.982	0.2	.			631	8	632	9	633	11		633	11
FM-035	335	33.2	0.00E+00	10296	0.06007	0.00071	0.85587	0.01404	0.103333	0.001167	0.688	4.8	.			606	25	628	8	634	7		634	7
FM-142	1102	117.4	0.00E+00	8090	0.06046	0.00025	0.86666	0.01092	0.103962	0.001236	0.943	3	.			620	8	634	6	638	7		638	7
FM-143	115	12.2	0.00E+00	3488	0.06091	0.00037	0.87314	0.0096	0.103963	0.000947	0.829	0.2	.			636	12	637	5	638	6		638	6
FM-128	59	6.2	0.00E+00	2778	0.06148	0.00052	0.88348	0.01044	0.104218	0.000853	0.693	-2.7	.			656	18	643	6	639	5		639	5
FM-019	105	10.4	0.00E+00	4902	0.06042	0.0007	0.87194	0.01351	0.104665	0.001071	0.66	3.9	.			619	25	637	7	642	6		642	6
FM-150	245	26.1	0.00E+00	9660	0.06067	0.00029	0.8787	0.00873	0.105045	0.000913	0.874	2.7	.			628	10	640	5	644	5		644	5
FM-082	242	24	0.00E+00	12809	0.06111	0.00025	0.88707	0.01891	0.105288	0.002204	0.982	0.4	.			643	8	645	10	645	13		645	13
FM-123	131	11.4	0.00E+00	2678	0.0611	0.00095	0.88692	0.01808	0.105277	0.001388	0.646	0.4	.			643	32	645	10	645	8		645	8
FM-064	183	18.3	0.00E+00	5896	0.06109	0.00026	0.88781	0.01772	0.1054	0.002055	0.977	0.6	.			642	9	645	10	646	12		646	12
FM-090	121	12	0.00E+00	4342	0.06119	0.00029	0.8927	0.01989	0.105803	0.002305	0.978	0.4	.			646	9	648	11	648	13		648	13
FM-066	317	32.2	0.00E+00	13092	0.0626	0.00028	0.9169	0.01906	0.106225	0.002156	0.976	-6.7	-3.3			695	9	661	10	651	13		651	13
FM-088	104	10.4	0.00E+00	3938	0.06157	0.00036	0.90547	0.02	0.106657	0.002274	0.965	-1	.			659	12	655	11	653	13		653	13
FM-130	97	10.6	0.00E+00	3557	0.0621	0.00033	0.91509	0.01174	0.106874	0.001248	0.910	-3.6	.			678	11	660	6	655	7		655	7
FM-071	18	1.8	0.00E+00	1254	0.06346	0.00056	0.94236	0.02125	0.107699	0.002236	0.921	-9.4	-3.1			724	18	674	11	659	13		659	13

Table 18 Raw data of concordant and disconcordant U-Pb analysis of all samples.

Name	ppm U	^{206}Pb	$^{206}Pb_c$(%)	206/204	Ratios $^{207}Pb/^{206}Pb^*$	1SE	$^{207}Pb/^{235}U^*$	1SE	$^{206}Pb/^{238}U^*$	1SE	Rho	Discordance Central (%)	Minimum rim (%)	Ages 207/206	1σ	207/235	1σ	206/238	1σ	Preferred Age	1σ
FM-091	174	17.7	0.00E+00	6225	0.06178	0.00031	0.92164	0.02045	0.108191	0.002339	0.975	-0.7	.	667	10	663	11	662	14	662	14
FM-020	41	4.2	0.00E+00	1509	0.0614	0.0008	0.91698	0.01497	0.108311	0.001075	0.608	1.5	.	653	27	661	8	663	6	663	6
FM-118	119	10.7	0.00E+00	4624	0.0617	0.00096	0.9218	0.01811	0.108348	0.001291	0.606	-0.1	.	664	32	663	10	663	8	663	8
FM-105	420	38.3	0.00E+00	14294	0.06218	0.00093	0.93013	0.01748	0.108492	0.001244	0.61	-2.5	.	680	30	668	9	664	7	664	7
FM-060	68	7.2	0.00E+00	2548	0.06162	0.00033	0.94067	0.01843	0.110718	0.002084	0.961	2.5	.	661	11	673	10	677	12	677	12
FM-073	56	5.9	0.00E+00	1694	0.06306	0.0004	0.96362	0.02055	0.110824	0.002255	0.954	-4.9	.	710	13	685	11	678	13	678	13
FM-107	95	8.9	0.00E+00	3879	0.06362	0.00098	0.97491	0.01886	0.111137	0.00131	0.609	-7.2	.	729	31	691	10	679	8	679	8
FM-057	112	11.9	0.00E+00	5194	0.06247	0.0003	1.0	0.01881	0.111214	0.002119	0.97	-1.6	.	690	10	682	10	680	12	680	12
FM-053	499	52.9	0.00E+00	21956	0.06154	0.00023	0.9457	0.01804	0.111457	0.002086	0.981	3.7	.	658	8	676	9	681	12	681	12
FM-030	31	3.2	0.00E+00	1426	0.06274	0.00084	0.96434	0.01763	0.111469	0.001387	0.681	-2.8	.	700	28	686	9	681	8	681	8
FM-002	61	6.5	0.00E+00	1870	0.06234	0.00075	0.95845	0.01476	0.111511	0.001071	0.624	-0.6	.	686	25	682	8	682	6	682	6
FM-080	288	30.3	0.00E+00	10268	0.06206	0.00024	0.95642	0.02044	0.111769	0.002349	0.984	1.1	.	676	8	681	11	683	14	683	14
FM-038	234	24.9	0.00E+00	13424	0.06208	0.00073	0.95622	0.0148	0.111721	0.001132	0.655	0.9	.	677	24	681	8	683	7	683	7
FM-037	194	20.7	0.00E+00	8327	0.06244	0.00073	0.96167	0.01514	0.11171	0.001179	0.670	-1	.	689	23	684	8	683	7	683	7
FM-044	542	58.1	0.00E+00	68328	0.06239	0.00074	0.96331	0.0155	0.111982	0.001226	0.680	-0.5	.	688	25	685	8	684	7	684	7
FM-005	97	10.4	0.00E+00	3307	0.06233	0.00076	0.96436	0.01496	0.112219	0.001067	0.613	.	.	685	25	686	8	686	6	686	6
FM-126	193	22.2	0.00E+00	5027	0.06272	0.0003	0.97754	0.0114	0.113043	0.001204	0.913	-1.3	.	699	10	692	6	690	7	690	7
FM-137	118	13.7	0.00E+00	2768	0.06225	0.00034	0.97734	0.00984	0.113871	0.000968	0.844	1.9	.	683	11	692	5	695	6	695	6
FM-041	81	8.9	0.00E+00	2575	0.06196	0.00074	0.97589	0.01583	0.114227	0.001255	0.677	3.8	.	673	25	691	8	697	7	697	7
FM-084	89	9.5	0.00E+00	3219	0.0631	0.00035	0.99313	0.02196	0.114154	0.002444	0.968	-2.2	.	712	11	700	11	697	14	697	14
FM-065	245	26.6	0.00E+00	14744	0.0632	0.00026	1.0	0.02007	0.114221	0.002256	0.979	-2.6	.	715	9	701	10	697	13	697	13
FM-047	348	38.1	0.00E+00	11176	0.06335	0.00075	0.99723	0.01604	0.11417	0.001238	0.674	-3.4	.	720	25	702	8	697	7	697	7
FM-079	212	22.9	0.00E+00	8355	0.0625	0.00028	0.98548	0.02121	0.114352	0.002406	0.978	1	.	691	9	696	11	698	14	698	14
FM-093	274	29.5	0.00E+00	16617	0.06264	0.00028	0.9894	0.02244	0.114552	0.002549	0.981	0.5	.	696	9	698	11	699	15	699	15
FM-075	803	87.3	0.00E+00	75089	0.06196	0.00021	0.98259	0.02035	0.115014	0.00235	0.987	4.5	.	673	7	695	10	702	14	702	14
FM-022	158	17.6	0.00E+00	6188	0.06453	0.00075	1.03006	0.01691	0.115772	0.001339	0.704	-7.4	-0.1	759	23	719	8	706	8	706	8
FM-015	320	35.6	0.00E+00	17376	0.06186	0.00069	0.99562	0.01514	0.116734	0.001208	0.68	6.7	0.1	669	22	702	8	712	7	712	7
FM-140	172	20.4	0.00E+00	5119	0.06344	0.0003	1.02185	0.01178	0.116825	0.001229	0.913	-1.6	.	723	10	715	6	712	7	712	7
FM-031	28	3.1	0.00E+00	946	0.06271	0.00083	1.01773	0.01779	0.117703	0.001335	0.649	2.9	.	698	28	713	9	717	8	717	8
FM-023	562	63.5	0.00E+00	21099	0.06206	0.0007	1.01664	0.01536	0.118807	0.001202	0.67	7.4	0.9	676	23	712	8	724	7	724	7
FM-036	291	33.9	0.00E+00	13049	0.06297	0.00074	1.0601	0.01658	0.122106	0.001261	0.660	5.3	.	707	24	734	8	743	7	743	7
FM-063	72	8.5	0.00E+00	2571	0.06398	0.00042	1.09182	0.02278	0.123773	0.002451	0.949	1.6	.	741	13	749	11	752	14	752	14
FM-141	209	26.4	0.00E+00	8343	0.06453	0.00031	1.1	0.0109	0.123806	0.001074	0.877	-0.9	.	759	10	754	5	752	6	752	6
FM-138	169	21.4	0.00E+00	11869	0.06493	0.00034	1.11737	0.01078	0.124813	0.001008	0.837	-1.9	.	772	11	762	5	758	6	758	6
FM-054	259	30.9	0.00E+00	10343	0.06464	0.00027	1.113	0.02151	0.12488	0.002356	0.976	-0.6	.	763	9	760	10	759	14	759	14
FM-033	158	18.8	0.00E+00	5990	0.06345	0.00074	1.09582	0.01692	0.125249	0.001259	0.651	5.4	.	724	24	751	8	761	7	761	7
FM-011	222	26.6	0.00E+00	10083	0.06474	0.00074	1.12405	0.01664	0.125935	0.001175	0.630	-0.2	.	766	23	765	8	765	7	765	7
FM-110	49	5.2	0.00E+00	1629	0.06567	0.00109	1.2	0.02416	0.127187	0.001635	0.613	-3.2	.	796	34	778	11	772	9	772	9
FM-025	143	17.5	0.00E+00	6755	0.06337	0.00074	1.12423	0.01824	0.128659	0.00145	0.695	8.7	2	721	24	765	9	780	8	780	8
FM-134	143	18.8	0.00E+00	4664	0.06535	0.00031	1.15965	0.01112	0.128701	0.001073	0.870	-0.7	.	786	9	782	5	780	6	780	6
FM-116	95	10.2	0.00E+00	9760	0.06664	0.00108	1.1889	0.02461	0.129385	0.001659	0.619	-5.4	.	827	33	795	11	784	9	784	9
FM-062	53	6.7	0.00E+00	4492	0.0656	0.00035	1.1993	0.02509	0.132588	0.002682	0.967	1.2	.	794	11	800	12	803	15	803	15
FM-095	182	20.6	0.00E+00	3748	0.06701	0.00102	1.22787	0.02456	0.13289	0.00173	0.651	-4.3	.	838	31	813	11	804	10	804	10
FM-122	793	88.1	0.00E+00	33652	0.06524	0.00101	1.21123	0.02445	0.134659	0.001746	0.642	4.4	.	782	31	806	11	814	10	814	10
FM-086	118	15	0.00E+00	7540	0.06667	0.00029	1.23897	0.02749	0.134772	0.002931	0.980	-1.6	.	828	9	818	12	815	17	815	17
FM-009	212	27.3	0.00E+00	9366	0.06697	0.00078	1.24993	0.01903	0.135374	0.001325	0.643	-2.3	.	837	25	823	9	818	8	818	8
FM-070	544	70.1	0.00E+00	25230	0.0661	0.00023	1.23569	0.02561	0.135592	0.002772	0.986	1.4	.	809	7	817	12	820	16	820	16
FM-040	71	9.3	0.00E+00	2963	0.06657	0.00083	1.24627	0.02062	0.135781	0.001481	0.659	-0.5	.	824	25	822	9	821	8	821	8
FM-003	130	17	0.00E+00	6265	0.06732	0.00079	1.28135	0.01981	0.138048	0.00138	0.647	-1.8	.	848	24	837	9	834	8	834	8

Name	ppm U	^{206}Pb	$^{206}Pb_c$(%)	206/204	Ratios $^{207}Pb/^{206}Pb^*$	1SE	$^{207}Pb/^{235}U^*$	1SE	$^{206}Pb/^{238}U^*$	1SE	Rho	Discordance Central (%)	Minimum rim (%)	Ages 207/206	1σ	207/235	1σ	206/238	1σ	Preferred Age	1σ
FM-050	539	192.5	0.00E+00	61036	0.17319	0.00095	8.69924	0.24693	0.364294	0.010147	0.981	-26.3	-25.1	2589	9	2307	26	2002	48	2589	9
FM-001	45	16.2	0.00E+00	5608	0.16204	0.00305	8.18827	0.19551	0.366488	0.005375	0.614	-21.8	-18.4	2477	32	2252	22	2013	25	2477	32
FM-121	523	167.4	0.00E+00	61261	0.1705	0.00396	8.96301	0.2625	0.381269	0.006813	0.610	-21.9	-17.8	2563	37	2334	27	2082	32	2563	37

Table 19 Overview of youngest grains and youngest clusters with content of concordant grains within each age.

Sample	Concordant ages	Type	Youngest grain	Youngest cluster	Cadomian	Lower Neoproterozoic	'Rodinia'	Late Paleoproterozoic	Early Paleoproterozoic	Late Archean	Older
					560-650	700-950	1000-1200	1,8-2,1	2,2-2,5	2,5-2,8	<2,8
HE1 bottom*	n=152	mixed sample	524 Ma	547 Ma**	68.4	3.9	0.7	5.3	2.0	2.6	0.7
CB	n=122	quartz-arenite	581 Ma	587 Ma**	21.3	35.2	3.3	8.2	3.3	1.6	0.8
FM	n=128	arenite	549 Ma	585 Ma**	34.4	30.5	3.1	2.3	1.6	2.3	0.0
CG2	n=117	quartz-arenite	550 Ma	568 Ma**	33.3	32.5	2.6	1.7	6.0	4.3	0.0
CG	n=132	friable quiartz-arenite	566 Ma	569 Ma**	31.1	23.5	0.0	6.1	2.3	1.5	0.0
HE3 top*	n=123	mixed sample	542 Ma	546 Ma**	30.1	4.9	0.0	34.1	5.7	8.1	8.1

8.3 CL images of all analyzed zircon grains

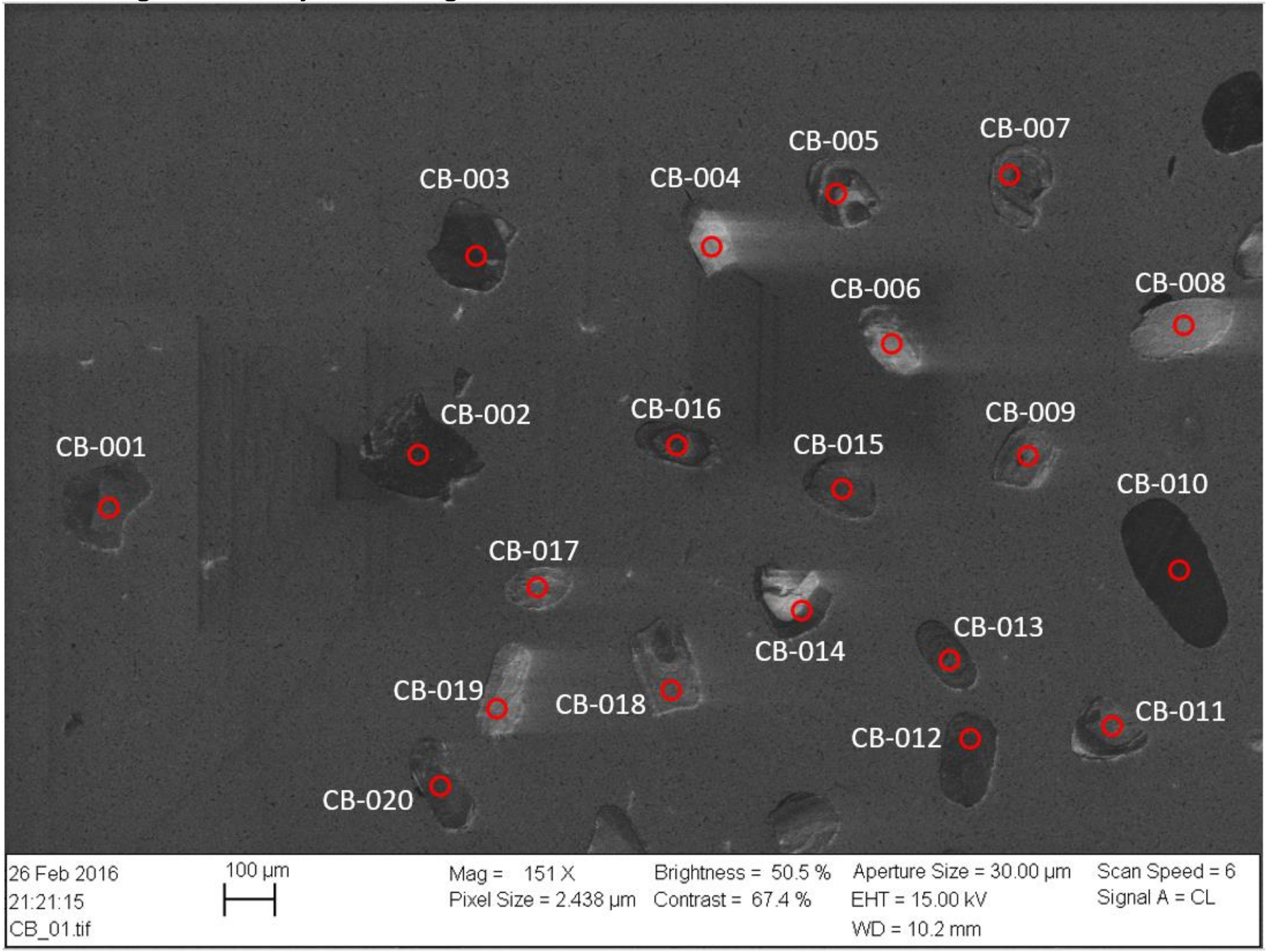

Figure 29 CL image overview of dated zircon grains.

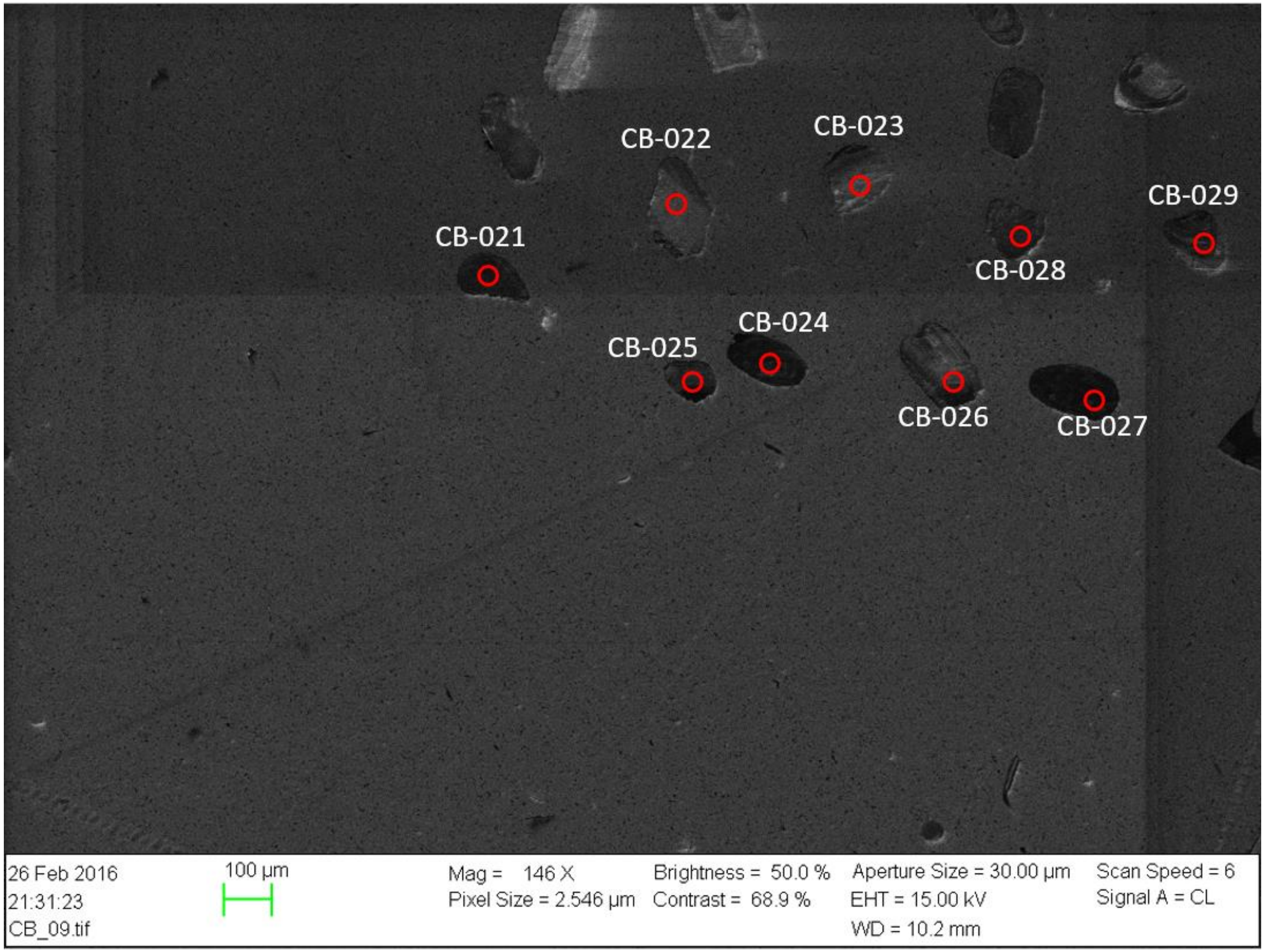

Figure 30 CL image overview of dated zircon grains.

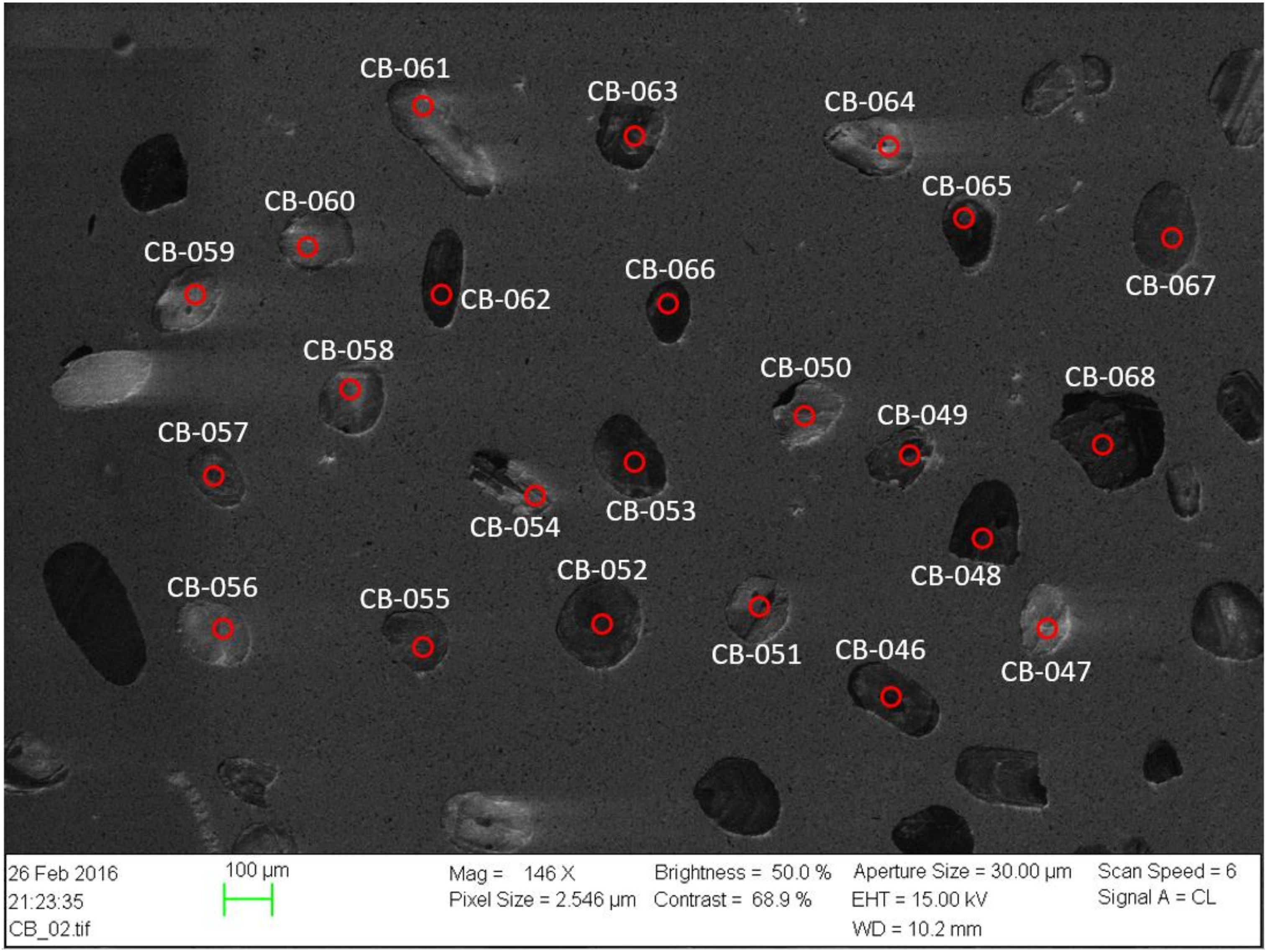

Figure 31 CL image overview of dated zircon grains.

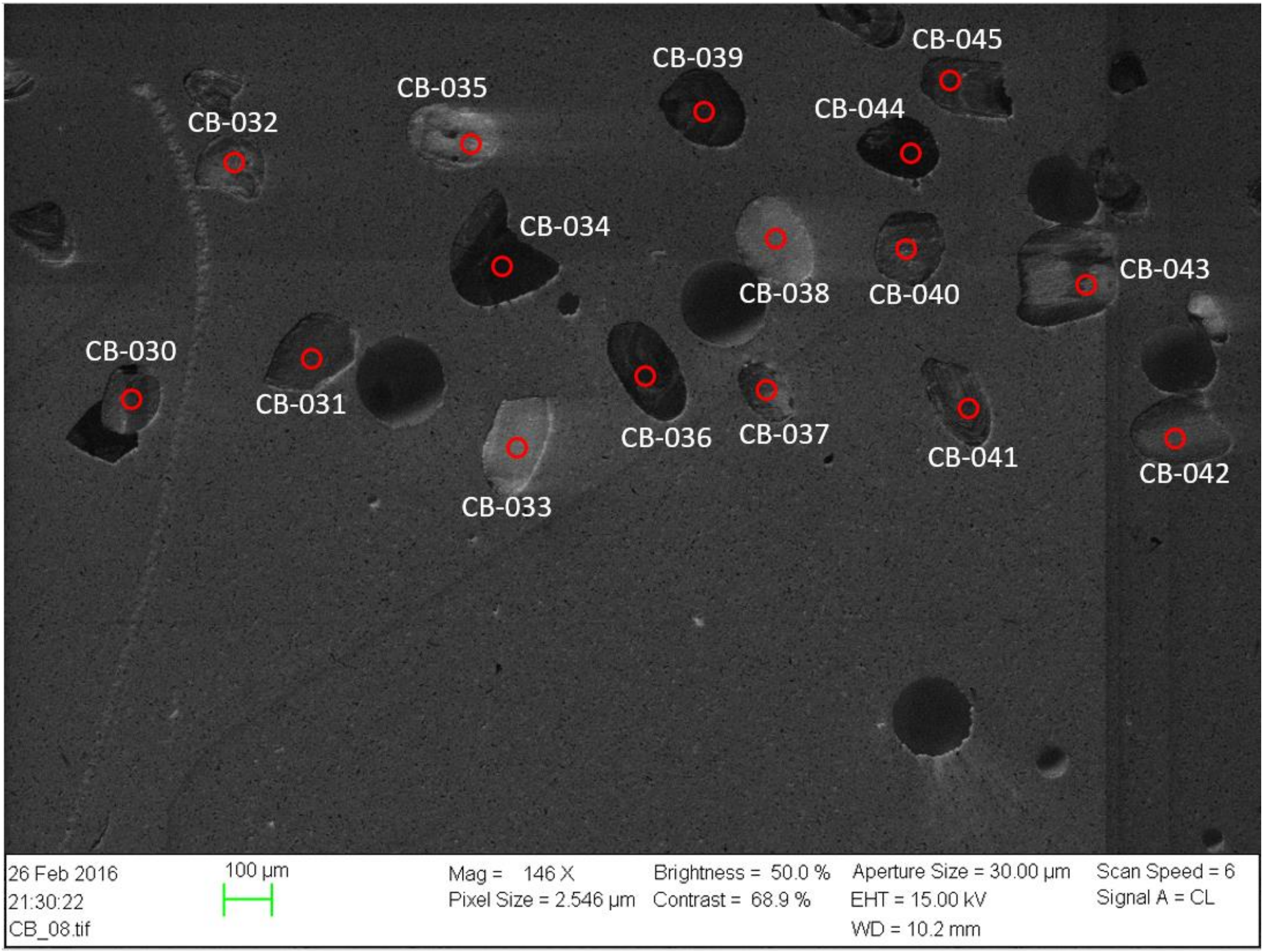

Figure 32 CL image overview of dated zircon grains.

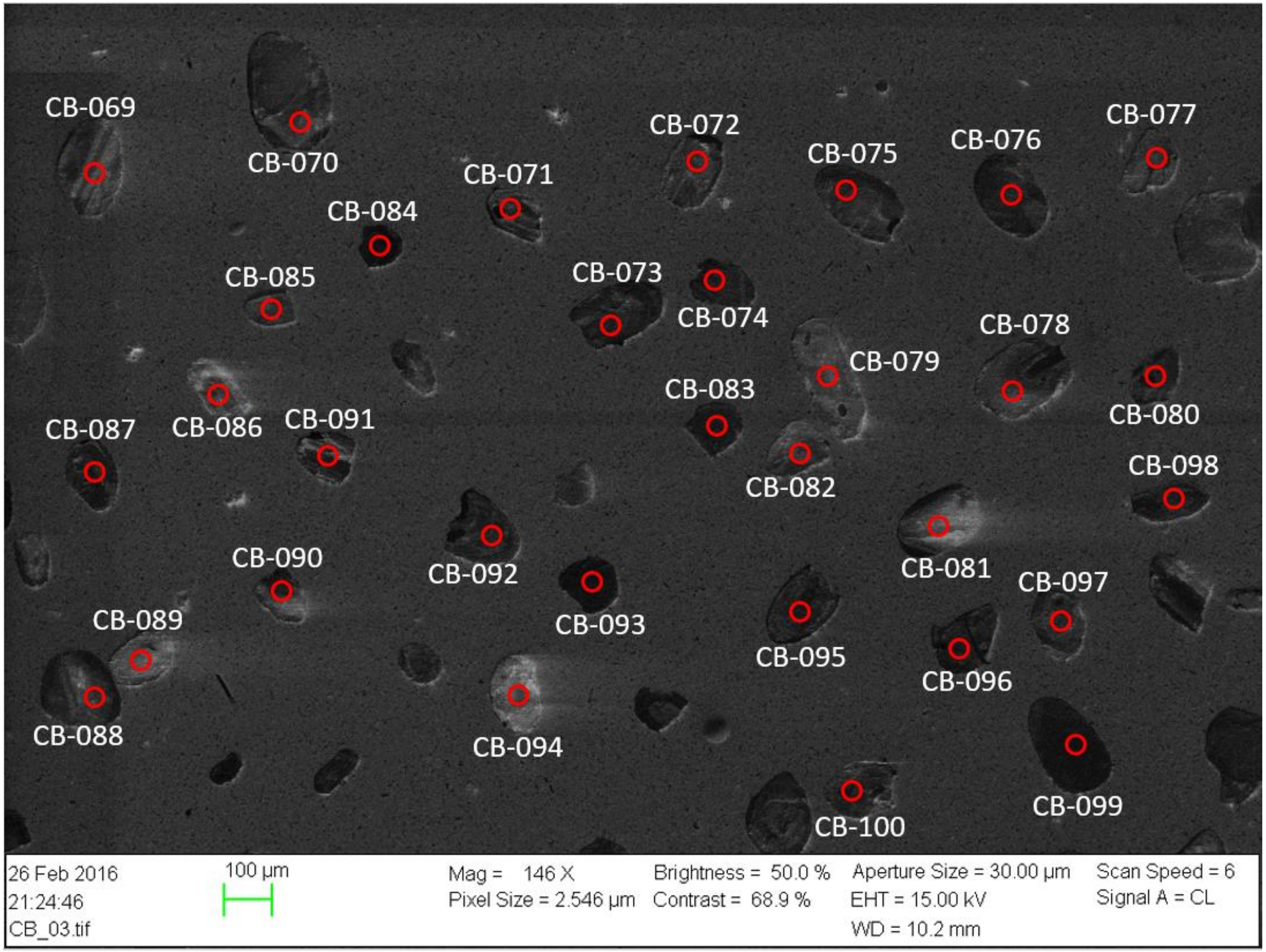

Figure 33 CL image overview of dated zircon grains.

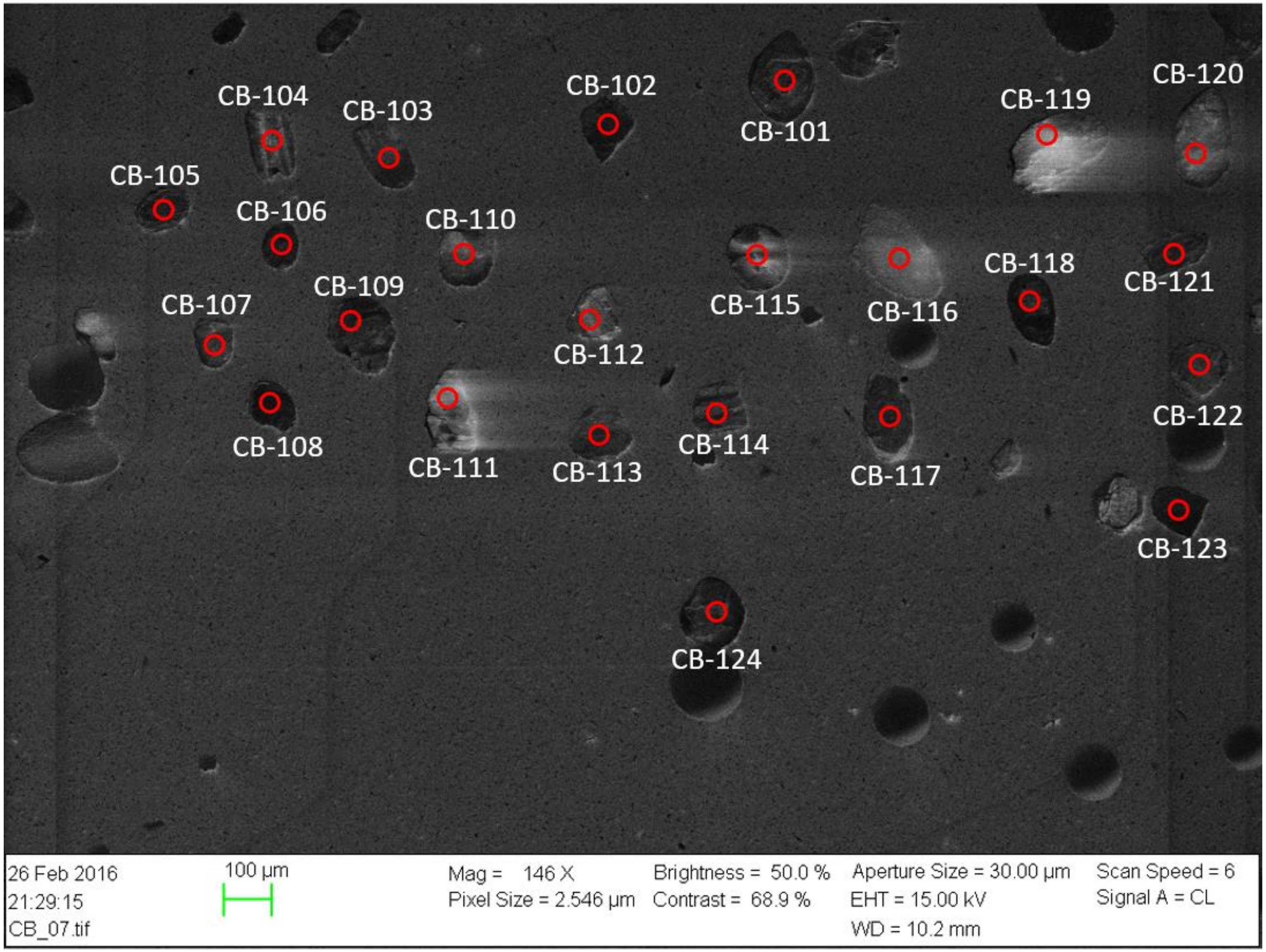

Figure 34 CL image overview of dated zircon grains.

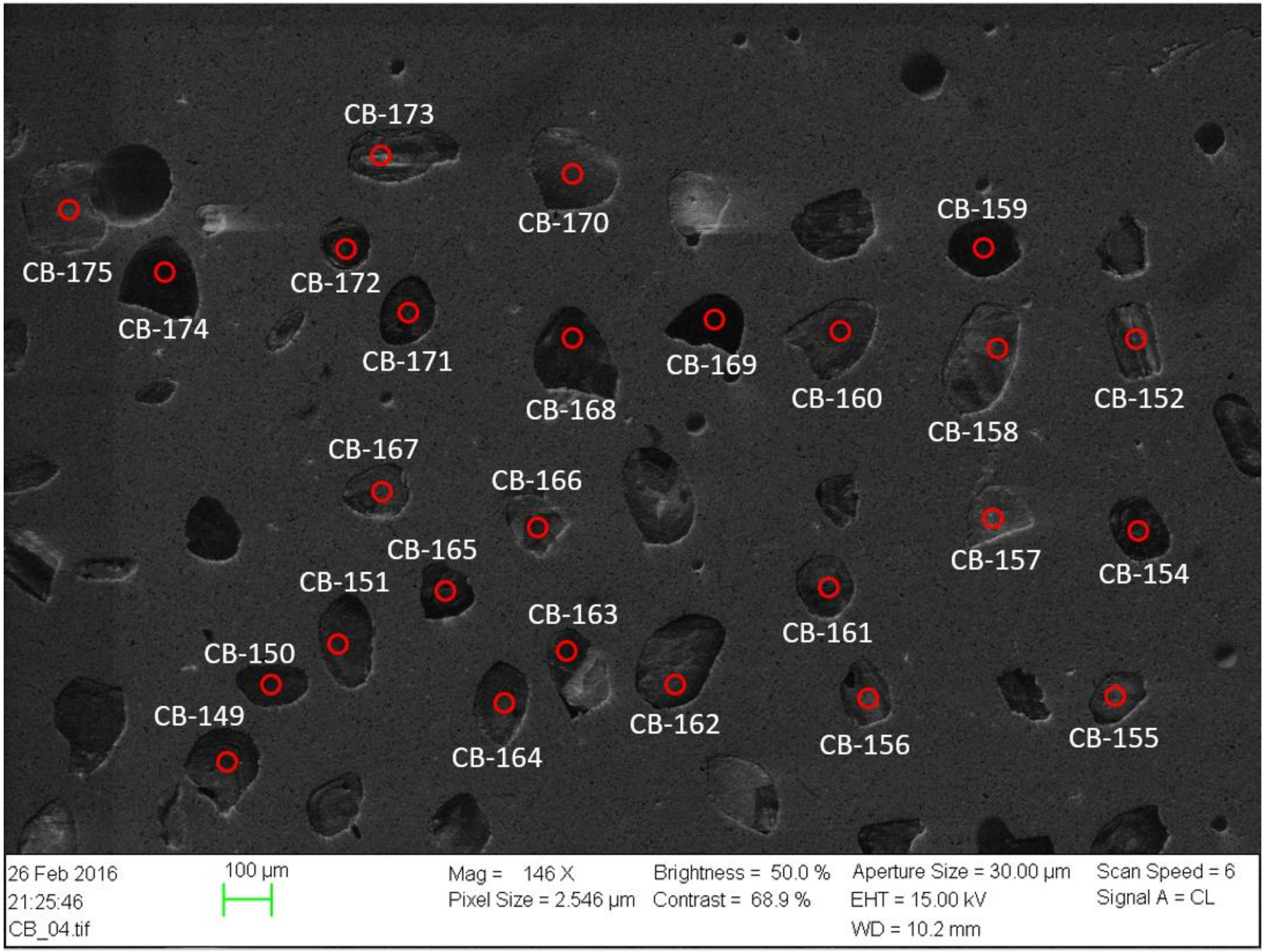

Figure 35 CL image overview of dated zircon grains.

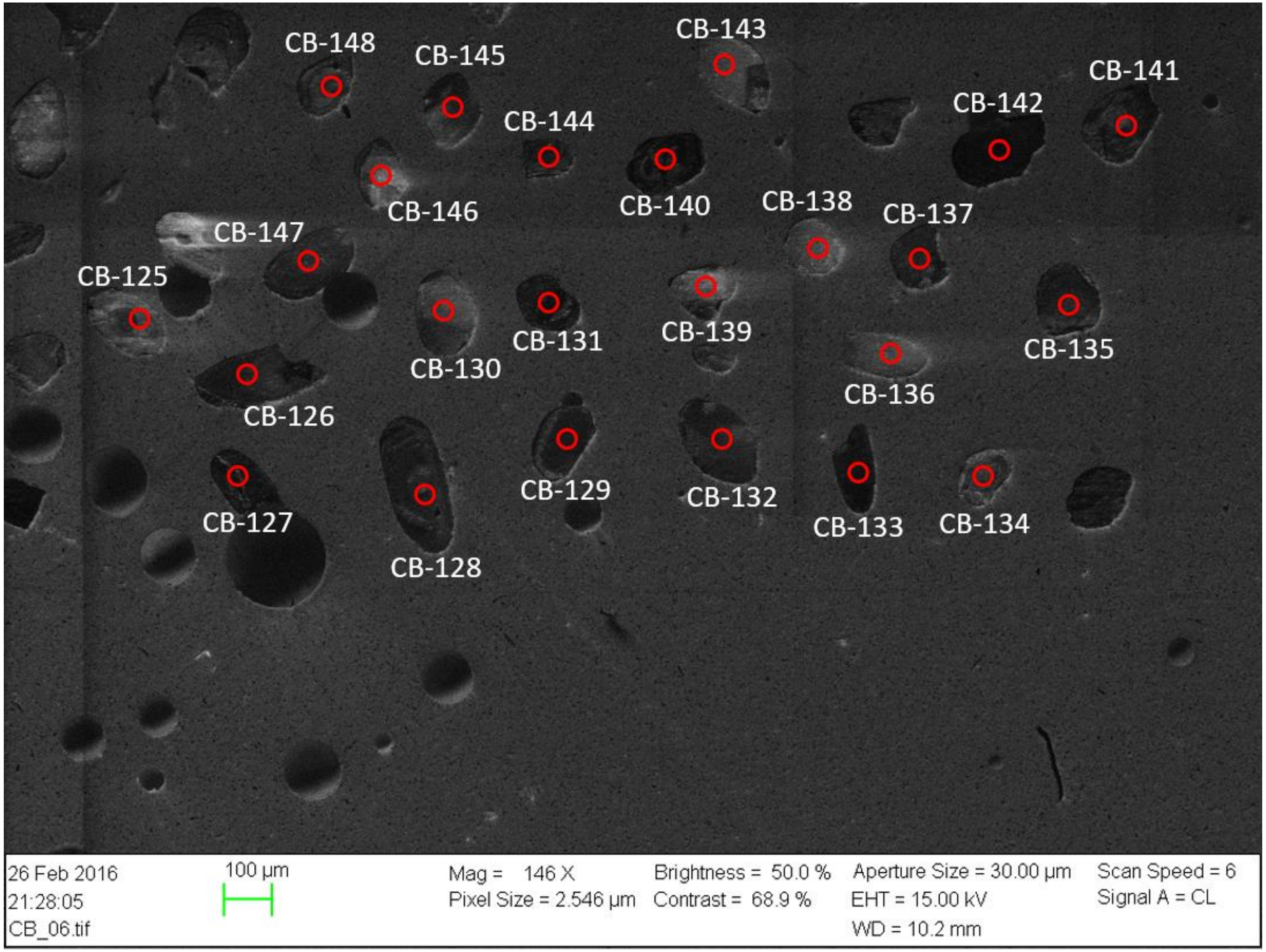

Figure 36 CL image overview of dated zircon grains.

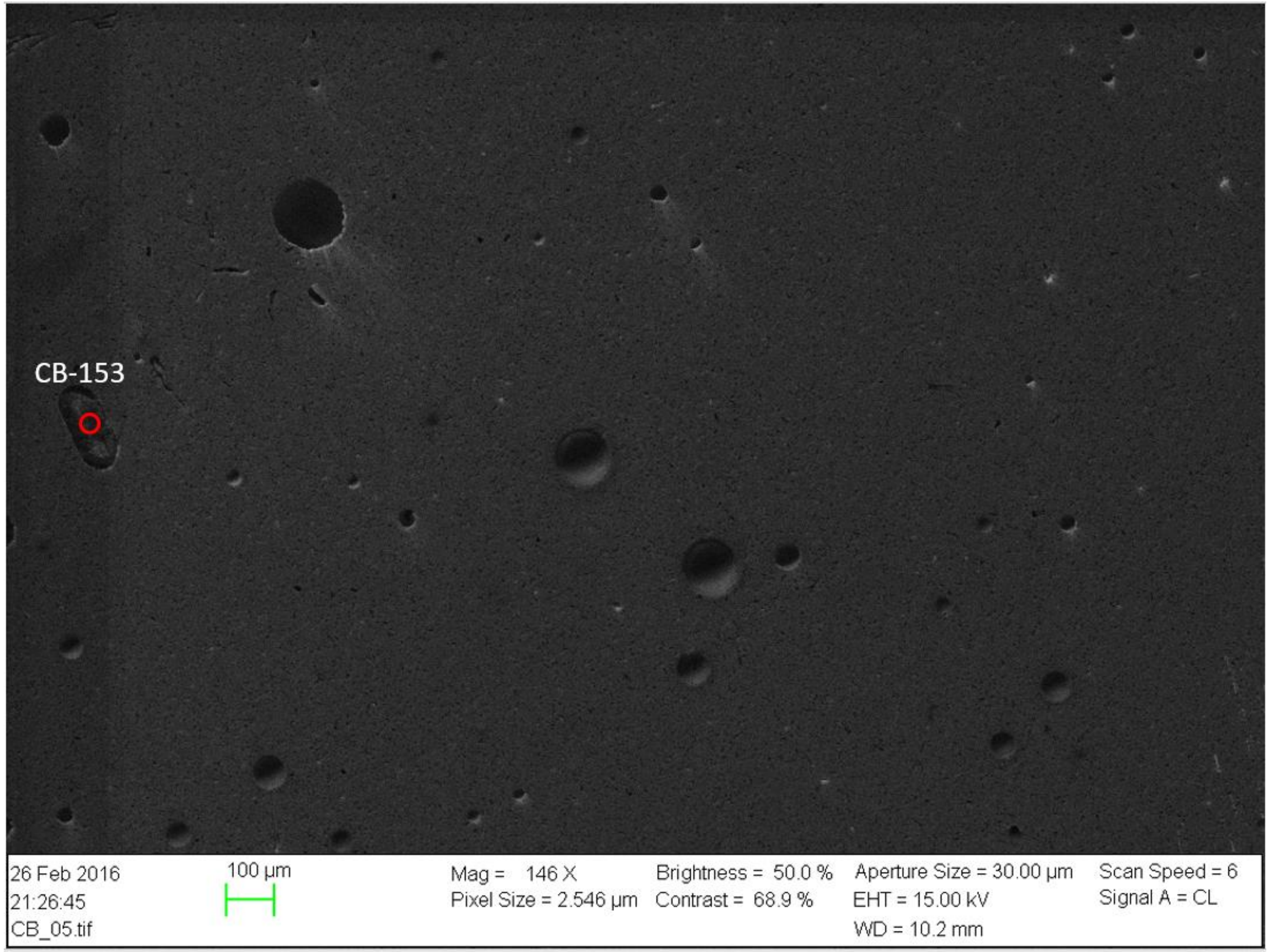

Figure 37 CL image overview of dated zircon grains.

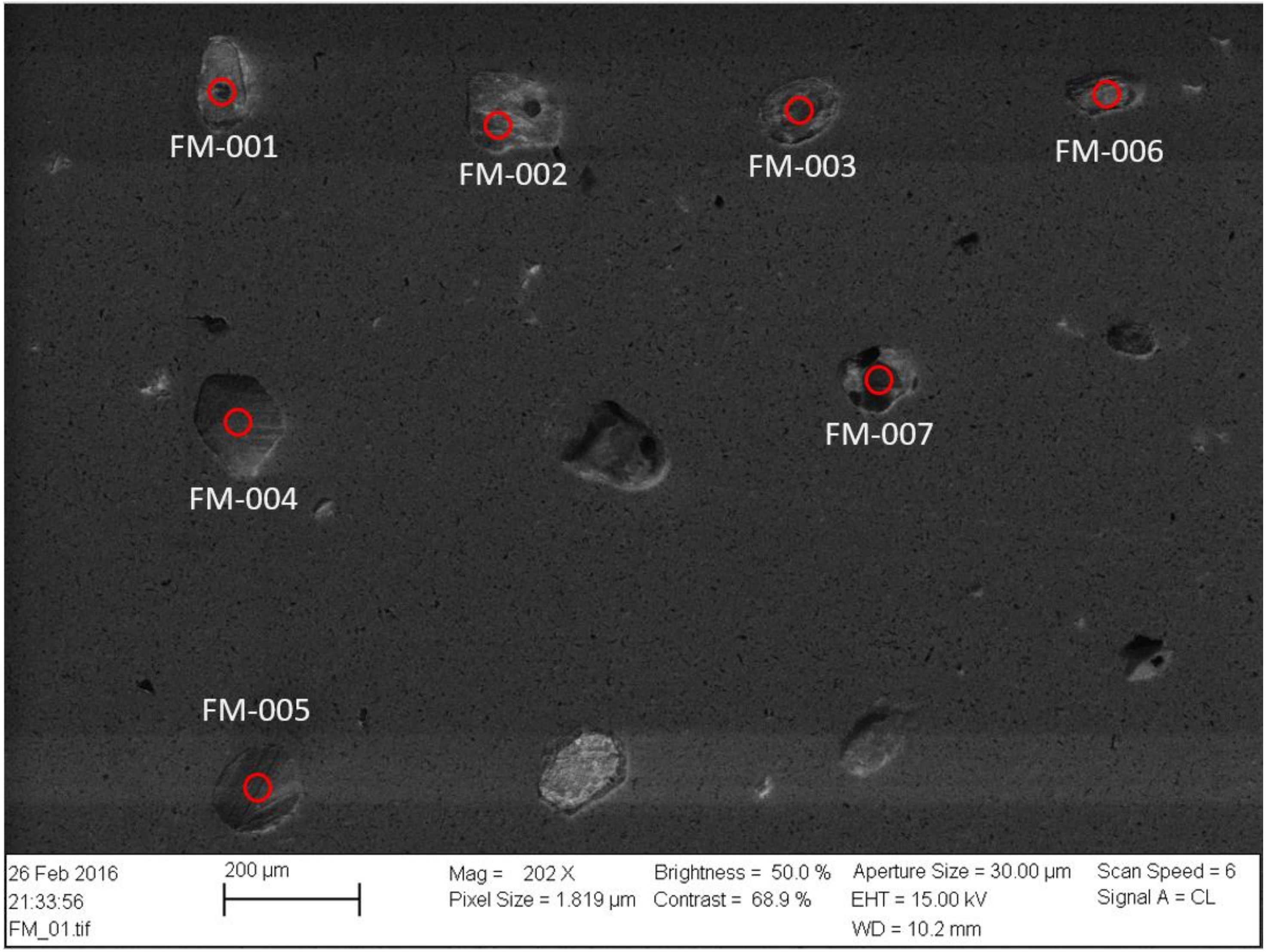

Figure 38 CL image overview of dated zircon grains.

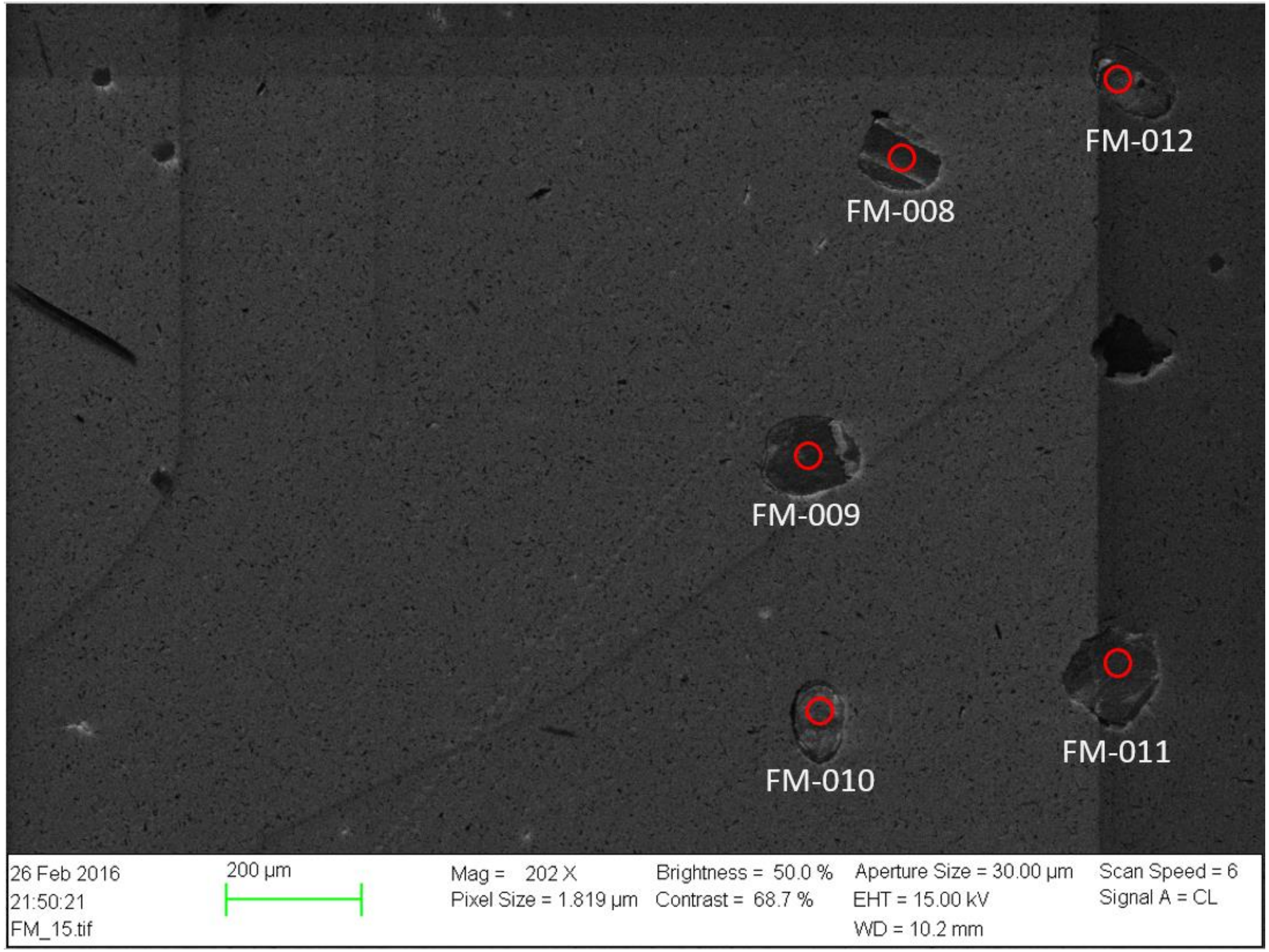

Figure 39 CL image overview of dated zircon grains.

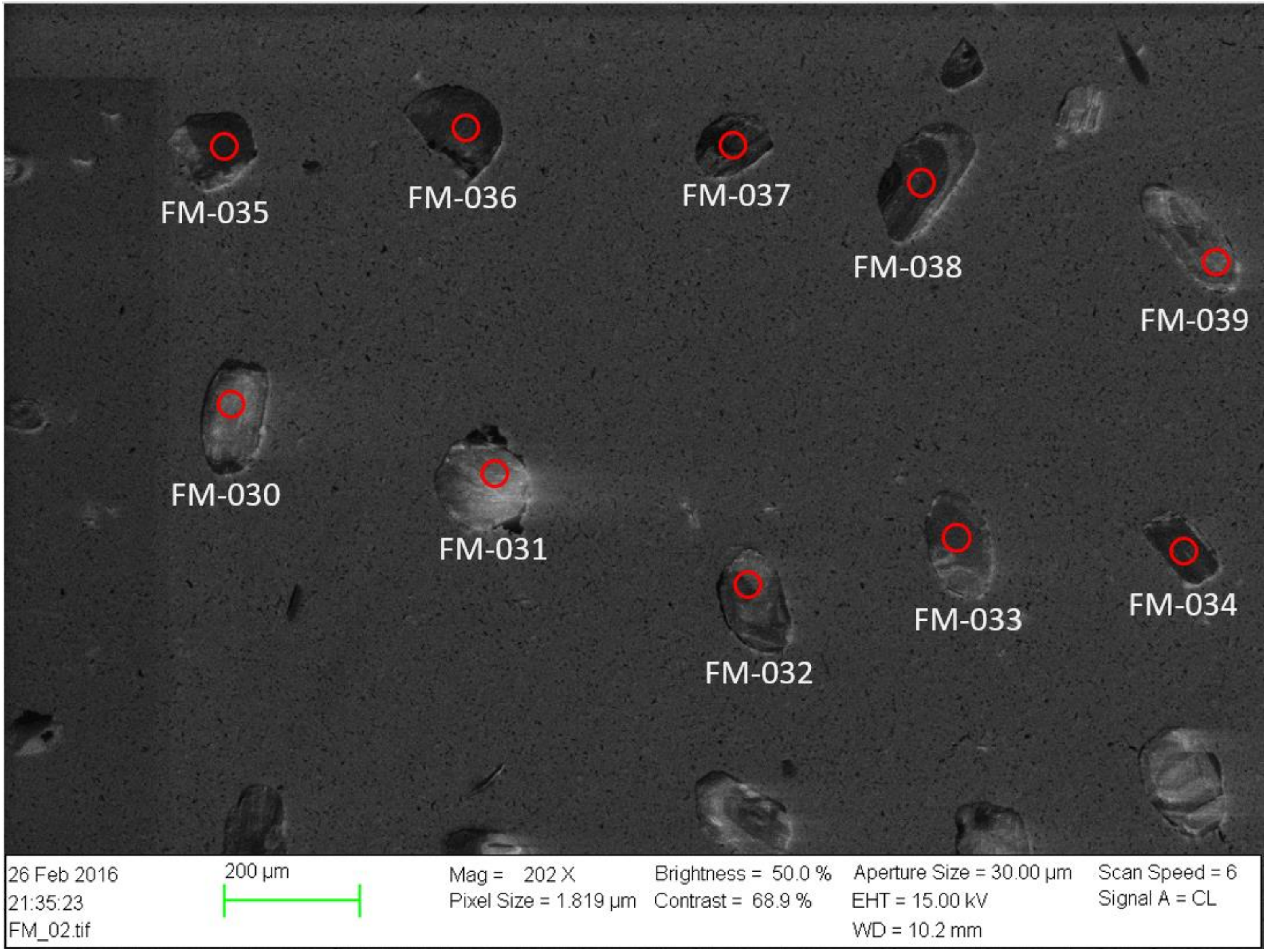

Figure 40 CL image overview of dated zircon grains.

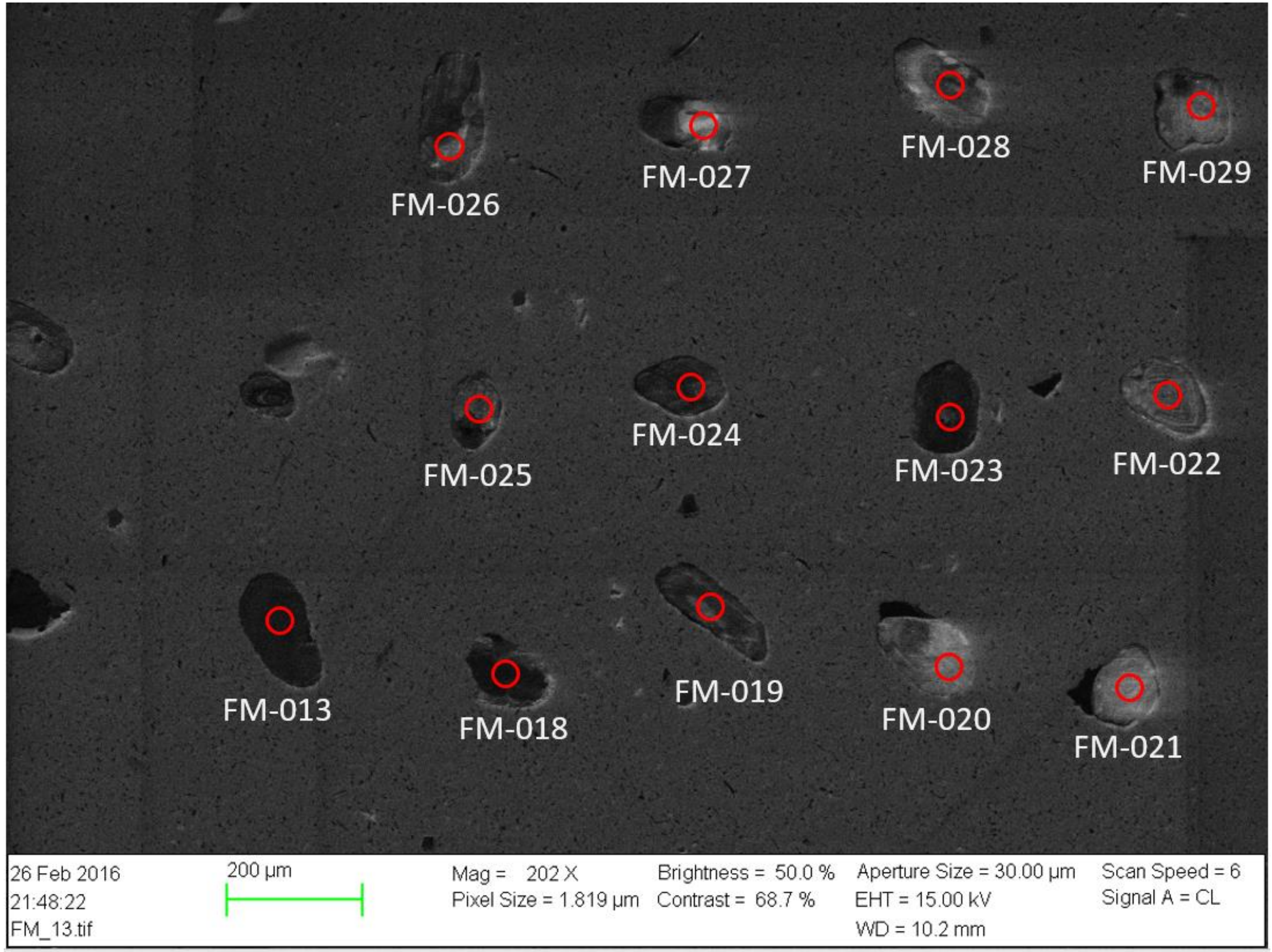

Figure 41 CL image overview of dated zircon grains.

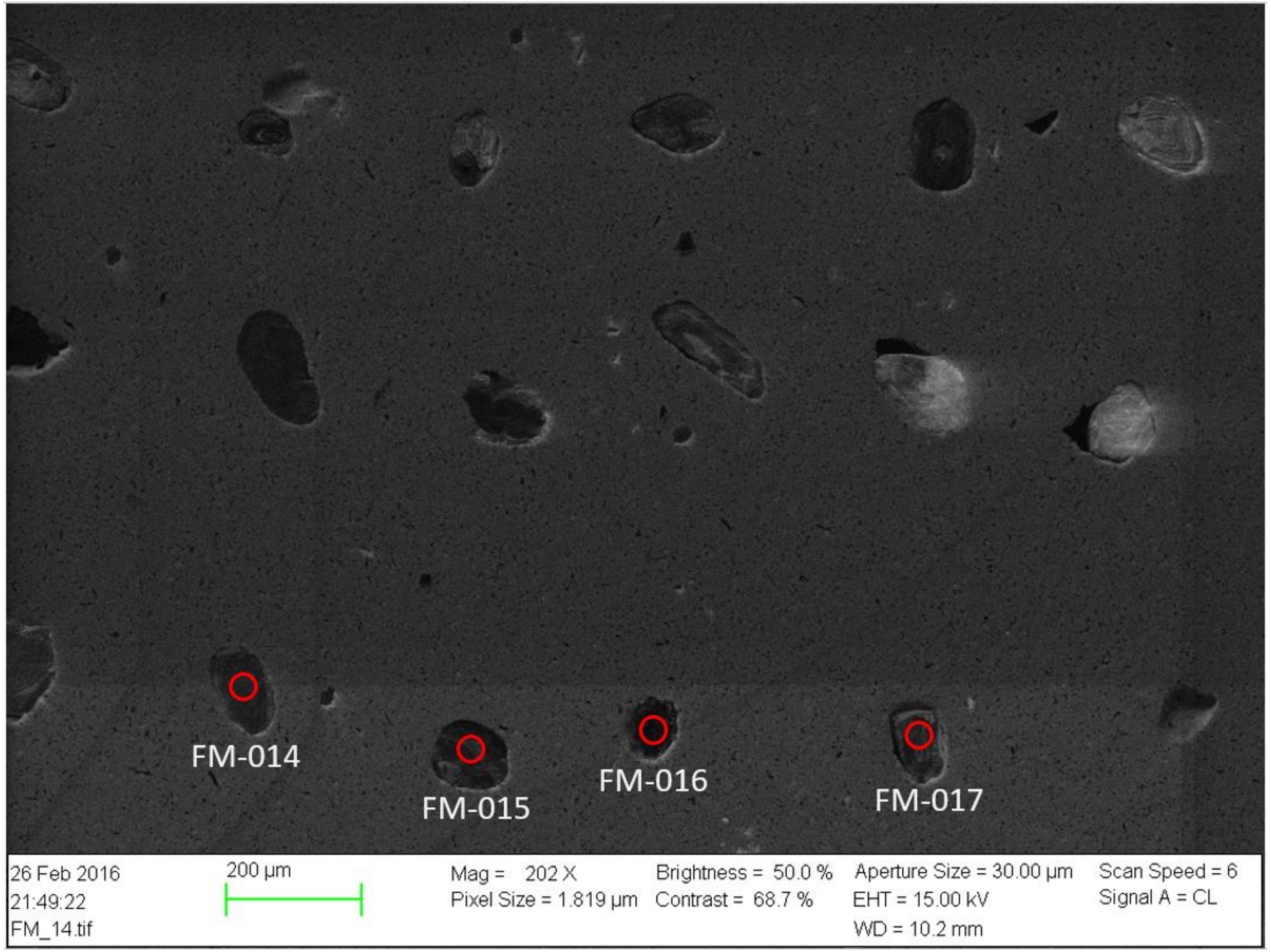

Figure 42 CL image overview of dated zircon grains.

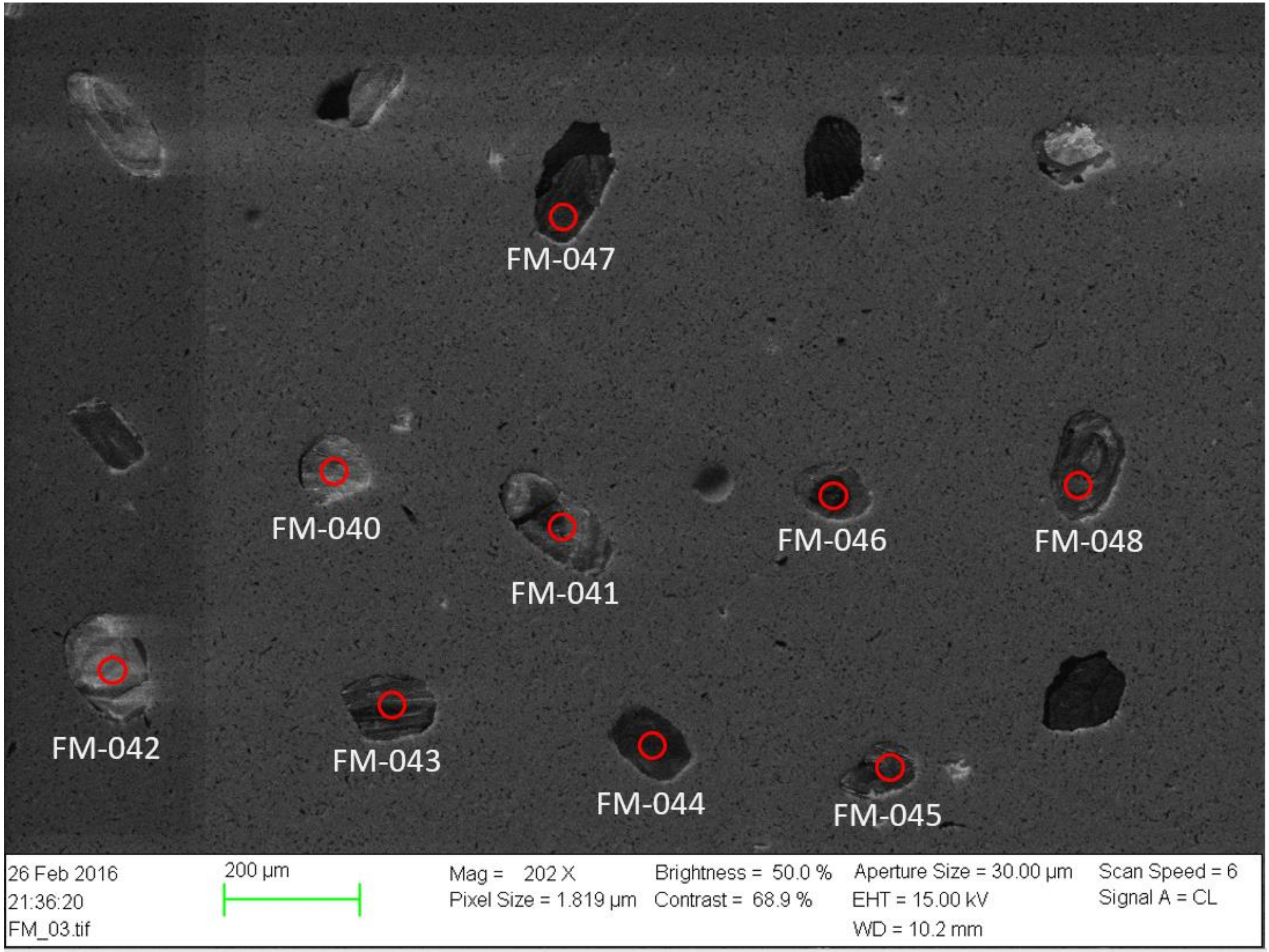

Figure 43 CL image overview of dated zircon grains.

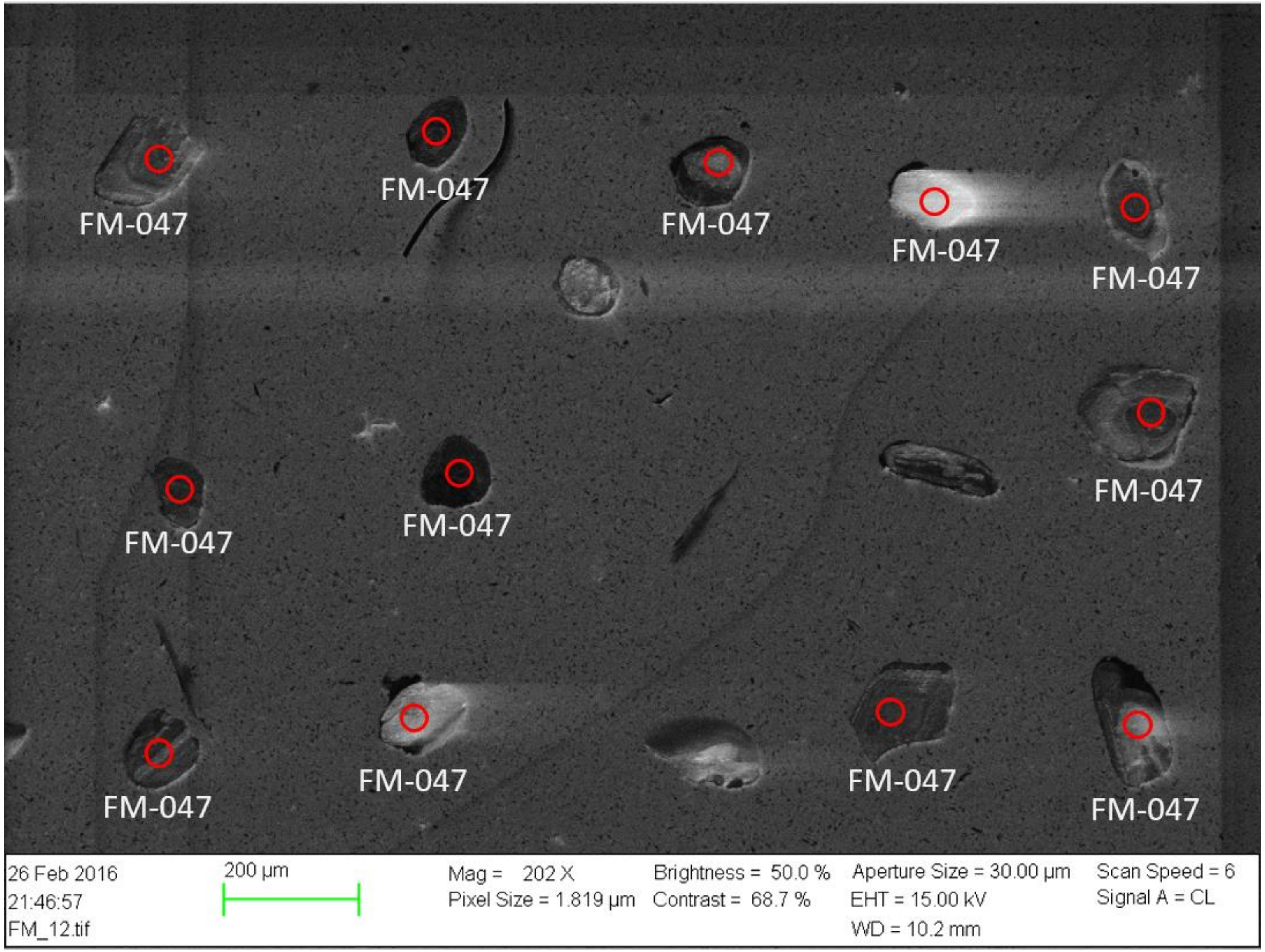

Figure 44 CL image overview of dated zircon grains.

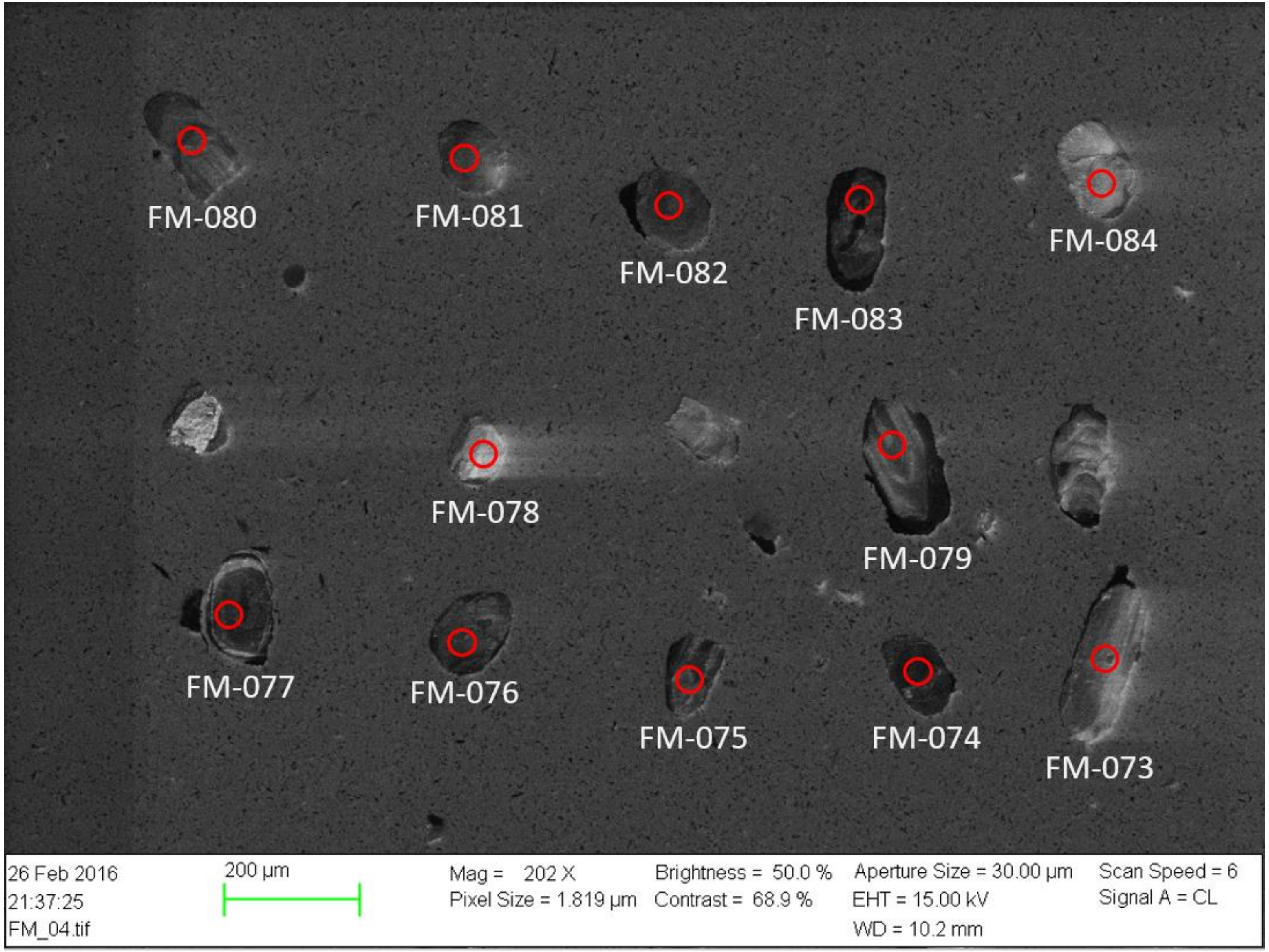

Figure 45 CL image overview of dated zircon grains.

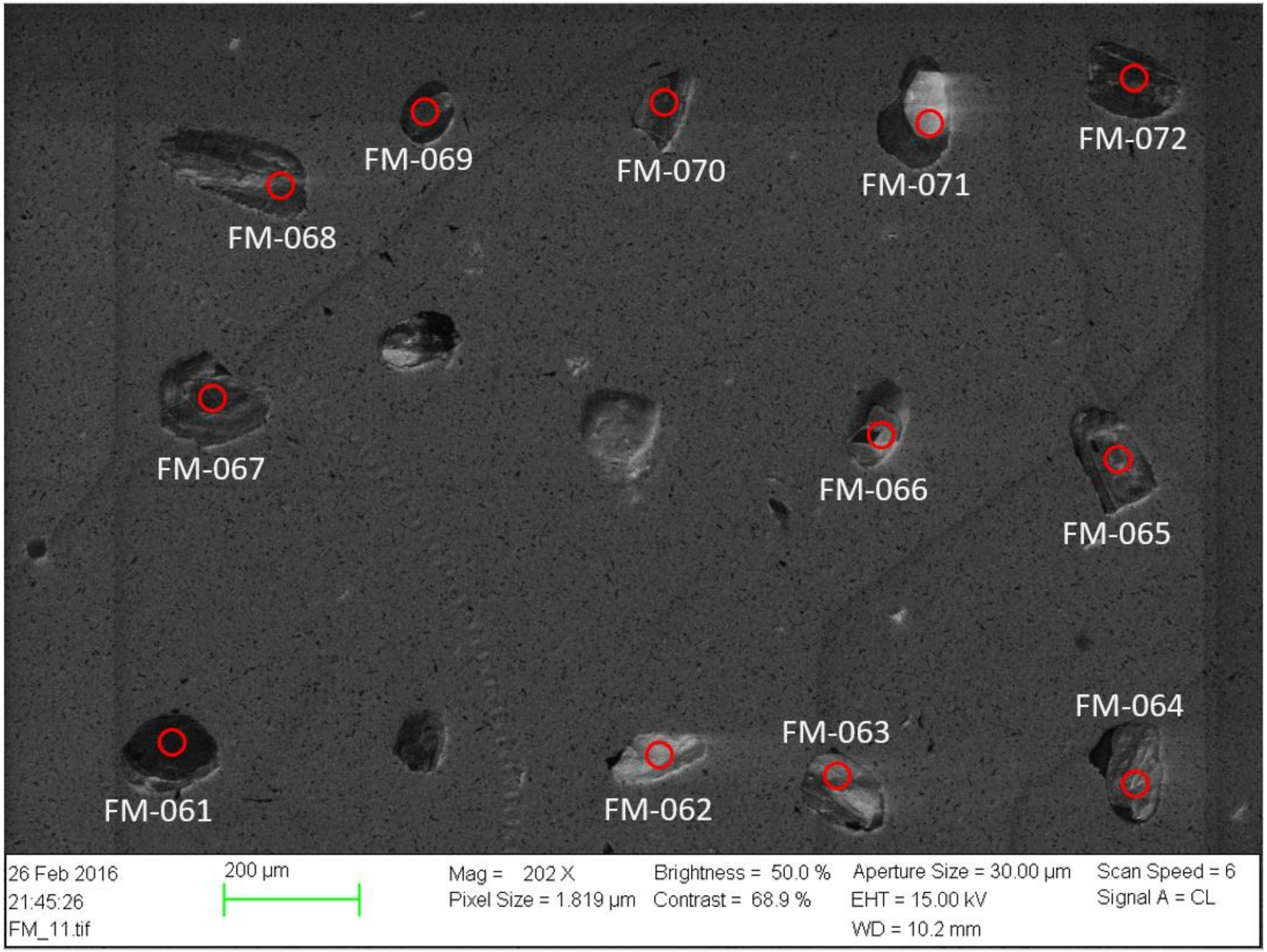

Figure 46 CL image overview of dated zircon grains.

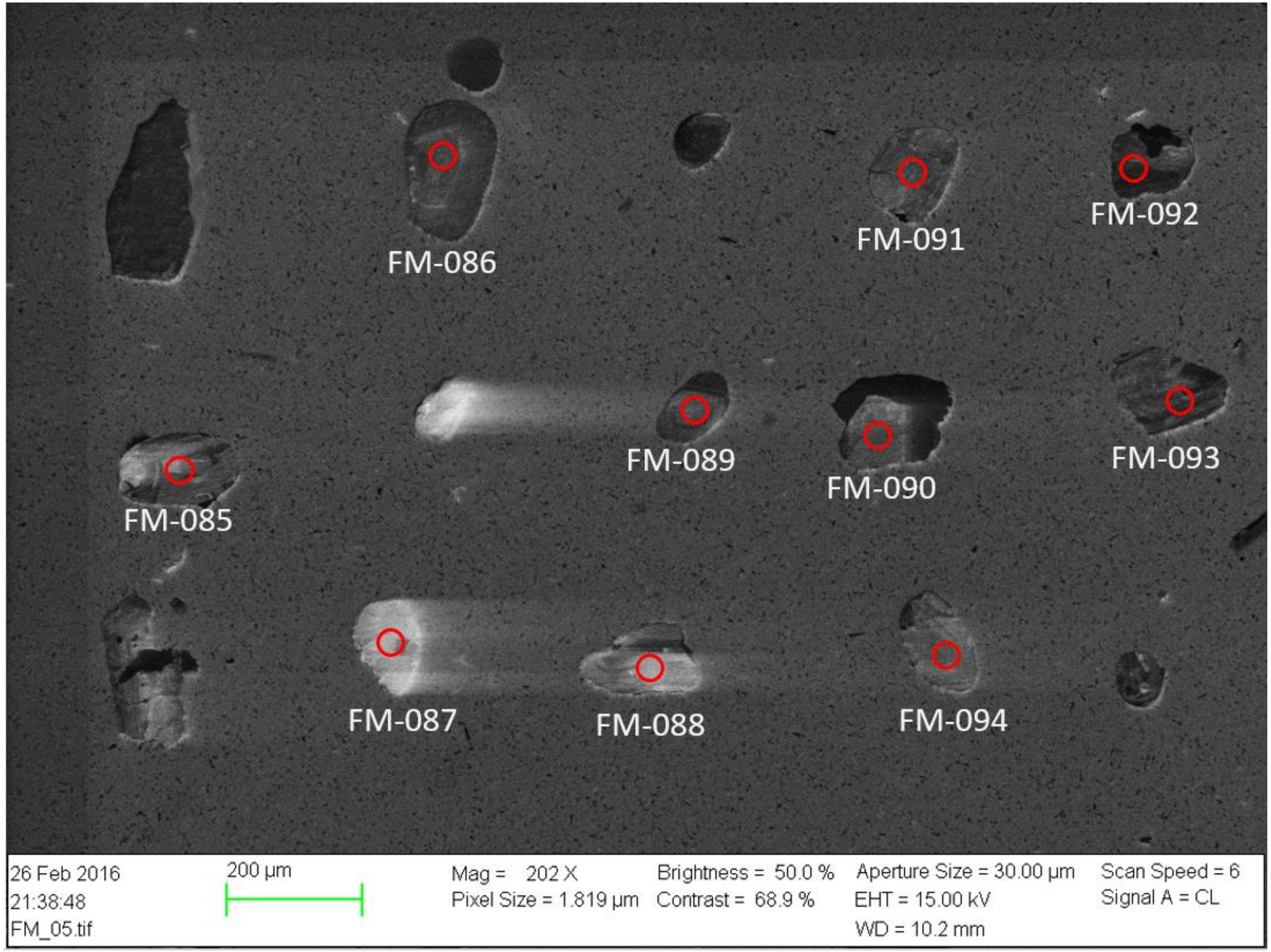

Figure 47 CL image overview of dated zircon grains.

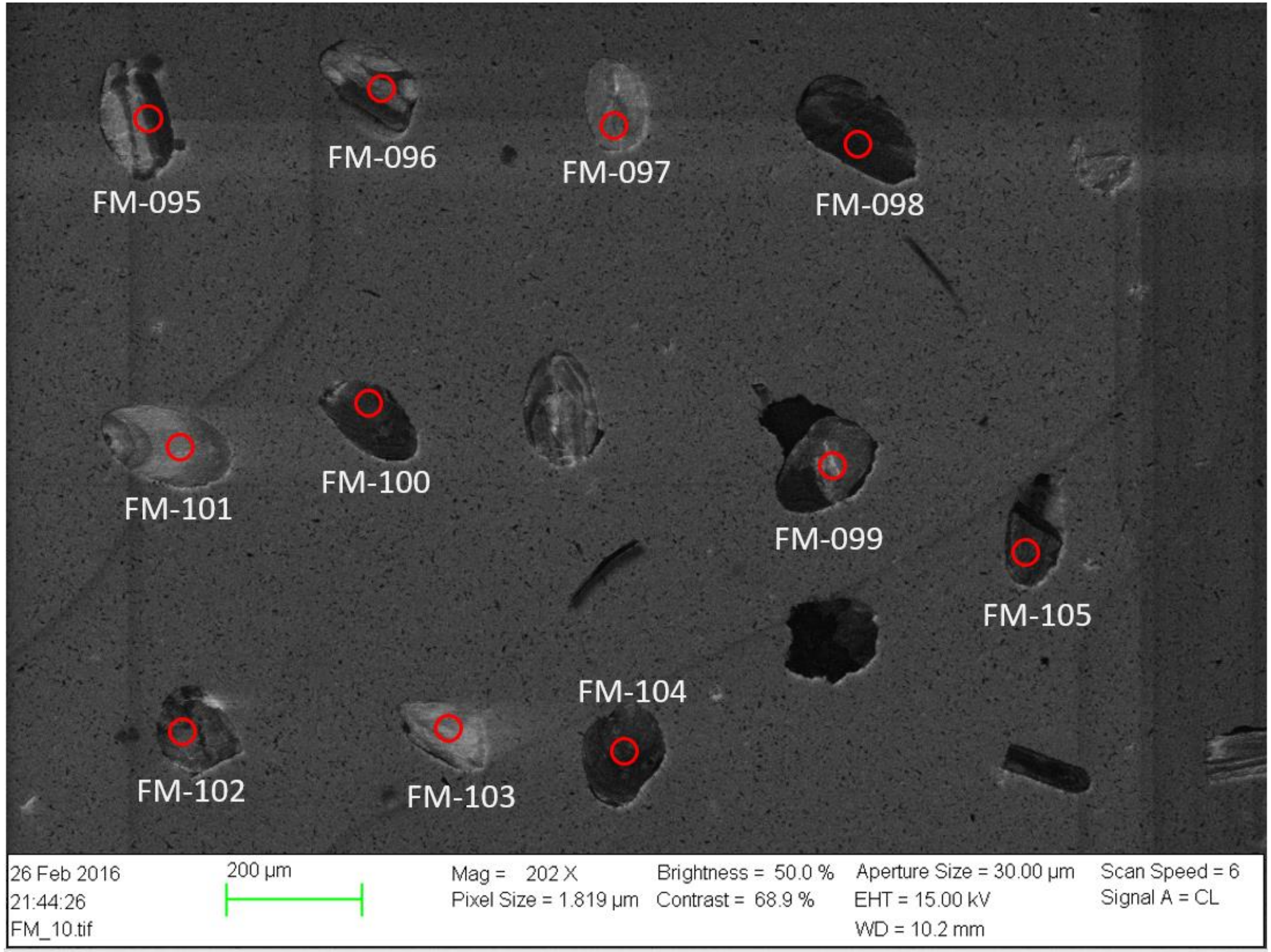

Figure 48 CL image overview of dated zircon grains.

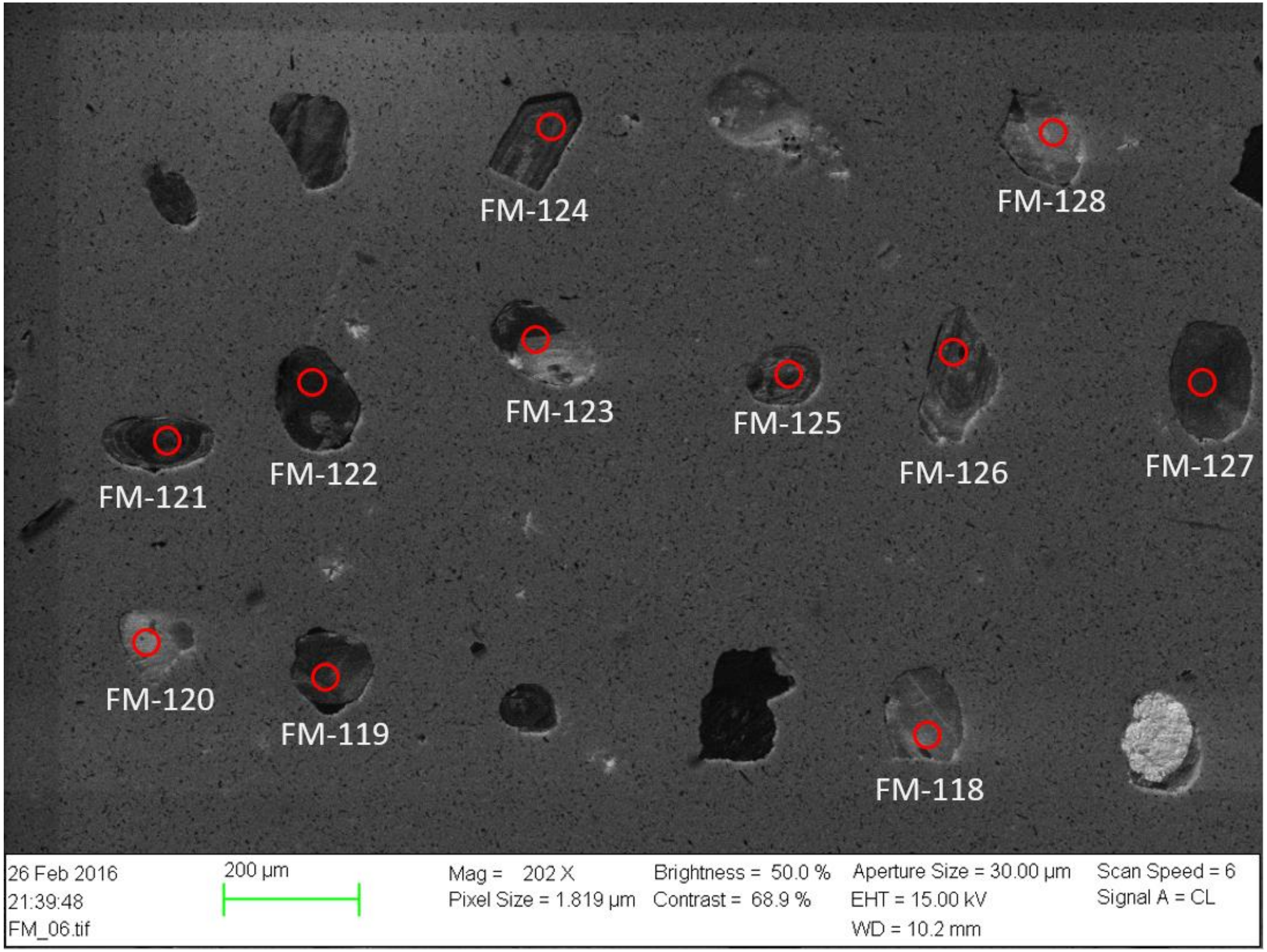

Figure 49 CL image overview of dated zircon grains.

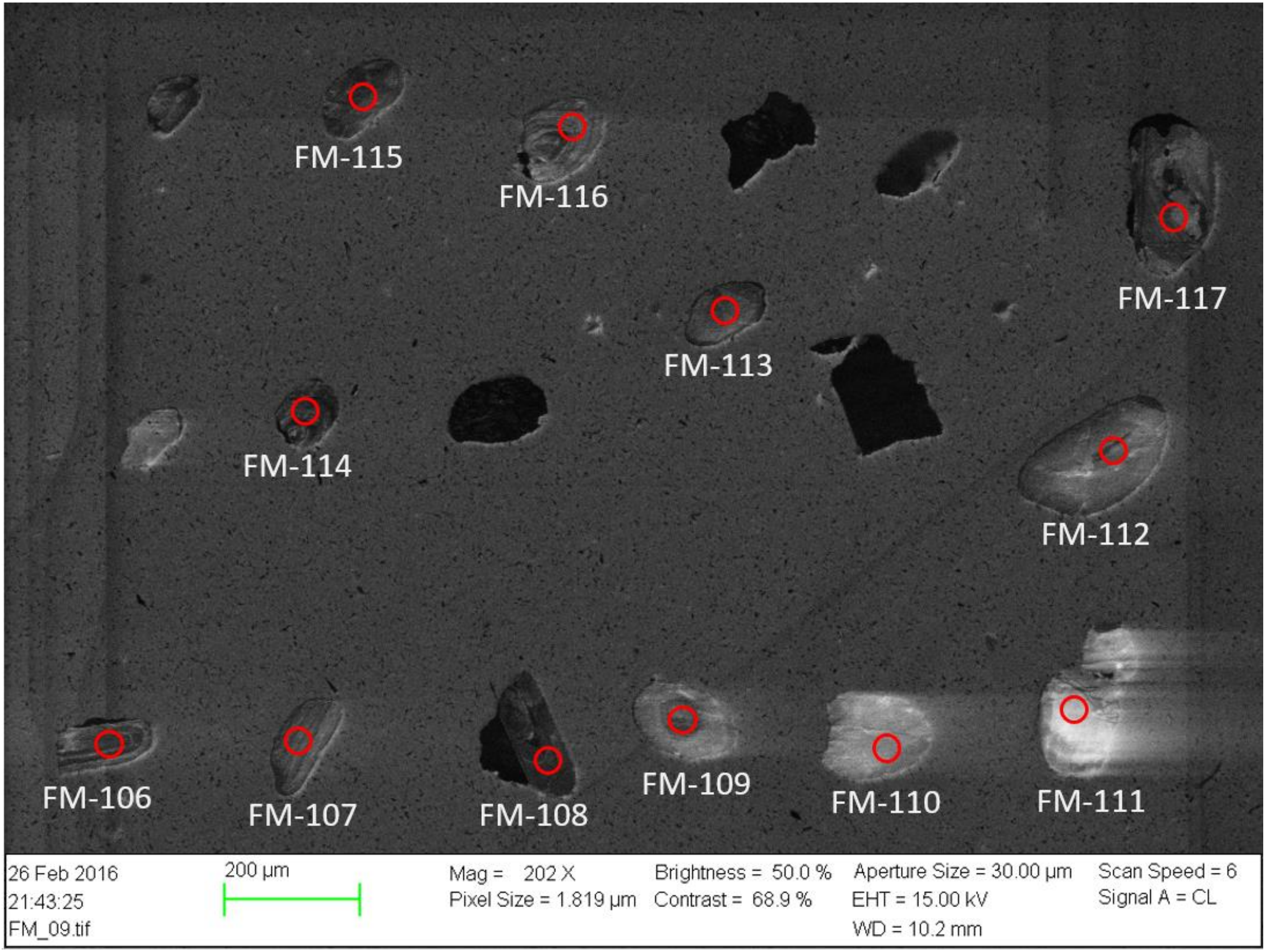

Figure 50 CL image overview of dated zircon grains.

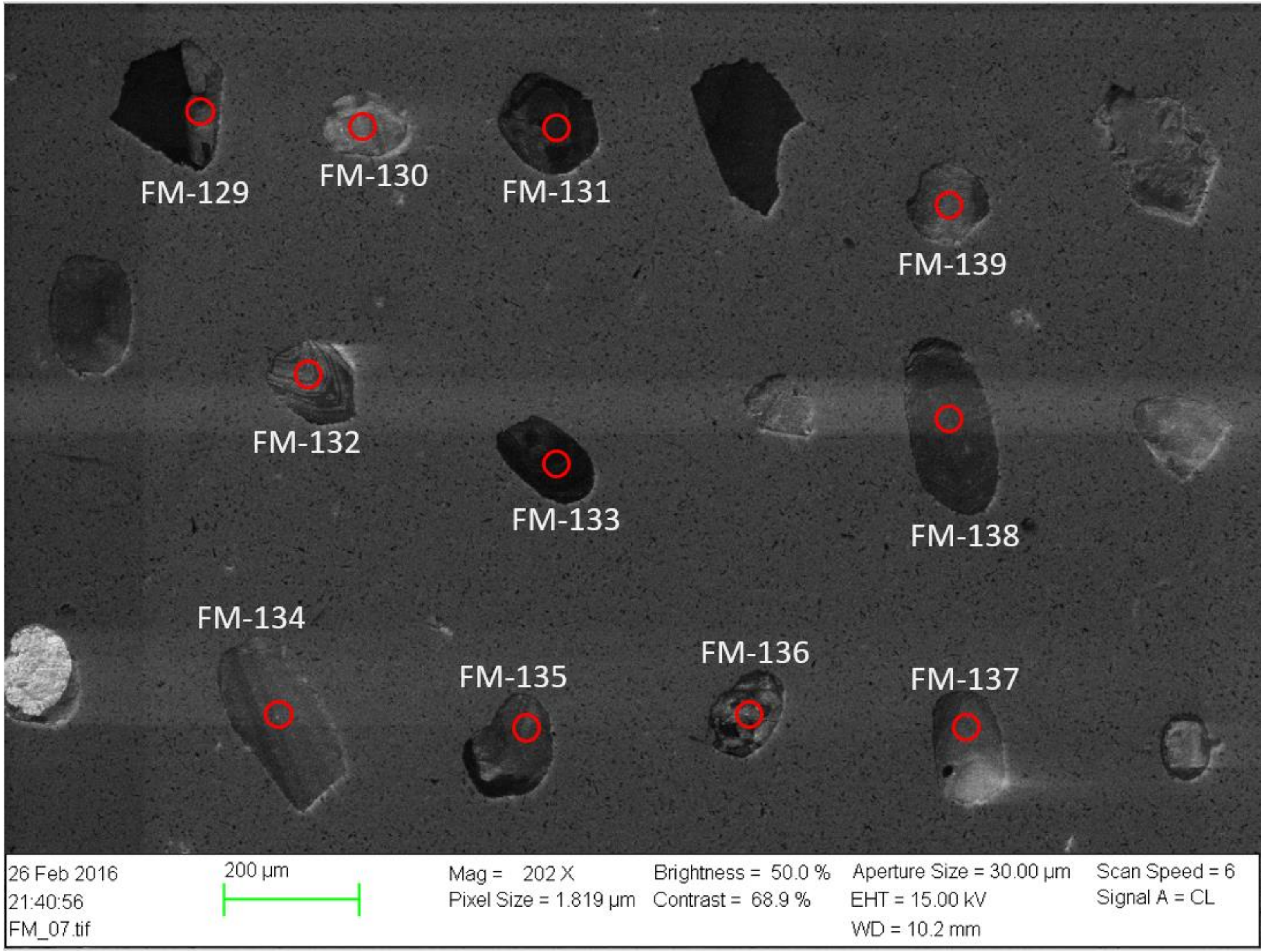

Figure 51 CL image overview of dated zircon grains.

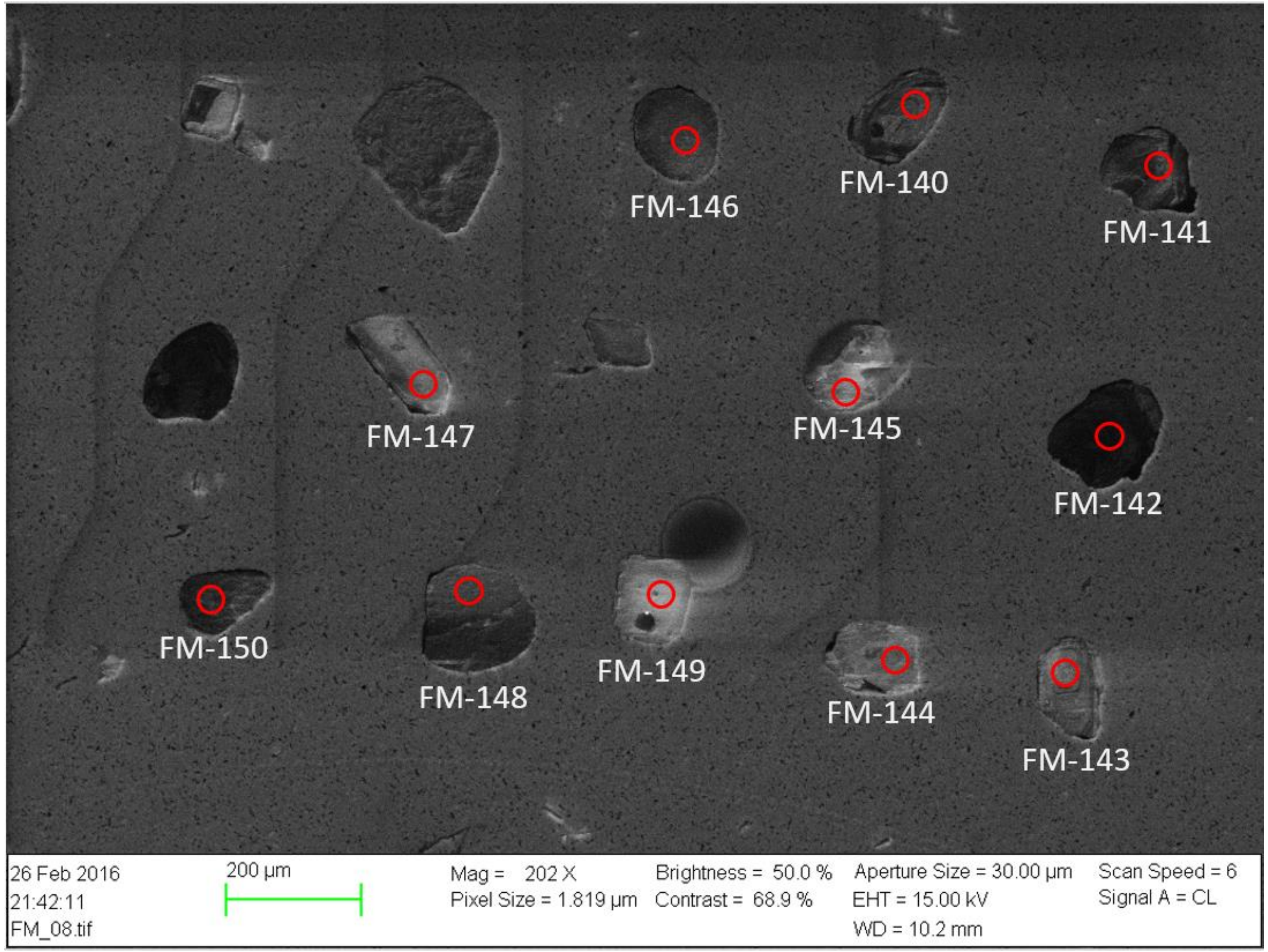

Figure 52 CL image overview of dated zircon grains.

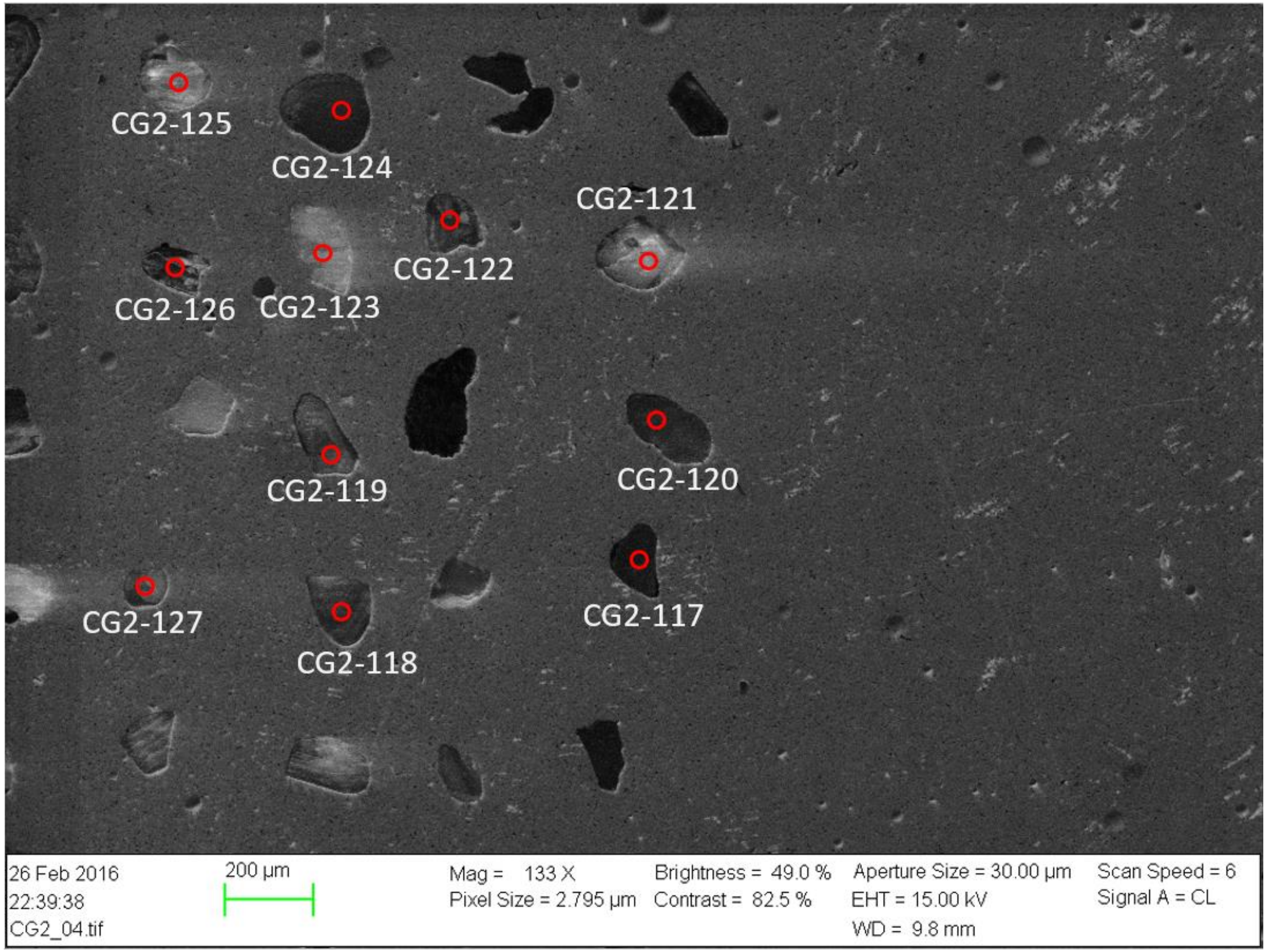

Figure 53 CL image overview of dated zircon grains.

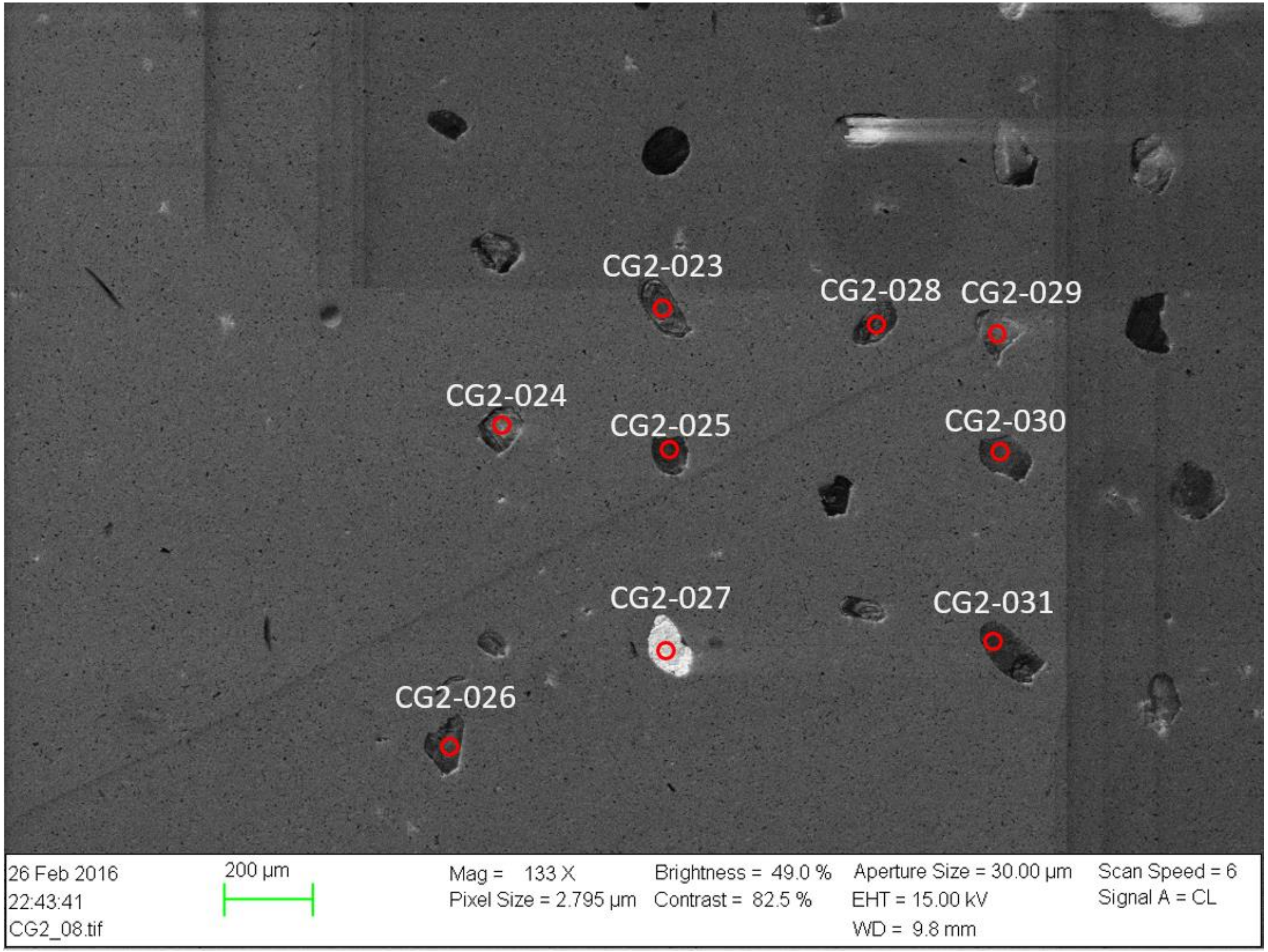

Figure 54 CL image overview of dated zircon grains.

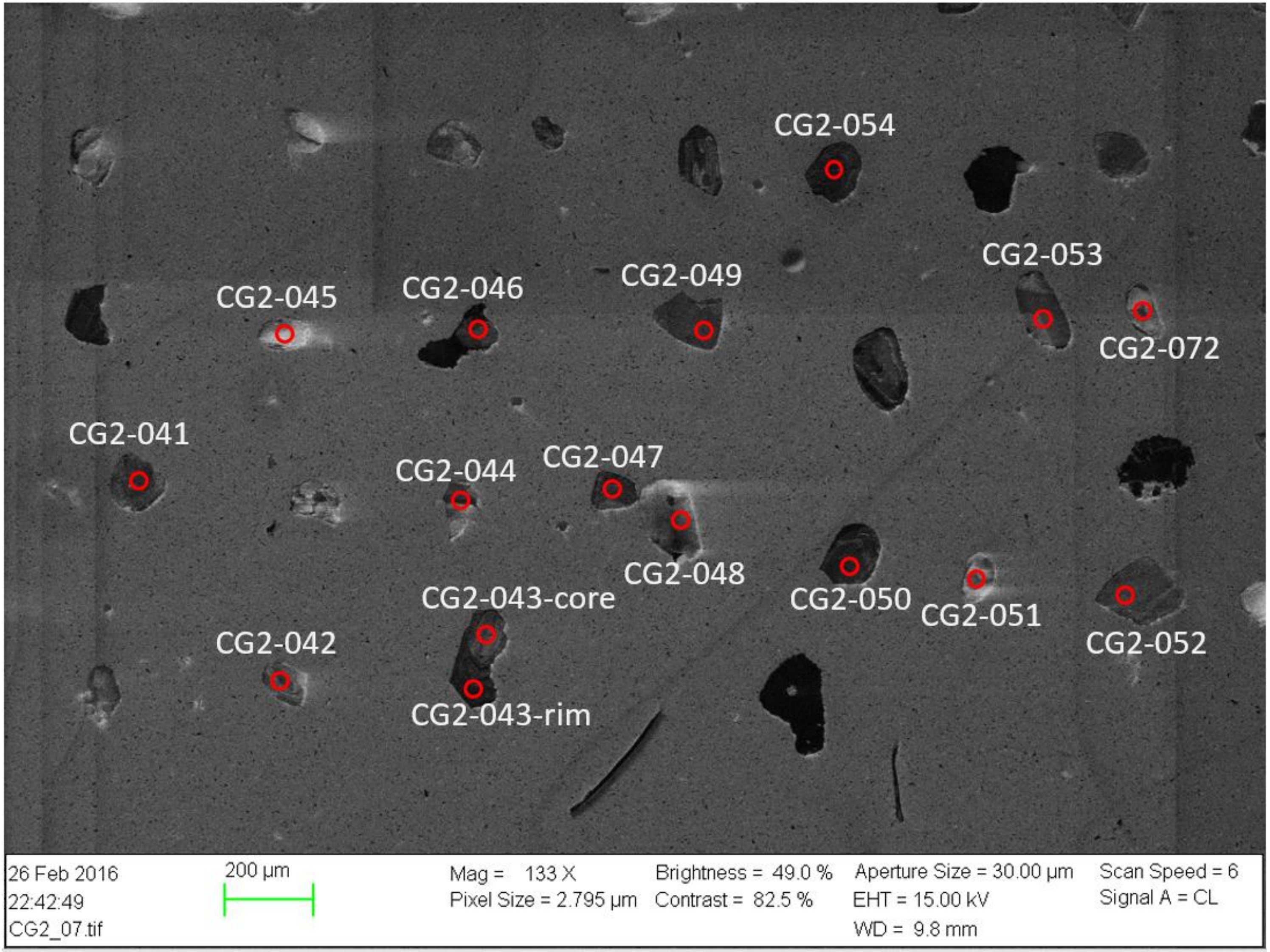

Figure 55 CL image overview of dated zircon grains.

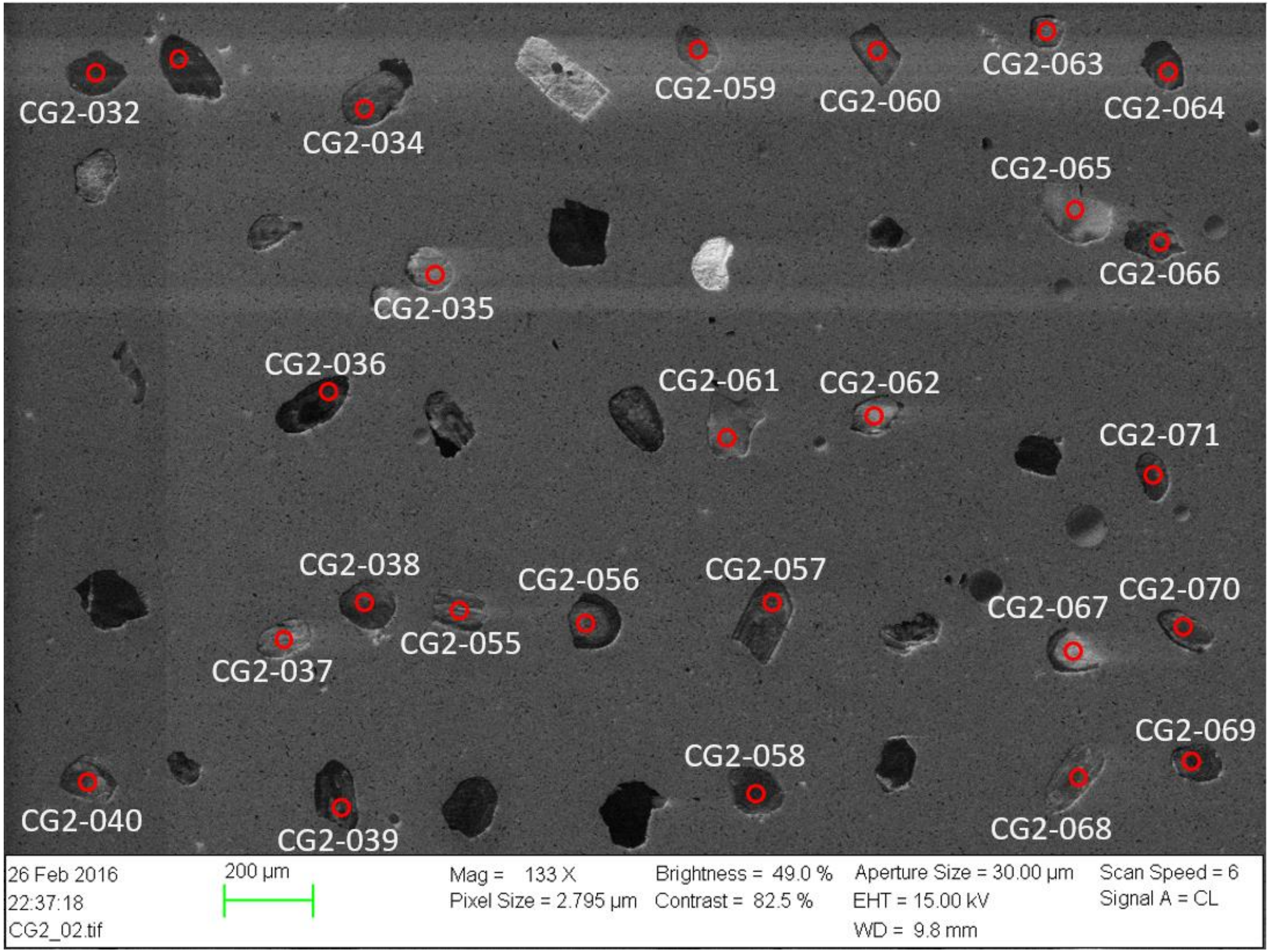

Figure 56 CL image overview of dated zircon grains.

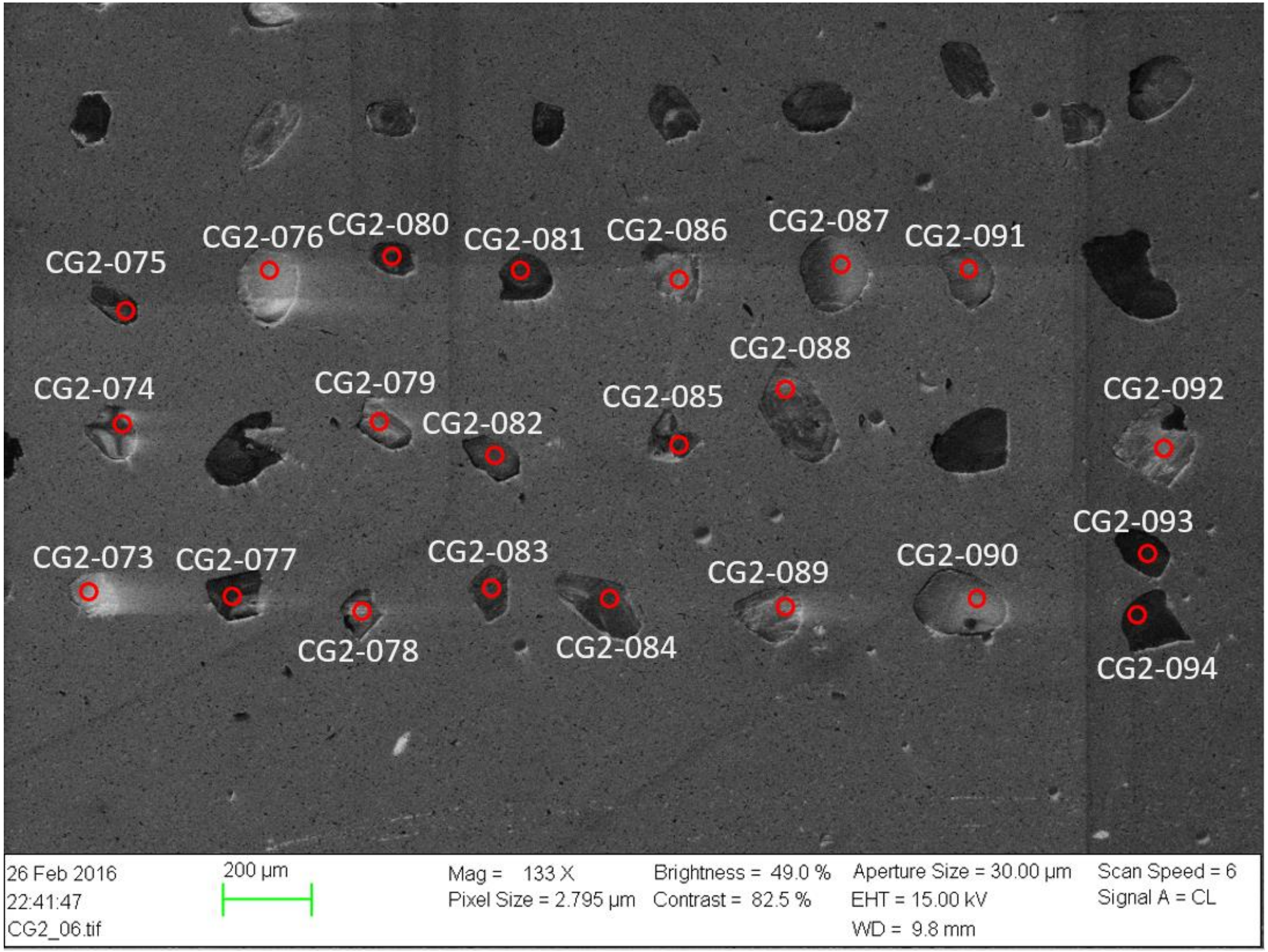

Figure 57 CL image overview of dated zircon grains.

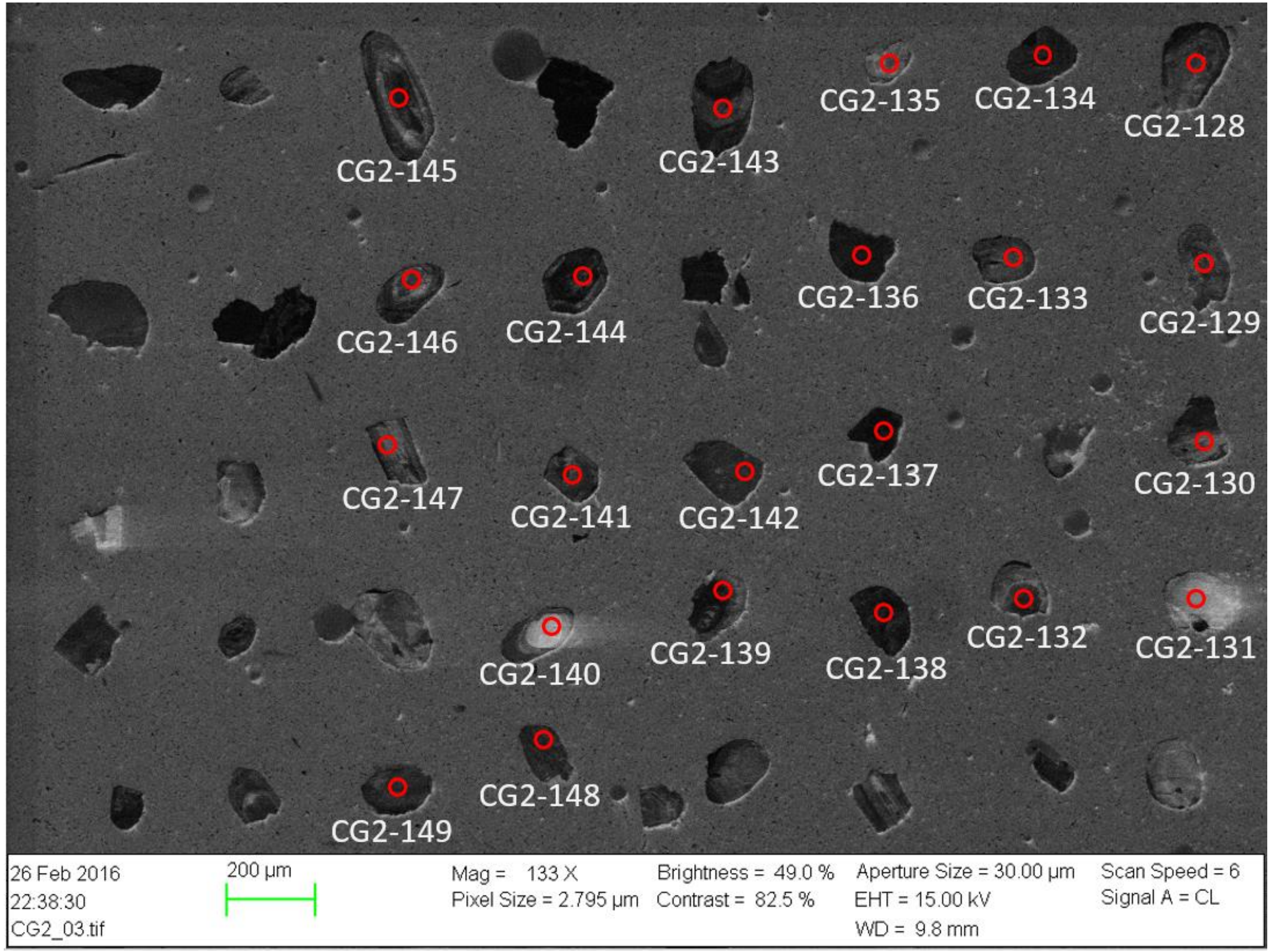

Figure 58 CL image overview of dated zircon grains.

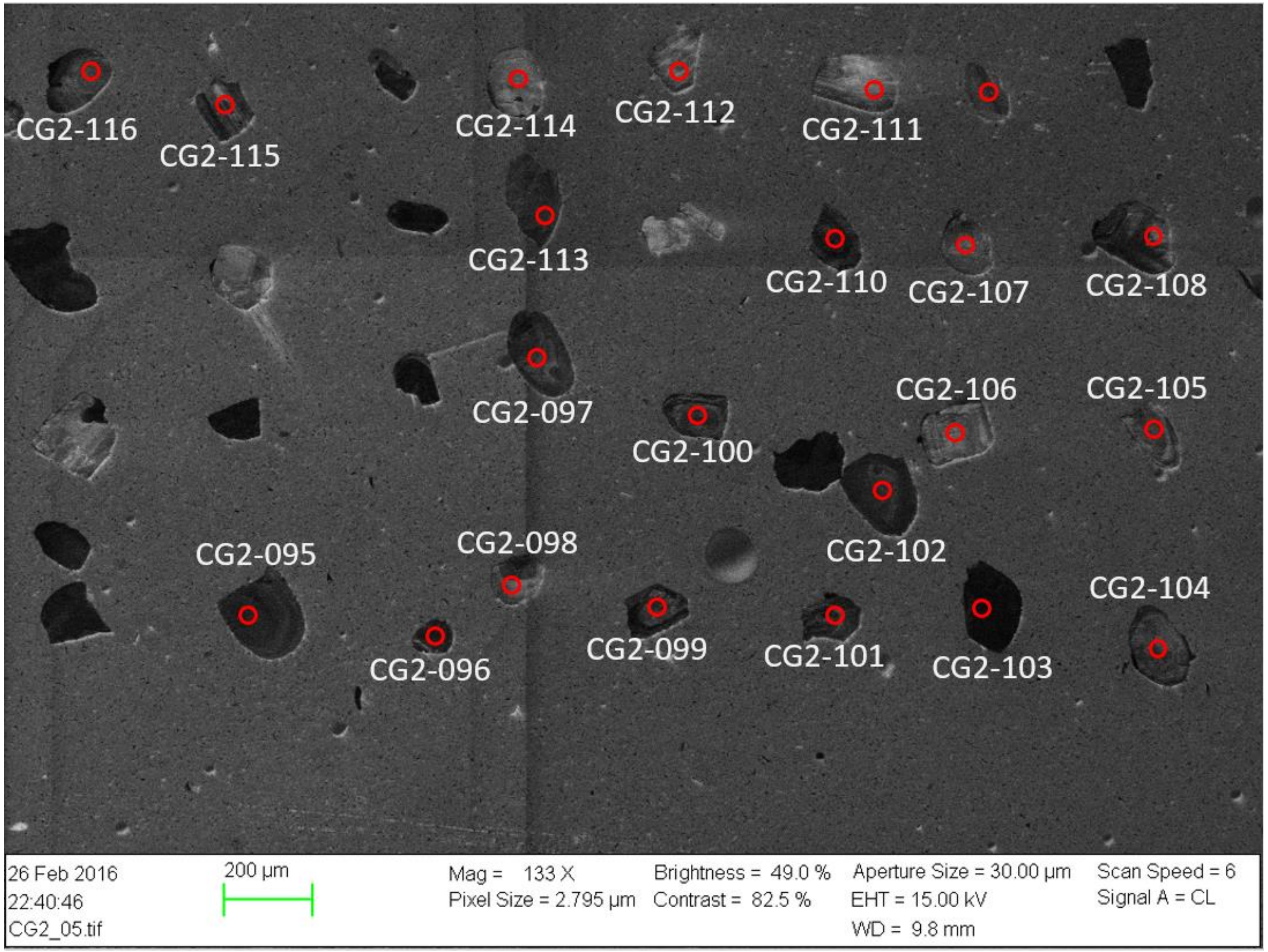

Figure 59 CL image overview of dated zircon grains.

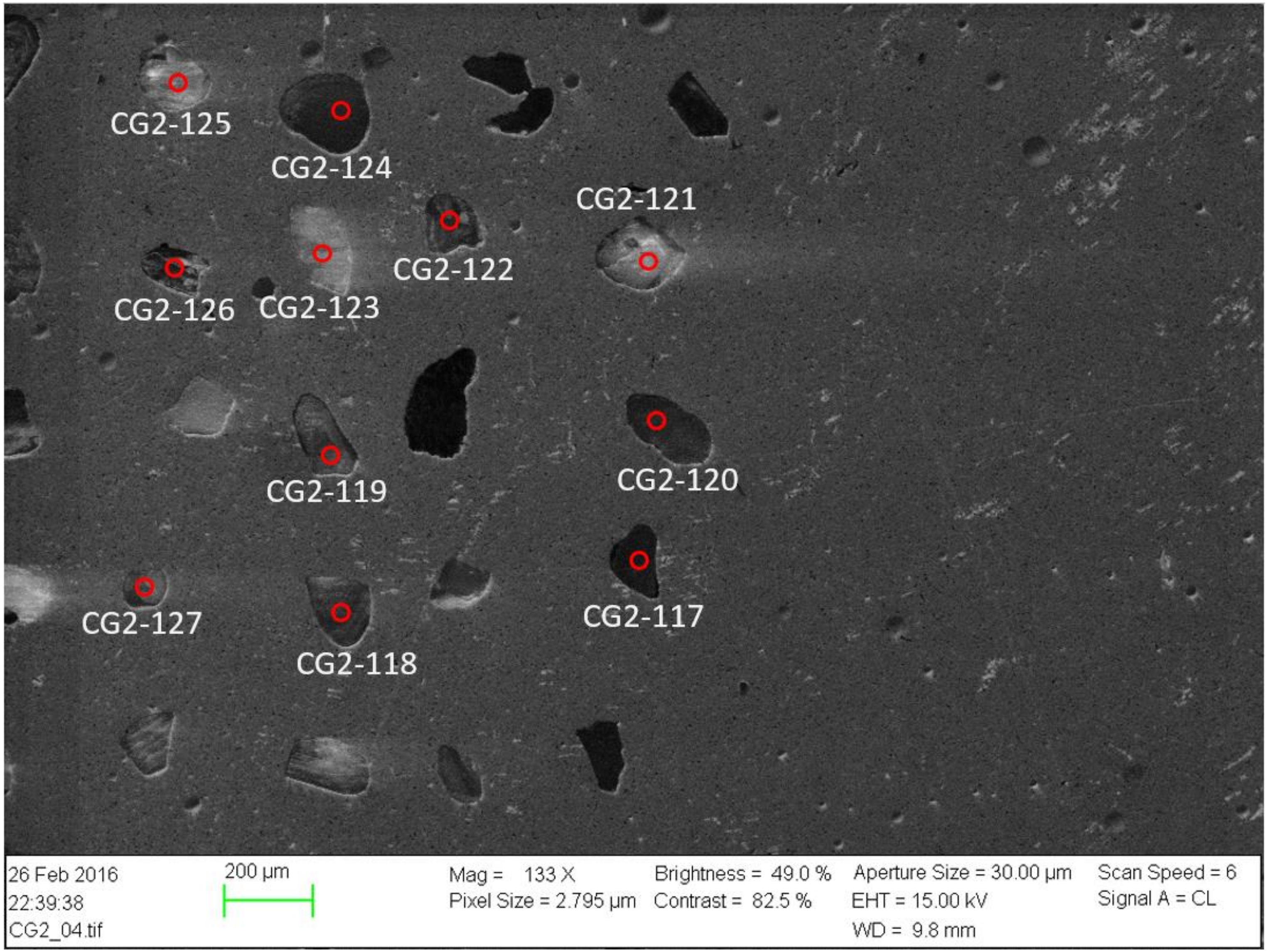

Figure 60 CL image overview of dated zircon grains.

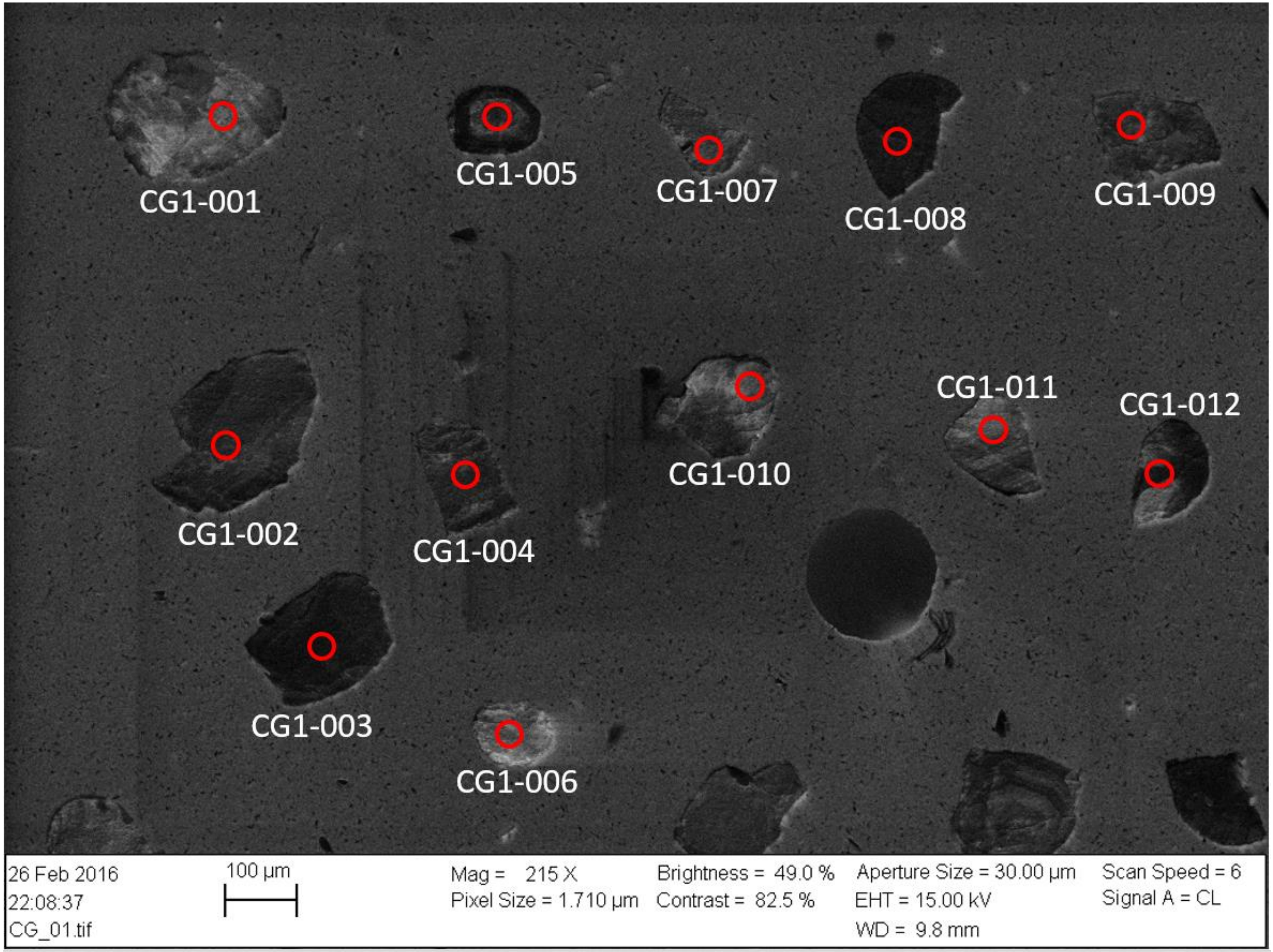

Figure 61 CL image overview of dated zircon grains.

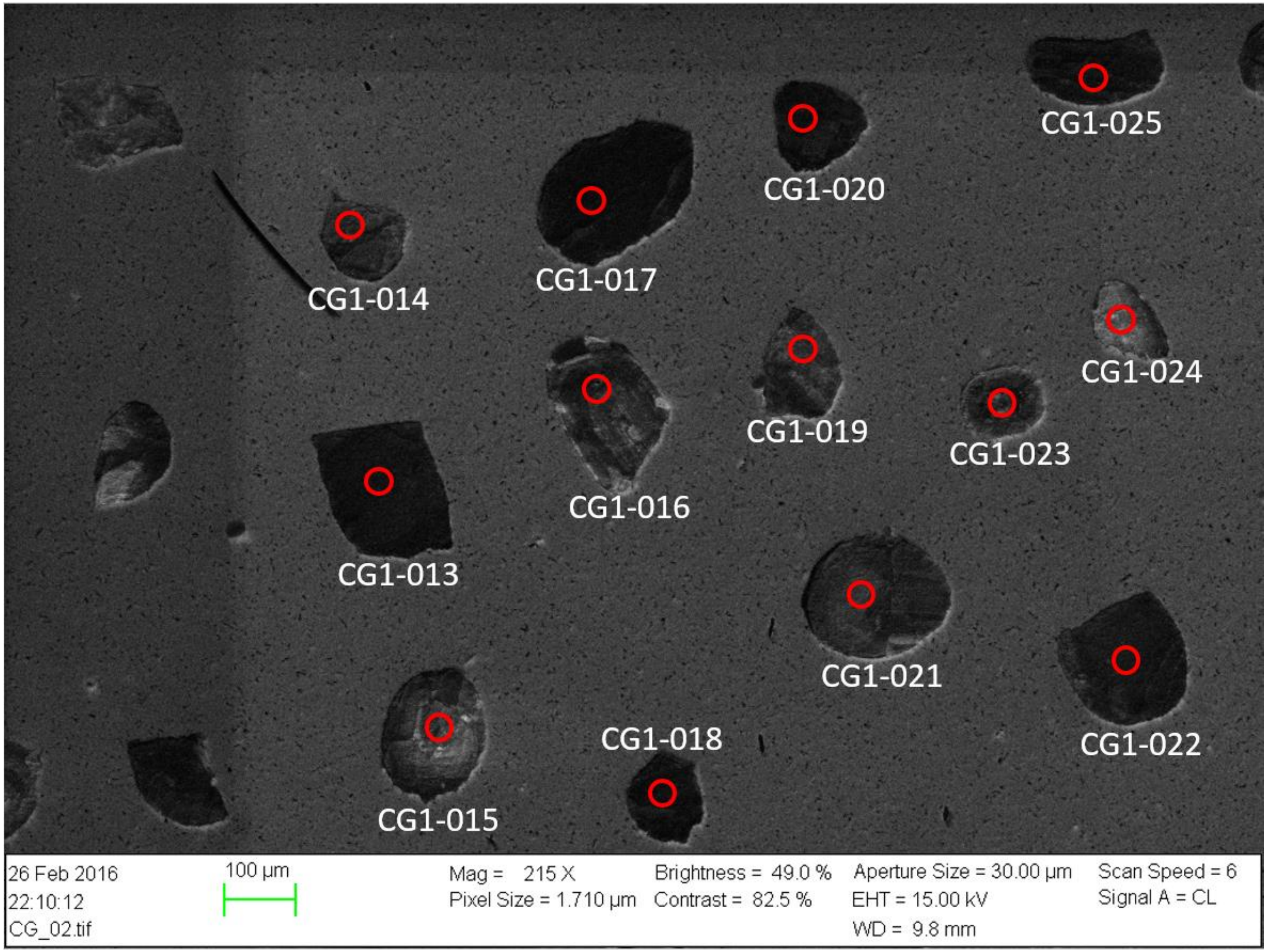

Figure 62 CL image overview of dated zircon grains.

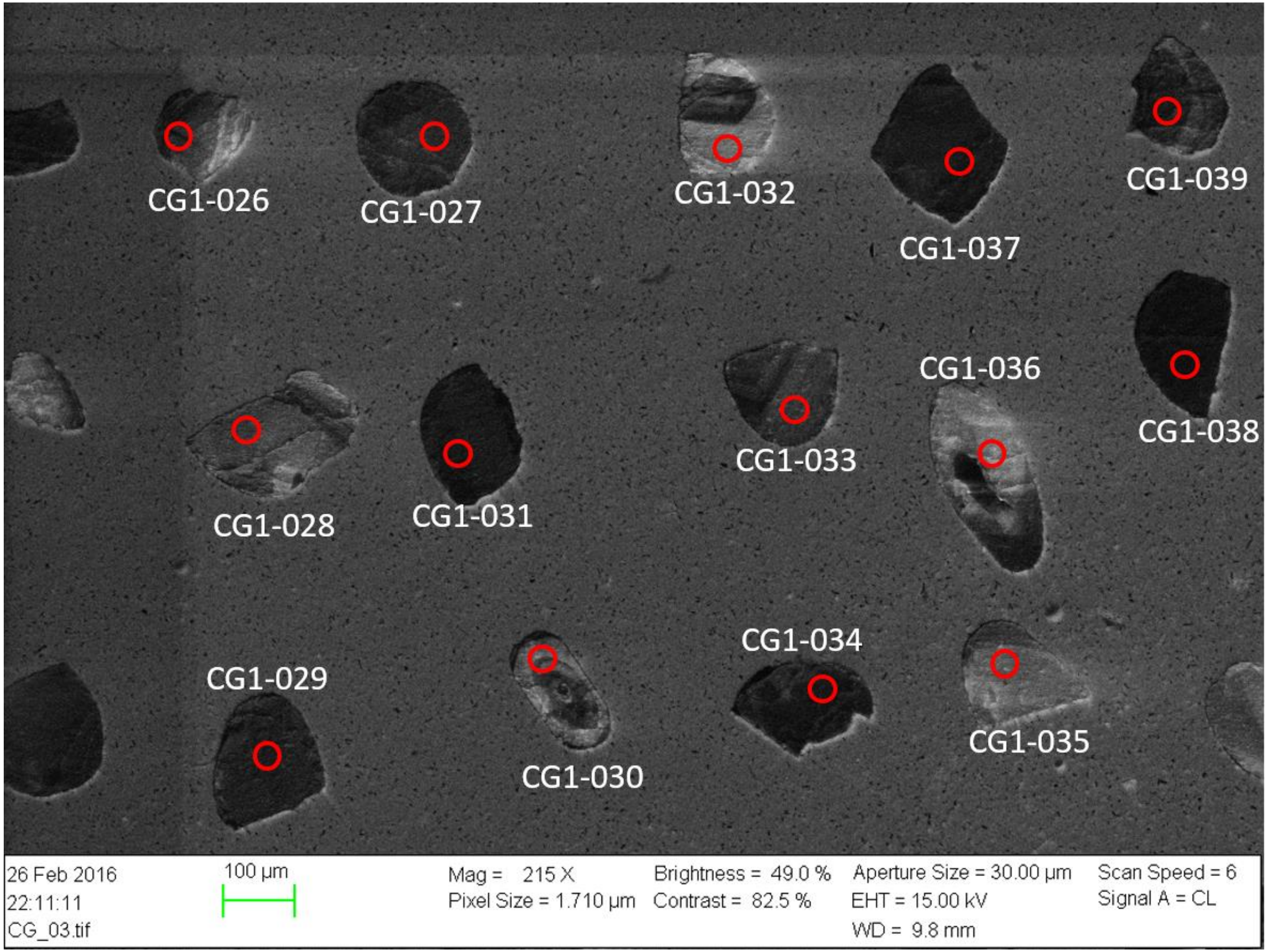

Figure 63 CL image overview of dated zircon grains.

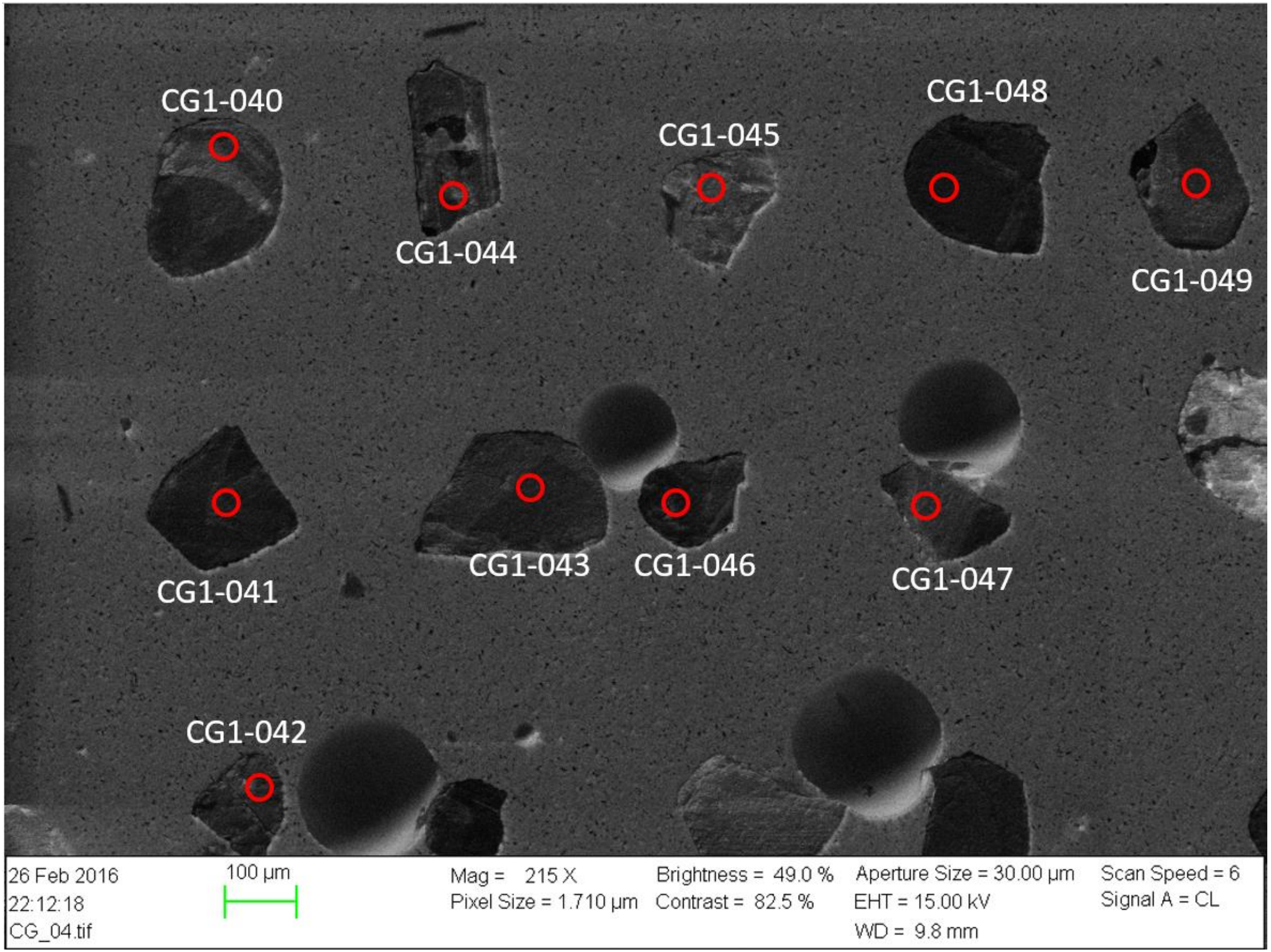

Figure 64 CL image overview of dated zircon grains.

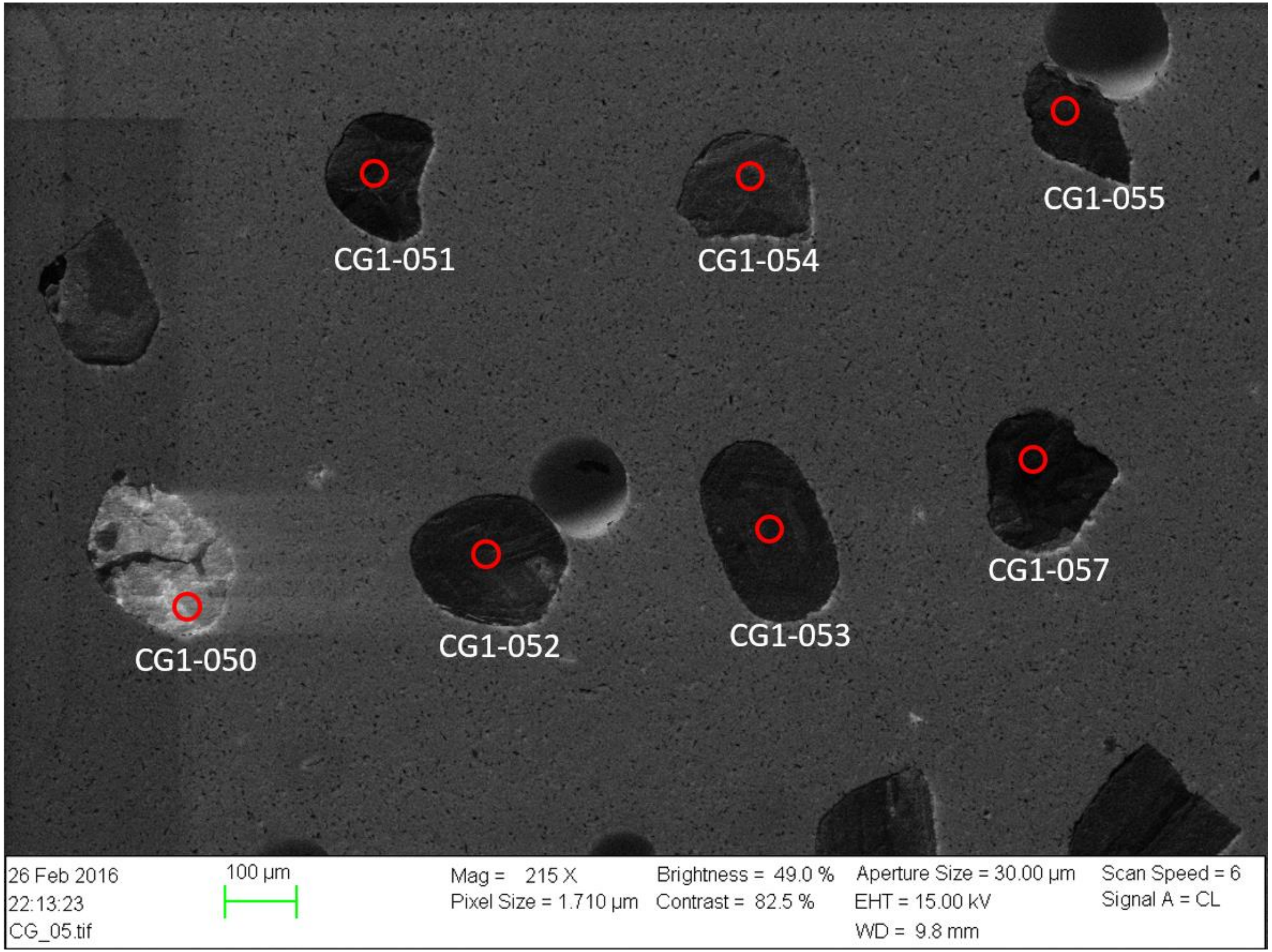

Figure 65 CL image overview of dated zircon grains.

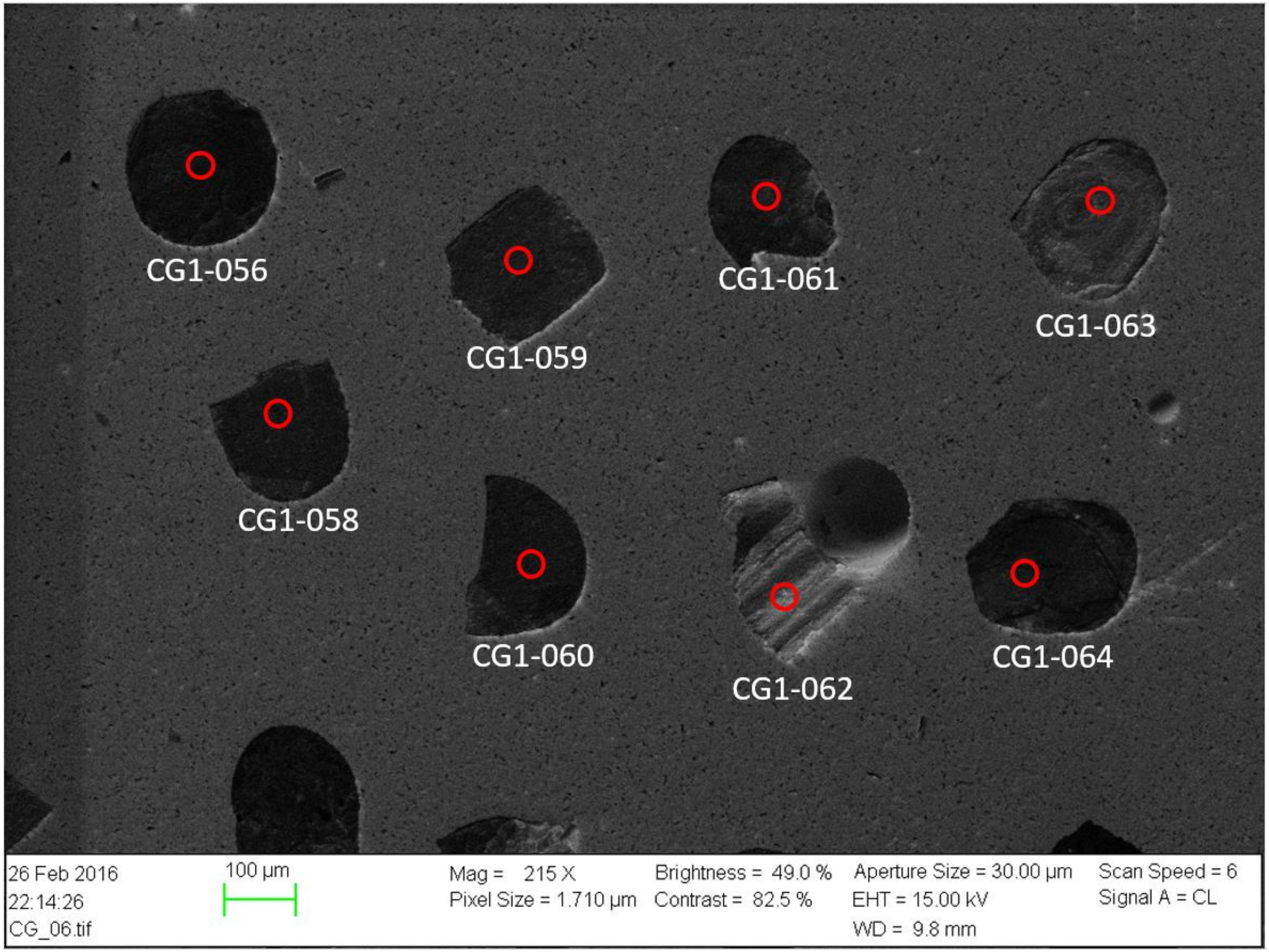

Figure 66 CL image overview of dated zircon grains.

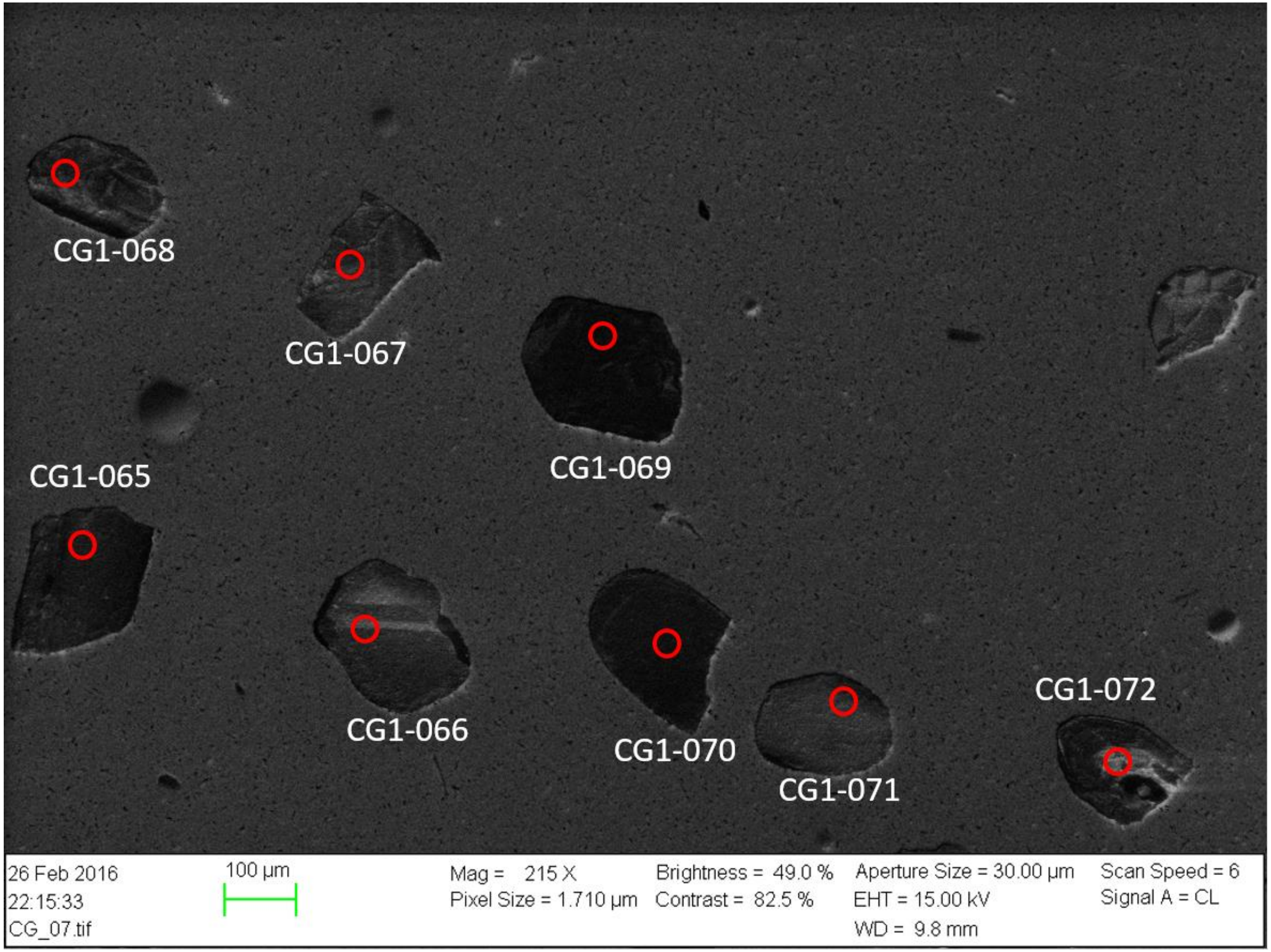

Figure 67 CL image overview of dated zircon grains.

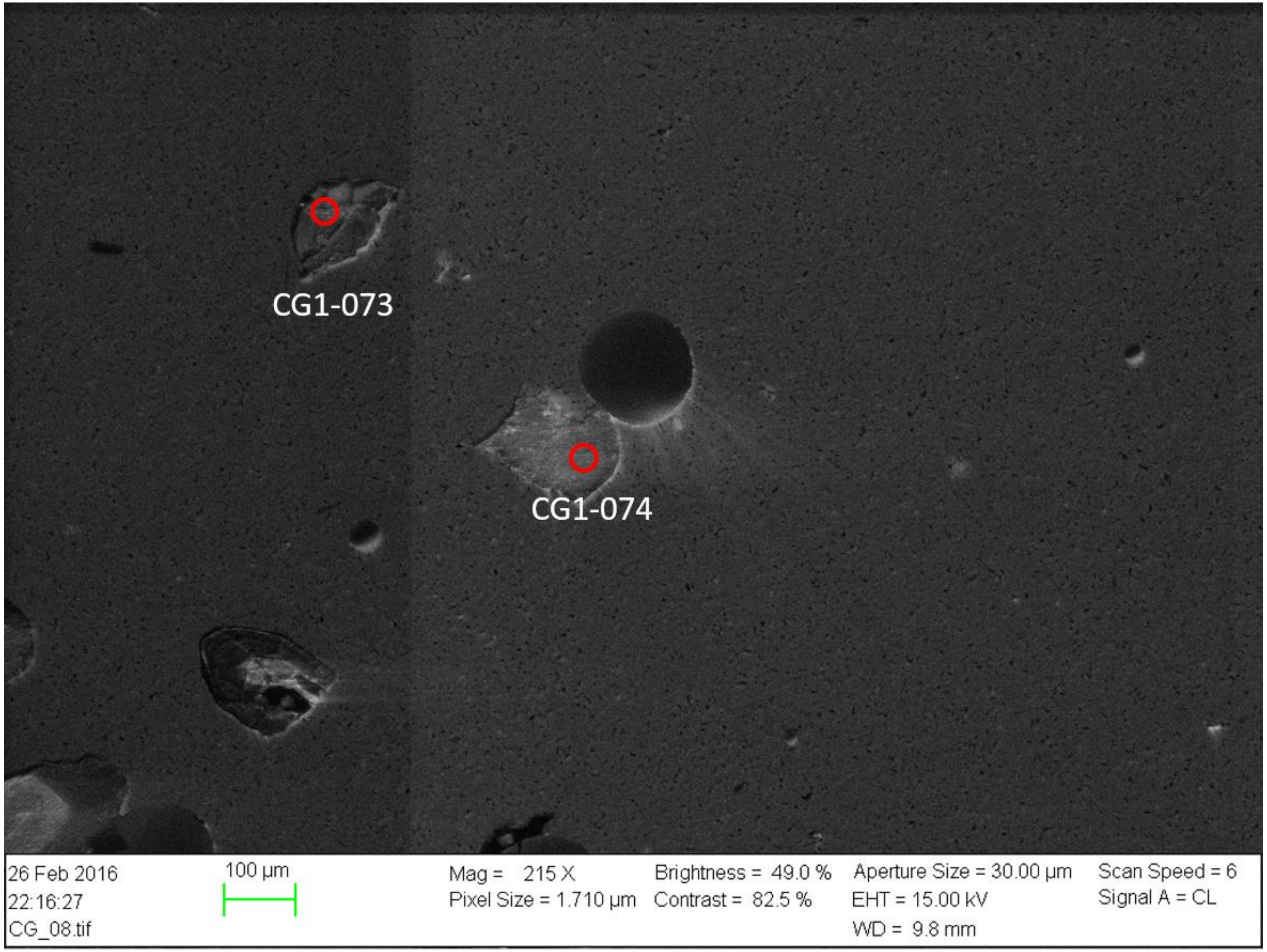

Figure 68 CL image overview of dated zircon grains.

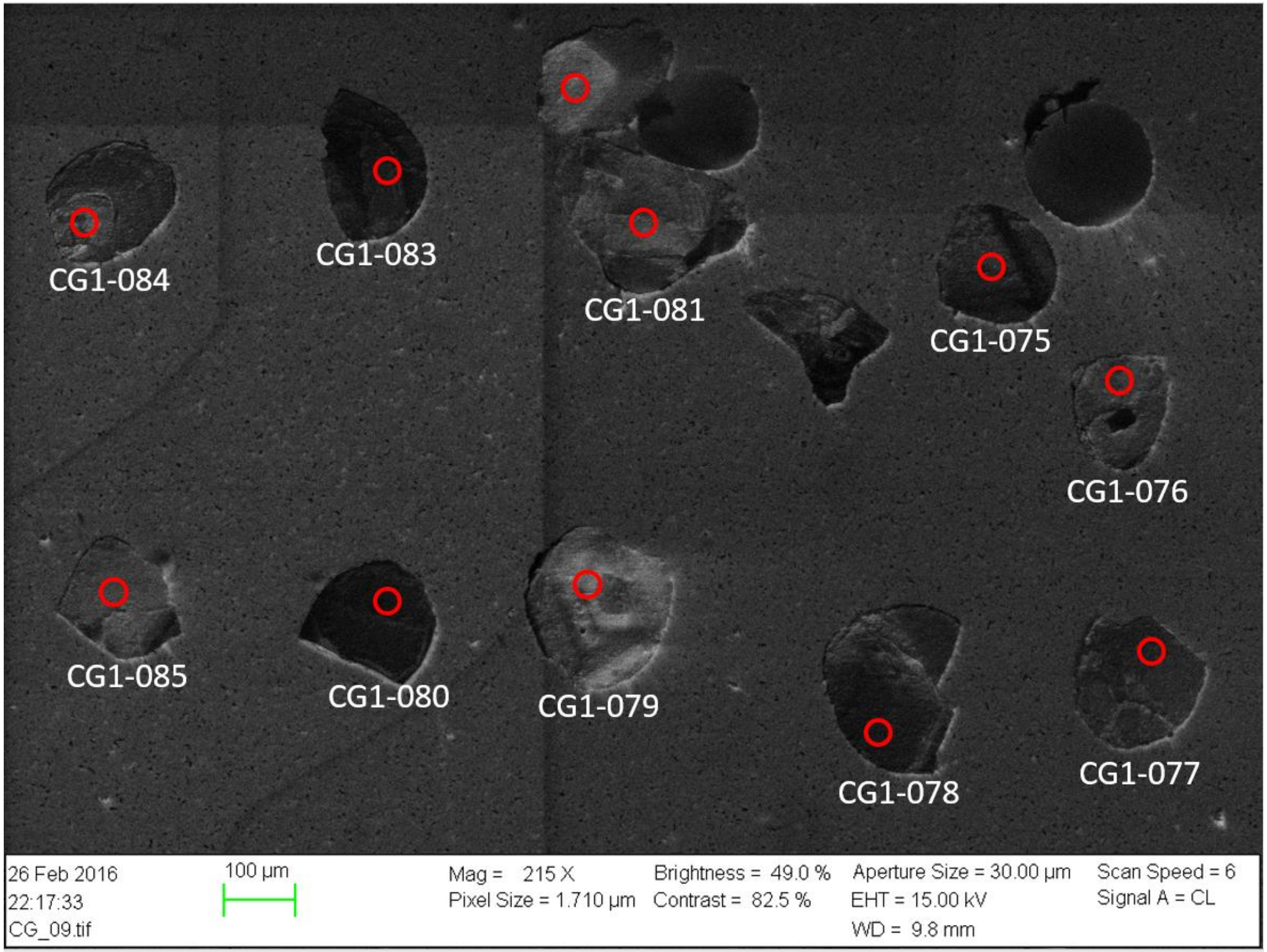

Figure 69 CL image overview of dated zircon grains.

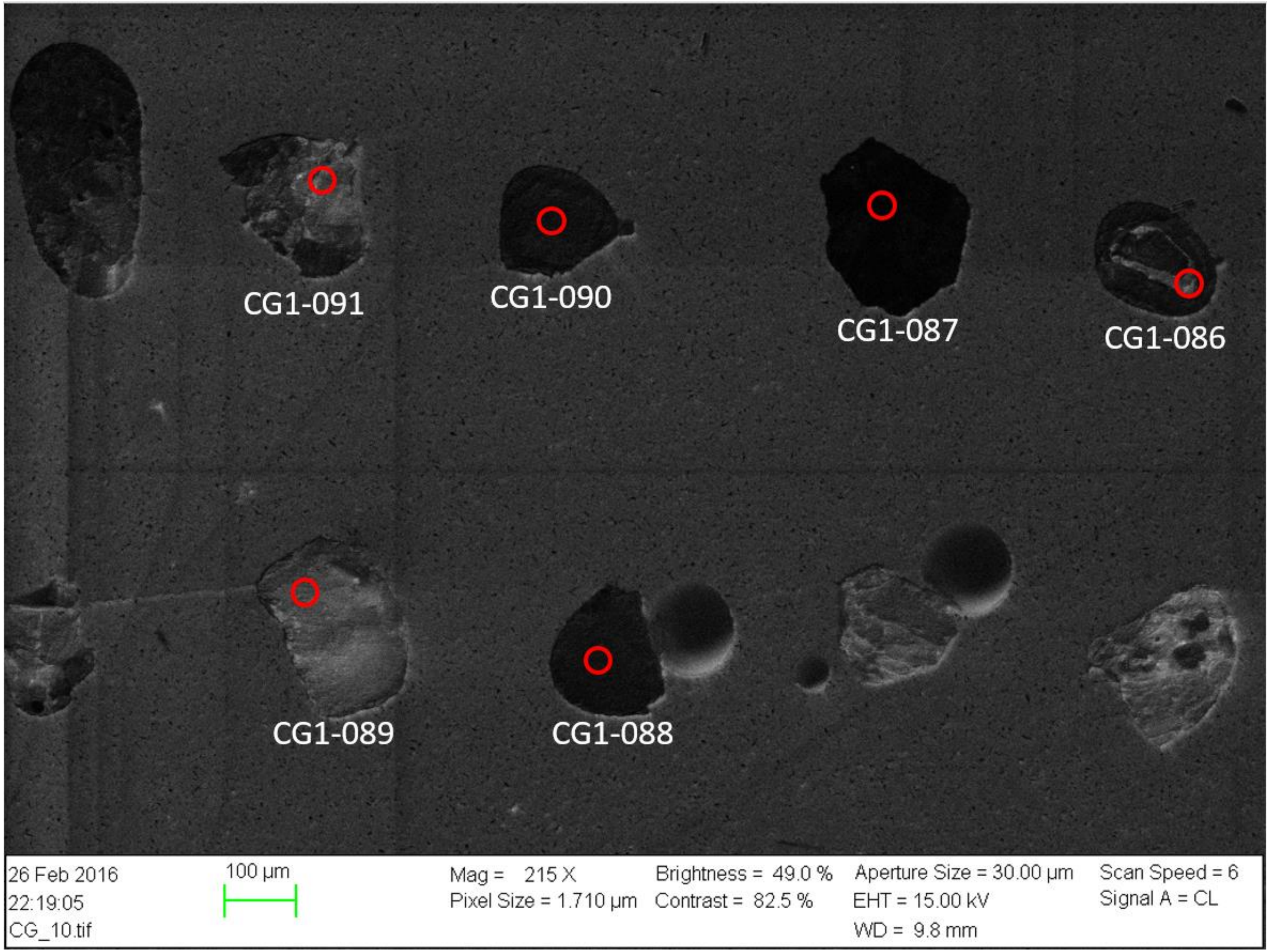

Figure 70 CL image overview of dated zircon grains.

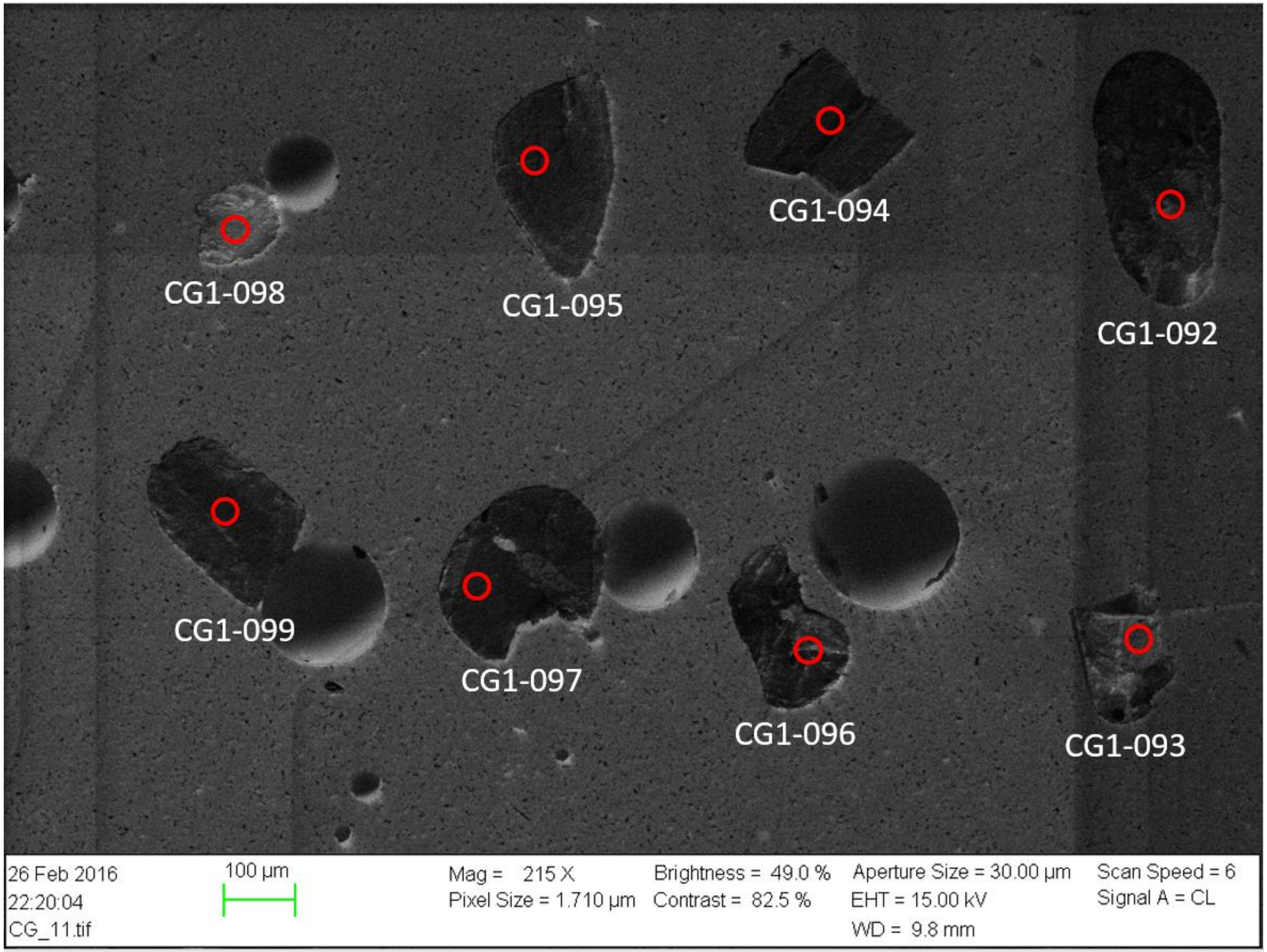

Figure 71 CL image overview of dated zircon grains.

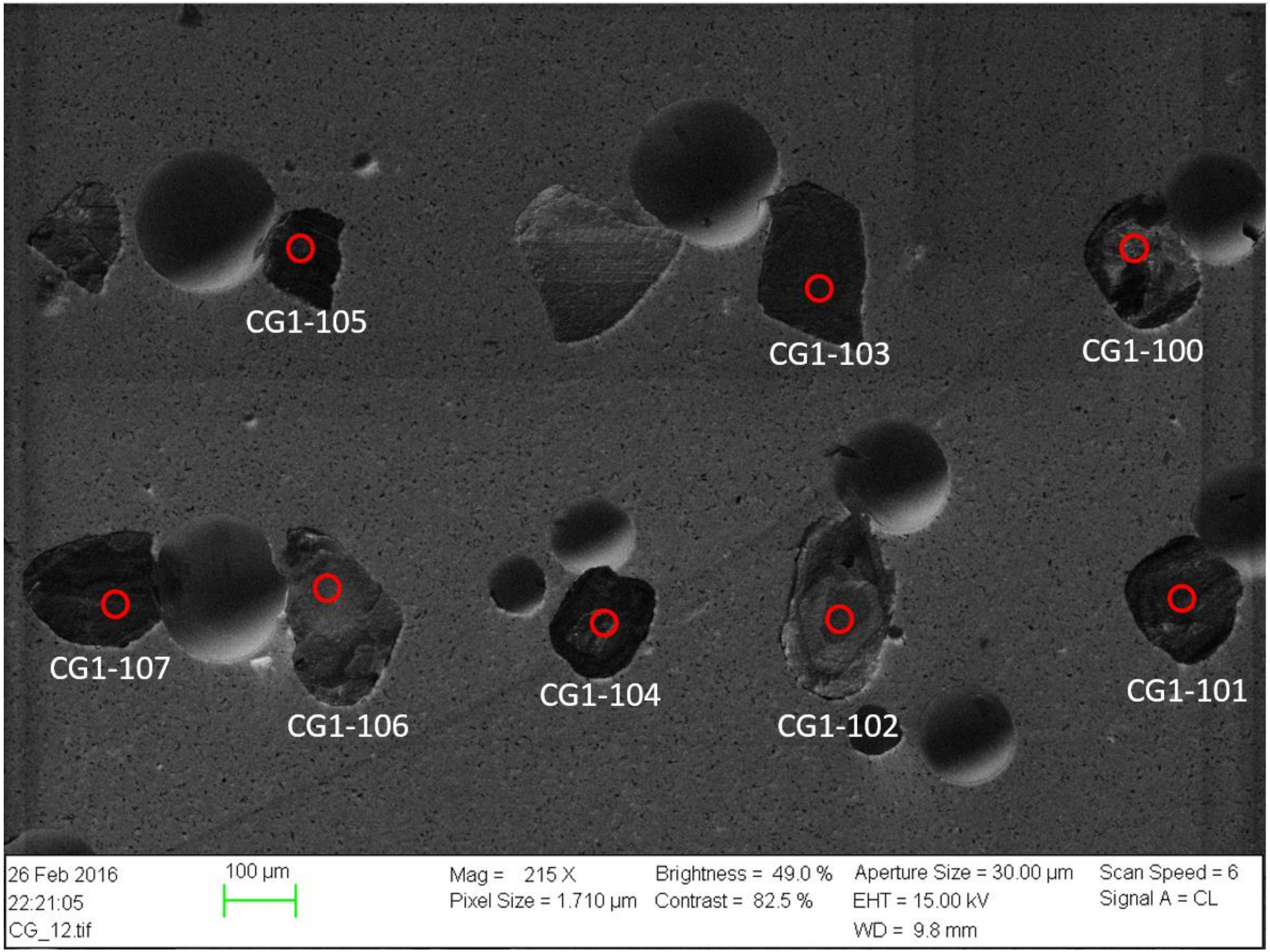

Figure 72 CL image overview of dated zircon grains.

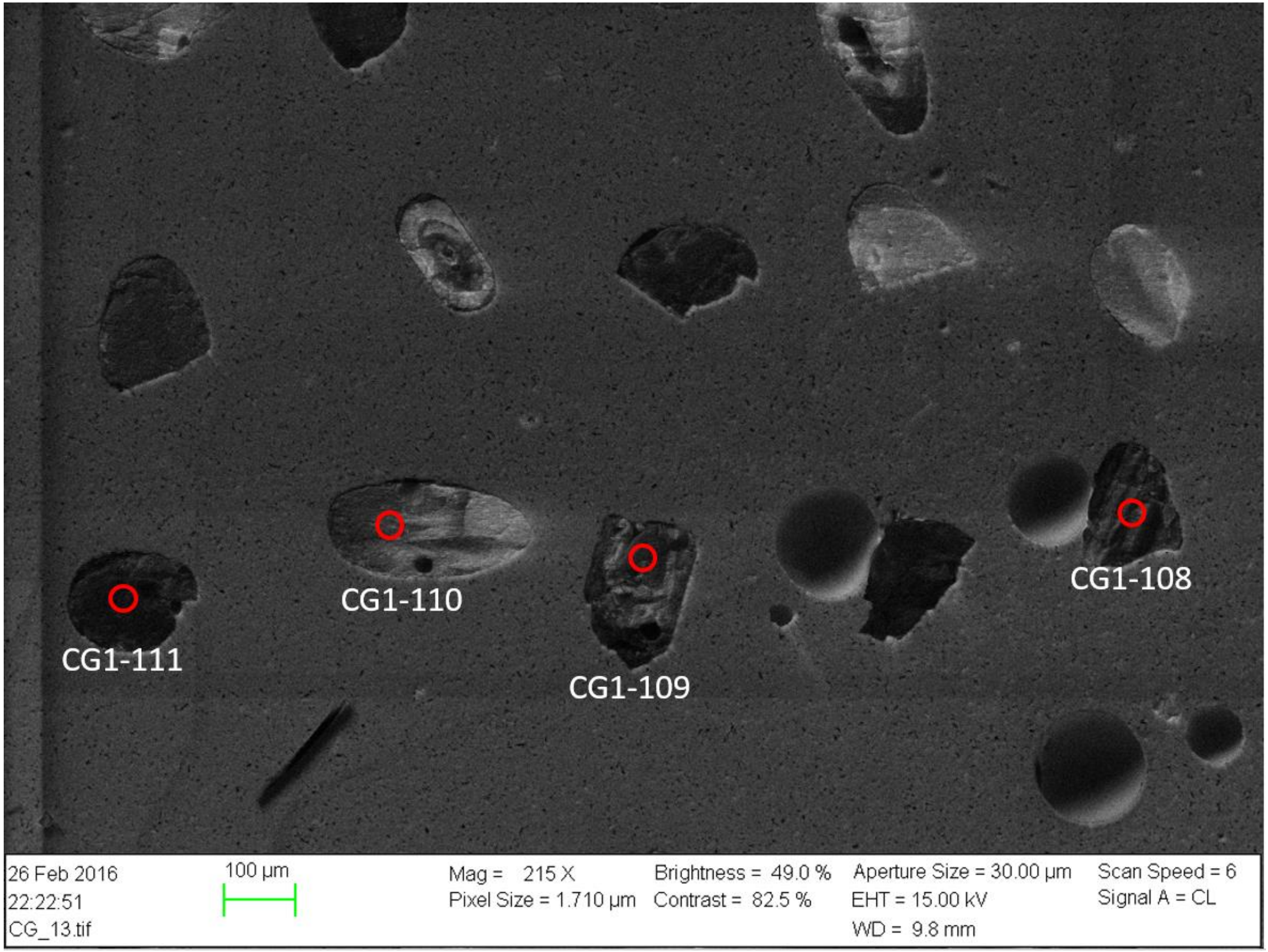

Figure 73 CL image overview of dated zircon grains.

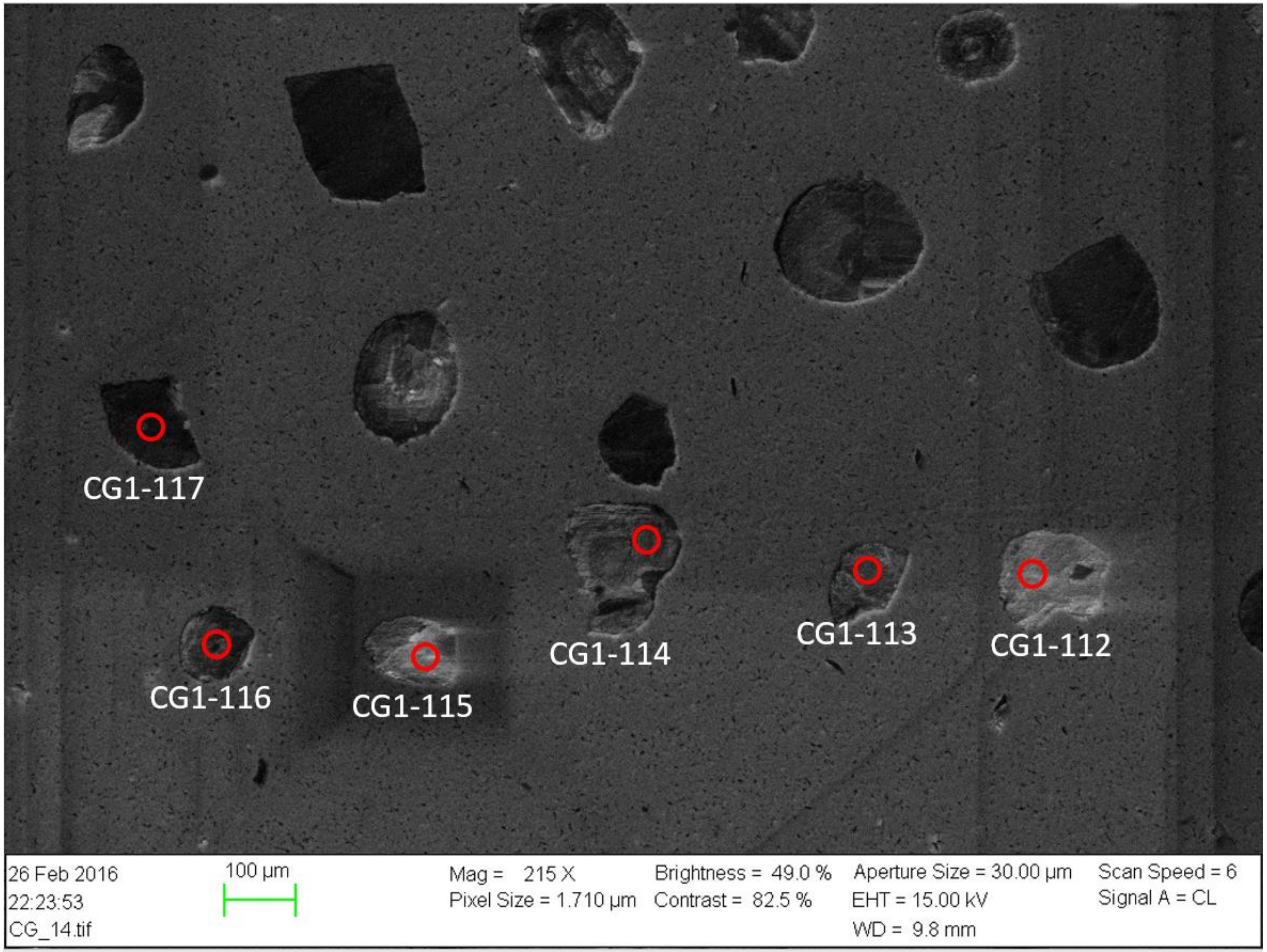

Figure 74 CL image overview of dated zircon grains.

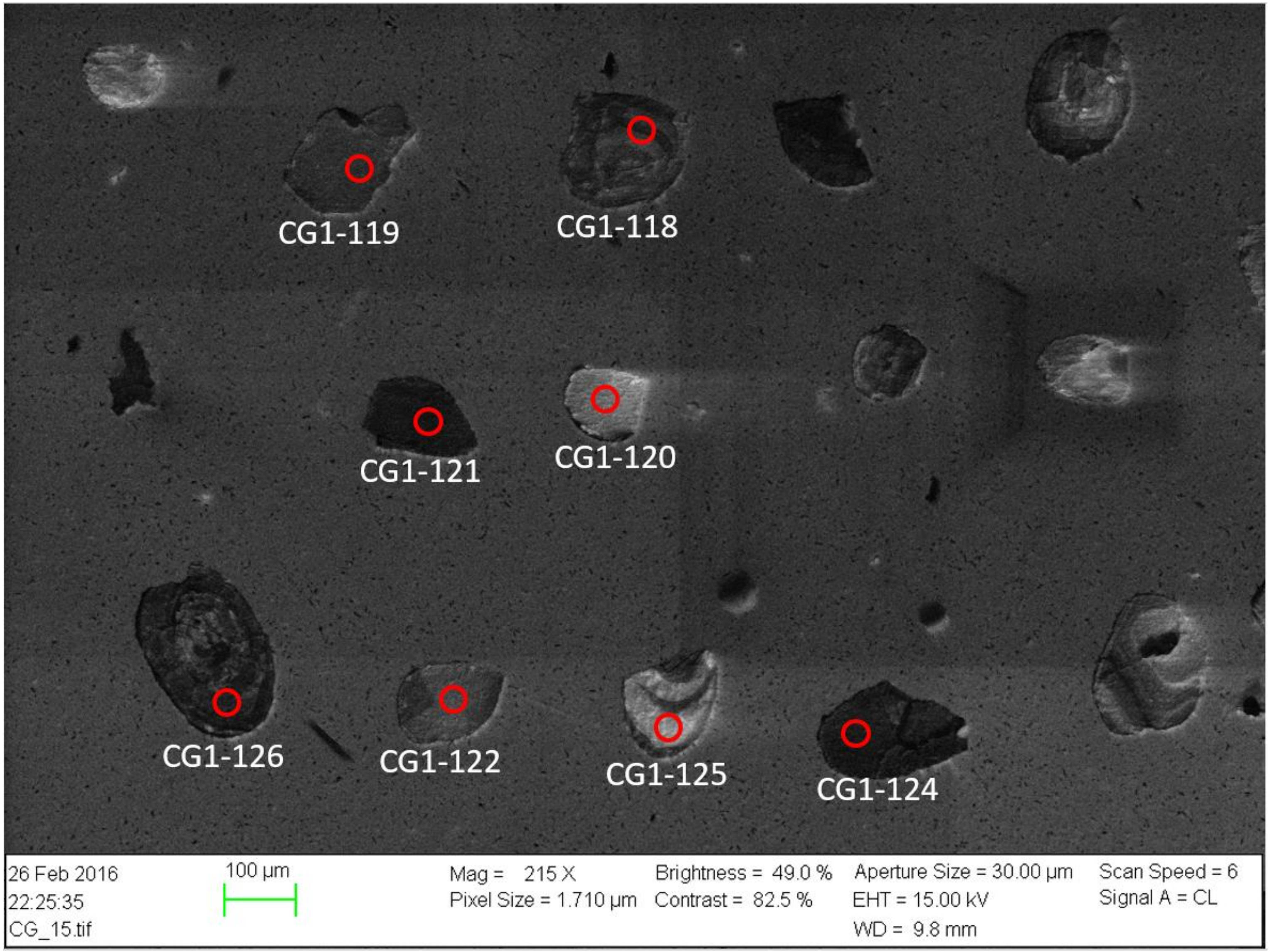

Figure 75 CL image overview of dated zircon grains.

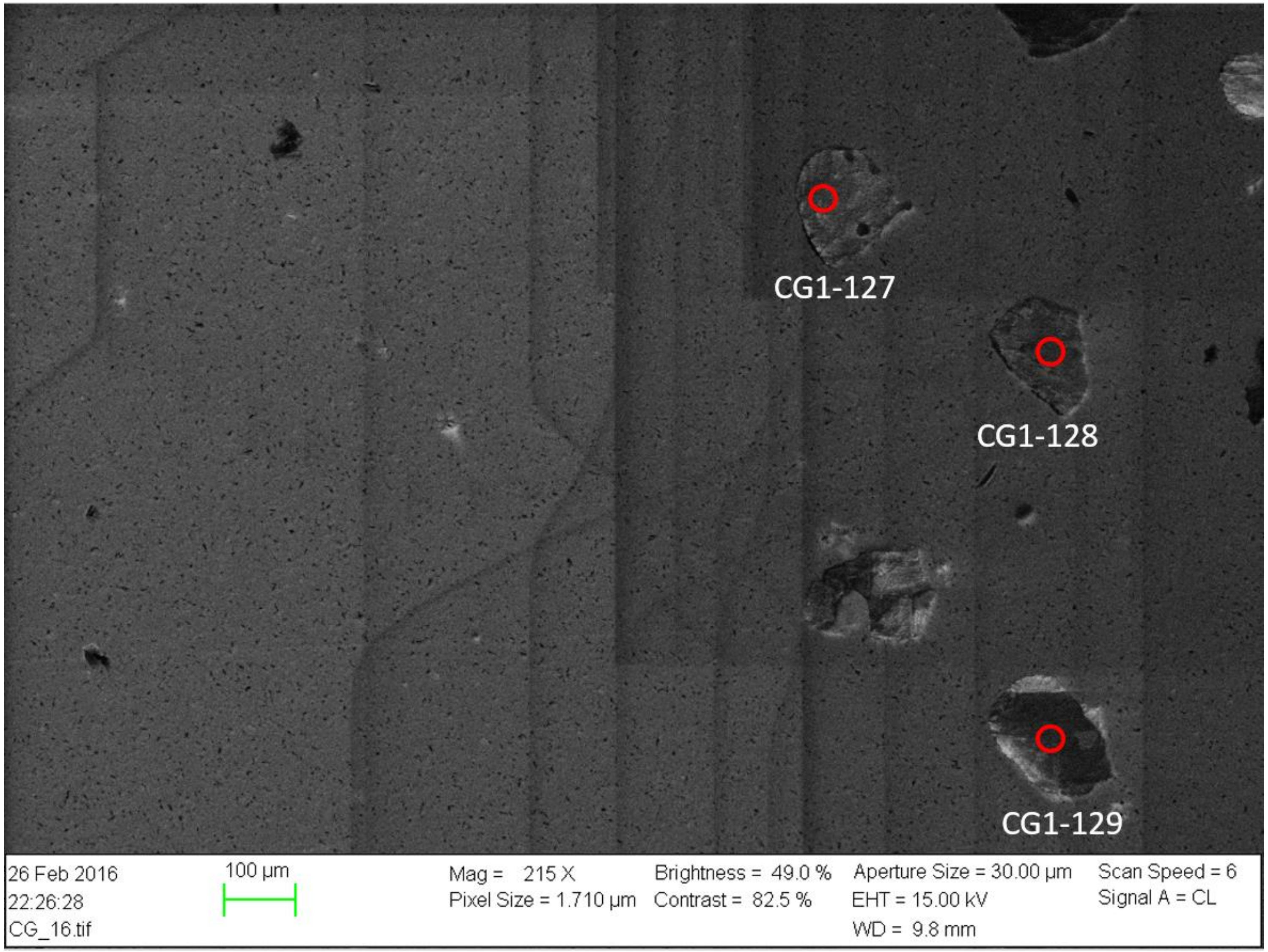

Figure 76 CL image overview of dated zircon grains.

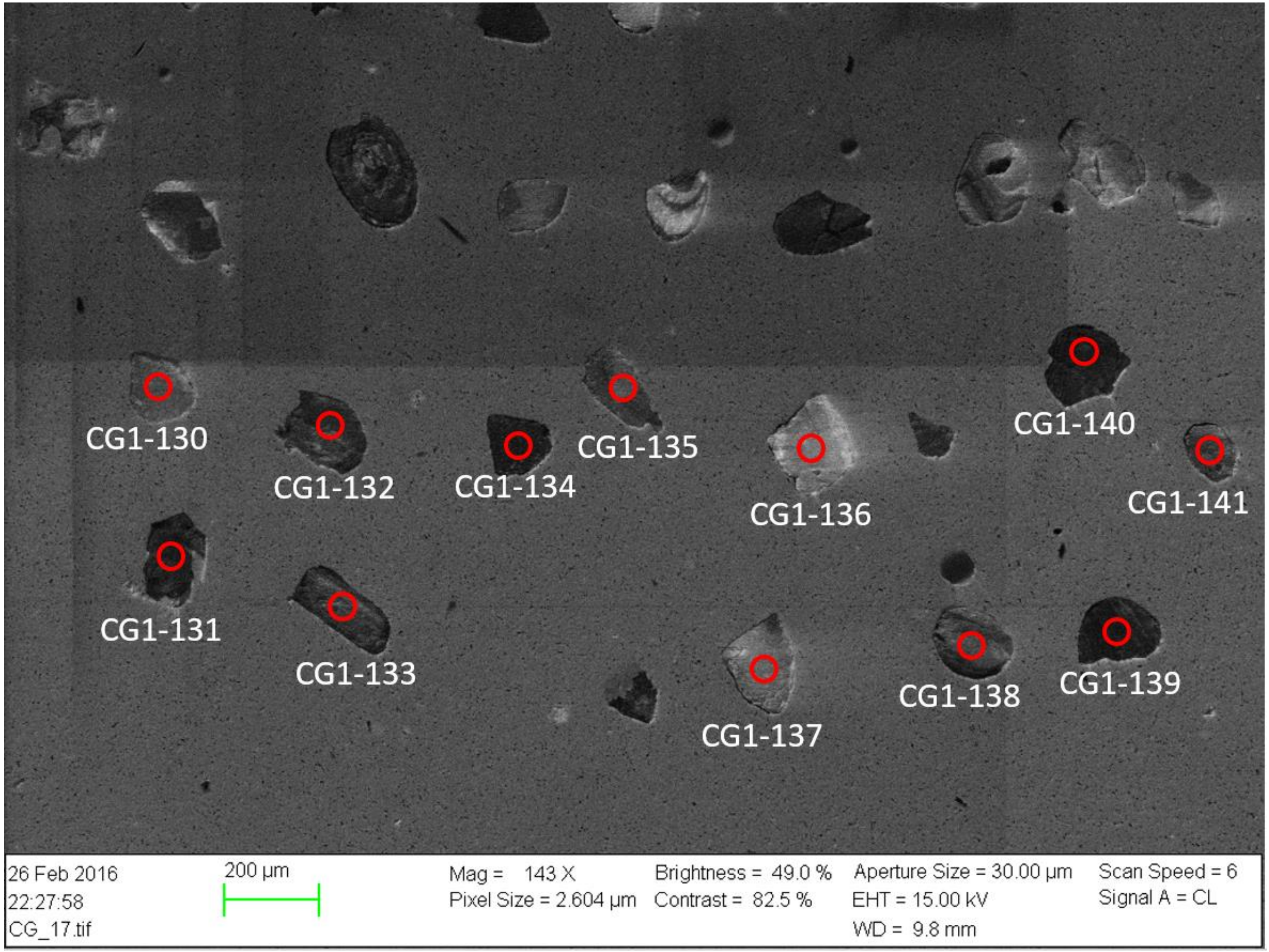

Figure 77 CL image overview of dated zircon grains.

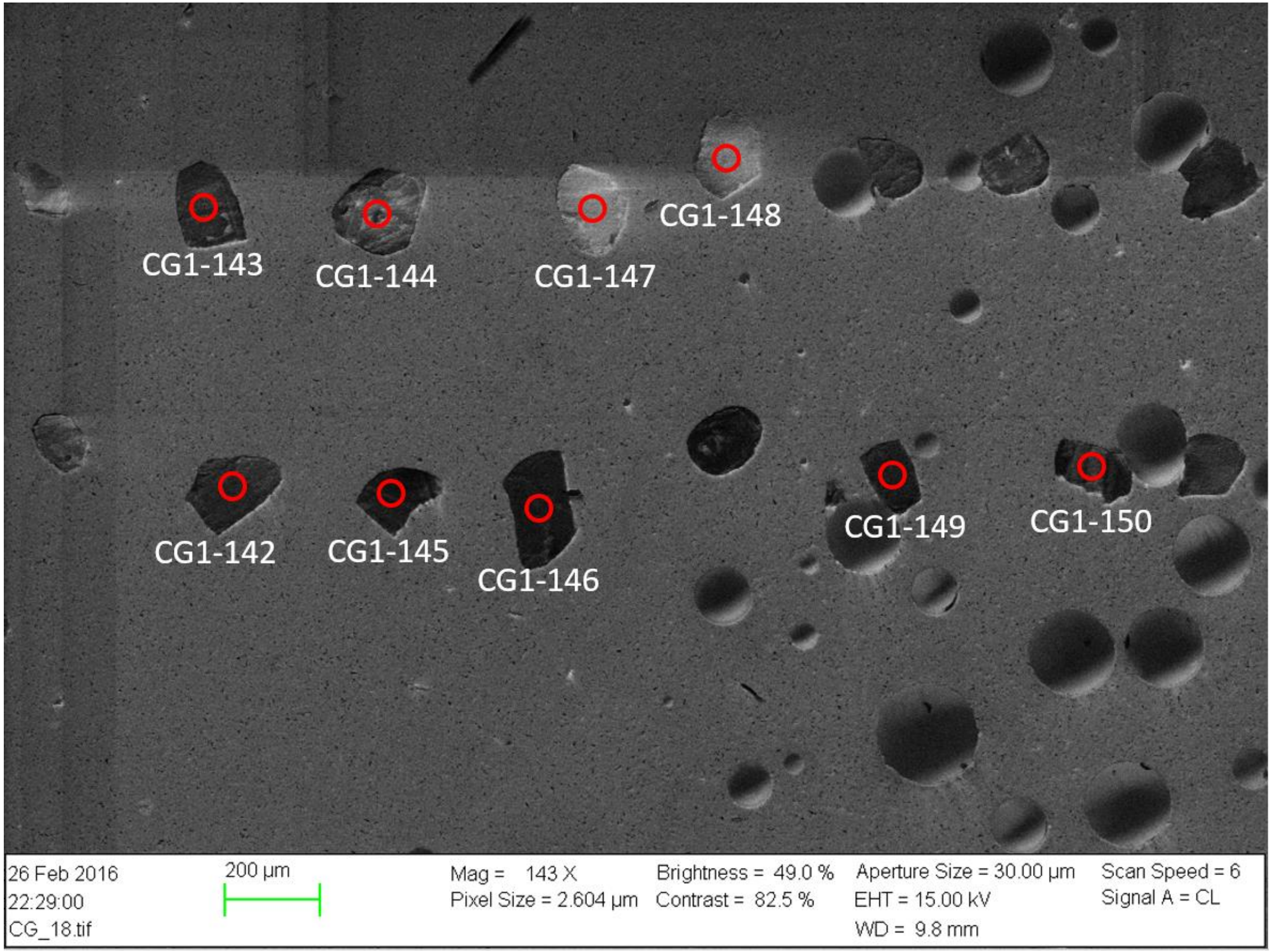

Figure 78 CL image overview of dated zircon grains.

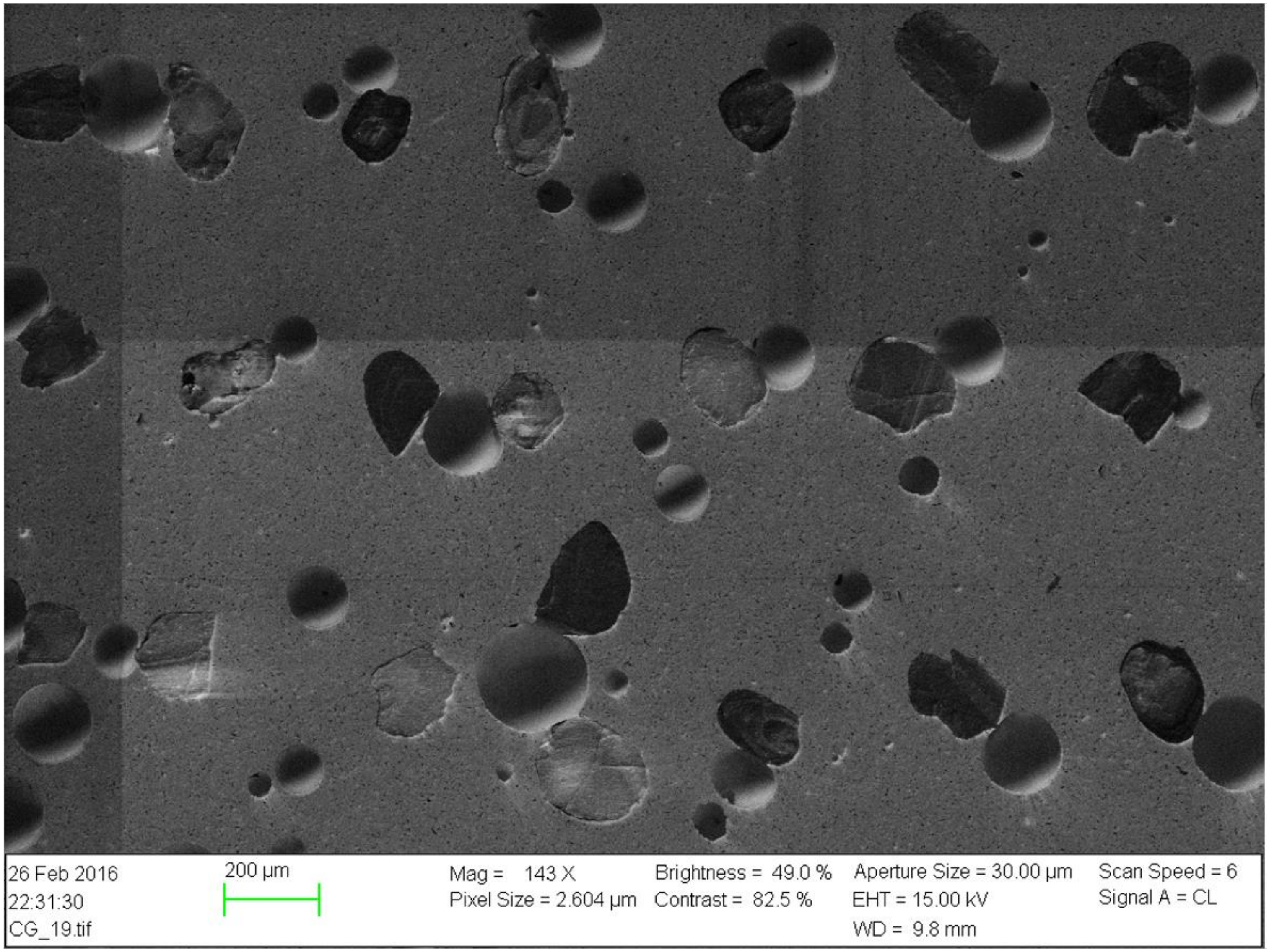

Figure 79 CL image overview of dated zircon grains.

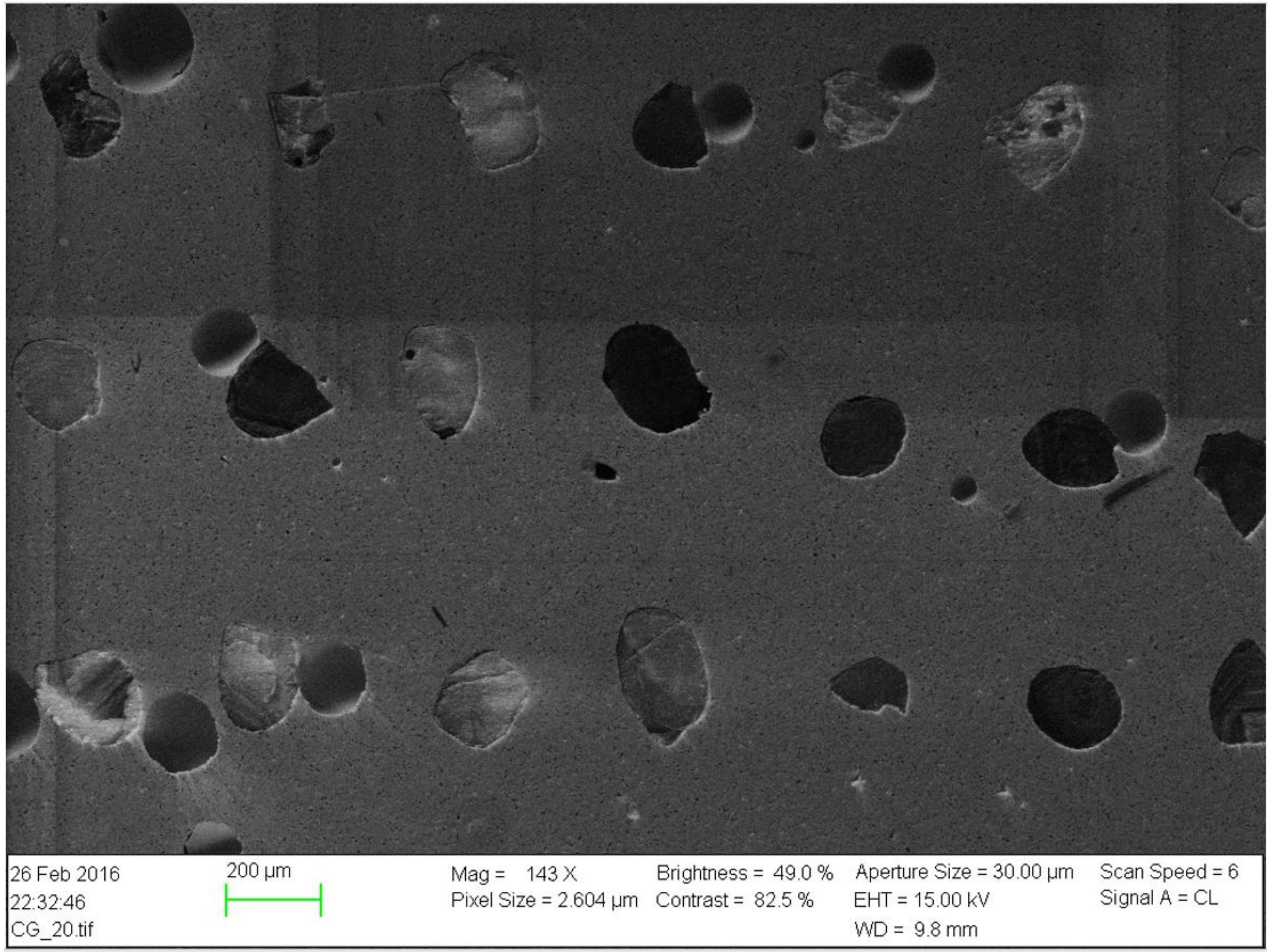

Figure 80 CL image overview of dated zircon grains.

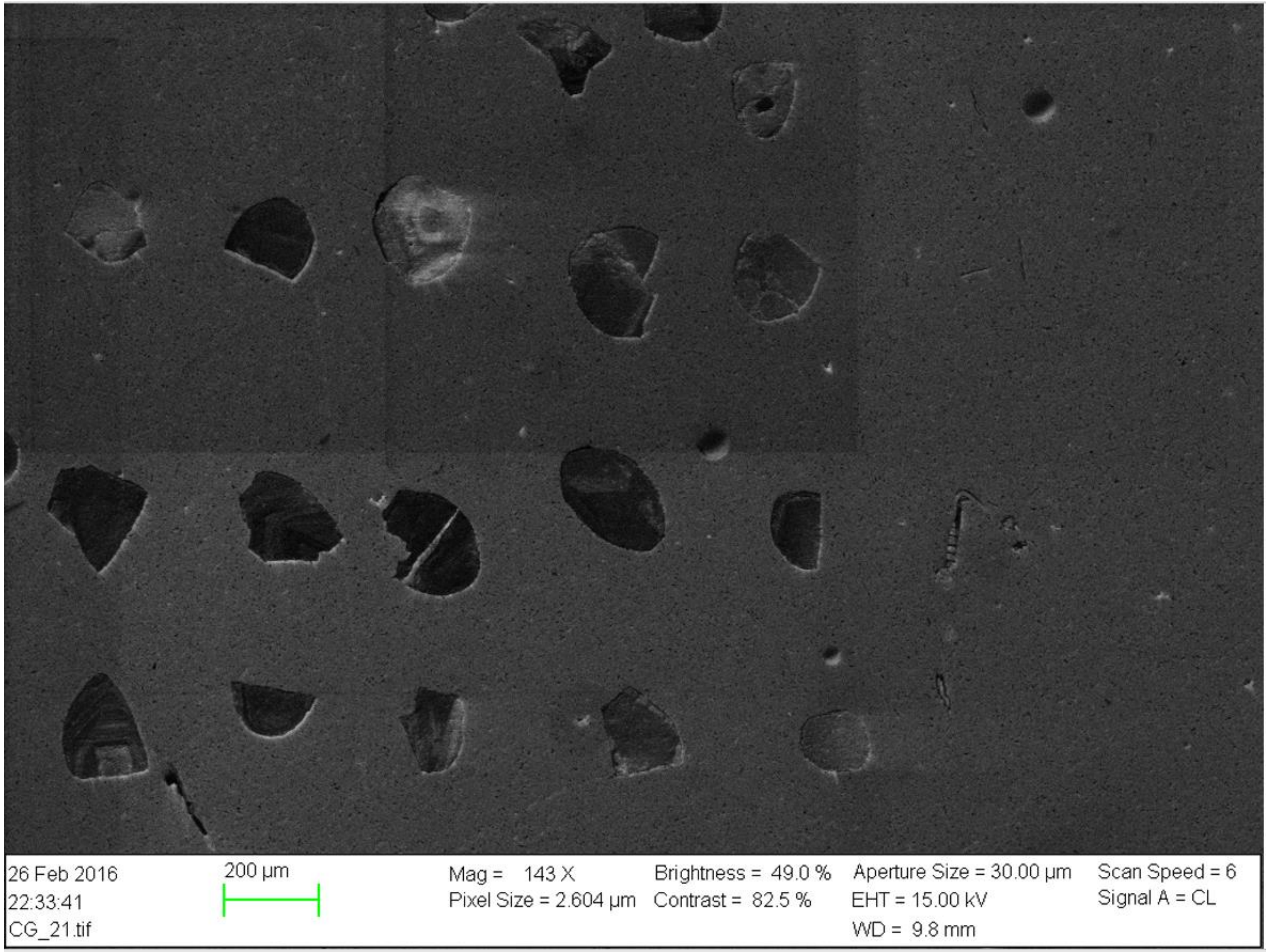

Figure 81 CL image overview of dated zircon grains.